THE UNIVERSITY
of EDINBURGH

11β-hydroxysteroid dehydrogenase type I inhibition in solid tumours

Callam Davidson

Doctor of Philosophy

The University of Edinburgh

2018

Abstract

Glucocorticoids, key hormonal regulators of the stress response, powerfully influence inflammation and metabolism. Reducing excessive glucocorticoid exposure is beneficial in treating metabolic and cognitive disorders, but manipulating systemic endogenous glucocorticoids risks compromising their beneficial effects. The enzyme 11β-hydroxysteroid dehydrogenase type 1 (11β-HSD1) activates glucocorticoids in target tissues and thus inhibition of this enzyme presents a clinical opportunity to reduce tissue-specific glucocorticoid action. Active glucocorticoids also exert potent angiostatic effects by binding the glucocorticoid receptor (GR), and 11β-HSD1 inhibitors have proven beneficial in models of myocardial infarction by promoting angiogenesis. The possibility that 11β-HSD1 inhibitors may increase pathological angiogenesis, such as that seen in solid tumours, remains unaddressed. This project tested the hypothesis that 11β-HSD1 inhibition promotes tumour growth as a result of increased angiogenesis, using murine models of squamous cell carcinoma (SCC) and pancreatic ductal adenocarcinoma (PDAC).

Murine SCC or PDAC cells were injected ($1x10^6$ cells/flank) into WT female mice fed either standard diet, or diet containing the 11β-HSD1 inhibitor UE2316 (175 mg/kg, N=6/group), or into 11β-HSD1 knockout (Del1) mice fed standard diet. Developing tumours were measured by callipers over several weeks, before animals were culled and tissues collected. SCC tumours grew more rapidly in UE2316-treated mice to reach a significantly ($P<0.01$) larger final volume (0.158 ± 0.037 cm^3) than in control mice (0.051 ± 0.007 cm3). PDA tumours were unaffected by 11β-HSD1 inhibition or deletion. Immunofluorescent co-staining of tumour sections for CD31/α-smooth muscle actin revealed no differences in vessel density, and RT-qPCR showed no difference in angiogenic factor expression, after 11β-HSD1 inhibition/deletion in either tumour type. GR and 11β-HSD1 RNA expression were greater in SCC vs PDAC tumours ($P<0.001$), as was 11β-HSD1 activity ($P<0.0001$).

In studies using the aortic ring assay of ex vivo angiogenesis, 11β-HSD1 deletion, but not inhibition with UE2316, was shown to prevent glucocorticoid-mediated angiostasis. The growth/viability of tumour cell lines was not affected by UE2316 or

corticosterone, as assessed by live cell imaging using the Incucyte imaging system. RNA-sequencing of SCC tumours revealed that multiple factors involved in the innate immune/inflammatory response were reduced in UE2316-treated tumours, and that extracellular matrix regulation was also altered by UE2316. Imaging of tumour sections using Second Harmonic Generation microscopy confirmed that UE2316 altered Type I collagen deposition in SCC ($P<0.001$) but not PDAC.

11β-HSD1 inhibition can increase tumour growth, possibly via suppression of inflammatory/immune cell signalling and alteration of the extracellular matrix, and tumours with higher GR and 11β-HSD1 content, such as SCC, may be more at risk. Interestingly this investigation found no evidence of increased angiogenesis in vivo or ex vivo after UE2316 treatment, suggesting that 11β-HSD1 inhibition does not promote angiogenesis in all ischaemic environments. Future work must focus on the effects of 11β-HSD1 inhibition on the immune and extracellular matrix component of the tumour microenvironment. While promotion of pathological angiogenesis does not appear to pose a major threat, 11β-HSD1 inhibitors may still interact with the immune and inflammatory environment in tumours to the detriment of health.

Lay Abstract

Glucocorticoids are hormones that regulate the body's response to stress. Exposure to sustained high levels of glucocorticoids can be damaging to health, and so reducing levels is desirable for treating diseases such as diabetes and Alzheimer's. However, care must be taken not to disrupt glucocorticoid levels throughout the body. Glucocorticoids are activated in specific tissues by the enzyme 11β-hydroxysteroid dehydrogenase type I (11β-HSD1), and blocking the action of this enzyme is considered a safer method for reducing their detrimental effects in targeted areas. Glucocorticoids also prevent the growth of new blood vessels (that is, they are anti-angiogenic). 11β-HSD1 inhibitors therefore promote the growth of new blood vessels (angiogenesis) by reducing glucocorticoid levels. While this promotes recovery in mice that have suffered a heart attack, it could also cause tumours to grow more quickly by increasing their blood supply. This project tested the hypothesis that 11β-

HSD1 inhibition promotes tumour growth by increasing angiogenesis, using mouse models of skin and pancreatic cancer.

Mouse skin cancer or pancreatic cancer cells were injected into mice which had received either (1) no treatment, (2) a drug that stops 11β-HSD1 generating glucocorticoids, or (3) genetic deletion of 11β-HSD1. Developing tumours were measured by callipers over 11-16 days, before animals were killed and tissues collected. Skin tumours grew more quickly in mice given a drug to block 11β-HSD1 generating glucocorticoids; this meant that the tumours in these mice were bigger than in controls. Pancreatic tumours were unaffected by 11β-HSD1 inhibition or deletion. The number of blood vessels in tumours, and the angiogenic signals they produced, were not affected by 11β-HSD1 inhibition/deletion in either tumour type. Skin tumours had more 11β-HSD1 and more of the glucocorticoid receptor than pancreatic tumours.

Adding glucocorticoids to a piece of mouse aorta grown on a plate prevented new blood vessels forming. This effect was prevented in aortas from mice lacking 11β-HSD1, but was not prevented by the drug that blocked 11β-HSD1. The growth and survival of cancer cells cultured on a plate were also unaffected by 11β-HSD1 inhibition and by glucocorticoids. Profiling gene expression in skin tumours showed that 11β-HSD1 inhibition reduced immune cell signalling, and affected structural components of the tumour, in particular collagen. Imaging of tumour sections confirmed that the amount of collagen in skin tumours, but not pancreatic tumours, was reduced by 11β-HSD1 inhibition.

In summary, using a drug to stop 11β-HSD1 generating glucocorticoids can increase tumour growth, possibly by suppressing immune signalling and altering the structure of the tumour. Tumour types with more 11β-HSD1 and glucocorticoid receptor, such as skin cancer, may be more at risk. Interestingly this investigation found no evidence of increased blood vessel growth after 11β-HSD1 inhibition, suggesting that local glucocorticoids influence blood vessels differently in the heart and in tumours. While 11β-HSD1 inhibitors may not promote blood vessel growth, they may still pose a threat. Future work must determine the mechanisms by which 11β-HSD1 inhibition affects immune cells in tumours and tumour structure.

Declaration

I declare that this thesis is the result of my own work performed at The University of Edinburgh. Any assistance received has been acknowledged in the relevant sections.

I declare that this work has not been previously submitted for any other degree or qualification.

Callam Davidson

Acknowledgements

I would like to thank my supervisors Paddy Hadoke, Brian Walker and Val Brunton, for their encouragement and support throughout the PhD. The mantra ‘what is the question?’ will not be forgotten. Thanks also to the British Heart Foundation for making the PhD possible through their generous funding.

I’d like to thank; the mass spec team (George, Natalie, Karen and Logan), John, Ifi, Martin and Laura at the ECRC and the histology staff (Mike, Lyndsey, Debbie, Mel and Laura). Thanks to Ruth Andrew, Scott Webster, Andrea Caporali and Karen Chapman for their kind words and advice. Thanks also to Alan and Bryan Serrels for their advice and regular provision of cells.

Thanks to the staff and students of the CVS and ECRC for creating a friendly working environment. Special thanks are due to all of team Paddy (Mark, Rob, Steve Welbeck, Junxi, Eileen, Amber, Matt) and my office mates Mark(s), Cat, Junxi, Theresia, Julie and Amber for the good times and edible goods. Mark MacAskill in particular has at times acted as a fourth supervisor and I am indebted to him in terms of both my science, and my Weegie slang. Thanks also to Lynne and Morwenna, who have kept me on target with their kindness and incredible organisational skills.

Huge thanks to Roseanne and the family for always making me feel capable of overcoming the challenges I’ve faced during the PhD. Finally, thanks to Dr Hebden and Ms Davies of King Edward VII School for their encouraging me to pursue science.

Contents

List of Figures

List of Tables

Abbreviations

HPA	Hypothalamic-Pituitary-Axis
11β-HSD	11β-hydroxysteroid dehydrogenase
MR	Mineralocorticoid Receptor
GR	Glucocorticoid Receptor
PDR	Proliferative Diabetic Retinopathy
CYP	Cytochrome P450

ER	Endoplasmic Reticulum
CBG	Corticosteroid Binding Globulin
CRH	Corticotropin Releasing Hormone
ACTH	Adrenocorticotropic Hormone
11-DHC	11-Dehydrocorticosterone
NO	Nitric Oxide
VSMC	Vascular Smooth Muscle Cell
VEGF	Vascular Endothelial Growth Factor
Il	Interleukin
IFN	Interferon
TNF	Tumour Necrosis Factor
NADP	Nicotinamide Adenine Dinucleotide Phosphate
KO	Knockout
SMA	Smooth Muscle Actin
WT	Wild-type
LPS	Lipopolysaccharide
FGF	Fibroblast Growth Factor
ECM	Extracellular Matrix
ANG	Angiopoietin

HIF	Hypoxia Inducible Factor
BM	Basement Membrane
MMP	Matrix Metalloprotease
DLL	Delta-like Ligand
KLF	Kruppel-like Factor
NOS	Nitric Oxide Synthase
TGF	Transforming Growth Factor
PDGF	Platelet Derived Growth Factor
ApoE	Apolipoprotein E
TLR	Toll-like Receptor
LDL	Low Density Lipoprotein
MCP	Monocyte Chemoattractant Protein
MI	Myocardial Infarction
PPAR	Peroxisome Proliferator Activated Receptor
TSP	Thrombospondin
HUVEC	Human Umbilical Vein Endothelial Cell
HCC	Hepatocellular Carcinoma
CAF	Cancer Associated Fibroblast
NK	Natural Killer

MDSC	Myeloid Derived Suppressor Cell
ARG	Arginase
PDAC	Pancreatic Ductal Adenocarcinoma
ER	Estrogen Receptor
AR	Androgen Receptor
SCC	Squamous Cell Carcinoma
TPA	12-O-tetradecanoylphorbol-13-acetate
BCC	Basal Cell Carcinoma
HPLC	High Performance Liquid Chromatography
EDTA	Ethylenediaminetetraacetic acid
PBS	Phosphate Buffered Saline
DMBA	7,12-Dimethylbenz[a]anthracene
SHG	Second Harmonic Generation
GO	Gene Ontology
FACS	Fluorescence Associated Cell Sorting

Meetings and Awards

Poster presentations

'Targeting 11ß-HSD1 to promote angiogenesis; is there a risk of solid tumour growth?, Scottish Cardiovascular Forum, Edinburgh, UK, 2015

'Targeting 11ß-HSD1 to promote angiogenesis; is there a risk of solid tumour growth?', BHF PhD Students Annual Symposium, Cambridge, UK, 2015

'A pharmacological inhibitor of 11β-HSD1 promotes squamous cell carcinoma growth in a murine subcutaneous tumour model', BHF PhD Students Annual Symposium, Glasgow, UK, 2016. **Prize for Best Poster Presentation.**

'Targeting 11β-HSD1 to promote angiogenesis – consequences for solid tumour growth', Scottish Cardiovascular Forum, Edinburgh, UK, 2017

'Targeting 11β-HSD1 to promote angiogenesis – consequences for solid tumour growth', BHF PhD Students Annual Symposium, Cambridge, UK, 2017

Oral presentations

'Pharmacological inhibition of 11β-HSD1 promotes tumour growth in a murine subcutaneous tumour model', Scottish Cardiovascular Forum, Belfast, UK, 2016. **Prize for Best Oral Presentation.**

List of Publications

Davidson, C. T, Dover, A. R., McVicar, C. M., Megaw, R., Glenn, J. V., Hadoke, P. W. F., Stitt, A. W. and Walker, B. R. (2017), Inhibition or deletion of 11β-HSD1 does not increase angiogenesis in ischemic retinopathy, *Diabetes and Metabolism*, doi: 10.1016/j.diabet.2016.12.001

Davidson, C. T., Muir, M., Homer, N., Andrew, R., Brunton, V., Hadoke, P.W.F and Walker, B.R. (2017), Targeting 11β-HSD1 to promote angiogenesis – consequences for solid tumour growth, *Heart*, doi: 10.1136/heartjnl-2017-311433.11

Chapter 1

Introduction

1 Introduction

Glucocorticoids are vital modulators of the physiological stress response, with wide-ranging effects across almost every major organ system (Sapolsky *et al.*, 2000). These steroid hormones have been exploited clinically for over half a century for their anti-inflammatory and immunosuppressive effects (Hench & Kendall, 1949) and are today still commonly used to treat both acute and chronic inflammatory conditions. These include rheumatoid arthritis, dermatological conditions, inflammatory bowel disease, asthma and multiple sclerosis (Coutinho and Chapman, 2011). Their potent immunosuppressive effects are also exploited clinically in the treatment of leukaemia and immunosuppression before organ transplant (Coutinho and Chapman, 2011; Lin and Wang, 2016).

In terms of physiology, when a stressor is encountered, the hypothalamic-pituitary-adrenal (HPA) axis is activated, leading to a rise in circulating cortisol (in man) or corticosterone (in rats and mice) (Sapolsky *et al.*, 2000). Negative feedback to both the hypothalamus and the pituitary ensures basal systemic glucocorticoid levels are maintained within a predictable range, with a diurnal peak and nadir under circadian control (Oakley and Cidlowski, 2013). The major role of glucocorticoids is in the regulation of energy metabolism; glucocorticoids oppose the effects of insulin, inducing gluconeogenesis and increasing free energy stores to fuel skeletal muscle metabolism (Walker, 2007). Glucocorticoids also exert myriad effects on other systems in the body, influencing reproductive function, memory, vascular tone, immunity and adiposity (Sapolsky et al. 2000).

Whilst glucocorticoids are pivotal in coordinating the physiological stress response, they can become maladaptive if present at chronically high levels. Consequences of excessive glucocorticoid exposure are apparent in Cushing's syndrome, in which glucocorticoid levels are constantly elevated, due either to a pituitary tumour or long-term therapeutic steroid administration (Whitworth *et al.*, 2000). Patients with glucocorticoid excess present with a range of debilitating cardiometabolic disorders, including increased visceral adiposity, poor glycaemic control and slow wound healing (Walker, 2007). This poor wound healing is attributable in part to the anti-angiogenic

effects mediated by active glucocorticoids (Small *et al.,* 2005). For more than three decades, glucocorticoids have been known to potently inhibit angiogenesis, though to this day the mechanisms involved remain uncertain (Folkman *et al.*, 1983; Small *et al.*, 2005).

Reducing glucocorticoid action is, therefore, clinically desirable in the management of metabolic disorders, such as type II diabetes, but manipulating systemic glucocorticoid action risks inducing adrenal insufficiency. As well as the tight systemic regulation of circulating glucocorticoid concentrations by the HPA axis, intracellular glucocorticoid concentrations are controlled at the pre-receptor level by two isozymes: 11β-hydroxysteroid dehydrogenase (11β-HSD) types 1 and 2 (Seckl & Walker, 2001). 11β-HSD2 functions as a dehydrogenase in mineralocorticoid target tissues, where it converts glucocorticoids to their inactive metabolites and prevents glucocorticoid occupancy of the mineralocorticoid receptor (MR). 11β-HSD1 is expressed in glucocorticoid target tissues where it acts predominantly as a reductase, activating glucocorticoids to amplify their effects at the glucocorticoid receptor (GR) (Chapman *et al.,* 2013b).

Manipulation of the 11β-HSDs presents a novel therapeutic opportunity to control tissue-specific glucocorticoid levels, without the risks associated with HPA axis perturbation. 11β-HSD1 selective inhibitors have been developed to improve glycaemic control in type II diabetes (Anderson and Walker, 2013) and these have also shown considerable promise in the treatment of Alzheimer's disease (Webster *et al.*, 2017). Pre-clinical evidence has also shown that 11β-HSD1 inhibition can promote angiogenesis, improving recovery post-myocardial infarction (Small *et al.*, 2005; McSweeney *et al.*, 2010) and reducing intra-adipose tissue hypoxia in obesity (Michailidou *et al.*, 2012). Whilst these are encouraging findings, the potential for 11β-HSD1 inhibitors to promote angiogenesis could also pose a risk in diseases associated with pathological angiogenesis, such as proliferative diabetic retinopathy (PDR) and solid tumour growth (Chung and Ferrara, 2011). These diseases are more common in the elderly, a population that are likely to benefit from the positive effects of 11β-HSD1 inhibitors on glycaemic control and cognitive function. Therefore, this risk cannot be taken lightly.

Few studies to date have directly addressed this risk. Recent work in a neonatal retinal hypoxia model suggests that 11β-HSD1 inhibition may not pose a threat to PDR (Davidson *et al.*, 2017) but evidence suggests that 11β-HSD1 manipulation can influence tumour growth (Liu *et al.*, 2016; Cirillo *et al.*, 2017). Tumours require their own blood supply if they are to grow beyond 1-2mm in size (Hanahan and Folkman, 1996). This is achieved via an angiogenic 'switch', by which tumours stimulate the excessive growth of a disorganised and tortuous neovasculature (Carmeliet, 2003). Targeting this blood supply is an important focus of cancer research (Carmeliet & Jain 2011; Folkman 2001). Furthermore, glucocorticoids are known to inhibit tumour angiogenesis and growth in certain contexts (Folkman *et al.* 1983; Yano *et al.* 2006). The question of whether local glucocorticoid regeneration plays an important role in regulating tumour angiogenesis and growth forms the focus of this thesis.

1.1 Glucocorticoid production

1.1.1 Synthesis, secretion and clearance

Glucocorticoids are part of the corticosteroid family of steroid hormones. They are synthesised from cholesterol, predominantly in the zona fasciculata of the adrenal cortex, via a pathway catalysed by members of the cytochrome P450 (CYP) oxidative enzyme family located on the inner membrane of the endoplasmic reticulum (ER) (**Figure 1.1**) (Parente, 2001). Cortisol is the major glucocorticoid produced in the human adrenal gland, whilst in rats and mice corticosterone is the major glucocorticoid as rodent adrenal glands lack the enzyme 17α-hydroxylase (Luu-The *et al.*, 2005). The zona glomerulosa of the adrenals produces mineralocorticoids (Curnow *et al.*, 1991), the other major class of corticosteroid which are primarily involved in the regulation of sodium retention, blood volume and blood pressure. Aldosterone is the primary mineralocorticoid (Briet and Schiffrin, 2010).

Glucocorticoids are released from the adrenals into the blood stream where they circulate bound to plasma proteins. Under non-stressed conditions, less than 6% of circulating cortisol is unbound in humans, with 80-90% bound to corticosteroid binding globulin (CBG) and the remainder bound to albumin (Lewis *et al.*, 2005).

Clearance of glucocorticoids occurs predominantly in the liver, where they are inactivated via one of several enzymatic pathways before excretion in the urine (Nixon *et al.*, 2012). The key route of relevance to this project is interconversion of active glucocorticoids and their inactive counterparts via the 11β-HSDs.

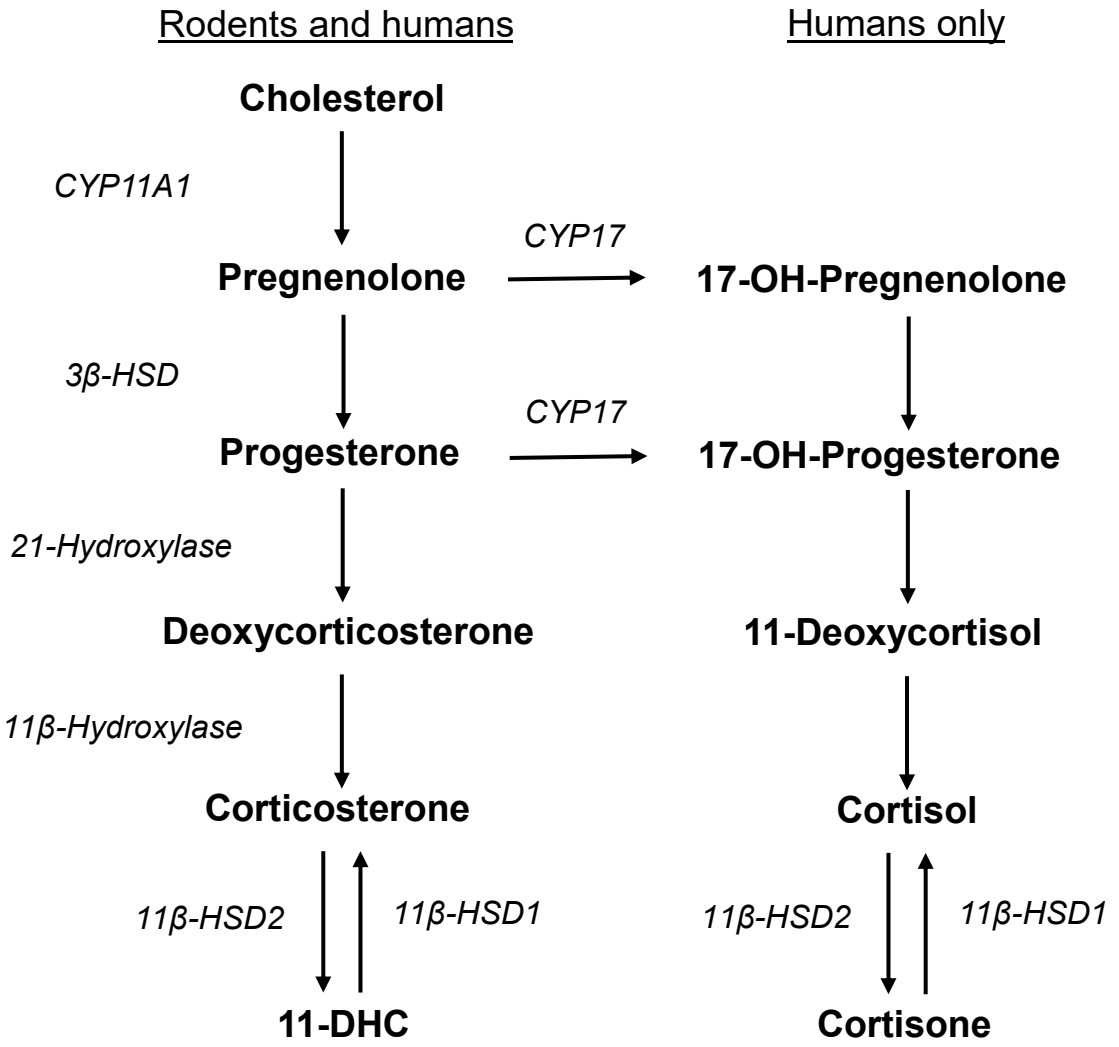

Figure 1.1 – Glucocorticoid synthesis in rodents and humans. The enzymatic pathway by which glucocorticoids are produced from cholesterol, in the zona fasciculata of the adrenal cortex. Rodents lack CYP17 (17α-hydroxylase) and thus do not produce those steroids shown in the right half of the figure. Adapted from Boucher *et al*., 2014.

1.1.2 Systemic regulation

Adrenal glucocorticoid release is under the control of the HPA axis. Upon the triggering of the stress response, neurons of the paraventricular hypothalamus release corticotropin releasing hormone (CRH) which in turn stimulates the corticotrophs of the anterior pituitary gland to release adrenocorticotropic hormone (ACTH) into the systemic circulation. ACTH stimulates increased adrenal production of glucocorticoids by both enhancing the delivery of cholesterol into the inner mitochondrial membrane, and by increasing the expression of steroidogenic enzymes. The HPA axis is maintained by a negative feedback system; corticosteroids bind the GR in the hypothalamus to inhibit CRH release, and in the pituitary to reduce CRH action and prevent ACTH secretion (Briassoulis *et al.*, 2011; Oakley and Cidlowski, 2013).

Under non-stressed conditions, glucocorticoid release is regulated in a circadian fashion by the suprachiasmatic nucleus of the hypothalamus (Malisch *et al.*, 2008). Human plasma cortisol levels are at their nadir between 8pm and midnight, peaking around 7-11am and declining throughout the day (Weitzman *et al.*, 1971; Nomura *et al.*, 1997; Chan and Debono, 2010). This circadian pattern is reversed in rodents, with plasma corticosterone levels at their lowest early in the morning (Harris *et al.*, 2001; Oster *et al.*, 2006). Typical nadir human serum cortisol levels are <50 nmol/l rising to peak levels of ~500 nmol/l (Parente, 2001; Debono *et al.*, 2009; Jung *et al.*, 2014), while cortisone ranges from ~10 - 60 nM (Nomura *et al.*, 1997). In mice, baseline corticosterone ranges from ~25nmol/l at nadir to ~600nmol/l, and 11-dehydrocorticosterone (11-DHC) from ~2.5 - 10nM, but levels vary between strains (Kotelevtsev *et al.*, 1997; Harris *et al.*, 2001; Yau *et al.*, 2007; Benedetti *et al.*, 2012; Gong *et al.*, 2015). Aldosterone circulates at a lower concentration than cortisol in humans; levels in human plasma are ~100 - 800 pmol/L (Fischbach and Dunning, 2009).

1.2 Glucocorticoid action

1.2.1 Receptor binding

Upon reaching target cells, glucocorticoids dissociate from their transport proteins and diffuse directly through the plasma membrane due to their lipophilic structure. They then bind to intracellular steroid hormone receptors in the cytoplasm, which form homodimers and are translocated to the nucleus where they bind DNA response elements and regulate transcription (Walker, 2007). Around ~2% of the human genome is regulated by glucocorticoids (Reddy *et al.*, 2009). Glucocorticoids bind to both the GR (type 2 corticosteroid receptor) and the MR (type I corticosteroid receptor). GR is ubiquitously expressed whilst MR is expressed in the kidney, colon, vasculature, hippocampus, heart, and adipose tissue (Walker, 2007). The GR binds cortisol with high affinity (K_D = ~20-25nM) compared with aldosterone (Hollenberg *et al.*, 1985; Mulatero *et al.*, 1997). The MR binds both glucocorticoids with relatively similar affinity (K_D = ~0.5-1.3nM) (Krozowski and Funder, 1983; Arriza *et al.*, 1987). As cortisol circulates at a 100-1000-fold higher levels than aldosterone, the MR is usually tonically occupied by cortisol in the absence of pre-receptor metabolism (Arriza *et al.*, 1987). Glucocorticoids may also exert some rapid non-genomic effects via cell surface receptors (Tasker *et al.*, 2006).

GR and MR are both ligand-activated transcription factors (Parker, 1993). Upon binding their ligands, receptors dissociate from their associated heat shock proteins and are translocated to the nucleus where they form homodimers. These homodimers bind to specific sequences of DNA in the promoter regions of target genes, termed glucocorticoid response elements (GREs). Receptor-ligand complexes are able to activate transcription (transactivation) or to repress transcription (transrepression) of target genes (McKenna and O'Malley, 2002; Walker, 2007). Some of the immunomodulatory effects of glucocorticoids are mediated via direct protein-protein binding of GR to other transcription factors, such as nuclear factor kappa-light-chain-enhancer of activated B cells (NF-κB) – this transrepression does not depend on GREs (Coutinho and Chapman, 2011).

1.2.2 Effects of glucocorticoids

Glucocorticoids are vital modulators of the physiological stress response and, as such, interact with most major organ systems, exerting a huge range of physiological effects that have been reviewed thoroughly elsewhere (Andrews and Walker, 1999; Sapolsky *et al.,* 2000; Walker, 2007; Coutinho and Chapman, 2011). Background of relevance to the present project can be categorised as effects on the cardiovascular system, the immune system and inflammatory response and metabolism.

1.2.2.1 **The cardiovascular system**

1.2.2.1.1 *Cardiac output*

Glucocorticoids prepare the body for stressful conditions, and their effects on the cardiovascular system reflect this. Glucocorticoids increase arterial pressure, heart rate and, consequently, cardiac output. They also induce dynamic changes in blood flow to favour skeletal muscle over the gastrointestinal and renal systems (Galosy *et al.*, 1981). The importance of glucocorticoids in regulating blood pressure can be seen in endocrine disorders; hypertension is a symptom of Cushing's syndrome whilst hypotension is evident in cases of adrenal insufficiency (Sapolsky *et al.*, 2000; Whitworth *et al.*, 2000; Goodwin and Geller, 2012). These effects are mediated predominantly by the permissive effect of glucocorticoids on sympathetic function, which include increased production of enzymes involved in adrenaline synthesis and reduced expression of enzymes involved in catecholamine breakdown at neuromuscular junctions (Dailey and Westfall, 1978; Kennedy and Ziegler, 1991; Sapolsky *et al.*, 2000).

1.2.2.1.2 *Vessel tone*

Both GR and MR are expressed in cardiovascular tissues, including in cardiomyocytes of the myocardium (Lombès *et al.*, 1992; Fraccarollo *et al.*, 2011; Lother *et al.*, 2011; Rog-Zielinska *et al.*, 2013, 2015) and the arterial wall (Hadoke *et al.*, 2006; Walker, 2007). GR and MR have been detected in the medial layer of mouse vessels (Christy *et al.*, 2003) and rabbit (Kornel *et al.*, 1982; Lombès *et al.*, 1992). MR has been detected in cultured rat smooth muscle cells and fibroblasts (Meyer and Nichols, 1981) and glucocorticoid and mineralocorticoid binding demonstrated in human smooth

muscle cells (Scott *et al.*, 1987) and endothelium (Inoue *et al.*, 1999; Oberleithner *et al.*, 2003). By acting at the GR, glucocorticoids increase smooth muscle responsiveness to noradrenaline (Sudhir *et al.*, 1989). This is likely mediated by reduced prostaglandin synthesis (Handa *et al.*, 1984). As GR activation has been shown to prevent the release of prostaglandins from rabbit endothelial cells (Rosenbaum *et al.*, 1986), this may indicate a paracrine mechanism between the layers of the vessel wall. Glucocorticoids also bind GR to inhibit acetylcholine-induced vasodilation of the endothelium via reduced nitric oxide (NO) synthesis (Mangos *et al.*, 2000). GR activation also contributes to hypertension by increasing expression of angiotensin type II receptors in rat vascular smooth muscle cells (VSMCs) (Sato *et al.*, 1994; Provencher *et al.*, 1995) but paradoxically has also been shown to downregulate levels of the powerful vasoconstrictor endothelin-1 (Provencher *et al.*, 1995). This latter effect may be associated with the regulation of vascular inflammation rather than vessel tone. The matter is complicated by action of glucocorticoids at the MR, which are sometimes paradoxical (Adler and Williams, 2007) – MR activation in the endothelium can enhance arterial vasodilatation via endothelial NO synthesis (Liu *et al.*, 2003; Uhrenholt *et al.*, 2003) but in the smooth muscle, MR activation causes vasoconstriction (Arima *et al.*, 2004). In healthy vessels, these two opposing actions likely balance one another, but in vessels in which the endothelium is damaged, the vasodilatory effects at the endothelium may be lost (Adler and Williams, 2007).

1.2.2.1.3 *Inflammation and fibrosis in vascular tissues*

MR activation causes perivascular and cardiac inflammation with associated fibrosis (Funder, 2005; Joffe and Adler, 2005). MR antagonists, such as spironolactone or the more selective eplerenone, are used clinically to treat congestive heart failure and left ventricular hypertrophy (LVH) (Pitt *et al.*, 1999; Soberman and Weber, 2000). Whilst the detrimental effects of MR activation are mediated by aldosterone (particularly in combination with high-salt diet), tonic occupancy of the MR is predominantly by cortisol.

Both long-term treatment with exogenous glucocorticoids and chronic over-production of endogenous glucocorticoids (as present in Cushing's syndrome) are

associated with an increased risk of atheromatous disease (reviewed by Walker, 2007). Glucocorticoids influence a variety of factors likely to influence this process.

1.2.2.1.4 *Angiogenesis*

Angiogenesis, the growth of new vessels from the existing vasculature, is potently inhibited by glucocorticoids. Folkman *et al.* (1983) were the first to describe the angiostatic effects of glucocorticoids, discovered during their studies of tumour angiogenesis. Steroids were shown to inhibit vessel growth in the presence of heparin leading to the conclusion that steroids may interact with endogenous heparins to tonically inhibit new vessel growth (Folkman and Ingber, 1987). In separate studies, glucocorticoids were shown to inhibit VSMC proliferation, possibly via decreased sensitivity to mitogenic stimulation (Longenecker *et al.*, 1982, 1984). The mechanism of angiostasis was not determined, but during this initial period of interest the mechanism was proposed to involve disruption of the capillary basement membrane, possibly related to reduced collagen deposition (Maragoudakis *et al.*, 1989).

These early studies used supraphysiological concentrations of glucocorticoids. More recently, physiological glucocorticoid concentrations have been shown to inhibit angiogenesis both *in vitro* and *in vivo* (Small *et al.*, 2005). Importantly, these effects were shown to be mediated via the GR, as the GR antagonist RU38486 abolished the angiostatic effects of glucocorticoids whereas spironolactone had no effect. The mechanism involved remains unclear. Corticosteroids decrease expression of vascular endothelial growth factor (VEGF) in cultured human VSMCs (Nauck *et al.*, 1998) and in human proximal renal tubular epithelial cells (Leonard *et al.*, 2005). Glucocorticoids alter cytoskeletal arrangement in endothelial cells (Logie *et al.*, 2010) and increase expression of the angiostatic protein thrombospondin-1 (Rae *et al.*, 2009; Logie *et al.*, 2010). Importantly, when TSP-1 was blocked using siRNA, cortisol no longer caused angiostasis *in vitro* (Rae *et al.*, 2009). Yano *et al.* (2006) also demonstrated the angiostatic (and consequently anti-tumour) effects of glucocorticoids in a murine model of prostate cancer.

1.2.2.2 **The immune system and inflammatory response**

1.2.2.2.1 *Therapeutic use*

Glucocorticoids are used therapeutically to suppress the immune system before organ transplantation and to treat a range of inflammatory and auto-immune conditions, such as rheumatoid arthritis, psoriasis and asthma (Maxwell *et al.*, 1994). In the clinic, therapeutic glucocorticoids are usually synthetic derivatives of the endogenous glucocorticoids, structural alterations of which confer variable characteristics in terms of receptor binding and metabolism by the 11β-HSDs (Diederich *et al.*, 2004). For example, dexamethasone and prednisolone are commonly used synthetic glucocorticoids which are relatively selective and potent GR agonists. Dexamethasone and prednisolone are metabolised by 11β-HSD2 but crucially 11-dehydroDex retains potency at the GR (Best *et al.*, 1997; Diederich *et al.*, 2004).

Glucocorticoids exert their anti-inflammatory and immunosuppressive effects on most cells of the immune system by downregulation of a huge range of pro-inflammatory chemokines and cytokines, including many interleukins (IL), interferon gamma (IFN-γ) and tumour necrosis factor alpha (TNF-α), as well as mediators of inflammation such as histamine and adhesion molecules. They reduce T cell activation and proliferation and promote the pro-inflammatory Th1 response while suppressing the anti-inflammatory Th2 response. They also alter the balance of leukocyte survival and apoptosis, and prevent leukocyte infiltration into sites of inflammation (Sapolsky *et al.*, 2000; Coutinho and Chapman, 2011). These actions are mediated by binding at the GR (Cronstein *et al.*, 1992). The importance of glucocorticoids in constraining the immune and inflammatory responses is evident in mice administered endotoxin; adrenalectomised mice do not survive doses of endotoxin that control mice can withstand, and dexamethasone pre-administration completely prevents lethality (Bertini *et al.*, 1988).

1.2.2.2.2 *Pro-inflammatory actions of glucocorticoids*

Whilst high dose clinically-administered glucocorticoids exert anti-inflammatory and immunosuppressive effects, physiologically they can exert immunostimulatory effects. Sapolsky *et al.* (2000) described the effects of glucocorticoids on the stress

response in terms of four criteria: permissive; suppressive, preparative and stimulatory. Glucocorticoids have been reported to have permissive inflammatory effects by elevating TNF-α and IL-6 concentrations in plasma after lipopolysaccharide (LPS) administration (Barber *et al.*, 1993); these cytokines promote the growth and activation of T-cells (Kuhweide *et al.*, 1990). Likewise, Wiegers *et al.* (1993, 1994, 1995) showed that physiologically-relevant concentrations of corticosterone (500-1000nM) directly enhanced T-cell growth *in vitro* (Wiegers *et al.*, 1993, 1994, 1995) and *in vivo* (Wiegers *et al.*, 1993) in rat tissues.

The explanation Wiegers *et al.* (1993) offer for this differential effect between pharmacological and physiological glucocorticoids is that low concentrations of glucocorticoids enhance the T-cell response via T-cell MR activation, while high concentrations of glucocorticoids may inhibit this response via T-cell GR activation. In further support of this theory, MR blockade in obese mice reduced the expression of pro-inflammatory mediators such as TNF-α and MCP-1 (Guo *et al.*, 2008). Sapolsky *et al.* (2000) highlight the importance of re-interpreting previous studies that made use of synthetic glucocorticoids with a low affinity for MR, and studies that made use of the GR antagonist RU38486, in light of this theory. Increased immune cell responses after GR blockade could result from preferential activation of MR rather than removal of the suppressive GR-mediated effects (Sapolsky *et al.*, 2000).

Whilst MR-mediated effects may explain enhanced T-cell activation by glucocorticoids, they cannot explain some of the observed pro-inflammatory actions of glucocorticoids. Low concentrations of corticosterone (100 pM) administered to rat macrophages stimulated them to produce pro-inflammatory cytokines, chemokines and NO, an effect that was not attributable to activation of the MR as lentiviral inactivation of the MR had no effect (Lim *et al.*, 2007). Thus both GR and MR may play a role in mediating the pro-inflammatory effects of glucocorticoids, particularly in macrophage populations which express both receptors (Liu *et al.*, 1999; Barish *et al.*, 2005). Of note, the same study found high concentrations of glucocorticoids (1 μM) potently inhibited this inflammatory activation (Lim *et al.*, 2007), again demonstrating the importance of glucocorticoid concentration when considering effects.

1.2.2.3 **Metabolism**

Though focus has thus far centred on their role in inflammation, the name glucocorticoid is derived from the key role that glucocorticoids play in glucose homeostasis. Glucocorticoids in most respects oppose the action of insulin by mobilising energy stores for use in combating a stressor. Glucocorticoids rapidly elevate blood glucose through a combination of mechanisms: they stimulate hepatic gluconeogenesis and glycogenolysis by elevating glucagon levels, and promote insulin resistance to redirect glucose from storage sites to active muscle (Sapolsky *et al.*, 2000). These effects last for longer than the acute metabolic effects elicited by adrenaline. Longer-term elevation of glucocorticoid levels also stimulates lipolysis and proteolysis to mobilise fatty acids and amino acids as alternative energy sources (Peckett *et al.*, 2011; Wang *et al.*, 2016).

The maladaptive effects of chronic glucocorticoid excess on metabolism are apparent in Cushing's syndrome, which is characterised by central obesity, dyslipidaemia, muscle wasting, hyperglycaemia and insulin resistance (Walker, 2007). While short-term glucocorticoid action mobilises energy stores and opposes insulin, chronic elevation of glucocorticoids causes increased insulin secretion and can lead to redistribution of fat from subcutaneous to intraabdominal depots associated with increased risk of adverse cardiometabolic consequences (Dallman *et al.*, 2004). The preferential storage in these depots may be due to the higher levels of GR expression in omental compared to subcutaneous adipocytes (Veilleux *et al.*, 2010).

Glucocorticoids thus influence and regulate a wealth of integral physiological processes across the body. Manipulating glucocorticoid action could be of benefit to myriad metabolic, cardiovascular, cognitive and systemic inflammatory disorders. The tissue-specific regulation of glucocorticoids by 11β-HSD1 and 2 offers a novel therapeutic opportunity to regulate the levels of glucocorticoids reaching target tissues.

1.3 The 11β-hydroxysteroid dehydrogenases

1.3.1 Function

Glucocorticoids are systemically governed by the HPA axis and plasma protein binding. On a local level, they are subject to pre-receptor regulation by the 11β-HSD isozymes, allowing for tissue-specific differences in glucocorticoid activity. 11ß-HSD1 is a dihydronicotinamide adenine dinucleotide phosphate (NADP(H))-dependent bidirectional oxidoreductase which acts predominantly as a reductase *in vivo* (Cai *et al.*, 2001; Seckl and Walker, 2001; Dover *et al.*, 2007), though *in vivo* dehydrogenase activity has been reported (Morris *et al.*, 2003). It is highly expressed in glucocorticoid target tissues such as liver, brain, adipose and vascular tissues, where it amplifies local glucocorticoid concentrations to increase binding at the GR (Seckl and Walker, 2001).

11βHSD-2 functions uniformly as a nicotinamide adenine dinucleotide phosphate (NADP+)-dependent dehydrogenase, converting cortisol (and corticosterone in rodents) to inactive 11-keto metabolites (Stewart and Krozowski, 1999). It acts primarily to allow selective access of aldosterone to the MR, but also has a protective role in the placenta (Edwards *et al.*, 1993). Loss of 11β-HSD2 function (as seen in the syndrome of apparent mineralocorticoid excess; SAME) mimics the effects of excessive aldosterone on cardiovascular tissues (Funder, 2005). The respective activity of the isozymes is shown in **Figure 1.2**.

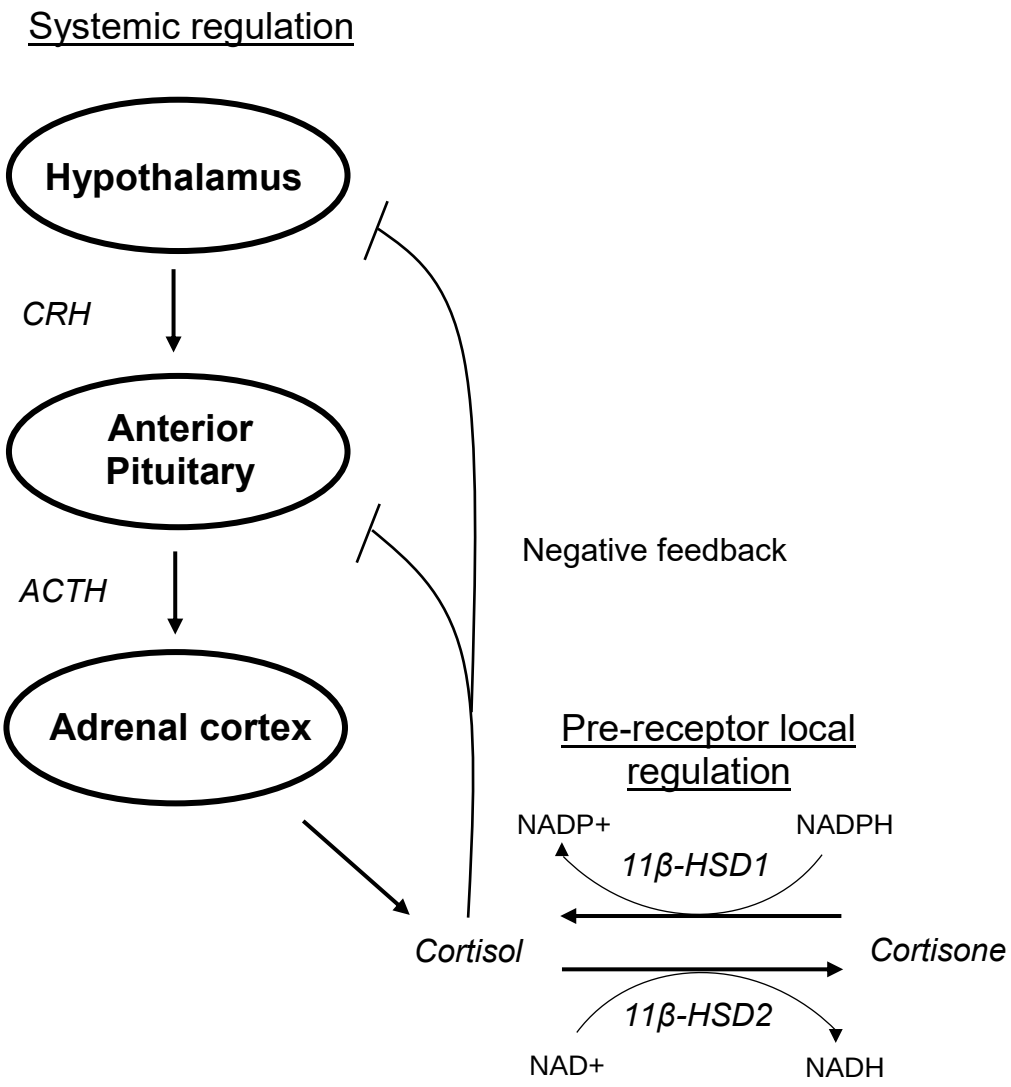

Figure 1.2 – Systemic and local glucocorticoid regulation. The Hypothalamic-Pituitary-Adrenal (HPA) axis maintains systemic glucocorticoids within tight parameters under normal healthy conditions through the regulated release of CRH and ACTH. The isozymes 11β-hydroxysteroid dehydrogenase (11β-HSD) 1 and 2 control pre-receptor metabolism of local glucocorticoids in specific tissues. 11β-HSD1 acts predominantly as a reductase *in vivo*, converting cortisone to cortisol, using NADPH as a co-factor. 11β-HSD2 catalyses the reverse reaction, acting as a dehydrogenase *in vivo* to inactivate cortisol to cortisone, using NAD+ as a co-factor.

1.3.2 Structure

Both 11β-HSD1 and 2 are microsomal isozymes of the short chain alcohol dehydrogenase superfamily (Stewart and Krozowski, 1999). 11β-HSD1 (in human and mouse) is a 292 amino acid protein with a molecular mass of 34kDa (Chapman *et al.*, 2013b). The type I isozyme is encoded by the *Hsd11b1* gene located on chromosome 1 and is highly conserved between species (Zhou *et al.*, 2012). The enzyme is comprised of a cofactor binding site, a substrate binding site facing the luminal space (Odermatt & Klusonova, 2015), and a highly hydrophobic N-terminal domain that anchors the enzyme to the membrane of the smooth ER where it is located. It has an affinity of ~ 2μM for cortisol (Zhou *et al.*, 2012) and a huge range of reported affinities for cortisone (K_m: ~150nM - 20μM, Chapman *et al.*, 2013b).

1.3.3 Discovery of the 11β-HSD isozymes

Extra-adrenal interconversion of cortisone and cortisol was first demonstrated over 60 years ago (Amelung *et al.* 1953). Over three decades later, the first evidence of 11β-HSD emerged, though at this time there was thought to be only one enzyme (Lakshmi & Monder, 1988). Two groups published simultaneously on the role of 11β-HSD in SAME, sufferers of which exhibit sodium retention, hypokalaemia and hypertension without an associated elevation in circulating aldosterone. This syndrome could be explained by congenital deficiency of 11β-HSD (or its inhibition by the liquorice derivative glycyrrhetinic acid) allowing inappropriate access of glucocorticoids to the MR (Edwards *et al.*, 1988; Funder *et al.*, 1988). Stewart *et al.* (1988) described the first adult case of 11β-HSD insufficiency, in which the patient presented with hypertension, hypokalaemia and suppressed renin-angiotensin-aldosterone system (RAAS) activity due to excessive MR activation by cortisol in the kidney and likely also in the blood vessel wall. This syndrome could be treated using dexamethasone, which selectively activated the GR and suppressed the HPA axis. A second interesting case study (Conn *et al.*, 1968) describes a patient presenting with these same symptoms. It was deduced that excessive liquorice consumption (2-3 36 g bars per day for 7 years) was responsible, as its removal from the patient's diet led to recovery. At the time, this was considered to be due to direct mineralocorticoid action by liquorice-derived compounds, but glycyrrhetinic acid has since been confirmed to be a liquorice

derivative that potently inhibits 11β-HSD activity (Stewart *et al.*, 1987). Subsequent purification and cloning revealed the distinct expression sites and substrate affinities of the type I and type II isozymes (Monder & Lakshmi 1989; Stewart *et al.* 1991; Albiston *et al.* 1994).

1.3.4 Activity

Whilst 11β-HSD2 is unidirectional in its dehydrogenase activity (Brown *et al.*, 1996), there has been some debate over the predominant activity of 11β-HSD1 (Seckl & Walker 2001; Morris *et al.*, 2003), with varying results seen between studies. Early studies examining 11β-HSD1 purified from rat liver showed bidirectional activity; however, the enzyme showed predominant reductase activity across a number of intact cell lines, including hepatocytes (Jamieson *et al.*, 1995), adipocytes (Bujalska *et al.*, 1997), VSMCs (Brem *et al.*, 1995) and skin fibroblasts (Hammami & Siiteri, 1991).

Some cell lines, such as Leydig cells (Phillips *et al.* 1989; Leckie *et al.* 1998), have generated contrasting results, though developmental stage of these cells may cause a switch in activity (Ge *et al.*, 1997). Culture conditions and metabolic conditions may also influence activity (Zhou *et al.*, 2012), making it difficult to interpret some contradictory evidence.

Critically, the same cells showing predominant reductase activity in culture often displayed bidirectional activity when homogenised (Brem *et al.*, 1995; Jamieson *et al.*, 1995), suggesting that 11β-HSD1 only exhibits bidirectional activity when released from the intracellular compartment. 11β-HSD1 is located within the SER luminal compartment in close proximity with another enzyme - hexose-6-phosphate dehydrogenase (H6PDH). H6PDH interacts with its substrate glucose-6-phosphate (G6P) and generates a large pool of NADPH. The abundance of NADPH then drives the reductase activity of 11β-HSD1 activity in intact cells (Lavery *et al.*, 2006; Walker *et al.*, 2007; Atanasov *et al.*, 2008; Zhang *et al.*, 2009), resolving the differential activity between intact and disrupted tissues.

Evidence of high cortisol-to-cortisone ratio in the hepatic circulation in humans also suggests predominance of reductase activity *in vivo* (Walker *et al.*, 1992). The generation of 11β-HSD1 knockout (KO) mice at the University of Edinburgh

demonstrated that 11β-HSD1 is the sole enzyme capable of reducing 11-keto metabolites to their active counterparts (Kotelevtsev *et al.*, 1997). The enzyme has several other substrates, including bile acids and xenobiotics. It is not within the scope of this introduction to cover these but they have been reviewed in detail elsewhere (Zhou *et al.*, 2012; Chapman *et al.*, 2013b).

1.3.5 Regulation

Several factors regulate 11β-HSD1 expression. Sexual dimorphism of hepatic enzyme expression is apparent in rats, with male animals expressing more 11β-HSD1 due to a pulsatile release in pituitary growth hormones as opposed to the continuous release in females (Low *et al.*, 1994). Note that this is not the case in mice (Rajan *et al.*, 1995); thus there are both inter-species and inter-gender differences in 11β-HSD1 expression. Glucocorticoids themselves increase expression of the enzyme in many cultured cell types, including: adipocytes (Engeli *et al.*, 2004), fibroblasts (Hammami and Siiteri, 1991), hepatocytes (Jamieson *et al.*, 1995) and neuronal cells (Rajan *et al.*, 1996). In intact tissues this only remains true for some tissue types (adipose for example) (Balachandran *et al.*, 2008) whilst in tissues such as liver, enzyme expression is reduced by exposure to glucocorticoids (Smith *et al.*, 1982).

Pro-inflammatory stimuli such as TNF-α and IL-1 stimulate increased 11β-HSD1 expression across a range of cell types *in vitro,* including stromal mesenchymal cells (Ahasan *et al.*, 2012) and keratinocytes (Itoi *et al.*, 2013). Furthermore, transgenic mice expressing TNF-α show increased hepatic 11β-HSD1, suggesting that inflammation may promote enzyme expression *in vivo* (Ignatova *et al.*, 2009). Co-administration of pro-inflammatory cytokines with glucocorticoids appears to augment this effect (Sun and Myatt, 2003; Ahasan *et al.*, 2012). There is evidence to suggest this may not hold true in the murine vasculature, as Dover *et al.* (2007) did not see increased 11β-HSD1 expression or activity *ex vivo* or *in vivo* after introducing an inflammatory stimulus. Importantly, pro-inflammatory stimuli do not necessarily increase enzymatic expression in immune cells (Freeman *et al.*, 2005).

1.3.6 Key sites of expression

11β-HSD1 expression is typically high in glucocorticoid target tissues, and enzyme expression is associated with GR expression in many tissues (Whorwood *et al.*, 1992). Distribution of 11β-HSD1 is generally similar in mice and humans, with the exception of the testis (Tannin *et al.*, 1991; Rajan *et al.*, 1995). mRNA expression is highest in liver, with activity also high in adipose tissue (Bujalska *et al.*, 1997), vasculature and heart (Walker *et al.*, 1991; Dover *et al.*, 2007), ovary (Benediktsson *et al.*, 1992), brain (Lakshmi *et al.*, 1991), uterus and placenta (Burton *et al.*, 1998; Waddell *et al.*, 1998), skeletal muscle (Whorwood *et al.*, 2002), as well as immune and inflammatory cells (Thieringer *et al.*, 2001; Gilmour *et al.*, 2006) and fibroblasts (Lee *et al.*, 2013; Tiganescu *et al*., 2013; Terao *et al.*, 2014).

1.3.6.1 11β-HSDs in the vasculature

Early suggestions of a role for 11β-HSD in the vasculature arose from studies using glycyrrhetinic acid to inhibit the enzyme in the skin; this potentiated the vasoconstrictor response to cortisol suggesting enhanced activation of the GR in smooth muscle (Teelucksingh *et al.*, 1990). 11β-HSD1 expression was later confirmed in rat vascular smooth muscle, with higher expression in smaller resistance vessels than in aorta (Walker *et al.* 1991). 11β-HSD2 has also been detected in human VSMCs (Smith *et al.*, 1996) and both isozymes have been reported in rat endothelial cells (Brem *et al.*, 1998). Hadoke *et al.* (2001), using 11β-HSD1 and 11β-HSD2 KO mice, found that 11β-HSD2 KO reduced the release of endothelium-derived-NO, inhibiting vasorelaxation. This suggests that 11β-HSD2 is the predominant isoform in the endothelium. This effect was reversible with the addition of L-arginine (Christy *et al.*, 2003). Christy *et al.* (2003) confirmed that 11β-HSD1 expression co-localised with α-smooth muscle actin (α-SMA) while 11β-HSD2 expression co-localised with angiopoietin receptor 2 (TIE-2) expression, further suggesting this differential distribution in the vessel wall. The same study also suggested that the effects of 11β-HSD2 deletion on vasomotor function may be mediated, at least in part, by renal enzyme loss. 11β-HSD2 was also the only isozyme detected in endometrial endothelial cells (Rae *et al.*, 2009).

1.3.6.2 **11β-HSDs in immune and inflammatory cells**

Given the powerful immunomodulatory effect of glucocorticoids, the expression of the 11β-HSDs in immune and inflammatory cell types has been studied extensively. 11β-HSD1 is not expressed in human monocytes until their differentiation into macrophages; enzyme expression is increased 10-fold by exposure to pro-inflammatory cytokines (IL-4/IL-13), and induction is inhibited by IFN-γ, a functional antagonist of ILs (Thieringer *et al.*, 2001). 11β-HSD2 is undetectable, or present at very low levels, in macrophages and monocytes (Gilmour *et al.*, 2006; Chapman *et al.*, 2013b). Wild-type (WT) murine macrophages can convert 11-DHC to corticosterone, promoting phagocytosis of apoptotic neutrophils in WT mice. This effect is not seen in macrophages from 11β-HSD1 KO mice, demonstrating a functional role for 11β-HSD1 in the resolution of inflammation (Gilmour *et al.*, 2006). This finding suggests that 11β-HSD1 inhibition could impede the resolution of inflammation.

Activation of human macrophages, but not monocytes, with LPS polarises them to a 'classically activated' M1 phenotype and enhances 11β-HSD1 expression, whereas alternative activation (M2) has no effect on expression of this enzyme (Chapman *et al.*, 2013b). Furthermore, phagocytosis of apoptotic neutrophils reduces 11β-HSD1 expression in macrophages (Chapman *et al.*, 2009), suggesting that the enzyme plays a dynamic role in the inflammatory process. Dendritic cell differentiation induces 11β-HSD1 expression. Interestingly, this expression is maintained by signals associated with innate immune activation (TNF-α, LPS), but is markedly decreased by CD40, a surface marker associated with activated antigen presenting cells (Freeman *et al.*, 2005). 11β-HSD1 is also expressed both in neutrophils and in mast cells (Chapman *et al.*, 2013a; Coutinho *et al.*, 2016).

Murine lymphocytes show only low levels of 11β-HSD1 activity and no 11β-HSD2 activity, though 11β-HSD1 activity is increased in response to activation or polarisation to Th1 or Th2 states (Zhang *et al.*, 2005). Not only does this imply a physiological role for pre-receptor glucocorticoid regulation in the mounting of the immune response, it also offers a therapeutic opportunity to control aspects of lymphocyte function without perturbing the HPA axis.

1.4 Angiogenesis

1.4.1 Process

To appreciate the effects of 11β-HSD1 manipulation on angiogenesis, an understanding of blood vessel development is required. In the developing embryo, many endothelial progenitor cells assemble to form a simple network of capillaries, in a process termed vasculogenesis. The remodelling of the vasculature to form a complex network of mature vessels is called angiogenesis, though there is some mechanistic crossover between these two processes (Carmeliet, 2003). As vessels mature, they acquire mural cells, including pericytes and VSMCs, which provide structural integrity and stability. This process is called arteriogenesis. Angiogenesis is complex, and its regulation in adult life is governed by a balance of stimulatory and inhibitory factors (Carmeliet, 2005b), some of which act upon many cell types and several of which act specifically upon the vascular endothelium (Yancopoulos *et al.*, 2000).

Blood vessels are vital in providing oxygen and nutrients for healthy tissues, for providing a means by which immune cells can travel between sites, and for allowing the transport of waste metabolites for excretion (Carmeliet and Jain, 2011). Finding a means by which to promote angiogenesis after ischaemic events, while highly desirable clinically (Isner, 2002), has proven challenging due to the myriad factors involved in orchestrating the complex angiogenic process. Furthermore, aberrant angiogenesis forms part of the pathology of several diseases, including proliferative diabetic retinopathy, rheumatoid inflammatory conditions and tumour growth (Folkman, 1995). Efforts to prevent angiogenesis have seen more success, with several angiogenesis inhibitors now in use; yet these are still limited in their efficacy. This section will provide an overview of physiological angiogenesis (for thorough reviews see Carmeliet & Jain 2011; Potente *et al.* 2011). Tumour vessels are abnormal and tumour angiogenesis will be described in more detail in **Section 1.6.3.**

1.4.2 Vasculogenesis

Vasculogenesis describes the formation of the primitive vascular network in the developing embryo. The early vascular plexus originates from the mesoderm, based

on signalling by members of the fibroblast growth factor (FGF) family. Both haematopoietic and endothelial cell lineages share a common precursor – the haemangioblast - as evidenced by experiments showing that deletion of VEGF Receptor 2 (VEGFR2) disrupts both haematopoietic and angioblastic lineages (Shalaby *et al.*, 1997).

In the yolk sac, heamangioblasts form cell aggregates, the inner cells of which are haematopoietic in origin and the outer of which are angioblastic. VEGF signalling is pivotal in determining angioblast cell fate at this stage; deletion of a single copy of the VEGF gene results in embryonic lethality with associated aberrant vessel formation in the yolk sac (Carmeliet *et al.*, 1996; Ferrara *et al.*, 1996). Signalling via VEGF receptors 1 and 2 (encoded by the *Flt1* and *Kdr* genes, respectively) influences cell fate. VEGFR1 suppresses commitment to the haemangioblast lineage (Fong *et al.*, 1999), a limiting mechanism vital in the functional assembly of vessels during vasculogenesis, while VEGFR2 is critical for endothelial cell formation and migration (Shalaby *et al.*, 1997). VEGFR3 is expressed in embryonic vasculature, but later becomes largely confined to the lymphatic system with the notable exception of endothelial sprouting (Tammela *et al.*, 2008). VEGF signalling functions in combination with molecules determining the interaction between endothelial cells and the extracellular matrix (ECM) to guide the process of vasculogenesis (Carmeliet, 2000). Even at this early stage, genetically-determined molecular differences can influence long term endothelial cell fate (Swift and Weinstein, 2009); Ephrin signalling, for example, governs arterial/venous commitment (Gale and Yancopoulos, 1999). Once formed, angioblasts can migrate to form a new vascular plexus at a distant site (Risau, 1997).

The molecular processes of vasculogenesis were originally thought to be independent from angiogenic processes in adult life, but the consensus has now shifted (Carmeliet and Jain, 2011), such that now there is interest in ‘therapeutic vasculogenesis’ (reviewed extensively in Luttun *et al.* 2002). This concept is based on findings such as the secretion of potent pro-angiogenic factors by circulating endothelial progenitor cells derived from monocytes and macrophages (Rehman *et al.*, 2003). The

involvement of endothelial progenitor cells in tumour angiogenesis is now subject to debate (Patenaude *et al.*, 2010); discussed further in **Section 1.6.4.3**).

1.4.3 Angiogenesis

Vasculogenesis results in the formation of a homogenous vascular plexus, which undergoes sprouting and is remodelled extensively to form a functional and complex vascular bed – this is the process of angiogenesis (Potente *et al.*, 2011). Angiogenesis occurs most commonly as sprouting angiogenesis, during which an angiogenic stimulus causes new vessels to bud and branch off from existing vessels. Less commonly, networks can be formed via intussusception, which involves pillars of ECM splitting vessels. This process occurs under specific circumstances, such as lung development (Risau, 1997), but its relevance to typical adult angiogenesis is unclear (Carmeliet and Jain, 2011).

Endothelial cells in mature vessels are quiescent and experience relatively low cell turnover, maintained by the coordinated signalling of VEGFs (Lee *et al.*, 2007; Stockmann *et al.*, 2008; Tvorogov *et al.*, 2010) and FGFs (Murakami *et al.*, 2008), as well as Notch (Benedito *et al.*, 2009; Jakobsson *et al.*, 2010) and angiopoietin-1 (ANG-1) (Sato *et al.*, 1995; Suri *et al.*, 1996; Saharinen *et al.*, 2008). Several of these signals are released in a paracrine fashion by stabilising pericytes. In this quiescent state, endothelial cells form a tight monolayer secured with claudins and VE-cadherin, and share a basement membrane with their supporting mural cells (Eble and Niland, 2009).They are oxygen-sensitive, dynamically responding to signals from the hypoxia inducible factors (HIF) to regulate flow (Carmeliet and Jain, 2011).

Upon sensing an angiogenic stimulus (such as VEGF, FGFs, ANG-2, or chemokines), vessels undergo a process comprised of several distinct steps; basement membrane disintegration, endothelial cell migration, channel formation and vessel maturation and survival (**Figure 1.3**).

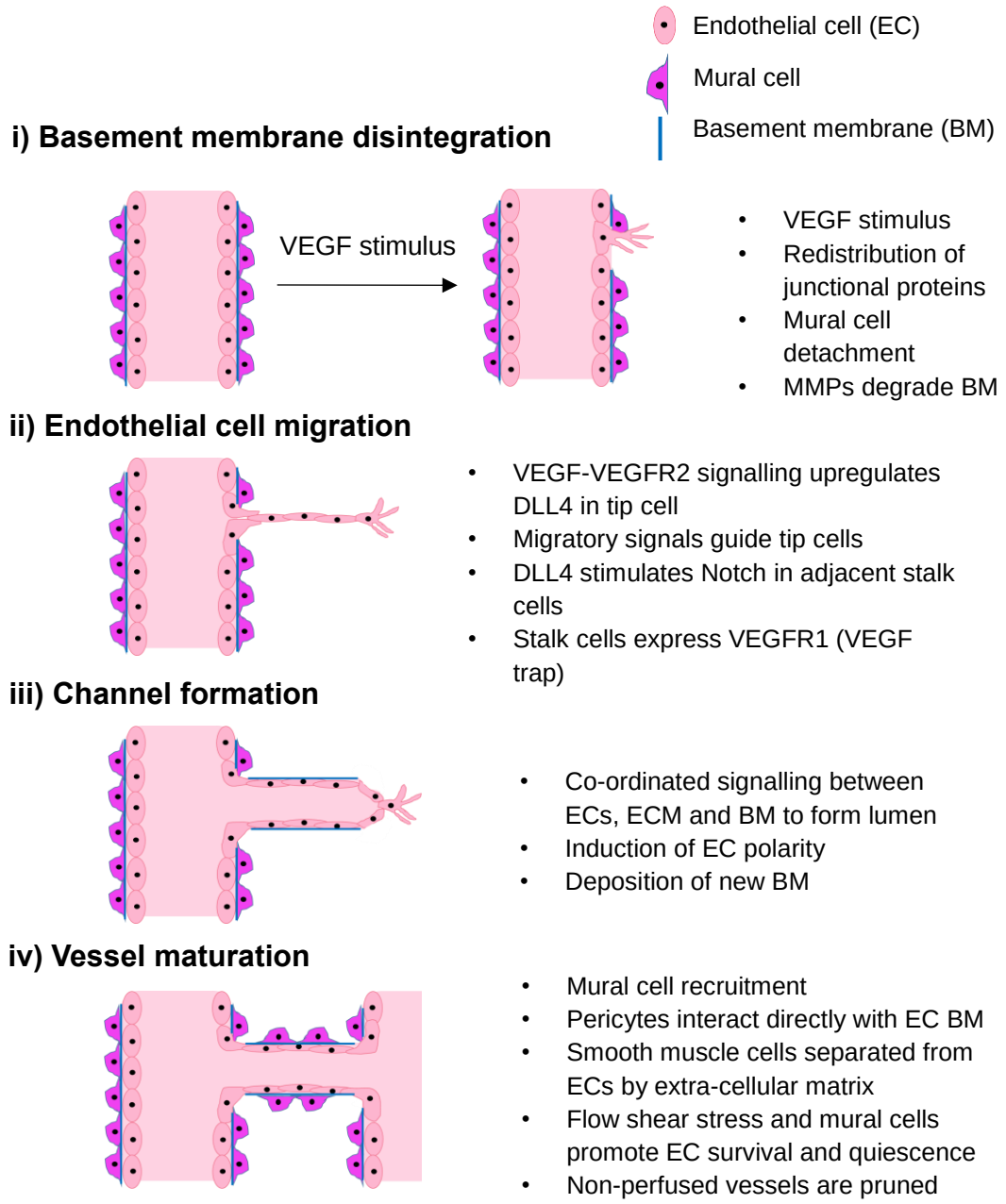

Figure 1.3 – Sprouting angiogenesis. Physiological angiogenesis can be divided into four major processes; i) Basement membrane (BM) disintegration, in which an angiogenic stimulus promotes the redistribution of cell junctions, the breakdown of the underlying BM, and the loss of mural cell coverage; ii) Endothelial cell (EC) migration, in which the coordinated signalling of VEGF and Notch/DLL4 confers tip and stalk cell identity; iii) channel formation, in which ECs communicate with the ECM to produce a lumen and new BM; and iv) vessel maturation, in which mural cells are recruited and cell become perfused, promoting EC survival and quiescence. Non-perfused vessels are pruned and regress. Adapted from Francavilla *et al.*, 2009.

1.4.3.1 Basement membrane disintegration

When a vessel receives an angiogenic signal, be it part of an inflammatory or hypoxic event, vasodilation occurs (mediated by NO) and vessels become hyper-permeable due to the redistribution of VE-cadherin and other junctional proteins. This allows plasma proteins to extravasate and deposit a provisional ECM (Carmeliet, 2000). Supporting pericytes detach from the vessel wall and break away from the basement membrane. ANG-2 stimulates this detachment (Augustin *et al.*, 2009), whilst matrix metalloproteases (MMPs) degrade the basement membrane (Carmeliet and Jain, 2011). This has the added benefit of liberating sequestered growth factors, such as VEGF and FGF (Arroyo and Iruela-Arispe, 2010). Targeting MMP2 and 9 has been seen to inhibit angiogenesis (Brooks *et al.*, 1998; Liu *et al.*, 2014). Evidence from the rat aortic ring assay also suggests that VEGF and ANG-1 stimulate the recruitment of innate immune cells from the adventitia of large vessels which contribute further pro-angiogenic cytokines (Aplin *et al.* 2006).

1.4.3.2 Endothelial cell migration

VEGF signalling at VEGFR2 causes endothelial cells to upregulate Delta like canonical notch ligand-4 (DLL4) expression. The endothelial cells that expresses the most DLL4 becomes the ‘tip cell’, which leads the migration of endothelial cells into the new ECM by extending numerous filopodia (Phng and Gerhardt, 2009). These extensions sense environmental cues like ephrins and semaphorins that guide their migration (Carmeliet and Jain, 2011). Tip cell identity is specified by Notch pathway signalling (Eilken and Adams, 2010), and endothelial cells dynamically compete for this role (Jakobsson *et al.*, 2010). High expression of DLL4 in the tip cell allows for activation of notch signalling in the adjacent endothelial cells, which suppresses tip cell behaviour and confers the identity of ‘stalk cell’. Disruption of Notch-DLL4 signalling results in excessive branching and filopodia (Thurston *et al.*, 2007). Stalk cells also express high levels of VEGFR1 which function as a VEGF trap and prevent further branching (Jakobsson *et al.*, 2010). Several other upstream pathways, such as Wnt/β-catenin, also feed into this process by regulating DLL4 expression (Corada *et al.*, 2010).

1.4.3.3 Channel formation

Stalk cells are able to form the vascular lumen required for perfusion, as well as producing junctional proteins with adjacent cells and depositing basement membrane to stabilise the new vessel (Phng and Gerhardt, 2009). The mechanism of lumen formation may depend on the vascular bed in question (Zeeb *et al.,* 2010; Potente *et al.*, 2011). Cadherins are required for lumen formation, evidenced by cadherin-deficient mice which die during embryogenesis due to impaired lumen formation (Carmeliet *et al.*, 1999). VE-cadherin is a key player in that it links endothelial cells to one another and also interacts with F-actin, a cytoskeletal fibre that is vital for forming the vessel lumen (Zeeb *et al.*, 2010). Endothelial cell polarity is also vital for lumen formation, as the apical surface must form the lumen whilst the basolateral surface interacts with the ECM and mural cells. This polarity is mediated by cell-cell and cell-ECM interactions, and may involve transport of intracellular vesicles. The process of lumen formation is reviewed extensively by Zeeb *et al.*, (2010).

1.4.3.4 Vessel maturation and survival

For a new vessel to become functionally mature, it must produce a basement membrane and inter-cell junctions, as well as recruiting mural cells to provide integrity and to maintain endothelial cell survival and quiescence (Potente *et al.*, 2011). Endothelial cells differentiate based on signals from the surrounding tissue and thus differ based on the vascular bed in question (Dyer and Patterson, 2010). Blood flow introduces mechanical shear stress, which is sensed by Kruppel-like factor 2 (KLF2), and enhances vessel maintenance via upregulation of nitric oxide synthase (NOS) and anticoagulation factors (Potente *et al.*, 2011). Nutrients and oxygen delivered by the blood also reduce VEGF signalling to encourage quiescence. Non-perfused vessels will regress (Carmeliet and Jain, 2011).

Two types of mural cell associate with vessels. Pericytes are supporting cells that interact directly with capillaries and immature vessels to provide the vessel with integrity and maintenance signals, and also interact with the surrounding ECM (Gaengel *et al.*, 2009). VSMCs are associated with mature arteries and veins and are separated from endothelial cells by ECM (Gaengel *et al.*, 2009). The phenotypic crossover between these two fibroblast-like cell types, and the lack of specific markers,

leaves the possibility for interconversion between the two open to debate (Adams and Alitalo, 2007). Transforming growth factor β (TGF-β) signalling enhances mural cell induction, migration and proliferation (Pardali *et al.*, 2010). Typically, the NG2 proteoglycan and α-SMA are used to demarcate these cells experimentally. A variety of integrated signals drive mural cell recruitment, but a key player is platelet-derived growth factor B (PDGF-B) which binds the PDGF receptor-B receptor on mural cells (Adams and Alitalo, 2007; Gaengel *et al.*, 2009).

Once recruited, mural cells produce signals that act on endothelial cells in a paracrine fashion. ANG-1 is released by mural cells and binds to the TIE2 receptor on endothelial cells, tightening endothelial junction to enhance vessel stability. These tight junctions allow vessels to effectively regulate vessel wall permeability and the extravasation of cells. Cadherins, occludins and members of the claudin family are all important in forming tight junctions (Cavallaro and Dejana, 2011). Recent evidence has shown that ANG-1 may play a more important role after injury, whilst in quiescent vessels it may be dispensable (Jeansson *et al.*, 2011). Ephrin-B2 and Notch signalling are also required for association of mural cells with endothelial cells, and deficiency of either causes vascular defects (Gridley, 2010; Pitulescu and Adams, 2010).

Once in a quiescent state, survival is a priority for endothelial cells. Autocrine release of VEGF reinforces endothelial cell survival (Warren and Iruela-Arispe, 2010). FGFs are also important in annealing adherens junctions, which link the cytoskeleton, between endothelial cells. Loss of FGF signalling subsequently results in vessel disintegration (Murakami *et al.*, 2008). The aforementioned TIE2/ANG-1 signalling, Notch pathway and mechanical shear stress are also key in maintaining survival and quiescence (Potente *et al.*, 2011).

1.4.4 Dynamic regulation of angiogenesis

Once a functional vascular bed is established, it remains under regulation by a variety of environmental stimuli. HIFs regulate perfusion of vessels by stabilising VEGF mRNA and enhancing VEGF signalling during hypoxia (Ema *et al.*, 1997; Iyer *et al.*, 1998). In normoxic conditions, oxygen-sensing prolyl hydroxylase domain proteins on endothelial cells label HIFs for degradation, but in hypoxia this does not occur,

allowing them to dynamically regulate endothelial cells shape in low oxygen conditions (Majmundar *et al.,* 2010).

Metabolic stimuli can also regulate angiogenesis, and endothelial cell metabolism is currently a subject of considerable interest (Vandekeere *et al.,* 2015). The observation that inhibiting mitochondrial respiration does not prevent angiogenesis challenged the notion that endothelial cells favour oxidative metabolism. Rather, upon stimulation by VEGF, endothelial cells increase the expression of the glycolytic activator phosphofructokinase-2/fructose-2,6-bisphosphatase 3. 85% of glucose metabolism in active endothelial cells is via glycolysis (De Bock *et al.*, 2013). Blockade of this enzyme can also suppress pathological angiogenesis in ocular and inflammatory models (Schoors *et al.*, 2014). This offers endothelial cells several advantages; it allows endothelial cells to vascularise anoxic tissues, which would otherwise be impossible with oxidative phosphorylation; it allows cells to quickly produce a larger yield of adenosine triphosphate (ATP) (per unit time glycolysis allows for increased ATP production, despite reduced glucose efficiency); and it also produces by-products suitable for increasing vessel biomass (Eelen *et al.*, 2015; Vandekeere *et al.*, 2015). Inhibition of 6-phosphofructo-1-kinase, a rate limiting enzyme of glycolysis, also suppressed tumour glycolysis and growth (Clem *et al.*, 2008). Ongoing research is also likely to provide further insight into the importance of fatty acid oxidation in regulating angiogenesis (Schoors *et al.*, 2015).

1.4.5 Arteriogenesis

Once a functional network is in place, some vessels undergo arteriogenesis. This involves further muscularisation of the vessel by migration and growth of recruited VSMCs. Flow is of great importance, as evidenced by the earlier muscularisation of coronary arteries proximal to the aorta as compared to veins (Jain, 2003). Pathological arteriogenesis can also occur, such as that seen in the 20-fold enlargement of collateral arterioles after occlusion of a supply artery (Schaper, 2009). This pathological response, and much pathological angiogenesis, requires the involvement of the inflammatory system. Contralateral flow induces monocyte migration and results in the breakdown of the vessel wall by proteinases. This is followed by an upregulation of factors that induce regrowth of smooth muscle and subsequent vessel enlargement.

The response of resistance arteries to flow is determined by vimentin and linked to the ECM (Carmeliet, 2000).

1.4.6 Pathological angiogenesis

Developmental angiogenesis forms the mature vasculature network. In adult life, physiological angiogenesis is limited to discrete processes, such as the menstrual cycle, pregnancy, skeletal growth and wound healing (Chung and Ferrara, 2011). Pathological angiogenesis is associated with conditions including PDR and age-related macular degeneration, rheumatoid arthritis, psoriasis, and tumour growth (Carmeliet, 2003; Chung and Ferrara, 2011). In the case of pathological angiogenesis, reperfusion and restoration of adequate nutrients and oxygen does not resolve the angiogenic response, which can result in uncontrolled aberrant angiogenesis.

Whilst both developmental and adult angiogenesis involve a highly coordinated cascade of stimulatory and inhibitory angiogenic factors (Chung and Ferrara, 2011), there are also key differences. Angiogenesis in adults must also remodel vessels that are quiescent and tightly encapsulated by smooth muscle as opposed to loosely assembled and active as during development. Inflammation is also frequently involved in pathological angiogenesis; monocyte/macrophages, platelets, mast cells and leukocytes are attracted to sites of inflammation, where they produce a variety of pro-angiogenic factors (Möhle *et al.*, 1997; Coussens *et al.*, 1999; Schaper, 2009; Newman and Hughes, 2012). Pathological interaction with the tumour microenvironment is also of relevance is cancer; this is discussed further in **Section 1.6.4**.

1.4.6.1 Manipulating angiogenesis in pathology

In the context of ischaemic injury, wound healing and obesity, enhanced angiogenesis can facilitate recovery (Vernieri *et al.*, 2001; McSweeney *et al.*, 2010; Michailidou *et al.*, 2012; Tiganescu *et al.*, 2013; Gordon *et al.*, 2014), whilst anti-angiogenic therapies are required for the treatment of heavy menstrual bleeding, cancer and several diseases of the eye (Folkman *et al.*, 1983; Rae *et al.*, 2009). Attempts to manipulate angiogenesis therapeutically are challenging, due primarily to the immense complexity of the angiogenic response – targeting or promoting any single part of this process is unlikely to result in a solution (Koh *et al.*, 2010).

1.4.6.1.1 *Promoting angiogenesis*

Previous attempts to promote angiogenesis therapeutically (for the treatment of coronary and peripheral artery disease) have focussed on manipulation of the VEGF pathway; however pro-angiogenic VEGF-based therapies have seen limited success due to the poor quality and disorganised nature of the neovasculature that forms (Mac Gabhann *et al.*, 2010; Zachary and Morgan, 2011). More recent attempts to use therapeutic stem cell injection have shown more promise but are still in their infancy and remain controversial in terms of their mechanism of action (Hou *et al.*, 2016). Shifting focus onto targets other than VEGF ligands may also improve the prospects of pro-angiogenic therapy in the future (Mac Gabhann *et al.*, 2010).

To consider increased vessel density alone as an indicator of successful pro-angiogenic therapy is overly simplistic, as increased vessel quality (integrity, perfusion, mural cell coverage) is also vital for effective revascularisation (Falcón *et al.*, 2009). This is the principle behind the concept of vessel normalisation (Carmeliet and Jain, 2011; Goel *et al.*, 2012), which has gained momentum in recent years. An increase in vessel density is only of long-term benefit to an ischaemic tissue if this vasculature matures appropriately (Eelen *et al.*, 2013), and thus vessel normalisation involves stimulating those features of angiogenesis that promote mural cell recruitment and maturation of the vessel. This approach could potentially be effective in treating ocular conditions and, controversially, tumours; both are associated with an aberrant leaky vasculature which contributes to the pathology. In retinopathies, the tortuous, leaky nature of the vasculature leads to unresolved hypoxia and blindness, whilst in tumours it hampers the effectiveness of radiotherapy and drug delivery (Carmeliet and Jain, 2011). As mentioned above, targeting endothelial cell metabolism is currently the subject of much interest, after the observation that the majority of endothelial cell energy is generated by glycolysis (De Bock *et al.*, 2013), and that inhibiting this process can suppress tumour growth (Clem *et al.*, 2008).

1.4.6.1.2 *Inhibiting angiogenesis*

Anti-angiogenic therapies have seen more success than pro-angiogenic therapies. Judah Folkman was the pioneer of the modern clinical approach to targeting tumour angiogenesis (Folkman, 1972). Several anti-angiogenic drugs are already in use for

treating cancer and eye diseases. The first of these was Bevacizumab, a VEGF-specific antibody, which improved overall survival in lung, colorectal and breast cancer patients (Jain *et al.*, 2006). Several tyrosine kinase inhibitors that block VEGF receptor signalling in endothelial and cancer cells are also in use, and have shown improved survival in gastrointestinal stromal tumour, renal-cell-carcinoma and hepatocellular carcinoma patients (Ferrara, 2009). Unfortunately, anti-angiogenic therapies are still hampered by toxicity when delivered in combination with chemotherapy (Jain *et al.*, 2006) and are also ineffective in patients who are refractory or develop resistance (Carmeliet and Jain, 2011). Perhaps most worrying are reports of adaptation and increased cancer malignancy after inhibition/deletion of VEGF in pre-clinical models (Ebos *et al.*, 2009; Pàez-Ribes *et al.*, 2009). In pathologies other than cancer, Ranibizumab (an antibody that blocks the VEGF-A isoform) and pegaptanib (a VEGF aptamer) have both been approved (in 2006) for use in treating age-related macular degeneration (Ferrara, 2009; Carmeliet and Jain, 2011). Overall, while not entirely unsuccessful, anti-angiogenic therapies have, as yet, failed to meet expectations in the clinic (McIntyre and Harris, 2015).

1.5 11β-HSD1 inhibition and the vasculature

1.5.1 11β-HSD1 inhibitors

Clearly, manipulation of local glucocorticoid concentrations is a highly desirable clinical intervention in terms of enhancing glycaemic control, regulating local inflammation and treating cardiometabolic disorders generally. Inhibition of 11β-HSD1 offers a novel therapeutic avenue for reducing tissue glucocorticoid exposure without risking affecting the systemic stress response.

For centuries, Japanese herbal medicine made use of the liquorice plant extract, Glycyrrhizin, which is itself a potent 11β-HSD inhibitor and could explain some of the anti-tumour effects of such medicines (Motoo and Sawabu, 1994). In 1995, the non-selective 11β-HSD inhibitor carbenoxolone was shown to improve insulin sensitivity in man via reduced binding of hepatic GR (Walker *et al.*, 1995). Further beneficial effects have been shown on blood glucose (Alberts *et al.*, 2002; Alberts *et al.*, 2003) and lipid handling (Berthiaume *et al.*, 2007) using the 11β-HSD1 selective inhibitors

BVT.2733 and compound A, respectively. As well as these general cardiometabolic benefits, 11β-HSD1 inhibition using compound 544 also markedly reduced the progression of atherosclerosis (Hermanowski-Vosatka *et al.*, 2005).

A number of 11β-HSD1 inhibitors progressed to clinical trial (reviewed extensively by Anderson and Walker, 2013), but have shown only mild improvements in terms of glycaemic control, lipid handling, blood pressure and weight loss. More recently, 11β-HSD1 inhibitors are showing promise in the improvement of cognitive function (Sooy *et al.*, 2010, 2015; Yau *et al.*, 2015), with UE2343 (Xanamem) currently in Phase II clinical trials (Webster *et al.*, 2017). In this section, the preclinical data on 11β-HSD1 inhibition or deletion in the vasculature are introduced.

1.5.1.1 **Atherosclerosis**

11β-HSD1 inhibition reduces atherosclerotic plaque formation in mice (Hermanowski-Vosatka *et al.*, 2005; Nuotio-Antar *et al.*, 2007). Though several studies report reduced low-density lipoprotein and improved glycaemic control, different inhibitors show variability; the 11β-HSD1 inhibitor 2922 showed no effect on atheroma (Lloyd *et al.*, 2009).

Though 11β-HSD1 deletion confers an atheroprotective phenotype in mice (Morton *et al.*, 2001; Kipari *et al.*, 2013), evidence suggests that the enzyme may have a direct role in regulating vascular inflammation distinct from plasma lipid profile and blood pressure. 11β-HSD1 KO Apolipoprotein E-deficient ($11\beta HSD1^{-/-}/apoE^{-/-}$) mice showed a significant reduction in plaque size, necrotic core area and macrophage content compared to $apoE^{-/-}$ mice (Garcia *et al.*, 2013; Kipari *et al.*, 2013). Transplantation of $11\beta HSD1^{-/-}/apoE^{-/-}$ bone marrow into $apoE^{-/-}$ mice conferred these atheroprotective features onto recipients, demonstrating the importance of leukocyte-derived 11β-HSD1 in this process (Garcia *et al.*, 2013; Kipari *et al.*, 2013). Furthermore, extracted peritoneal macrophages from $11\beta HSD1^{-/-}/apoE^{-/-}$ mice had significantly reduced cholesterol content, although 11βHSD1 deletion did not affect inflammatory cell migration in this study (Garcia *et al.*, 2013).

Perhaps most interestingly, gene expression analysis revealed a decrease in toll-like receptor (TLR) signalling and an attenuation of the inflammatory state in $11\beta HSD1^{-/-}$

mice, with a reduction in the amount of pro-inflammatory cytokines (e.g. TNF-α, MCP-1) released by 11βHSD1$^{-/-}$ peritoneal macrophages in response to stimulation with oxidised low density lipoprotein (LDL) (Garcia *et al.*, 2013). Similar data have been reported elsewhere, including reduced monocyte chemoattractant protein 1 (MCP-1) and vascular cell adhesion molecule 1 (VCAM-1) expression, along with decreased T-cell infiltration into atherosclerotic plaques from 11βHSD1$^{-/-}$/apoE$^{-/-}$ mice (Luo *et al.*, 2012; Kipari *et al.*, 2013). The effects of glucocorticoids on MCP-1 appear to vary between inflammatory cell types and VSMCs, where in contrast, GR binding has been shown to decrease MCP-1 expression (Dhawan *et al.*, 2007). Overall, these findings strongly suggest that 11β-HSD1 influences inflammation in the vascular wall and that enzymatic inhibition may decrease inflammation in an atherosclerotic context.

1.5.1.2 Neointimal proliferation

Restenosis after coronary angioplasty is a clinical problem when treating occlusive vascular disease. It is caused by neointimal proliferation of VSMCs and, thus, glucocorticoids have been considered to be of potential benefit based on their anti-proliferative effects on VSMCs (Longenecker *et al.*, 1982, 1984; Berk *et al.*, 1988, 1991; Goncharova *et al.*, 2003). 11β-HSD1 inhibition in this context, therefore, could potentially be pathogenic.

Cai *et al.* (2001) found that pro-inflammatory cytokines (IL-1β or TNF-α) induced greater expression of 11β-HSD1 in VSMCs, supporting a potential role for the enzyme in regulating local inflammation; although this finding could not be replicated in intact aortic tissue or *in vivo* (Dover *et al.*, 2007). Iqbal *et al.* (2012) demonstrated that both glucocorticoid binding to GR, and MR antagonism can reduce neointimal proliferation. Importantly, they also found that 11β-HSD1 deletion reduced neointimal proliferation, with an associated reduction in macrophage infiltration and increased collagen content. This effect was seen only in double KO (11β-HSD1$^{-/-}$ apoE$^{-/-}$) mice with a hyperlipidaemic phenotype which promotes lesion formation, suggesting that this effect was due to systemic rather than local enzyme deletion. Overall, it is unlikely that 11β-HSD1 in the vascular wall affects neointimal proliferation.

1.5.1.3 Promotion of angiogenesis

Glucocorticoids are anti-angiogenic (Folkman *et al.,* 1983). This manifests clinically as poor wound healing associated with Cushing's disease (Gordon *et al.,* 1994) and increased risk of heart failure associated with chronic glucocorticoid therapy (Souverein *et al.,* 2004). Given these effects and the potential role for 11β-HSD1 in regulating vascular inflammation, 11β-HSD1 inhibition or deletion was hypothesised to enhance angiogenesis. Small *et al.* (2005) were the first to test this using physiological concentrations of glucocorticoids. *Ex vivo* aortic rings showed reduced vessel outgrowths after exposure to both 11-DHC and corticosterone, an effect that was blocked with GR antagonist RU38486 but not the MR antagonist spironolactone. Both carbenoxolone and 11β-HSD1 deletion protected aortic rings from the angiostatic effects of 11-DHC, suggesting that conversion of the inactive substrate results in angiostasis. *In vivo* subcutaneous sponges showed enhanced angiogenesis after mice were given RU38486 and reduced angiogenesis when sponges were impregnated with cortisone or cortisol. In 11β-HSD1 KO animals, cortisone did not inhibit sponge angiogenesis, and both RU38486 and 11β-HSD1 deletion increased angiogenesis in dermal wounds. These data support the *ex vivo* observations and suggest they are highly relevant *in vivo.* Of note, Terao *et al.* (2011) also reported enhanced wound healing after 11β-HSD1 inhibition; however, they attribute this effect to increased proliferation of keratinocytes rather than enhanced angiogenesis.

The most striking data concerning angiogenesis comes from studies using the induced myocardial infarction (MI) model in mice. Both GR antagonism (Small *et al.,* 2005) and 11β-HSD1 deletion increase myocardial revascularisation after coronary artery ligation resulting in improved recovery (Small *et al.,* 2005; McSweeney *et al.,* 2010; White *et al.,* 2015; Mylonas *et al.,* 2017). The same finding has been reproduced using the selective 11β-HSD1 inhibitor UE2316 delivered at the time of injury (McGregor *et al.,* 2014). Given the clinical burden of heart failure after MI, these results show promise for 11β-HSD1 inhibitors.

Inflammatory cells play a crucial role in angiogenesis. After myocardial injury, macrophages secrete pro-angiogenic TGF-β and VEGFA, and promote angiogenesis, myofibroblast infiltration and collagen deposition (van Amerongen *et al.,* 2007). 11β-

HSD1 KO mice showed increased recruitment of neutrophils (McSweeney *et al.*, 2010; Mylonas *et al.*, 2017) and macrophages to the healing infarct after coronary artery ligation, with an increase in MCP-1 and IL-8 mRNA and an increased number of 'alternatively activated' YM-1-positive macrophages, suggesting a pro-reparative phenotype (McSweeney *et al.*, 2010). Enhanced neutrophil recruitment was associated with reduced expression of C-X-C chemokine receptor 4 (CXCR4) in neutrophils in 11β-HSD1 KO mice, a cell surface receptor which enhances bone marrow retention of neutrophils (Mylonas *et al.*, 2017). After 28 days, vessels in the healing infarct had increased α-SMA coverage in 11β-HSD1 KO mice, suggesting maturity and stability.

The beneficial effect of 11β-HSD1 inhibition/deletion on recovery post-MI cannot be attributed to 11β-HSD1 expressed in vascular smooth muscle or cardiomyocytes, as mice with targeted deletion of the enzyme in these cell types did not recover faster than wild type control mice after myocardial injury (White *et al.*, 2015; Mylonas *et al.*, 2017). Experiments using bone marrow chimeric 11β-HSD1 KO mice confirmed the importance of the enzyme in host tissues rather than donor myeloid cell lineages (Mylonas *et al.*, 2017). Cardiac fibroblasts from the infarcted hearts 11β-HSD1 KO animals expressed more CXC-motif ligand (CXCL) 2 and CXCL5 than WT controls, and exposure of these cells in culture to corticosteroids reduced expression of CXCL2 and CXCL5 (Mylonas *et al.*, 2017). Thus, the mechanism for enhanced recovery after MI is likely to involve enhanced expression of chemoattractant proteins from cardiac fibroblasts as a result of reduced GR binding, resulting in enhanced neutrophil recruitment and polarisation of macrophages towards a pro-reparative phenotype.

Potentially the enhanced angiogenesis seen in the myocardium is a consequence of an altered inflammatory environment rather than a direct influence of 11β-HSD1 on vascular remodelling. Indeed, the 11β-HSD1 inhibitor compound A has been shown to reverse cardiac hypertrophy in a VEGF-based transgenic model intended to uncouple reversal of hypertrophy from neovascularisation (Gordon *et al.*, 2014). In these studies, 11β-HSD1 expression was increased in hypertrophied myocardium and its inhibition was proposed to alter cardiac muscle myofilament composition. Thus, there remains some debate surrounding cardiac mechanisms, and the importance of angiogenesis in this context is unclear.

11β-HSD1 KO mice with diet-induced obesity show increased angiogenesis, resulting in reduced hypoxia and reduced fibrosis in their adipose tissue (Michailidou *et al.*, 2012). HIF-1α signalling, Col1a1 mRNA, picrosirius red staining and α-SMA staining were all reduced in adipose tissue of 11β-HSD1 KO animals. *In vivo*, 11β-HSD1 KO adipose tissue showed a greater vessel-to-adipocyte ratio. *Ex vivo*, aortic rings showed a greater angiogenic response when exposed to 11β-HSD1 KO periaortic fat conditioned media (PACM) compared to WT PACM. In keeping with these findings, 11β-HSD1 KO adipose tissue also showed increased expression of pro-angiogenic mediators VEGF, apelin and angiopoietin-like protein 4 (ANGPTL4), expression of which was further increased by the addition of a peroxisome proliferator-activated receptor-γ (PPAR-γ) agonist (Michailidou *et al.*, 2012). Interestingly, 11β-HSD1 expression in mouse embryonic fibroblasts is decreased by HIF-1α (Lee *et al.*, 2013), and fibroblastic preadipocytes show enriched 11β-HSD1 expression in adipose tissue, suggesting once again that this enzyme may be of particular importance in fibroblasts.

It is important to note the distinction in proposed mechanism between MI (an acute ischaemic event) and obesity (a chronic inflammatory environment). Although enhanced angiogenesis is reported in both scenarios, reported data concerning inflammation are polarised. In the myocardium, enhanced neutrophil and macrophage recruitment are at the centre of the improved functional recovery. In adipose tissue from 11β-HSD1 KO animals, a decrease in inflammatory signalling (MCP-1 expression, T-cell infiltration and macrophage infiltration) has been reported (Wamil *et al.*, 2011), similar to that seen in atherosclerosis (Luo *et al.*, 2012). Itoi *et al.* (2013) observed enhanced IL-6 production after exposing keratinocytes to a low cortisol concentration (0.1 pM) but attenuated IL-6 levels when using a high cortisol concentration (10 μM). Thus the context of inflammation may be pivotal in predicting the response to 11β-HSD1 inhibition (this concept is reviewed more thoroughly in Chapman *et al.*, 2013a). An important similarity to note in both contexts is that of altered fibrosis and the potential importance of 11β-HSD1 in fibroblasts.

1.5.2 11β-HSD1 inhibition and pathological angiogenesis

Whilst angiogenesis can promote recovery and attenuate ischaemia, it can also contribute to the pathology of a disease. The involvement of local glucocorticoid

metabolism has been examined in three such contexts. Endometrium from women experiencing heavy menstrual bleeding was found to express higher levels of 11β-HSD2 and reduced levels of the anti-angiogenic factor thrombospondin-1 (TSP-1) (Rae *et al.*, 2009). The angiostatic effects of cortisol on endothelial tube-like structure formation were blocked with the addition of siRNA against TSP-1, presenting a possible mechanism – increased 11β-HSD2 in endometrial stromal cells reduces the amount of glucocorticoids accessing the GR in adjacent endothelial cells, causing them to secrete less TSP-1 and, thus, enhancing pathological angiogenesis. Note that the proposed mechanism here has a paracrine action, unlike the autocrine hypotheses suggested in the myocardium and adipose tissue.

Recently, 11β-HSD1 inhibition has been investigated in the context of the retina to assess its potential for worsening PDR. Surprisingly, the 11β-HSD1 inhibitor compound 544 reduced pathological neovascularisation in the retinas of neonatal mice exposed to hypoxic conditions, despite the absence of the enzyme from the retinal vasculature (Davidson *et al.*, 2017), possibly as a result of off-target effects. Critically, no differences were seen in retinal vasculature between 11β-HSD1 KO and WT mice, suggesting that 11β-HSD1 inhibitors are unlikely to exacerbate PDR.

Inflammatory arthritis is characterised by pathological angiogenesis as the expansion of the synovium increases the demand for nutrients and oxygen (Paleolog, 2002). Zhang *et al.* (2017) recently demonstrated that resolution of joint inflammation was impaired in mice with macrophage-specific deletion of 11β-HSD1 compared to WT littermates, to a similar degree as was previously seen in global 11β-HSD1 KO animals (Coutinho *et al.*, 2012). This was associated with a two-fold increase in VE-cadherin mRNA, suggesting a potentially altered vessel phenotype, although no changes were seen in VEGF mRNA (also the case in previous papers reporting increased angiogenesis, such as McSweeney *et al.* (2010)). The same mice showed an enhanced angiogenic response on subcutaneous insertion of a polyurethane sponge, suggesting that myeloid 11β-HSD1 plays an important role in the pro-angiogenic phenotype after enzyme inhibition.

Aberrant angiogenesis is also a hallmark of cancer (Hanahan and Weinberg, 2011) and its induction occurs during the transition from hyperplasia to neoplasia (Folkman *et*

al., 1989). Solid tumours, like healthy tissue, require a system of nutrient transfer to thrive. Above a few millimetres in size, this transfer must be in the form of vasculature as distances are too great for simple diffusion to suffice (Folkman, 1995). A concern is that 11β-HSD1 inhibition could enhance tumour angiogenesis, leading to increased tumour growth and metastasis. This concern has barely been addressed in the literature thus far. Liu *et al.* (2016) reported an anti-angiogenic and anti-tumour effect of 11β-HSD1 overexpression in murine hepatocellular carcinoma (HCC), both *in vitro* and *in vivo*. The same study also demonstrated reduced 11β-HSD1 expression in malignant tissue compared to non-neoplastic liver (a commonly reported phenomenon), and argued that loss of 11β-HSD1 in malignancy enhances glycolysis and subsequent tumour growth.

1.6 Cancer

1.6.1 Hallmarks of cancer

Cancer describes a collection of diseases characterised by uncontrolled cell proliferation and invasiveness. As one of the leading cause of death globally (after ischaemic heart disease and stroke), it is the focus of intense research to reduce the impact it has on wellbeing and the burden it places on health organisations. Cancers can affect almost any tissue in the body, but are considerably more common in highly proliferative tissues. Cancers with high mortality include lung, liver, colorectal, stomach and breast cancer, and progression to metastasis greatly decreases the chances of long-term survival after treatment (World Health Organisation, 2017).

In 2000, Hanahan and Weinberg (2000) published their seminal paper ‘Hallmarks of Cancer’ which defined the common features of malignancy. Those hallmarks are cancerous tissue’s ability to: sustain proliferative signalling; evade growth suppressors; activate invasion and metastasis; enable replicative immortality; resist cell death; and induce angiogenesis. In 2011, this paper was updated to reflect the progress made over the previous decade. Emerging hallmarks now also include the ability to deregulate cellular energetics and to avoid immune destruction (Hanahan and Weinberg, 2011). Targeting these hallmarks offers the best chance of curing cancer, though the picture is complicated immensely by the vast heterogeneity between cancer

types and subtypes, and by the resistance and adaptation many cancers show in response to therapy.

1.6.2 Tumour formation

Typically, cancerous tissues arise from healthy tissues through a series of genetic and environmental insults, resulting in loss-of-function mutations in tumour suppressor genes and gain-of-function mutations in oncogenes, driving a malignant phenotype (Weinberg *et al.*, 1999), with associated replicative immortality linked to telomerase expression (Blasco, 2005). This process has been likened to Darwinian evolution, in the sense that mutations conferring a survival advantage to cells are typically maintained and lead to clonal selection of a tumour cell population (Nowell, 1976; Hanahan and Weinberg, 2000). TP53, for example, is a prototypical tumour suppressor gene; it integrates signals relating to cell stress (oxygen and glucose availability, DNA damage, etc.) and can halt progression of the cell cycle if quality standards are not met (Hanahan and Weinberg, 2011).

Leukaemias (cancers of the blood), do not typically form solid tumours, whereas cancer in other tissues results in the formation of a primary tumour, comprised of tumour cells and an array of supporting mesenchymal, inflammatory and vascular cell types that form the tumour microenvironment. Interest in the tumour microenvironment has intensified in the last decade, and has provided new avenues for treatment that target more subtle components of the tumour (Hanahan and Coussens, 2012). In this section, the components of the tumour microenvironment, and their influence on tumour growth, will be introduced.

1.6.3 Tumour angiogenesis

During the very early stages of development, tumours can achieve nutrient and waste exchange via simple diffusion. As the tumour grows beyond 1-2 mm in size however, an ‘angiogenic switch’ (Hanahan and Folkman, 1996b) is required and the tumour must develop its own blood supply to maintain its growth and to successfully metastasise. A powerful driver for this process are the HIFs, which stimulate cells of the tumour to release VEGF (Dayan *et al.*, 2008). HIF can become upregulated in tumours as a result of mutations in tumour-suppressor genes or oncogenes (Chung and

Ferrara, 2011), leading to sustained high levels of VEGF and pathological angiogenesis. The resultant vasculature is tortuous, hyper-permeable and lacking in sufficient mural cell coverage, creating regions of hypoxia and necrosis which in turn stimulate further angiogenesis (Verdegem *et al.*, 2014). Unlike physiological angiogenesis, tumour angiogenesis is not self-limiting (Polverini and Leibovich, 1984).

Vessels in tumours are heterogenous, with six classifications of vessel types now in use; mother vessels; three types of daughter vessels; feeder arteries and draining veins (reviewed by Nagy *et al.*, (2010)). Whilst it is not within the scope of this introduction to describe each type individually, the vasculature overall is characterised by irregular vessel diameter, thin walls comprised of abnormally shaped endothelial cells with compromised basement membrane, and variable mural cell coverage. These features have been observed in a variety of preclinical models (Morikawa *et al.*, 2002; Baluk *et al.*, 2003; Ozawa *et al.*, 2005; Hagendoorn *et al.*, 2006) and in clinical samples (Less *et al.*, 1997). Another process unique to tumour angiogenesis is vascular mimicry, whereby tumour cells are able to adopt an endothelial-like phenotype and form functional channels, creating 'mosaic vessels' and further complicating the therapeutic targeting of tumour angiogenesis (Hess *et al.*, 2006; Lin *et al.*, 2007). This vascular mimicry has principally been observed in melanoma (Hendrix *et al.*, 2003).

Cells can often be identified by markers they express on their surface. Tumour endothelial cells express different markers from their 'normal' counterparts, presenting an opportunity for targeted therapies (reviewed by Ruoslahti, (2002)). As well as the tumour and tumour endothelial cells, an array of stromal cells also release proangiogenic factors to further stimulate the angiogenic process. These include immune inflammatory cells, fibroblasts and pericytes.

1.6.4 The tumour microenvironment

Tumour cells are characterised by their unconstrained replication and invasiveness, the result of acquired mutations. While autocrine growth signals within tumour cells are dysregulated, the paracrine effects of other cell types within the tumour also have a powerful influence upon tumour growth (Hanahan and Weinberg, 2011). These cell

types include endothelial cells, fibroblasts and immune/inflammatory cell types. Whilst many of these supporting cells are likely to migrate from the surrounding healthy tissues, it is also now thought that bone-marrow-derived progenitor cells migrate into tumours and contribute to immune inflammatory, fibroblast and mural cell populations (Mishra *et al.*, 2008; Fang and Salven, 2011; Quante *et al.*, 2011).

1.6.4.1 **Fibroblasts in tumours**

Fibroblasts comprise one of the most prevalent and important regulatory cell types in the stroma of carcinomas. Outside of cancer, fibroblasts may be categorised as one of two types: normal tissue-derived fibroblasts are responsible for laying down the fibrous ECM; myofibroblasts are a specialised cell type found in large quantities in wounds and at sites of chronic inflammation (Kalluri, 2016), where their role is to promote tissue repair. The majority of the fibroblasts forming part of the tumour stroma are referred to as cancer-associated fibroblasts (CAFs) (De Wever *et al.*, 2008) though some normal fibroblasts are present and produce ECM that forms the palpable tumour mass. CAFs are similar to myofibroblasts; they display an 'activated' pro-reparative phenotype, but in the chronic inflammatory setting of a tumour they can contribute to lesion growth through pathological stromal ECM deposition. Unlike typical myofibroblasts, which return to a 'normal' phenotype after resolution of inflammation, CAFs maintain their activated state to drive tumour progression (Shiga *et al.*, 2015). The growth factors, chemokines and proteases they release can promote tumour cell proliferation, angiogenesis and metastasis (Orimo *et al.*, 2005; Karnoub *et al.*, 2007; Mishra *et al.*, 2011; Quante *et al.*, 2011; Dumont *et al.*, 2013; De Wever *et al.*, 2014; Kalluri, 2016).

Evidence exists to suggest CAFs promote an immunosuppressive tumour microenvironment (Harper and Sainson, 2014). Yet evidence to the contrary also exists, and there is now debate as to whether CAFs could in fact promote anti-tumour immune cell infiltration (Özdemir *et al.*, 2014; Rhim *et al.*, 2014); CAFs adopt a pro-inflammatory phenotype early during neoplasia development (Erez *et al.*, 2010) and their depletion causes intra-tumour immunosuppression and enhanced tumour growth in carcinomas (Özdemir *et al.*, 2014), highlighting the importance of appreciating the

complex interplay between different components of the tumour microenvironment and their impact on tumour growth.

1.6.4.2 Inflammatory and immune cells in tumours

Cells of both the innate and adaptive immune systems infiltrate tumours, much as they would a wound. Tumours can be thought of as wounds that do not heal and, as such, present a chronic inflammatory situation (Flier *et al.,* 1986). Chronic inflammatory conditions themselves are a risk factor for later dysplasia (Schäfer and Werner, 2008). While acute inflammation functions to clear cellular debris and repair tissue, chronic inflammation in cancer is associated with pathological fibrosis, angiogenesis and neoplasia. A vast array of immune and inflammatory cell types are present within tumours, and these are review extensively by Grivennikov *et al.* (2010).

The immune system, when functioning correctly, eradicates threats within the body, including many tumour types. Avoiding this anti-tumour response is a feature of malignancy (Hanahan and Weinberg, 2011), and tumours that do form have found a way to evade immune destruction. An abundance of evidence exists to support anti-tumour immunity (see Kim *et al.*, 2007; Cirillo *et al.*, 2017). Evidence for this is seen in the increased incidence of cancers, in particular those associated with oncogenic viruses but also several with no infectious cause, after immunosuppression (Vajdic and van Leeuwen, 2009). Immunosuppression for renal transplant has been associated with increased incidence of non-melanoma skin cancer (such as squamous cell carcinoma) (Glover *et al.*, 1997; Euvrard *et al.*, 2003; Moloney *et al.*, 2006). In one study, this was associated with reduced circulating CD4+ T-cells (Ducloux *et al.*, 1998). In rare cases, transmission of donor malignancy to the immunocompromised host via organ transplant has been reported, suggesting that the immunocompromised host was unable to destroy the transmitted tumour cells (Strauss and Thomas, 2010).

In preclinical models of tumourigenesis, depletion of immune cell populations (such as cytotoxic T-cell and natural killer (NK) cells) also increases the growth of some tumour types (Kim *et al.*, 2007). IFN-γ secreted by cells of the innate immune system (cytotoxic T-cells) and NK cells is able to destroy tumour cells, and IFN-γ-insensitive tumour cells showed increased *in vivo* growth and reduced rejection when implanted

into mice (Dighe *et al.*, 1994). Similarly, mice lacking IFN-γ or all of the IFN family members showed enhanced tumourigenicity and more rapid tumour growth compared to immunocompetent WT mice (Kaplan *et al.*, 1998), suggesting the existence of an IFN-γ-dependent tumour surveillance system. Further studies using transgenic mice have demonstrated the importance of an interplay between lymphocytes and IFN-γ in mediating anti-tumour immunity (Shankaran *et al.*, 2001). PDV cells (a squamous cell carcinoma cell line) also grew more readily in mice lacking γδ T-cells (Girardi *et al.*, 2001).

Immune and inflammatory cells can also promote tumour progression. M1 macrophages and neutrophils are the major cell types associated with the classical inflammatory response, while M2 'alternatively' activated macrophages and myeloid progenitor cells are associated with a reparative phenotype. It is the latter of these two responses that is thought to enhance tumour growth (Mantovani *et al.*, 2002). Cells of the innate immune system, including macrophages, neutrophils and dendritic cells, can promote tumour progression by producing myriad growth factors, cell survival signals, angiogenic factors, cytokines and chemokines, ECM modifying proteases and inductive signals (reviewed by Coffelt *et al.*, 2010; DeNardo *et al.*, 2010). Mast cells and tumour associated macrophages (TAMs) encourage tumour angiogenesis directly through release of angiogenic factors and proteinases (e.g. MMP 9, IL-6 and TNF-alpha) which remodel the ECM (Hori *et al.*, 1996). They also indirectly stimulate tumour cells to release their own proangiogenic molecules (Sica *et al.*, 2002; Carmeliet, 2003). The lymphocytes of the adaptive immune system may play an important role in recruiting such tumour-promoting myeloid cells.

As well as these differentiated immune inflammatory cells, an important emerging player is the myeloid-derived suppressor cell (MDSC), a myeloid progenitor associated with suppression of anti-tumour immunity. Through production of arginase 1 (ARG1) and inducible nitric oxide synthase (iNOS), these MDSCs promote tumour progression by reducing the anti-tumour function of NK cells and cytotoxic T cells (Murdoch *et al.*, 2008). These cells exhibit functional and phenotypic crossover with Tie-2 expressing monocytes (TEMs); both cell types are known to promote tumour angiogenesis, suggesting that myeloid cells can both stimulate tumour growth by

increasing blood supply and by suppressing anti-tumour immunity (De Palma *et al.*, 2005; Qian and Pollard, 2010). Furthermore, Varga *et al.* (2008) found that glucocorticoids upregulated monocytes with a phenotype similar to MDSCs – immunosuppressive and anti-inflammatory. Such cells are thought to contribute to tumour progression (Sica and Bronte, 2007).

In mice lacking monocytes, tumour growth is drastically reduced (Sica *et al.*, 2002) and NSAIDs have also been shown to reduce tumour angiogenesis (Dermond and Ruegg, 2001). The story is complicated by evidence that macrophages can inhibit angiogenesis in some contexts (Carmeliet, 2003), possibly via TSP-1 (Salvesen and Akslen, 1999). Mast cells too have been shown to increase with an accompanying reduction in angiogenesis in haemangiomas treated with glucocorticoids (Hasan *et al.*, 2000).

1.6.4.3 **Vascular cell types in tumours**

Whilst endothelial cells in the adult vasculature are normally maintained in a quiescent state, tumour angiogenesis involves an 'angiogenic switch' which renders vessels constantly active and stimulates continual sprouting angiogenesis (Hanahan and Folkman, 1996a). This switch is often tripped in the pre-malignant stages of tumourigenesis, suggesting it is an important target from an early stage (Menakuru *et al.*, 2008). Tumours typically alter the balance of angiogenic factor expression to favour pro-angiogenic factors (e.g. VEGF-A) over anti-angiogenic factors (e.g. TSP-1) (Baeriswyl and Christofori, 2009). Increased expression of VEGF-A, as well as other growth factors such as the FGFs, can be driven by both the hypoxic environment in a tumour or by oncogenic activation (Carmeliet, 2005a). This chaotic unbalanced angiogenic stimulus results in tortuous, leaky vessels that branch excessively, are often enlarged, and are prone to microhaemorrhage (Nagy *et al.*, 2010).

Patterns of neovascularisation vary drastically between tumour types. Pancreatic ductal adenocarcinoma (PDAC) tumours grown in mice, for example, display large avascular regions and are overall hypovascularised (Olive *et al.*, 2009) whereas other tumour types (such as renal carcinomas) are highly angiogenic (Hanahan and Weinberg, 2011). The source of major angiogenic stimuli can also vary between

tumour types, with immune inflammatory cells having a greater influence over angiogenesis in certain tumours, whilst in others tumour cells themselves stimulate the process.

Bone marrow-derived cells, including cells of the innate immune system (macrophages, mast cells, neutrophils), can also powerfully stimulate pathological angiogenesis and the tripping of the angiogenic switch (De Palma *et al.,* 2007; Qian and Pollard, 2010). Necrosis within tumours can lead to the recruitment of immune inflammatory cells, which can in turn stimulate angiogenesis and tumour growth. Bone-marrow-derived vascular progenitor cells may also become intercalated within vessels and contribute to angiogenesis, though the extent of this contribution is now thought to be minimal (Patenaude *et al.,* 2010; Fang and Salven, 2011).

Supporting pericytes also function differently between normal and cancerous blood vessels. Mural cell coverage is markedly reduced in most tumours, as the chaotic nature of tumour angiogenesis does not result in functional maturation. Pericytes, however, do associate with tumour vessels and may in fact play an important role in angiogenesis (Raza *et al.,* 2010). Whilst pericytes are recruited to tumour vessels, they do not adhere as tightly as in normal vessels, and remain slightly detached (Morikawa *et al.,* 2002; Abramsson *et al.,* 2003). Tumour vessels are highly dependent on pericyte coverage for their integrity and provision of endothelial survival factors like VEGF (Reinmuth *et al.,* 2001). Inhibiting pericyte PDGFβ receptor signalling with kinase inhibitors prevents the binding of PDGF-B (released from endothelial cells), a vital signal for recruiting pericytes (Gaengel *et al.,* 2009). This approach has been shown to reduce growth in several tumour models by reducing coverage and stability of tumour vessels (Shaheen *et al.,* 2001; Bergers *et al.,* 2003). Whilst these results are promising, there is a risk that compromising vessel integrity could encourage metastasis, and overexpression of PDGFβ has been shown to reduce tumour growth in models of pancreatic and colorectal cancer (McCarty *et al.,* 2007).

1.6.5 Glucocorticoids and tumours

Glucocorticoids have been in used for the treatment of lymphoid cancers for over 70 years (Pearson and Eliel, 1950; Inaba and Pui, 2010). Synthetic glucocorticoids, such

as dexamethasone, are effective in this setting but their associated side-effects (metabolic disorder, muscle wasting, osteoporosis etc.) limit their usefulness (Pufall, 2015). In treatment of these haematopoietic cancers, the curative mechanism is thought to be predominantly upregulation of pro-apoptotic signalling pathways such as Bim (Wang *et al.*, 2003; Pufall, 2015). In terms of other cancer types, glucocorticoids have shown moderate beneficial effects in the treatment of endocrine responsive tumour types (breast and prostate cancer), either as monotherapy or in conjunction with cytotoxic drugs (Lin and Wang, 2016). These beneficial effects are poorly understood but may involve cooperation between GR and the estrogen receptor (ER, breast cancer) (Karmakar *et al.*, 2013) or the androgen receptor (AR, prostate cancer) (Sahu *et al.*, 2013).

As well as their use to treat malignancy itself, glucocorticoids are also commonly prescribed for the side effects associated with chemo- and radiotherapy, such as loss of appetite and weight, fatigue, vomiting and pain (Lin and Wang, 2016). Controversially, many preclinical studies suggest that dexamethasone inhibits the apoptotic effects of chemotherapy. This has been seen in tumours or tumour cells from a range of cancer types, predominantly carcinomas. These include: bladder, renal and testicular carcinoma (Zhang *et al.*, 2006b); glioma (Gorman *et al.*, 2000; Benedetti *et al.*, 2003); breast (Mikosz *et al.*, 2001; Wu *et al.*, 2004) and ovarian cancer (Sui *et al.*, 2006); cervical carcinoma (Rutz *et al.*, 1998; Kamradt *et al.*, 2000); HCC and colorectal cancer (Zhang *et al.*, 2006b); lung carcinoma (Bergman *et al.*, 2001; Gassler *et al.*, 2005; Gündisch *et al.*, 2012) and pancreatic cancer (Zhang *et al.*, 2006a). A comprehensive study of multiple solid tumour types by Zhang *et al.* (2007) led to the conclusion that dexamethasone induces chemotherapy resistance in the majority of solid tumours. No clinical studies have been able to validate these pre-clinical observations as yet (Lin and Wang, 2016). It is also important to bear in mind that the majority of these studies used pharmacological doses of dexamethasone (which is itself highly potent and selective for the GR), thus the same cannot necessarily be assumed when manipulating systemic glucocorticoids at physiologically relevant concentrations.

GC-mediated resistance to cell death in breast cancer was found to be via upregulation of survival factors such as serine/threonine survival kinase 1 (Mikosz *et al.*, 2001; Wu *et al.*, 2004). Feng *et al.* (2012) also found that chronic restraint stress led to the induction of serum- and glucocorticoid-induced protein kinase, which attenuated p53 tumour-suppressor function and promoted tumour colorectal cancer xenograft growth.

As well as influencing cell survival, glucocorticoids are also likely to alter the anti-tumour immune response (Flint *et al.*, 2017). The concept of glucocorticoids influencing immunological resistance to tumours stretches back over 40 years (Rettura *et al.*, 1973). The complexity of anti-tumour immunity is vast and a huge amount remains to be discovered. However, the last decade has seen great progress (Fearon, 2017; Flint *et al.*, 2017). CXCR3 is now considered a vital mediator of T-cell migration into tumours (Mikucki *et al.*, 2015). The interaction of key chemokines such as CXCL9-11, and their various receptors, are central to the process of immune control in cancer. Cancer cells, myeloid cells, endothelial cells and CAFs may all be involved (reviewed by Fearon (2017)). Colorectal cancer can generate immunoregulatory glucocorticoids to reduce anti-tumour immunity (Sidler *et al.*, 2011). Furthermore, administration of physiologically-relevant levels of corticosterone abolished the beneficial effects of immunotherapy on murine pancreatic cancer (Flint *et al.*, 2016). Both studies suggest that manipulation of physiological glucocorticoids could affect anti-tumour immunity.

IL-6 stimulates the growth of cancer cells, promotes tumour angiogenesis and is influenced by cortisol (Bernabé *et al.*, 2011), making it an important therapeutic target. This is particularly true of squamous cell carcinoma (SCC), discussed in more depth in **Section 1.6.5.1.1.** Bernabé *et al.*, (2011) found that stress levels of corticosterone elevated IL-6 levels, while pharmacological levels decreased IL-6 expression in SCC. Elevated IL-6 levels predict poor prognosis in SCC (Duffy *et al.*, 2008). Reducing the disruptive influence of IL-6-producing pro-inflammatory CAFs on downstream chemokine signalling has been proposed in PDAC (Flint *et al.*, 2016), a tumour type with a relatively high proportion of CAFs (Öhlund *et al.*, 2017). The same approach has shown promise in melanoma (Jobe *et al.*, 2016).

Tumour cells undergo a shift towards aerobic glycolysis during their transition towards malignancy (Hanahan and Weinberg, 2011); a process termed the Warburg effect (Warburg, 1956). The impact of glucocorticoids on glucose availability is therefore a concern, as the increased amount of available glucose could stimulate enhanced glycolysis and increased proliferation of cancer cells. This has been suggested to occur during treatment of glioblastoma with corticosteroids (Seyfried *et al.*, 2010) although it has not yet been thoroughly investigated. The same argument is of relevance to tumour angiogenesis, as endothelial cells are also highly glycolytic (De Bock *et al.*, 2013; Vandekeere *et al.*, 2015) and inhibiting glycolysis suppresses tumour growth (Clem *et al.*, 2008).

Determining the influence of glucocorticoids on intra-tumour immunity and inflammation is highly complex, not only because of the sometimes contrasting effects of immune inflammatory cells on tumour progression, but also due to the differential effects of glucocorticoids on inflammation, depending on concentration (Bernabé *et al.*, 2011; Itoi *et al.*, 2013) and inflammatory context (Chapman *et al.*, 2013a). Likewise, different cancer subtypes express variable levels of GR and of the 11β-HSDs, affecting their sensitivity to glucocorticoids (reviewed by Azher *et al.*, (2016)). Viaje *et al.* (1977) demonstrated the anti-tumour effects of synthetic glucocorticoids in preventing the induction of 12-O-tetradecanoylphorbol-13-acetate (TPA)-induced mouse skin cancer, but did not examine the role of anti-inflammatory steroid in established carcinoma progression.

Despite this large body of evidence suggesting that glucocorticoids can promote tumour progression, there are also findings in the contrary. Over three decades ago, Folkman *et al.*, (1983) performed their pioneering experiments demonstrating the angiostatic and anti-metastatic effects of glucocorticoids (in combination with heparin) on tumours. More recently, Yano *et al.* (2006) demonstrated that dexamethasone (1-1000nM) suppressed VEGF and IL-8 production via binding at the GR *in vitro*, and glucocorticoids have shown suppressive effects in preclinical models of ovarian cancer via activation of mIR-708, leading to suppressed metastasis (Lin *et al.*, 2015). Furthermore, mice injected with 1µg dexamethasone showed reduced growth of xenograft tumours *in vivo*, though potential metastases were not investigated. Work by

Schiffelers *et al.* (2005) also found that prednisolone encapsulated in liposomes could accumulate within colon-carcinoma and melanoma-derived tumours and inhibit their growth. Of note, these studies, like others (Crowley *et al.*, 1988), did not observe an inhibitory effect of glucocorticoids on tumour cell growth *in vitro* and did not see a change in tumour vessel number, potentially implicating other cells of the microenvironment (immune inflammatory cells/fibroblasts) in the anti-tumour process. The role of local glucocorticoid signalling within the tumour microenvironment has been subject to increasing interest in recent years (for reviews see Volden and Conzen, 2013; Azher *et al.*, 2016; Lin and Wang, 2016).

In some circumstances, it is overly simplistic to view the effects of glucocorticoids on tumour as 'positive or negative' alone. In bladder cancer, for example, dexamethasone binding at the GR was shown to, on the one hand, inhibit apoptosis and slightly augment the growth of xenografts in mice, but on the other hand it reduced the expression of MMP 2/9 and IL-6, and prevented epithelial-mesenchymal-transition (EMT), leading to reduced invasiveness (Zheng *et al.*, 2012).

1.6.5.1 **11β-HSDs and tumours**

An abundance of evidence indicates that glucocorticoids can affect tumour growth. However, the majority of this work has focussed on delivery of pharmacological doses of synthetic glucocorticoids, as opposed to manipulation of endogenous levels. The role of the 11β-HSDs in tumour growth has only attracted relatively recent interest (Azher *et al.*, 2016; Liu *et al.*, 2016; Cirillo *et al.*, 2017). Glucocorticoids exert a powerful influence on the immune system, the inflammatory response, fibrosis and ECM deposition, and angiogenesis. Thus, 11β-HSD1 inhibition and subsequent changes in local glucocorticoid levels could affect almost every aspect of the tumour microenvironment, as well as potentially glucose handling in the highly metabolically-active tumour cell population (**Figure 1.4**).

Review of cancer genomics data sets available via the cBioPortal for Cancer Genomics (Cerami *et al.*, 2012) reveals amplification of *HSD11B1* expression in 8-10% of breast and hepatobiliary cancer studies, while around 8% of cutaneous melanomas show either mutation (4%) or amplification (4%) of the gene. Altered expression of

HSD11B1 is also apparent in around 5% of studies on endometrial cancers, non-Hodgkin lymphomas, non-small cell lung cancers and melanomas. Of note, around 3-5% of oesophageal and lung SCC studies and around 2% of PDAC studies show amplified *HSD11B1* expression. Examination of *HSD11B2* in the same data sets reveals amplification of the gene in 2-3% of adrenocortical carcinoma and bladder cancer studies, loss of the gene in around 2% of prostate and ovarian cancers and altered gene expression in 1.5-2% of esophogastric, breast and endometrial cancers. Overall, alterations in expression are marginally more common for *HSD11B1* (3.3% of samples) than for *HSD11B2* (1.1% of samples).

Only one recent study has directly addressed the impact of 11β-HSD1 overexpression on tumour growth (Liu *et al.*, 2016). In this study, decreased 11β-HSD1 expression was seen in HCC samples as compared to healthy liver tissue, and was predictive of poor prognosis. The liver is a key glucocorticoid-sensitive organ involved in regulating systemic glucose homeostasis (Kuo *et al.*, 2015). Liu *et al.*, (2016) report that 11β-HSD1 overexpression impaired glucose uptake and glycolysis in HCC cells *in vitro*, and also reduced angiogenic sprouting and HUVEC migration, in keeping with the known physiological effects of glucocorticoids (Small *et al.*, 2005; Kuo *et al.*, 2015). In terms of direct effects on tumour cells, overexpression of 11β-HSD1 (via lentivirally induction) significantly decreased HCC cell mobility and invasiveness *in vitro*. 11β-HSD1 overexpression also attenuated growth potential of HCC cells, an effect that was reversed by the GR antagonist mifepristone, suggesting it was mediated via increased cortisol availability. Injection of 11β-HSD1 overexpressing HCC cells into Balb/C nude mice resulted in decreased tumour growth, weight, vessel density and 18F-fludeoxyglucose (FDG) accumulation *in vivo* (Liu *et al.*, 2016). Analysis of factors expressed by cells showed that 11β-HSD1 overexpression reduced HIF-1α and VEGF expression, as well as several MMPs (2, 3, 9, 12 and 14) and ANGPTL4, suggesting an anti-angiogenic effect likely as a result of increased glucocorticoid levels. These findings strongly implicate glucose homeostasis as a mechanism, though a significant shortcoming of this study is the use of Balb/C mice; although necessary for use in conjunction with human cells, these mice lack a functional T-cell response and thus conclusions cannot be drawn relating to the inflammatory immune response. This is especially important in light of recent evidence demonstrating that locally produced

cortisol binds GR to inhibit anti-tumour CD8+ T-cell proliferation (Cirillo *et al.*, 2017). It is likely that 11β-HSD1 inhibition will have differential effects on different tumour types depending on the function of the original healthy tissue.

Alterations in the expression of the 11β-HSD isozymes is likely to be of great importance in malignancy. Rabbitt *et al.* (2002) generated osteosarcoma cell lines which overexpressed either 11β-HSD1 or 2 and saw decreased or increased proliferation, respectively, leading them to conclude that activated glucocorticoids constrain tumour cell proliferation, and that the 11β-HSDs provide pre-receptor control of this process. A second group has published similar findings (Woitge *et al.*, 2001). Of note, these changes in enzyme expression and proliferative potential were not accompanied by a change in GR expression. These findings suggest that a switch in enzyme expression may occur as part of both pathophysiology and normal development. 11β-HSD2 for example is expressed in bone during development (Condon *et al.*, 1998), while 11β-HSD1 expression increases with age (Cooper *et al.*, 2002). The opposite may be true in malignant tissues; a consistent observation across a variety of tumour types is that expression of the type I isozyme is decreased and the type II isozyme increased in comparison to healthy tissue. 11β-HSD2 has even been suggested as a putative oncogene that enhances proliferative and neoplastic potential in GR-rich tissues, while gene therapy to increase 11β-HSD1 expression could prove effective as an anti-tumour therapy (Rabbitt *et al.*, 2003b).

This pathophysiological 'switch' has been reported in adrenal carcinoma and adenoma (Coulter *et al.*, 1999), colon carcinoma (Pácha *et al.*, 2002; Takahashi *et al.*, 2008), myeloid leukaemia (Gingras and Margolin, 2000), prostate (Dovio *et al.*, 2009), osteosarcoma (Bland *et al.*, 1999; Cooper *et al.*, 2000) and HCC (Liu *et al.*, 2016). In breast (Hundertmark *et al.*, 1997; Koyama *et al.*, 2001) and endometrial (Koyama and Krozowski, 2001) cancer cell lines, the same patterns have been reported and inhibition of 11β-HSD2 activity reduced cell proliferation (Hundertmark *et al.*, 1997; Koyama and Krozowski, 2001). High 11β-HSD2 activity is also seen in ovarian cancer (Temkin *et al.*, 2006) and potentially enhances tumour progression by reducing the anti-inflammatory effects of cortisol. Importantly, the same effect has been observed in human pituitary tumours (Korbonits *et al.*, 2001; Rabbitt *et al.*, 2003a). This is of

particular relevance as the pituitary is responsible for negative regulation of ACTH release; thus enhanced inactivation of cortisol by elevated 11β-HSD2 is likely to blunt negative feedback and increase systemic cortisol levels. This process has been implicated in the pathophysiology of Cushing's syndrome (Korbonits *et al.*, 2001). A notable exception are the SCCs; in these cancers, 11β-HSD1 expression is reduced compared to healthy skin, but is still detectable (Gronau *et al.*, 2002) whereas 11β-HSD2 (and the MR) are undetectable (Suzuki *et al.*, 2000).

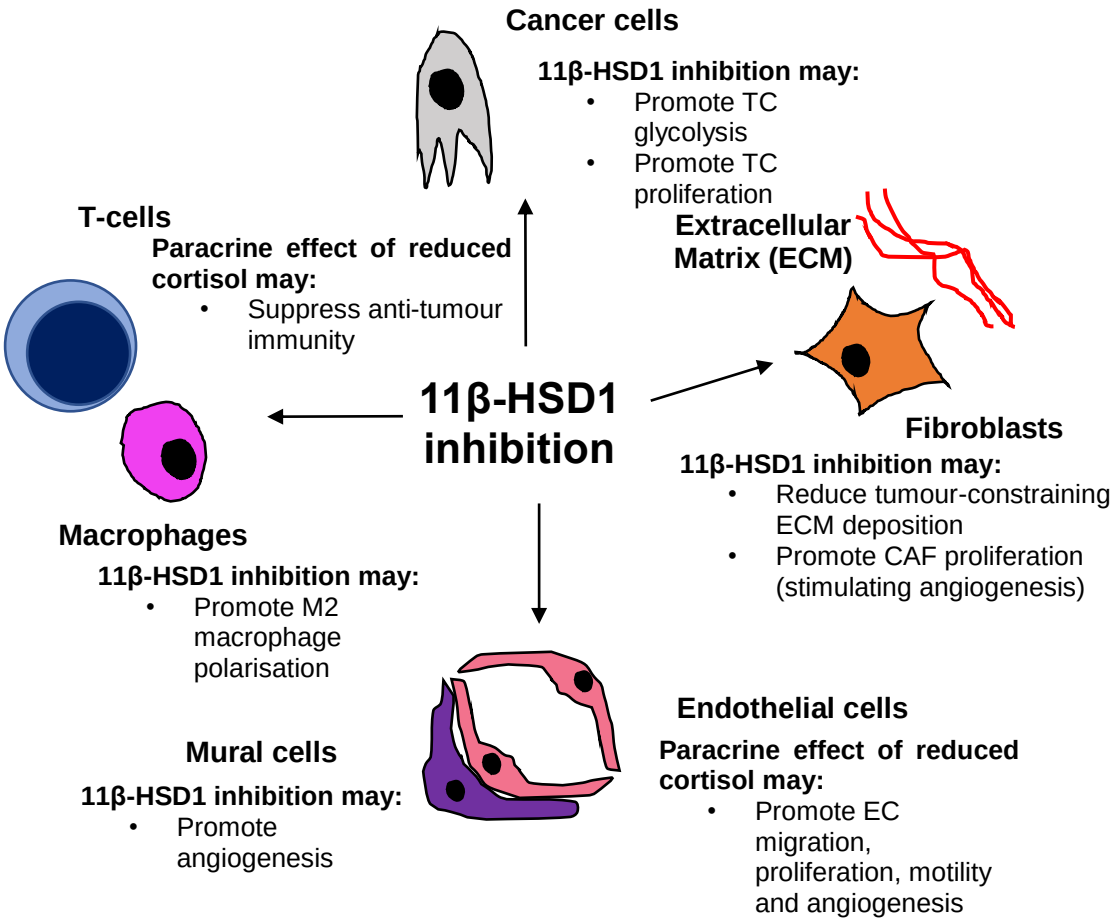

Figure 1.4 – Potential tumour-promoting effects of 11β-HSD1 inhibition. The tumour microenvironment is composed of tumour cells (TCs), cancer associated fibroblasts (CAFs), immune/inflammatory cells, and blood vessels (comprised of endothelial cells (ECs) and their supporting mural cells (pericytes/smooth muscle cells)). Most of these cell types contain 11β-HSD1, and the supporting literature suggests that inhibition of the enzyme may promote TC glycolysis and proliferation, a loss of tumour constraining extracellular matrix and anti-tumour immunosurveillance, and promotion of angiogenesis via increased inflammatory stimuli and possibly direct vascular interaction. Adapted from Hanahan and Weinberg, 2011.

1.6.5.1.1 *11β-HSD1 and skin cancer*

11β-HSD1 expression was originally described in the skin by Teelucksingh *et al.* (1990). Over the last decade, the role of *de novo* steroidogenesis and steroid regeneration by 11β-HSD1 in skin, both healthy and diseased, has proven to be of particular importance (Cirillo and Prime, 2011; Slominski *et al.*, 2014; Azher *et al.*, 2016; Terao and Katayama, 2016). 11β-HSD1 is expressed in all layers of the epidermis, as well as in dermal fibroblasts (Terao *et al.*, 2011; Tiganescu *et al.*, 2011). Pharmacological doses of glucocorticoids potently induce skin atrophy, associated with decreased Type I and III collagen deposition (Oishi *et al.*, 2002). Reducing physiological levels of glucocorticoids by 11β-HSD1 inhibition/deletion stimulates fibrosis (Tiganescu *et al.*, 2013). This is likely the result of increased fibroblast proliferation, as 11β-HSD1 inhibition/deletion was seen to increase fibroblast proliferation and dermal thickness in mice (Tiganescu *et al.*, 2013; Terao *et al.*, 2014). It is worth noting that Terao *et al.* (2014) did not observe increased fibroblast proliferation *in vivo* in 11β-HSD1 KO mice, only in WT mice given an 11β-HSD1 inhibitor. This could either suggest off-target effects or that acute inhibition of enzyme function may sometimes confer an alternative phenotype to chronic deletion. 11β-HSD1 inhibition also promoted keratinocyte proliferation and enhanced wound healing in mice (Terao *et al.*, 2011). 11β-HSD1 content in skin has been shown to increase with age (Tiganescu *et al.*, 2011) and after inflammatory stimuli (Itoi *et al.*, 2013), and 11β-HSD1 KO mice are protected from the adverse effects of skin aging (Tiganescu *et al.*, 2013). Together, the studies above suggest an important role for the enzyme in skin homeostasis.

Binding of glucocorticoids to the GR is thought to be of more importance than binding at the MR in terms of keratinocyte proliferation, motility and migration, as transgenic overexpression of the GR in mice slows wound healing, reduces macrophage and granulocyte recruitment, and reduces IL-1β, TNF and VEGF expression (Stojadinovic *et al.*, 2006; Sanchis *et al.*, 2012). Importantly, this effect must be mediated by endogenous GCs rather than exogenous synthetic equivalents. Glucocorticoids suppress a huge range of IFN-γ related genes (Stojadinovic *et al.*, 2006) and prolong epidermal turnover time (Choi *et al.*, 2006). The discovery that keratinocytes contain

all the enzymes required for non-adrenal steroidogenesis, and that glucocorticoid availability in these cells is under regulation by the 11β-HSDs (Cirillo and Prime, 2011), brings into question the importance of local glucocorticoid regeneration in skin cancer. Evidence suggests that the expression of GR is especially high across a variety of SCC cell lines (Budunova *et al.*, 1997; Spiegelman *et al.*, 1997), and is even sometimes upregulated in SCC compared to normal epidermis (Budunova *et al.*, 1997), emphasising the potential glucocorticoid sensitivity of this cancer type. GR function may be compromised in tumours, based on the lack of changes in metallothionein 1 (Budunova *et al.*, 1997; Spiegelman *et al.*, 1997) and connexin 26 (GR-regulated genes) (Budunova *et al.*, 1997) after exposure to glucocorticoids in tumour cells. Budunova *et al.* (1997) also saw GR mRNA was decreased in tumour cells after exposure to glucocorticoids, an effect interestingly absent in the surrounding skin.

The skin responds dynamically to inflammatory stimuli, with physiologically-relevant glucocorticoid concentrations inducing IL-6 expression in keratinocytes and pharmacological doses attenuating IL-6 release (Itoi *et al.*, 2013). The same differential effects of low and high dose corticosteroids have been seen in SCC cells (Bernabé *et al.*, 2011), with low doses stimulating IL-6 release and enhancing tumour cell proliferation. IL-6 is associated with angiogenesis and tumour progression (Heikkilä *et al.*, 2008) and is correlated with poor prognosis in SCC of the head and neck (Duffy *et al.*, 2008), suggesting that manipulating local glucocorticoid levels may affect SCC progression. Furthermore, inflammatory mast cells, which express 11β-HSD1 (Coutinho *et al.*, 2013), are known to promote fibroblast recruitment, angiogenesis and tumour progression in SCC (Coussens *et al.*, 1999). There is also evidence to suggest that steroid synthesised *de novo* by malignant keratinocytes may promote anchorage independence and promote invasiveness (Kennedy *et al.*, 2015).

In terms of enzyme expression, basal cell carcinoma (BCC), SCC and seborrheic keratosis all show reduced (but detectable) levels of 11β-HSD1 compared to healthy skin, potentially due to their hyperproliferative state (Terao *et al.*, 2013). 11β-HSD2 is elevated in SK and BCC compared to healthy skin, but is barely detectable in SCC (Cirillo *et al.*, 2012; Terao *et al.*, 2013), again highlighting the unusual glucocorticoid

regulation in this particular class of cancers. Cirillo *et al.* (2017) recently reported detection of both 11β-HSD1 activity and low levels of 11β-HSD2 in human SCC by immunohistochemistry, and argue that inhibition of the type 2 isozyme affects the invasiveness of some SCC cell lines; however, they were only able to demonstrate an effect on cell behaviour in one of the three SCC lines tested.

The phenotype and metastatic potential of a tumour is influenced by the non-cellular ECM network of the tumour microenvironment (Cretu and Brooks, 2007). Elevated 11β-HSD1 increases local glucocorticoid availability which reduces collagen deposition, which may enhance tumour progression and metastasis (Willhauck *et al.*, 2006; Cretu and Brooks, 2007). Thus 11β-HSD1 inhibition may promote collagen deposition and enhance ECM integrity. Enhancing ECM integrity has previously been shown to have a beneficial anti-tumour effect; stromal modulation inhibited tumour angiogenesis and the invasiveness of SCC cells – the fibrotic tissue induced led to the accumulation of myofibroblasts and collagen and enhanced the production of an intact basement membrane (Willhauck *et al.*, 2006). The beneficial alteration in tumour phenotype was not related to altered tumour cell proliferation, but was due rather to increased ECM condensation and reduction of peritumoural protease activity. VEGFR expression was altered, and a corresponding increase in TSP-1 and endostatin suggested an additional powerful anti-angiogenic phenotype. This ECM normalisation highlights the importance of the non-cellular TME and further implicates 11β-HSD1 in SCC progression (Tiganescu *et al.*, 2013).

1.7 Hypothesis and Aims

The work described in this thesis was designed to test the following hypothesis:

11β-HSD1 inhibition will promote tumour angiogenesis and, consequently, enhance solid tumour growth.

Specifically, the experiments presented were designed with the following primary aims:

1. To determine whether pharmacological inhibition or genetic ablation of 11β-HSD1 promote tumour growth and angiogenesis in murine models of squamous cell carcinoma and pancreatic ductal adenocarcinoma.
2. To determine the effects of pharmacological 11β-HSD1 inhibition and exogenous glucocorticoids on *ex vivo* angiogenesis, and *in vitro* tumour cell growth.
3. To determine the effects of 11β-HSD1 inhibition on the tumour microenvironment and investigate mechanisms by which glucocorticoid manipulation might influence tumour growth.

Chapter 2

Materials and Methods

2 Materials and Methods

2.1 Materials

2.1.1 Chemicals and reagents

Unless otherwise stated all chemicals and reagents were purchased from Sigma-Aldrich (Gillingham, UK). All High-Performance Liquid Chromatography (HPLC)-grade chemicals were purchased from VWR (Lutterworth, UK). Scintillation fluid (Pro-flow G+) was purchased from Meridian Biotech (Tadworth, UK).

2.1.2 Buffers

C buffer: 63g Glycerol, 8.77g NaCl, 186mg Ethylenediaminetetraacetic acid (EDTA), 3.03g Tris, made up to 500mL with distilled H_2O and pH adjusted to 7.7. Stored at 4°C.

Phosphate Buffered Saline (PBS): 10 x PBS tablets (Thermo-Fisher Scientific, Renfrew, UK) dissolved in 1L dH_2O. Stored at room temperature.

Tris-Buffered Saline (TBS): 6.05g Tris, 8.76g NaCl made up to 800mL with distilled H_2O and pH adjusted to 7.6. Made up to 1L with distilled H_2O and stored at 4°C.

Homogenisation buffer: 100g Glycerol, 300mg Tris, 186mg EDTA, made up to 500mL with distilled H_2O and pH adjusted to 7.5. Stored at 4°C. 7.7mg 1,4-Dithiothreitol (DTT) added per 50mL before use.

Citrate buffer: Prepared and stored as a 10x solution - tri-sodium citrate (dehydrate) 29.4g, 1000mL distilled H_2O. Diluted 1:10 in distilled H_2O, pH adjusted to 6.0 and 0.1% Tween-20 added before use.

EDTA

0.5M solution prepared by adding 93.05 grams EDTA disodium salt dissolved in 400mL distilled H_2O and pH adjusted to 8.0 with sodium hydroxide (NaOH). When salt dissolved, solution made up to 500mL with distilled H_2O.

TAE buffer

50x stock solution: 242 grams of Tris base dissolved in 750mL distilled H_2O + 57.1 mL glacial acid and 100 milliliters of 0.5 M EDTA. Made up to a final volume of 1L with distilled H_2O.

2.1.3 Drugs

2.1.3.1 **11β-HSD1 inhibition *in vivo***

Studies used the 11β-HSD1 inhibitor UE2316 ([4-(2-chlorophenyl-4-fluoro-1-piperidinyl][5-(1H-pyrazol-4-yl)-3-thienyl]-methanone), synthesised by High Force Ltd (Durham, UK) (Webster *et al.*, 2011). For *in vivo* studies, UE2316 was delivered *ad libitum* to animals via an adjusted RM1 diet (175mg/kg UE2316) prepared by Special Diet Services (Essex, UK). UE2316 has an IC_{50} of 162nM for mouse 11β-HSD1 (Sooy *et al.*, 2010) and no significant off-target activities in selectivity screening, including against 11β-HSD2, 17β-HSD1 and GR (Yau *et al.*, 2015).

2.1.3.2 **11β-HSD1 inhibition *in vitro***

For *in vitro* studies, a 20mM UE2316 stock solution was stored at -20°C and diluted incrementally to give an appropriate final concentration in experimental solvent. The novel 11β-HSD1 inhibitor UE2341 (High Force Ltd.) (Webster *et al.*, 2011) was used as an internal standard for mass spectrometry studies.

2.1.3.3 **Systemic glucocorticoid manipulation**

Metyrapone (Cambridge Bioscience, Cambridge, UK) was used to inhibit adrenal corticosteroid synthesis in mice; the drug was dissolved in saline solution (10mg/mL) for intraperitoneal injection and used the same day. Corticosterone was delivered to animals via drinking water; 100mg corticosterone was added to 8mL ethanol and topped up with 392mL H_2O to give a 10x holding stock (250µg/mL) which was diluted 1/10 (drinking water was replaced every 2-3 days).

2.1.4 Corticosteroids

11-dehydrocorticosterone (Kendall's compound 'A') and corticosterone (Kendall's compound 'B') were purchased from Steraloids (Newport, USA) and stored at -20°C

as 20mM stocks made up in ethanol (for *in vitro* studies) or methanol (for use in mass spectrometry). [9,11,12,12-$^{2}H_4$]cortisol was used as an internal standard in mass spectrometry studies. Stocks were diluted incrementally to an appropriate final concentration in experimental solvent. Tritiated steroid stocks (corticosterone and cortisone) were purchased from PerkinElmer (Wokingham, UK). For systemic glucocorticoid manipulation studies, corticosterone was delivered to animals via drinking water; 100mg corticosterone was added to 8mL ethanol and topped up with 392mL H_2O to give a 10x holding stock (250µg/mL) which was diluted 1/10 (drinking water was replaced every 2-3 days).

2.1.5 Software

Table 2.1 shows software details.

Software	**Use**	**Manufacturer**
Zen Blue edition	Slide Scanner/LSM 710 confocal microscope	Carl Zeiss Microscopy (Cambridge, UK)
ImageJ	Image analysis	See PMID 22743772
MCID Basic 7.0	Non-fluorescent microscopy	MCID
Lightcycler 480 software v1.5.1.62	RT-qPCR	Roche Diagnostics (Welwyn Garden City, UK)
Nanodrop 100 software v3.8.1	Nanodrop RNA quality	ThermoScientific
Chromeleon v6.5 SP4 Build 1000	HPLC output	ThermoScientific

Analyst software with MultiQuant v3.0.2	Mass spectrometry	SCIEX (Washington, USA)
Incucyte software	Incucyte Zoom live cell imaging	Essen Bioscience (Welwyn Garden City, UK)
Softmax Pro 4.8	Plate reader software	Molecular Devices
Cufflinks software	RNA sequencing bioinformatics	See PMID 20436464
Prism v7	Statistical analysis	Graphpad (San Diego, USA)

Table 2.1 – Software. Software used throughout project

2.1.6 Plastics

All sterile tissue culture plastic-ware was purchased from Corning (Wiesbaden, Germany).

2.2 Animals

C57BL6/J and FVB/N mice were purchased from Envigo (Blackthorn, UK) or Charles River (Elphinstone, UK). C57BL6/J mice globally deficient for 11β-HSD1 (Del1) were bred in house at the University of Edinburgh (Zhang et al., 2017). All experimental animals were female, and aged 9-14 weeks. Groups were age-matched. Animals were group housed (5 mice per cage maximum) and given free access to food and water unless otherwise stated. All procedures were carried out by a licensed individual and in strict accordance with the Animals (Scientific Procedures) Act 1986, under project Licence 70/8897 or 60/4523.

2.3 Methods

2.3.1 Cell culture

2.3.1.1 Preparation of reagents

All reagents were stored in sealed containers according to manufacturer's advice and opened only inside a sterile Class 2 fume hood. Before use, foetal calf serum (FCS; Gibco (Invitrogen, Carlsbad, USA) was heat-inactivated by incubation for 30 minutes in a 57°C water bath. Where required, FCS was stripped by adding 1g of dextran charcoal to 50mL serum and incubating at 4°C on a gentle shaker overnight. Serum was spun by centrifuge (180 RCF x 5 min) and passed through a sterile 0.2µm filter (Merck-Millipore, Cork, Ireland) three times to minimise particulate contamination. Aliquots (1mL) were stored at -20°C.

2.3.1.2 Source of cells

Studies made use of three immortalised murine cancer cell lines. Two SCC cell lines, WT-SCC cells (Serrels *et al.*, 2012) and SCC-B6-1 cells, were generated in-house by Dr Alan Serrels using a two-stage 7,12-Dimethylbenz[a]anthracene (DMBA)/TPA chemical carcinogenesis protocol as previously described (McLean *et al.* 2004). Squamous cell carcinoma was selected based on multiple reports of altered local glucocorticoid profile in this cancer type (Azher *et al.*, 2016). WT-SCC are syngeneically compatible with FVB/N mice, however the transgenic mouse line available in our group (Del1 - global 11β-HSD1 knockout) are bred on a C57BL6/J background. SCC-B6-1 cells served as an SCC cell-line compatible with Del1 mice to investigate the effects of enzyme deletion and inhibition. A PDAC cell line, Panc043 cells, were provided by the Beatson Institute in Glasgow – these cells were originally derived from tumours developed using the *KrasLSL.G12D/+; p53R172H/+; PdxCretg/+* (KPC) model (Hingorani et al., 2005) and were selected as an alternative tumour type that grow on the C57BL6/J background.

2.3.1.3 **Cell culture media**

2.3.1.3.1 *Panc043*

Panc-043 cells were cultured in Dulbecco's Modified Eagle Medium (DMEM) supplemented with 10% FCS.

2.3.1.3.2 *WT-SCC*

WT-SCC cells were maintained in Glasgow Minimum Essential Medium (GMEM) supplemented with 10% FCS, 2mM L-Glutamine, 1mM sodium pyruvate, MEM non-essential amino acids (Thermo-Fisher) and MEM vitamins. SCC-WT cells are Focal Adhesion Kinase (FAK) KO cells which have had FAK re-expressed using electroporation, and require selection via the addition of 0.25 mg/mL hygromycin B to media.

2.3.1.3.3 *SCC-B6-1*

SCC-B6-1 cells were maintained in Glasgow Minimum Essential Medium (GMEM) supplemented with 10% FCS, 2mM L-Glutamine, 1mM sodium pyruvate, MEM non-essential amino acids (Thermo-Fisher) and MEM vitamins.

2.3.1.4 **Freezing media**

Cells were stored at -80°C in the appropriate cell culture medium (see above) + 20% FCS + 10% dimethyl sulfoxide (DMSO).

2.3.1.5 **Cell maintenance**

2.3.1.5.1 *Serial passaging*

All cells were serially passaged (split 1/10 WT-SCC/Panc043 and 1/5 SCC-B6-1, every 2-3 days) and maintained at 37°C/5% CO^2 in 25mL media in T150 flasks (Corning). All cell lines were adherent and were split by replacing media with 4mL trypsin (Thermo-Fisher Scientific) and incubating for 5 min at 37°C. Once cells were detached, trypsin was inactived by diluting 5:1 with medium, and an appropriate volume taken into a new flask. All experimental cells were used at <20 passages.

2.3.1.5.2 *Cell storage, thawing and freezing*

Cells were stored in liquid nitrogen when not in use. Cells were frozen by trypsinising a >70% confluent flask, pelleting the resulting cells by centrifuge (5 min x 180 RCF) and re-suspending in 10mL freezing media. 1mL aliquots were added to cryovials and stored at -80°C for 24 hours before transfer to liquid nitrogen for long-term storage.

Cells were thawed quickly in a 37°C water bath and added to 25mL normal cell culture medium in a T150 flask. Cells were transferred to a 50mL Falcon tube, pelleted by centrifugation (5 min x 180 RCF) and resuspended in 25mL cell culture medium for transfer into a T150 flask.

2.3.2 Solid tumour model

In vivo studies of tumour growth used a model of subcutaneous tumour development (described previously in Serrels et al., 2015).

2.3.2.1 **Diet alteration**

Diet was changed 5 days prior to cell injection for all experiments, to allow animals to adjust to the new diet. Diet and animals were weighed every 2-3 days from the point of diet change.

2.3.2.2 **Cell injection**

Tumour cells in suspension were pelleted by centrifugation (180 RCF x 5 min) and re-suspended in 20mL sterile PBS twice to remove media. Cells were counted by haemocytometer before pelleting and re-suspension in Hank's Balanced Salt Solution (HBSS) to give a concentration of 10 x 10^6 cells/mL. Hair was removed from the flanks of mice by shaving and 100µL of cell suspension (1x10^6 cells) injected subcutaneously into each flank to produce 2 tumours per animal. As this procedure is relatively non-invasive, no analgaesia is required.

2.3.2.3 **Tumour development**

Tumours were allowed to develop over the subsequent 1-6 weeks during which they were measured by callipers every 2-3 days. Tumour volume was calculated as the volume of an ellipsoid (0.5*length*breadth^2). Mice and diet were weighed and mice

checked for any unexpected signs of ill health every 2-3 days. Tumour growth data is the mean ± SEM of the 2 tumours per animal. For UE2316-diet groups, diet was changed 5 days prior to cell injection and mice were weighed from the point at which diet was changed. Calliper measurements were blinded where possible by masking of cage labels and randomisation of cages by a second individual.

2.3.2.4 Tissue collection

At the end of the experiment, mice were culled by cervical dislocation and tissues harvested. Blood was collected rapidly from the thoracic cavity using a syringe without a needle and stored in anti-coagulant EDTA-treated tubes (Sarstedt, Leicester, UK). Plasma was separated from whole blood by centrifugation (2000 RCF x 10 min at 4°C) for storage at -20°C. Tumours were weighed upon removal and halved (one half was snap frozen in liquid nitrogen for storage at -80°C, the other half was fixed in formalin for 24 hours before transfer to 70% ethanol before processing and embedding in paraffin wax). All other required tissues were removed and snap frozen in liquid nitrogen before storage at -80°C.

2.3.3 Immunohistochemistry

2.3.3.1 Section preparation

Paraffin embedded tissues were sectioned by microtome (5µm) and dried at 37°C overnight on electrostatically-adherent microscope slides (Superfrost plus, Thermo-Fisher Scientific).

2.3.3.2 Hydration and dehydration of tissue sections

Sections were rinsed in xylene (2 x 5 min), rehydrated through serial dilutions of ethanol (100% x 20s, 100% x 20s, 95% x 20s, 80% x 20s, 70% x 20s) and washed in H_2O. Basic stains were rehydrated through serial dilutions of ethanol (50% x 20s, 75% x 20s, 95% x 20s, 100% x 20s) and rinsed in xylene (5 min) before mounting.

2.3.3.3 Haematoxylin and Eosin staining

Rehydrated sections were immersed in Harris haematoxylin (2 min), acid alcohol (15s), Scott's tap water (20s) and eosin (5s), with a thorough H_2O rinse between each step. Slides were dehydrated and mounted with DPX mountant.

2.3.3.4 Immunofluorescent staining

Heat-based antigen retrieval was performed by immersing sections in pH6 citrate buffer and pressure cooking (5 min). Sections were permeabilised by immersion in PBS + 0.4% Triton-X for 15 minutes. Slides were fitted into Sequenza cassettes (Thermo-Fisher Scientific) and rinsed with PBS before blocking with 200µL of 1% normal goat serum (Biosera, Nuaille, France) for 30 minutes. Slides were incubated with 200µL primary antibody (18h, 4°C) with the exception of a negative control, for which PBS was added in lieu of antibody. After primary incubation, slides were rinsed with PBS and incubated with 200µL secondary antibody (1 hour, room temperature). After secondary incubation, slides were rinsed with PBS and incubated with DAPI (1/1000 in deionised water x 5 min) before a thorough final rinsing with deionised water. Slides were mounted using Fluoromount G (SouthernBiotech, Cambridge, UK) and stored at 4°C.

2.3.3.5 Imaging

Slides were scanned at 200x magnification using an Axioscan.Z1 (Zeiss) digital slide scanner. Higher magnification images were obtained using the LSM710 confocal microscope (Zeiss). Gain and digital offset values were adjusted using negative control samples to remove background autofluorescence, and the same settings then used to image all specimens.

2.3.4 Specific staining protocols

2.3.4.1 Vessel staining

2.3.4.1.1 *CD31/α-SMA immunofluorescent co-stain*

Paraffin-embedded tumours (all types, 2 sections per tumour spaced 50µm apart, N=6/group) were stained using the basic protocol described in **Section 2.3.3.4**, using the antibodies detailed in Table 2.2.

Antibody	**Dilution**	**Catalogue #**
CD-31 (primary)	1/300	Ab28364 (Abcam, Cambridge, UK)
Goat anti-Rabbit IgG, Alexa Fluor 488 (secondary)	1/1000	A-11034 (Molecular Probes, Eugene, USA)
α-SMA-cy3 (conjugated primary antibody)	1/1000 – added with secondary antibody	C6198 (Sigma)

Table 2.2 – Antibodies used for vessel staining. Antibodies diluted in 200µL 1% goat serum/PBS. The conjugated primary and secondary antibodies were co-diluted and added to samples simultaneously.

2.3.4.1.2 *CD31 DAB stain*

CD31 staining was performed by L. Boswell based at the Shared University Research Facility (SuRF). Staining was performed using the Leica BOND-III automated staining system and the Leica Bond Polymer Refine detection kit (Leica, Milton Keynes, UK). Rehydrated slides underwent citrate buffer antigen retrieval as above, followed by: bond wash (buffer solution purchased from Leica; 10 min), peroxidase blocking (5 min, 4% hydrogen peroxide, room temperature), bond wash, CD31 (Table 2.2) antibody incubation (60 min), polymer incubation (15 min), bond wash, dH_2O rinse, 3,3′-Diaminobenzidine staining (DAB; 10 min) and haematoxylin counterstaining (5 min), bond wash. Sections were then dehydrated and mounted with DPX mountant.

2.3.4.2 **Vessel quantification**

2.3.4.2.1 *Manual vessel counts*

Tumour sections (prepared as described in **Section 2.3.4.1.1**) were imaged using the Axioscan.Z1 slide scanner (Zeiss). Vessels showed a relatively even distribution across the tumour, with no consistently predictable region associated with high vascular density, leading to the decision to use randomly generated fields of view for quantification. Zen Blue software (Zeiss) was used to demarcate 10 randomly selected

0.1mm^2 fields of view from which vessels were manually quantified. CD31-positive only vessels and CD31/α-SMA positive vessels were both quantified to allow the ratio of vessels with smooth muscle coverage to be calculated. Two sections from the centre of the tumours, spaced 50µm apart, were quantified per tumour. Quantification was performed blinded to treatment group.

2.3.4.2.2 *Chalkley counts*

As a secondary measure of vessel density, sections stained for CD31 (prepared as described in **Section 2.3.4.1.2**) were quantified by Chalkley count using the method described previously (Hansen *et al.*, 2000). One section (three hotspots) was quantified per tumour. Quantification was performed blinded to treatment group.

2.3.4.2.3 *Hotspot quantification*

As a tertiary measure of vessel density, sections were stained for CD31 (prepared as described in **Section 2.3.5.1.2**) and vascular hotspots identified for manual quantification (using an adapted version of the protocol described by Weidner, 2008). Hotspots were 0.74mm^2 in area. Quantification was performed blinded to treatment group.

2.3.4.3 **Identification of proliferating cells - Ki-67**

2.3.4.3.1 *Staining*

Ki67 staining was performed using the general methods described in **Section 2.3.3.4** using the antibodies described in Table 2.3.

Antibody	**Dilution**	**Catalogue #**
Ki-67 (primary)	1/100	Ab15580 (Abcam)
Goat anti-Rabbit IgG, Alexa Fluor 488 (secondary)	1/1000	A-11034 (Molecular Probes)

Table 2.3 – Antibodies used for Ki67 staining. Antibodies diluted in 200µL 1% goat serum/PBS.

2.3.4.3.2 *Quantification*

Whole section

Sections were imaged by slide scanner (x20 magnification) and quantified automatically using ImageJ. Whole section images were duplicated and one copy converted to binary. This binary imaged was used to create a region of interest encompassing the entire section, which was then applied to the original image. The 'Measure' function was then used to generate a read out of stain intensity.

Fields of view

Ki67-stained sections were also quantified semi-automatically; 2 sections/tumour were scanned at 200x magnification and the most proliferative region selected (this was performed by a blinded observer). This region was then imaged at 400x magnification and nuclei number calculated by ImageJ. Ki67-positive cells were then quantified manually per hotspot by a blinded observer and expressed as a percentage of total cells.

2.3.4.4 **Identification of inflammatory cells - F4/80**

2.3.4.4.1 *Staining*

F4/80 staining was optimised by L. Boswell based at the Shared University Research Facility (SuRF). Staining was performed using the Leica BOND-III automated staining system and the Leica refine detection kit (Leica). Rehydrated slides underwent trypsin-based antigen retrieval (10 min, 37°C, 0.5mg/mL), peroxidase blocking (5 min, 4% hydrogen peroxide, room temperature), serum blocking (30 min, anti-rat impress blocking serum; Vector labs, Peterborough, UK), primary antibody incubation (eBiosciences, cat no. 14-4801, 1:300, 30 min), ImmPRESS^{TM} anti-rat Ig reagent incubation (30 min, Vector labs), 3,3′-Diaminobenzidine staining (DAB; 10 min) and haematoxylin counterstaining (5 min). Sections were then dehydrated and mounted with DPX mountant.

2.3.4.4.2 *Quantification*

F4/80 stained sections were imaged by slide scanner and whole sections were automatically quantified using ImageJ software.

2.3.4.5 **Identification of T-cells – CD3 staining**

2.3.4.5.1 *Staining*

CD3 staining was performed by L. Boswell based at the Shared University Research Facility (SuRF). Staining was performed using the Leica BOND-III automated staining system and the Leica Bond Polymer Refine detection kit (Leica). Rehydrated slides underwent citrate buffer antigen retrieval as above, followed by: bond wash (10 min), peroxidase blocking (5 min, 4% hydrogen peroxide, room temperature), bond wash, CD3 antibody incubation (Santa-Cruz, Dallas, USA; cat no. sc-20047, 60 min), polymer incubation (15 min), bond wash, dH2O rinse, 3,3′-Diaminobenzidine staining (DAB; 10 min) and haematoxylin counterstaining (5 min), bond wash. Sections were then dehydrated and mounted with DPX mountant.

Whole section

Sections were imaged by slide scanner (x20 magnification) and quantified automatically using ImageJ. Whole section images were duplicated and one copy converted to binary. This binary imaged was used to create a region of interest encompassing the entire section, which was then applied to the original image. The 'Measure' function was then used to generate a readout of stain intensity.

Hotspots

1 section/tumour was scanned at 100x magnification and the two most intense regions of signal identified and imaged (this was performed by a blinded observer). Images were thresholded and percentage stain area measured on ImageJ. Data presented are the average of the two hotspots per tumour.

2.3.4.6 **Picrosirius-red staining**

2.3.4.6.1 *Staining*

Picrosirius red staining was performed by Debbie Mauchline (Shared University Research Facilities). Working solutions of Direct red (0.1%) and Fast green (0.1%) were combined in equal parts and added to picric acid (1:9 ratio for a working solution). This solution was then filtered and stored at room temperature in the dark. Slides were dewaxed and rehydrated then rinsed in tap water. Slides were incubated in the PSR solution (2 hours at room temperature) in a covered box to reduce light exposure. After incubation, slides were rinsed in tap water and very briefly rinsed in 100% ethanol (<5s). Slides were then allowed to dry before mounting with DPX mountant.

2.3.4.6.2 *Quantification*

Slide scanner images were obtained and quantified automatically using ImageJ.

2.3.4.7 **Second Harmonic Generation imaging**

2.3.4.7.1 *Image acquisition*

To visualise Type-I collagen specifically, Second Harmonic Generation (SHG) microscopy was performed by Dr Martin Lee on WT-SCC tumours (N=6/group), Panc043 tumours (N=3/group) and SCC-B6-1 tumours (Day 28 N=6/group, Day 41 N=3/group). A tunable pump laser (720–990 nm, 7 ps, 80 MHz repetition rate) and a spatially overlapped second beam, termed the Stokes laser (1064, nm, 5–6 ps and 80 MHz repetition rate), were both provided by a picoEmerald (APE) laser. The pump laser used 50 mW power (measured at the objective) and was tuned to 816.8 nm. The Stokes laser used 20 mW power (measured at the objective). This laser was inserted into an Olympus FV1000 microscope coupled with an Olympus XLPL25XWMP N.A. 1.05 objective lens. The objective lens used a short-pass 690 nm dichroic mirror (Olympus). A series of filters (FF552-Di02, FF483/639-Di01 and FF420/40) were used to filter the Second Harmonic Generation signal.

2.3.4.7.2 *Image analysis*

SHG images were quantified automatically using Image J.

2.3.5 Unsuccessful immunohistochemistry

2.3.5.1 Identification of fibroblasts - Vimentin

2.3.5.1.1 *Staining*

In an attempt to quantify fibroblasts, WT-SCC tumours from control and UE2316-diet-fed mice (N=6/group) were stained with vimentin. Vimentin staining was performed using the general methods described in **Section 2.3.3.4** using the antibodies described in Table 2.4.

Antibody	**Dilution**	**Catalogue #**
Vimentin (primary)	1/100	5741 (Cell Signalling Technology, Danvers, USA)
Goat anti-Rabbit IgG, Alexa Fluor 488 (secondary)	1/1000	A-11034 (Molecular Probes)

Table 2.4 – Antibodies used for vimentin staining. Antibodies diluted in 200µL 1% goat serum/PBS.

Unfortunately, this stain proved ineffective, as although it produced a strong cytoplasmic stain, it was expressed almost ubiquitously across the tumour (see Figure 2.1) rendering it unhelpful for quantifying fibroblasts.

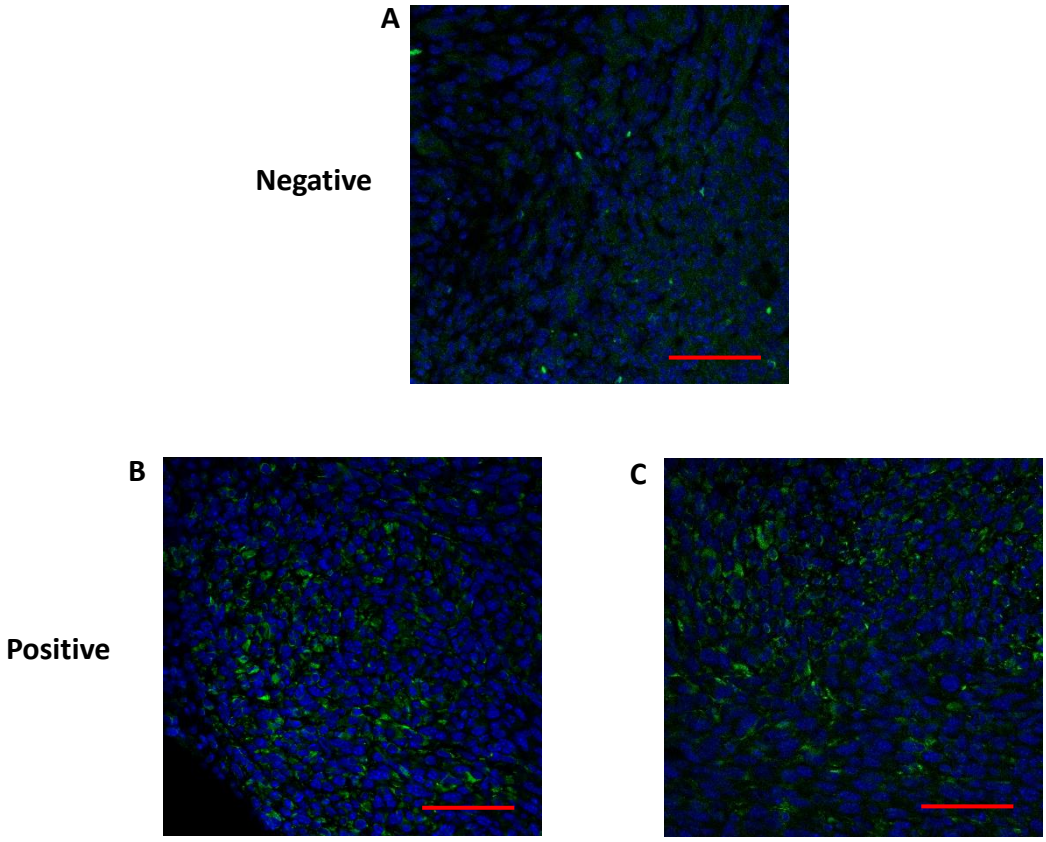

Figure 2.1 - Vimentin positive cells in WT-SCC tumours. Adding secondary antibody to tumours in the absence of primary antibody resulted in no immunoreactivity (A), while addition of the primary vimentin antibody produced a strong cytoplasmic stain (green) in most of the cells in the tumour (B and C). Blue counterstain = DAPI. Scale bar = 50µm.

2.3.5.2 **11β-HSD1 staining**

Early attempts to optimise staining for 11β-HSD1 using the protocol described in **Section 2.3.3.4** proved ineffective, with positive signal masked by excessive background. An alternative method was optimised on the BOND automated staining system by Lyndsey Boswell and emulated at the bench using an adapted protocol by combining both an Immpress HRP Anti-Goat Ig (Peroxidase) Polymer detection kit (Vector Labs) and tyramide signal amplification. Slides were dewaxed, rehydrated, antigen retrieved and permeabalised as described in **Section 2.3.3.4** (with TBS used instead of PBS to reflect BOND staining conditions). Blocking was performed using 2.5% horse serum (30 min) before incubation with 11β-HSD1 antibody (developed in-house by Dr Scott Webster, sheep-raised anti-rodent/human, diluted 1/200 in TBS + 1% BSA) for 1 hour at room temperature. Slides were then incubated with goat Immpress polymer (30 min) followed by Cy-3 conjugated tyramide (10 min 1/50 dilution, Perkin-Elmer) and counterstained with DAPI (1/1000 in distilled water). Slides were washed thoroughly with TBS between incubations, and with distilled water before mounting with aqueous mountant (Fluoromount-G, Southern Biotech) for imaging on an LSM710 confocal microscope (Zeiss).

The 11β-HSD1 staining protocol was used to stain liver tissue from wild-type FVB/N and 11β-HSD1 knockout (Del1) mice, and tumour tissue from wild-type FVB/N mice. Unfortunately, imaging on the LSM710 microscope showed that non-specific binding was apparent in the tissue of the knockout animals (Figure 2.2), confirming that this protocol was ineffective. 11β-HSD1 immunostaining was subsequently abandoned in favour of enzymatic transcript and activity measurements.

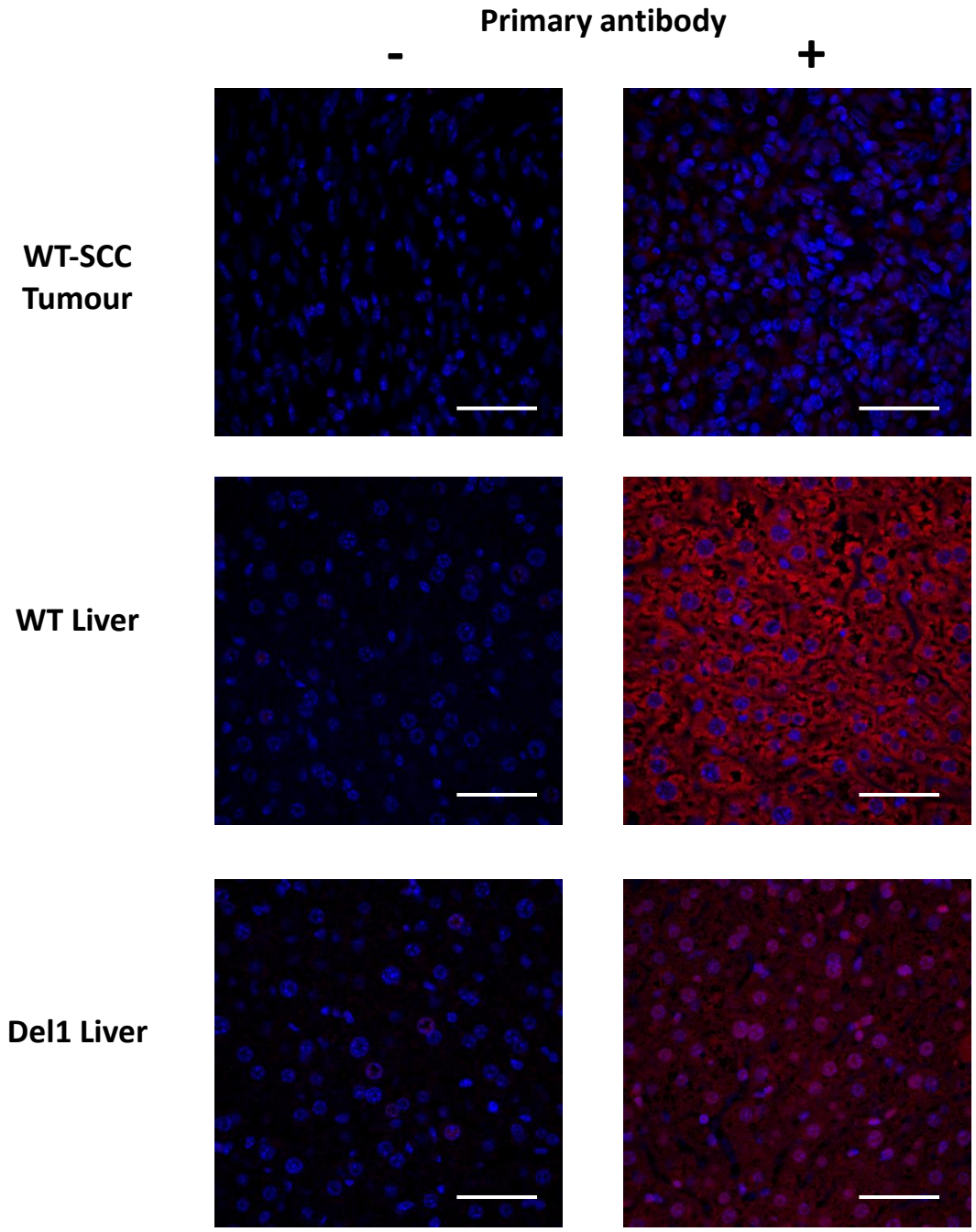

Figure 2.2 – 11β-HSD1 immunofluorescent staining. 11β-HSD1 staining was performed on tumour tissue from wild-type (WT) FVB/N mice (top), and liver tissue from wild-type FVB/N mice (middle) and 11β-HSD1 knockout (Del1) mice (bottom). Whilst primary antibody-negative controls did not show immunoreactivity, binding was apparent in all antibody-positive tissues, including in the knockout animals. Tissues imaged at 400x magnification, scale bar = 50μm.

2.3.6 Real-time qPCR

2.3.6.1 **RNA extraction**

Cell lines were grown to >70% confluence in a 6-well plate (Corning) and lysed for 2 minutes using 600µL Qiazol (Qiagen, Manchester, UK). A cell scraper was used to ensure cells were detached before Qiazol was transfered to 1.5mL Eppendorf tubes. For tissues (except sponges, described below), 30mg of frozen tissue was homogenised in 600µL of Qiazol reagent in a 1.5mL Eppendorf tube using a tissue homogeniser (T10 Basic, IKA, Staufen, Germany) and allowed to settle at room temperature for 5 minutes. 120µL of chloroform was added to samples which were vortexed and allowed to settle (2 min). Samples were subjected to centrifugation (12000 RCF x 15 min at 4°C) and the resultant aqueous phase mixed with an equal volume of 70% ethanol. All subsequent on-column steps were performed as per the RNeasy manufacturer protocol. RNA concentration and integrity were assessed using the Nanodrop 1000 (Thermo-Fisher Scientific).

2.3.6.1.1 *RNA extraction from subcutaneous sponge tissue*

Sponges required an alternative extraction protocol due to their fibrous nature. Tissues were thoroughly homogenised in 700µl of Qiazol (2 min disruption followed by splitting of sample across two Eppendorf tubes, addition of a further 350µl of Qiazol and a further 1 min disruption). Samples were incubated at room temperature (5 min) before 200µl chloroform was added. They were then mixed by vortex and incubated at room temperature (2 min) before being spun (12000 x g, 15 min, 4°) and the aqueous phases for the same samples combined and added to an equal volume of 70% ethanol. Where the aqueous phase was insufficient, a further 200µl Qiazol was added and samples re-spun. All subsequent on-column steps were performed as per RNeasy protocol.

2.3.6.2 **cDNA generation**

cDNA was generated from RNA using the QuantiTect Reverse Transcription Kit (Qiagen) as per manufacturer's protocol. For the PCR reaction, samples were incubated at 42° for 15 minutes followed by 95° for 3 minutes in a Thermal cycler

(Techne-Cole-Palmer, Staffordshire, UK). A H_2O control (H_2O replacing RNA) and no-RT control (H_2O replacing reverse transcriptase) were also prepared.

2.3.6.3 qPCR

cDNA was diluted 1/40 in RNase-free water and a standard curve constructed by pooling 2µL of each sample and serially diluting. In triplicate on a 384-well plate, 2µL of sample was combined with 5µL of Lightcyler 480 Probes Master mastermix (Roche), primers (0.1µl/sample Forward and Reverse), probe (0.1µl/sample) and RNase-free water to make up to 10µL total volume. Plates were spun (420 RCF x 2 min on LCM-3000 plate centrifuge (Grant Instruments, Royston, UK) before analysis on the Light Cycler 480 (Roche). Samples were run for 50 cycles (10s at 95° and 30s at 60°).

Primer sequences and UPL probes are detailed in Table 2.5. All data were normalised to the average of two housekeeping genes (GAPDH and TBP) (Figure 2.3A and 2.3B and Figure 2.4) with the exception of one experiment which was normalised to GAPDH only (Figure 2.3C).

Gene/accession number	**Sequence**	**UPL**
Gapdh (glyceraldehyde 3-phosphate Dehydrogenase) - NM_008084.3	cctgcttcaccaccttcttg	80
	tgtccgtcgtggatctgac	
Tbp (TATA-binding protein) -NM_013684	gatgggaattccaggagtca	97
	gggagaatcatggaccagaa	
Vegfa (vascular endothelial growth factor alpha) - NM_009505.4	ggttcccgaaaccct	4
	gcagcttgagttaaacgaacg	
	cagtggtactggcagctagaag	68

Vegfr2 (vascular endothelial growth factor receptor 2) - NM_010612.2	acaagcatacgggcttgttt	
Il6 (interleukin 6) - NM_031168.1	ccaggtagctatggtactccagaa	6
	gctaccaaactggatataatcagga	
Hif1a (hypoxia inducible factor 1 alpha) - NM_010431.2	cgctatccacatcaaagcaa	95
	gcactagacaaagttcacctgaga	
Thbs1 (thrombospondin 1) - NM_011580.3	gcaacaggaacaggacaccta	22
	cacctctccgggttactgag	
Gli3 (zinc finger protein GLI3) - NM_008130.2	caccaaaacagaacacattcca	71
	ggggtctgtgtaacgcttg	
Nr3c1 (nuclear receptor subfamily 3 group C member 1 - glucocorticoid receptor) - NM_008173.3	ggccgctcagtgttttctaa	17
	gcagagtttgggaggtggt	
Nr3c2 (nuclear receptor subfamily 3 group C member 2 -mineralocorticoid receptor) - NM_001083906.1	gcaggggtatggcatgtct	5
	gccggcatgaacttagga	
HSD11B1 (11β-hydroxysteroid dehydrogenase type I) - NM_008288.2	catgctgaagcagagcaatg	63
	tgcagagtagggagcaatca	
HSD11B2 (11β-hydroxysteroid dehydrogenase type II) - NM_008289.2	cactcgaggggacgtattgt	95
	ccctcttctgggctctgg	

Col1a1 (type I collagen) – NM_007742.3	ccgctggtcaagatggtc	1
	ctccagcctttccaggttct	
Cxcl9 (chemokine (C-X-C motif) ligand 9) - NM_008599.4	gcatcgtgcattccttatca	1
	cttttcctcttgggcatcat	
TNF (tumour necrosis factor) - NM_013693.3	ctgtagcccacgtcgtagc	25
	ttgagatccatgccgttg	
Acta2 (alpha smooth muscle actin) - NM_007392.3	atttaaaaagtctcactatgcacctg	69
	ggatgttggccaaaggag	
Tlr9 (toll-like receptor 9) - NM_031178.2	ctcggaacaacctggtgact	106
	actggaggcgtgagagattg	
Cxcl2 (chemokine (C-X-C motif) ligand 2 - NM_009140.2	aaaatcatccaaaagatactgaacaa	26
	ctttggttcttccgttgagg	
Itga10 (integrin alpha-10) - NM_001302471.1	gtgcttcaagctgacatgga	1
	cagcactttctgtcgtccac	
Tnfrsf9 (tumor necrosis factor receptor superfamily member 9) - NM_001077509.1	ttgaggggaatcttcagagc	2
	tgaaaagcctgacacagagg	

Tnfrsf21 (tumor necrosis factor receptor superfamily member 21) - NM_178589.3	catgctgcatatcctgaacc	17
	tcagcctggggaatctctt	
Tnfrsf23 (tumor necrosis factor receptor superfamily member 23) - NM_024290.4	ccataatgatgccccaatgt	4
	ttgataataaaagaataaggggtgatg	
Ccl11 (C-C motif chemokine 11) - NM_011330.3	cacggtcacttccttcacct	4
	tggggatcttcttactggtca	
Pf4 (platelet factor 4) - NM_019932.4	catctcctctgggatccatct	9
	ccattcttcagggtggctat	
Fas (tumour necrosis factor receptor superfamily member 6) - NM_007987.2	caagtgcaagtgcaaaccag	2
	gggttccatgttcacacga	
Csf1 (colony stimulating factor 1) - NM_007778.4	cagcctccttcctgttgtct	1
	ccagagcttgtgacaggaca	
Dcn (decorin) - NM_001190451.2	gagggaactccacttggaca	3
	ttgttgttgtgaaggtagacgac	
Stat2 (signal transducer and activator of transcription 2) - NM_019963.1	gggtgttactaccaggaaaaagtta	6
	cagctcgtccacctgtctg	

Angptl2 (angiopoietin-like 2) - NM_011923.4	ctggacagggaccatgatgt	88
	ggagtgagcacaggcgttat	
Cspg4 (Chondroitin Sulfate Proteoglycan 4) - NM_139001.2	ccacttcgacctctctgacg	2
	gccaccactcggaagaaat	
Nos2 (nitric oxide synthase (inducible) - NM_010927.4	ggagcctttagacctcaacaga	3
	aaggtgagctgaacgaggag	
Arg1 (Arginase) - NM_007482.3	gaatctgcatgggcaacc	2
	gaatcctggtacatctgggaac	

Table 2.5 – Details of primers and UPL probes used for qPCR. Forward (upper row) and reverse (lower row) primers are shown. UPL number refers to the probe used for the assay.

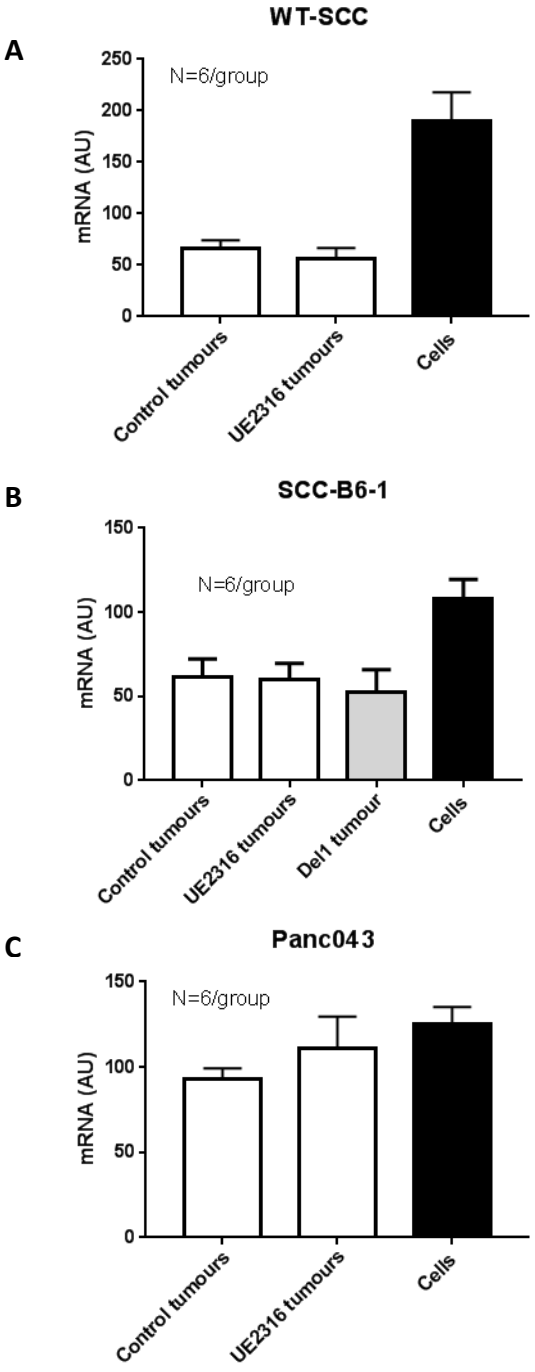

Figure 2.3 – Averaged housekeeping gene expression. GAPDH and TBP were selected and averaged to give housekeeping gene concentrations to which other gene expression could be normalised. A and B) No differences were seen between treatment groups within SCC tumour types, however higher expression was seen in SCC tumour cells. C) No differences were seen between treatment groups within Panc043 tumour types, and Panc043 cell expression did not differ from tumour.

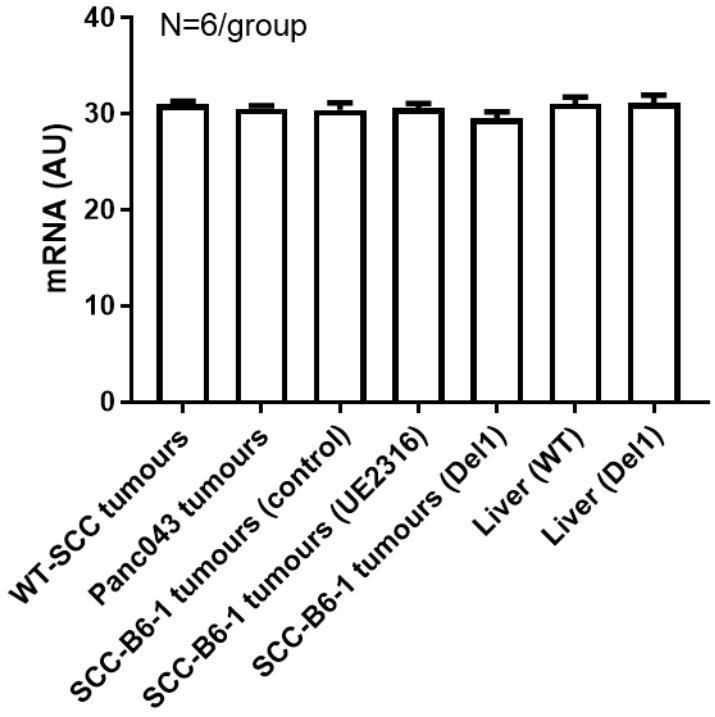

Figure 2.4 – Averaged housekeeping genes. GAPDH and TBP were selected and averaged to give housekeeping gene concentrations to which other gene expression could be normalised. No differences were seen between any of the tissues or treatment groups.

2.3.7 ELISA

To measure corticosterone in murine plasma, a corticosterone ELISA kit (Enzo Life Sciences) was used as per manufacturer's instructions. Plates were read using a microplate reader (OPTImax; 405-580nm, 22.1°C).

2.3.8 Enzyme activity assays

2.3.8.1 Protein assay

Tissue samples were homogenised in homogenisation buffer (**Section 2.1.2**) and diluted (1/20). A BioRad protein DC assay (BioRad, Hemel-Hempsted, UK) was performed as per manufacturer's instructions to determine protein concentration. Homogenates were stored undiluted at -80°C until needed.

2.3.8.2 Dehydrogenase activity assay for tissue homogenate

Samples were prepared in duplicate and kept on ice. Samples were diluted in C buffer (**Section 2.1.2**) to the required concentration in a 250µL final volume, but made up to 190µL in C buffer. For the final assay, 10µL ^{3}H-B (250nM), 50µL NADP+ (2mM; Cambridge Bioscience) and 190µL sample were added to 12x75mm borosilicate glass culture tubes, which were covered with parafilm and incubated in a shaking water bath (37°C) (three controls were run at each time-point: a protein-free control; a co-factor free control; and a protein/co-factor free control; with buffer used in lieu). After incubation, samples were placed on ice, mixed with 1mL ethyl acetate by vortex and allowed to settle. The top layer was transferred by glass pipette to a Chromacol vial (Thermo-Fisher) and condensed under nitrogen gas at 60°C. Samples were re-suspended in 600µL mobile phase (65% water, 15% acetonitrile, 25% methanol) and sealed. Based on optimisation experiments, protein concentration and incubation time differed between WT-SCC (0.5mg/mL, 90 min), Panc043 (0.5mg/mL, 24 hours) and SCC-B6-1 (0.125mg/mL, 90 min) tumour homogenates. The following controls were also prepared in duplicate: Buffer + B (buffer replacing protein and co-factor), no protein (buffer replacing protein) and no cofactor (buffer replacing cofactor).

2.3.8.3 **Reductase activity assay for intact tissue**

2.3.8.3.1 *Intact tissue incubation*

Whole liver and aorta were excised from mice killed by cervical dislocation. Liver was cut into small pieces and weighed (10-20mg). Aortae were weighed then sectioned into four rings (~3mm length). 4 pieces were cut from liver using sterile dissection equipment and weighed (5-20mg). Single liver pieces and whole aortae (four rings) were placed in wells of a 12 well plate in 1mL treatment media and incubated for 24 hours (5% CO_2, 37°C). Treatments were applied to each mouse in duplicate. UE2316-treated liver pieces (N=6) were cultured in 1mL DMEM-F12 medium containing 12.5nM ^{3}H-cortisone and1µM cold cortisone and 300nM UE2316. Control liver pieces (N=6) were cultured in the above medium with vehicle added in lieu of UE2316. All wells had a final DMSO concentration of 0.3%. The following controls were also prepared: blank media; treatment control (+ treatment, no tissue); standard control (+0.5µl substrate in 1mL media). Media was aspirated after incubation and stored in 7mL glass bijous (samples could be frozen at this point for later extraction). All samples were run in duplicate.

2.3.8.3.2 *Extraction*

Samples were passed through Sep-Pak C-18 cartridges (Waters, Elstree, UK); Sep-Paks were inserted into 20-position extraction manifold chamber (Waters) and a 5mL syringe used to prime columns with 5mL methanol, followed by 5mL HPLC-grade H_2O. Samples (1mL) were added to the column, washed with 5mL HPLC-grade H_2O and eluted with 2mL methanol for collection into 13 x 75mL tubes. These samples were dried down (N_2, 60°C), resuspended in 200µL HPLC-grade H_2O and ethyl acetate extraction performed (10:1, vortex sample with 2mL ethyl acetate and remove upper phase to 12.x75mL tube) to remove phenol red contamination. Samples were dried down, resuspended in 600µL mobile phase (60% water, 40% methanol), transferred to chromacol vials, and sealed.

2.3.8.4 **High-Performance Liquid Chromatography**

Samples were detected by HPLC with online scintillation counting. Set-up consisted of an autosampler (717 plus) maintained at 4°C, a mobile phase pump (pump600,

Berthold, Harpenden, UK), a column heater and a radioflow detector (LB509, Berthold) connected to a scintillation fluid pump (flow: 2ml/min).

2.3.8.4.1 *Elution of steroids*

200µL of sample were injected into the HPLC system, equipped with a C-18 Sunfire symmetry column (15cm length, 4.6mm diameter, pore size µm; Water, Edinburgh, UK). A run time of 35 minutes (60:15:25 mobile phase, 1.5ml.min flow, 35°C column temperature) was required to detect 11-DHC (elution time: 15.8 min) and corticosterone (elution time: 23.4 min). Detected peaks had a width <2 minutes and were at least 3x higher than background. A run time of 35 minutes (60:40 mobile phase, 1.2mL/min flow, 34°C column temperature) was used to detect cortisone (elution time: 22.9 min) and cortisol (elution time: 28.7 min).

2.3.8.4.2 *Quantitation*

Peaks were manually integrated and converted to % substrate and product formed. Amount of product formed (nmol) was then calculated from the known amount of substrate and data were expressed as the reaction velocity (product formed per unit incubation time per unit protein concentration; nmol/min/mg).

2.3.9 Liquid chromatography tandem mass spectrometry

Initially, optimisation of a dual-extraction method for corticosteroids and UE2316 was attempted to conserve plasma. This approach proved problematic due to differences in the extraction efficiencies between compounds/solvents (superior recovery of steroids was achieved using chloroform, while UE2316 recovery was better with ethyl acetate). Thus separate extractions were performed for corticosteroids and UE2316.

2.3.9.1 **Liquid-liquid extraction of corticosteroids from plasma samples**

A 12-point aqueous extracted standard curve was prepared in 100µL HPLC-grade H_2O (0 - 50ng A/B) alongside plasma samples. 2.5ng internal standard (d4F) was added to all samples/standards and a double blank was prepared (no internal standard). Samples/standards were mixed with a 10x volume of chloroform, vortexed and allowed to settle. The upper solvent phase was transferred by glass pipette into a 3.5mL vial. Samples were concentrated under nitrogen gas at 60°C before resuspension in

70µL mobile phase (70:30 water/acetonitrile) and transfer to liquid chromatography (LC) vials (Waters).

2.3.9.2 Liquid-liquid extraction of UE2316 from plasma samples

A 12-point aqueous-extracted standard curve was prepared in 150µL human plasma (0 - 500ng UE2316) alongside plasma samples. 2.5ng internal standard (UE2341) was added to all samples/standards and a double blank was prepared (no internal standard). Samples/standards were mixed with a 10x volume of ethyl acetate, vortexed and allowed to settle. The upper solvent phase was transferred by glass pipette into a 3.5mL vial. Samples concentrated under nitrogen gas at 60°C before resuspension in 70µL mobile phase (70:30 water/acetonitrile) and transfer to LC vials (Waters).

2.3.9.3 Liquid-liquid extraction of UE2316 and corticosteroids from liver and tumour samples

2.3.9.3.1 *Tissue homogenisation*

200-400mg liver tissue (weights recorded) or tumour tissue (whole tumour, ~30-50mg) was homogenised in 1mL Krebs buffer (**Section 2.1.2**) in 1.5mL Eppendorf tubes using a tissue homogeniser. Tissue was homogenised at full speed for 20s, allowed to settle, then homogenised for a further 10s to ensure complete tissue disruption. The homogeniser was cleaned with ethanol and 2 x distilled H_2O rinses between samples. 10µL of a 250ng/mL UE2341/d4f internal standard combined stock was added to samples.

2.3.9.3.2 *Tissue extraction*

Samples were spun by centrifuge (15 min x 16,100 x g, 4°C) and supernatant (approx. 1mL) removed to a 13 x 100mm vial. A 5x volume of ethyl acetate was added and samples vortexed for 20s. Samples were then spun by centrifuge (2 min x 1000 x g, 4°C) and the top (clear) layer transferred to a new 13 x 100mm vial by glass pipette (this step was performed twice). Samples were condensed under nitrogen gas at 60°C and resuspended in 2mL 30% methanol/H_2O. These were then passed through Sep-Pak C18 cartridges (5mL methanol prime, 5mL water prime, 2mL sample, 5mL water wash, elution with 2mL methanol), collected into 13 x 100 mL vials and condensed

under nitrogen gas at 60°C. Samples were then resuspended in 100µL of mobile phase (70:30 water:acetonitrile).

A 10 point standard curve was prepared and extracted as described above in 1mL Krebs in the absence of tissue.

2.3.9.3.3 *Optimisation of tissue extraction*

The method for extracting corticosteroids and UE2316 from tissue required optimisation to achieve clean samples with sufficient analyte detectability.

Ethyl acetate extraction

The optimal ratio of ethyl acetate to sample, and the number of ethyl acetate extractions required, were both determined by testing a range of ratios (3:1, 5:1 and 10:1 compared to unextracted analytes) and performing the extraction either once, twice or three times. Extractions were performed on 1mL H_2O samples spiked with 10ng of A/B/UE216/2341/d4F, with samples in triplicate for each condition. Ethyl acetate extractions were performed and samples then condensed and resuspended in 100µL mobile phase (70:30 water:acetonitrile). Samples were measured as described in **Section 2.3.8.4**. As shown in Figure 2.5A, maximum recovery was achieved using a 5:1 double extraction.

Sep-Pak recovery

Initial attempts to extract tissue without the addition of solid phase extraction resulted in cloudy samples with a fat-like contaminant. Solid phase extraction was thus considered as a clean-up step. To assess recovery with solid phase extraction, Sep paks were primed with 5mL methanol and 5mL H_2O, followed by the addition of 5mL H_2O spiked with 10ng A/B/UE2316/2341/d4F. Columns were washed with 5mL H_2O wash, and samples eluted with 2mL methanol. Eluted samples were then condensed (nitrogen gas, 60°C) and resuspended in 100µL mobile phase (70:30 water:acetonitrile) and run alongside an unextracted preparation of 10ng A/B/2316/2341/d4F (run conditions as described in **Section 2.3.8.4**). Recovery was calculated by dividing extracted peak area by unextracted peak area. Solid phase extraction resulted in reduced recovery of all analytes, though all were still well within the limits of detection (Figure 2.5B).

Extraction recovery and matrix recovery

To determine the relative contribution of the extraction process and the tissue matrix to signal loss, the recovery after solid phase extraction was calculated, as well as the matrix suppression caused by the tissue itself. This was determined by preparing, in triplicate; pre-spiked livers; post-spiked livers; and unextracted standards. Livers were from FVB/N mice. 10ng of analyte mixture (A/B/UE2316/UE2341/d4F) in 10µL methanol) was spiked onto pre-spiked liver, and extractions performed as described in **Sections 2.3.9.3.1-2** (internal standard was only added as part of the pre-spike mixture). Post-spiked livers had the analyte mixture added in 100µL mobile phase (70:30 water:acetonitrile) after the extraction process. Unextracted standards were 10µL of the analyte mixture condensed (nitrogen gas, 60°C) and resuspended in 100µL mobile phase. Extraction recovery was calculated by dividing pre-spike peak area by post-spike peak area. Matrix recovery was calculated by dividing post-spike peak area by unextracted peak area. A/d4F/UE2316 showed similar extraction and matrix recovery, while B showed superior recovery compared to other analytes (Figure 2.5C). UE2341 showed 41% signal attenuation in the presence of matrix however as an internal standard this was not considered problematic as levels were consistent between samples.

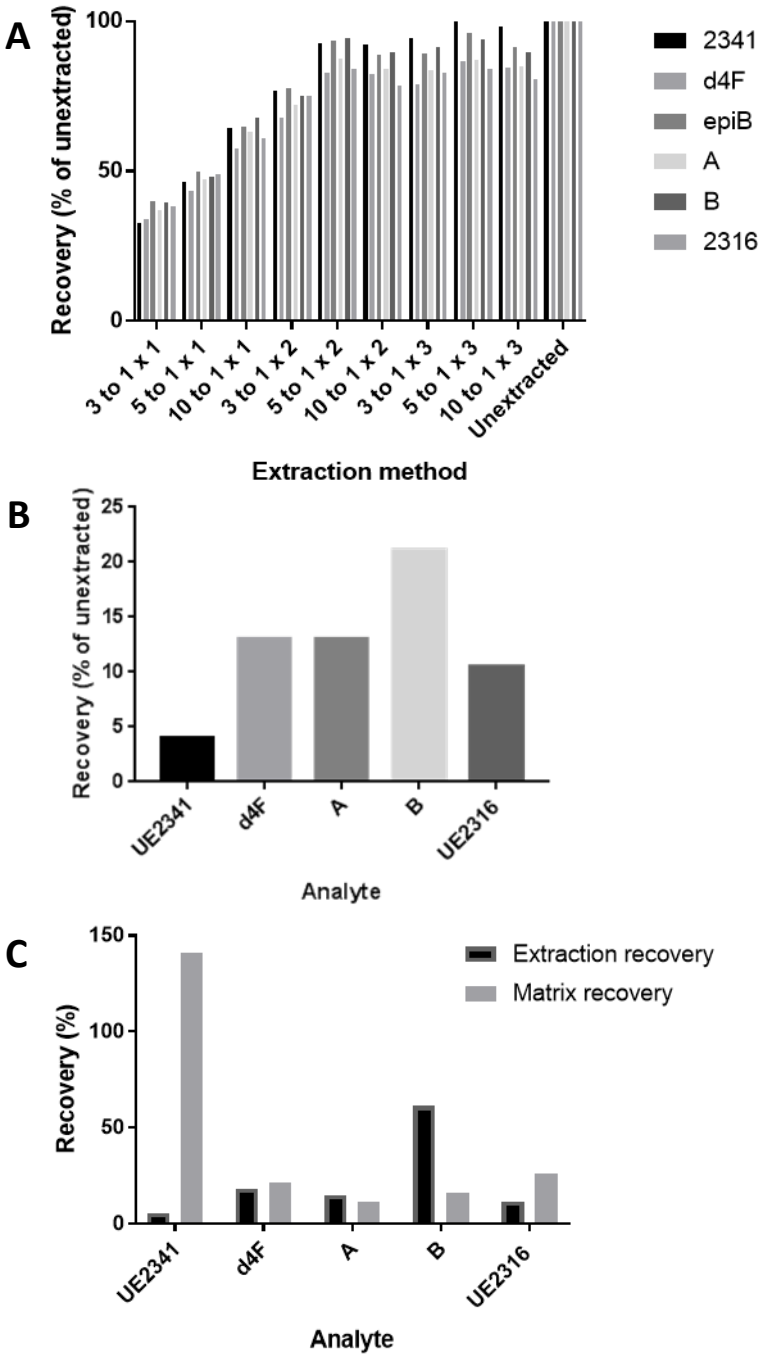

Figure 2.5 - Tissue extraction optimisation for mass spectrometry. A) Analyte recovery plateaus at a 5 to 1 double extraction, identifying this approach as optimal. B) Recovery of analytes in water after sep-pak extraction, as expressed as % of unextracted sample. C) Extraction and matrix recovery were acceptable for all analytes, though signal attenuation is apparent for UE2341 in the presence of matrix. All extractions performed in triplicate.

2.3.9.4 Tandem mass spectrometry

Mass spectrometry staff (Dr Natalie Homer, George Just and Dr Karen Sooy) operated the mass spectrometer and decided upon appropriate analytical parameters for all mass spectrometry experiments. The mass spectrometry system used was a Nexera LC-30AD Ultra High-Performance Liquid Chromatograph (UHPLC) connected to a Nexera SIL-30 AC autosampler (Shimadzu, Kyoto, Japan). The mass spectrometer was a QTRAP 6500+ operated with an electrospray ionisation Turbo V source (SCIEX, Framingham, USA). 30µL sample was injected onto a C18-AR column (Ace Excel, 2µm, 150x2.1mm). Analytes were eluted under a gradient of 30% acetonitrile increasing to 90% over 9 minutes at a flow rate of 0.5mL/min at 40°C. Column temperature was 40°C and sample temperature 10°C. Ionisation was achieved by positive ion electrospray, using a spray voltage of 5500 V, temperature of 700°C, curtain gas pressure of 40 psi, ion source gas 1 40psi, ion source gas 2 60psi and entrance potential 10. Analytes were measured by multiple reaction monitoring (declustering potential, collision energy, cell exit potential): corticosterone m/z 347→121 (66, 69, 8V); 11-DHC m/z 345→121 (51, 133, 8V); UE2316 m/z 389→177 (100, 39, 15V); UE2341 (internal standard) m/z 356→177 (85, 37.5, 17V); D4F (internal standard) m/z 367→121 (121, 25, 20V). Peaks area ratios were compared with corresponding standards.

2.3.10 Genotyping of Del1 animals

Genomic DNA isolation was performed using a GeneJET genomic DNA purification kit (Thermofisher) as per manufacturer's instructions.

Primers (100µM stocks, Table 2.6) were combined in equal proportions to make a primermix solution. A mastermix solution was prepared (12.5µL biomix red (Bioline, London, UK) + 8.5µL dH_2O per sample). 3µL primermix solution was added to 1µlL DNA/sample in a 0.2mL tube. Samples were transferred to a thermal cycler for initial denaturation (5 min x 95°C). 21µL mastermix was then added to each sample to give a total reaction volume of 25µl. Samples underwent 30 cycles (1 min x 95°C, 1 min x 61°C, 2 min x 72°C) and a final extension step (10 min x 72°C). Samples were then

run on an agarose gel (1% agarose in TAE buffer, 120V, 45 min) and imaged on a UV transilluminator.

Primer code	Sequence (5'-3')
Yuri2oligo4	CAC TGC ATT CTA GTT GTG GTT TGT CC
Ex1-3F1	TTC TTC GTG TGT CCT ACA GG
Ex1-3R1	CCC GCC TTG ACA ATA AAT TG

Table 2.6 - Genotyping primers.

2.3.11 Aortic ring assay

2.3.11.1 Tissue collection

8-12 week old female mice were culled (exposure to increasing concentration of CO_2) and the thoracic aorta dissected out and trimmed of adipose tissue and branching vessels. Mice were pinned out and fur washed with ethanol. The thoracic cavity was opened and the lungs and oesophagus removed using dissection scissors and forceps. The aorta was severed proximal to the diaphragm and 0.5mL Opti-MEM (Thermo) was injected into the heart to flush blood out of the aorta. The aorta was then removed by applying gentle tension to the vessel and cutting through the perivascular fat and connective tissue with micro scissors and fine tip forceps. Isolated aortae were transferred to opti-MEM and trimmed of perivascular fat and smaller branching vessels, then sectioned into 18 rings (1mm length) using micro scissors and fine tip forceps.

2.3.11.2 Tissue culture

Aortic rings were cultured in 96-well plates, prepared as follows; rat tail collagen (EMD Millipore, Massachusetts, USA) was diluted to 1mg/mL in Opti-MEM and pH adjusted using 10µl/mL 1N NaOH to give a pink colour. Collagen was stored on ice throughout the process. 50µL of collagen was added to wells and aortic rings embedded using forceps (this was performed quickly to prevent premature polymerisation of collagen). Rings were orientated so that the vessel lumen was

parallel to the bottom of the well. Plates were incubated for one hour at 37°C to allow collagen to set, after which 150µL of media was added. Treatments were added to rings in 150µl of Opti-MEM supplemented with 2% FCS (days 0-3), 0.5U/mL heparin and 5ng/mL VEGF. Media were changed on days 3 and 5 and vessels were imaged and quantified on day 7. An equal concentration of ethanol/DMSO was present in all wells (0.3%).

2.3.11.3 Vessel quantification

Vessels were counted manually using the 10x objective lens on a culture microscope (Olympus CK40, Olympus, Southend-on-Sea, UK) on day 7, using the method described by Nicosia & Ottinetti (1990). For the 11-DHC curve in Section 4.2.1, vessels counts from day 6/7 were pooled as equipment failure necessitated early conclusion of the study, however growth was sufficiently healthy to allow for this.

2.3.12 Optimisation of the aortic ring assay

In order to confirm the ideal experimental conditions under which to measure the effects of glucocorticoids and UE2316 on *ex vivo* angiogenesis, the standard lab protocol was optimised.

2.3.12.1 Tissue collection

Aortic rings were harvested from C57BL6/J mice (female, aged 10-12 weeks). For optimisation studies, a single mouse was used for each study.

2.3.12.2 Tissue culture

2.3.12.2.1 *Basal media conditions optimisation*

Rings were cultured as described in **Section 2.3.10.2**, with treatments (Table 2.7) added to rings in 150µL opti-MEM. Exposures were performed in triplicate. Media were added at day 0, and changed on days 3, 5 and 7. Vessel counts were performed on days 5, 7 and 10.

Condition	Day 0-3	Day 4-7
FCS + VEGF	2% FCS + 5ng/mL VEGF	5ng/mL VEGF
FCS only	2% FCS	2% FCS
VEGF only	5ng/mL VEGF	5ng/mL VEGF
Blank	-	-

Table 2.7 - Media conditions for aortic ring assay optimisation. Exposures were replicated in triplicate. 150µL of media were added to each well. Media were added at day 0 and changed on days 3, 5 and 7. Vessels were quantified on days 5, 7 and 10.

2% FCS + 5ng/mL VEGF caused sustained vessel growth that continued to day 10. Removal of VEGF from media led to a peak vessel count at day 7, after which vessels began to regress. 5ng/mL VEGF or opti-MEM alone led to poor growth with vessels beginning to regress after day 5 (Figure 2.6). Comparison of vessel counts performed at day 7 suggests that 2% FCS + 5ng/mL VEGF stimulate the most vessel growth (62.7 ± 22 vessels), leading to selection of these conditions for future experiments. Day 7 was selected as the optimal day for quantification.

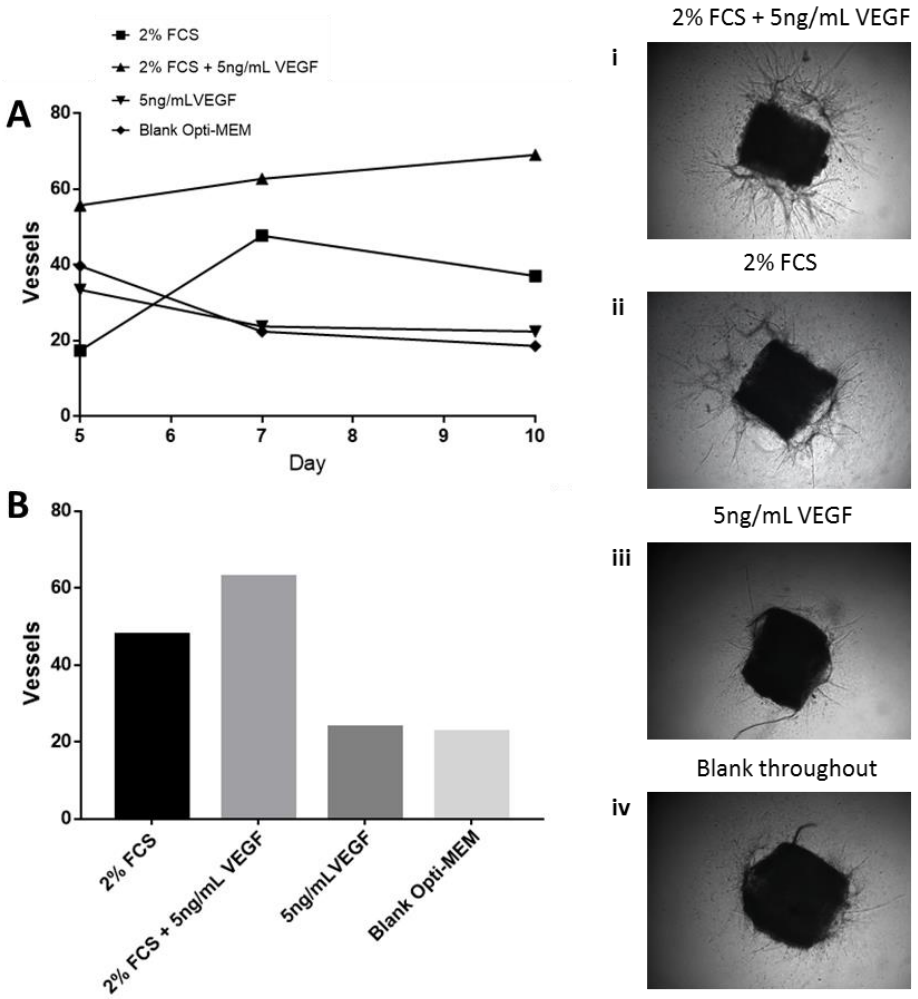

Figure 2.6 - Aortic ring assay optimisation. A) Aortic rings respond differently to different basal media conditions. Foetal Calf Serum (FCS) was used only between days 0-3 while VEGF was maintained throughout. Stimulation with both VEGF and FCS caused enhanced growth that was sustained for 10+ days (i), while stimulation with FCS alone led to a growth peak at day 7 (ii). VEGF (iii) and opti-MEM (iv) alone led to poor growth with vessel growth peaking at day 5 before regression. Images taken at day 7. B) Day 7 counts indicate that 2% FCS + 5ng/mL VEGF is the optimum basal media for the investigation. N=1, treatments in triplicate.

2.3.12.3 Effect of heparin on vessel growth

The presence of heparin is reportedly required to facilitate the angiostatic effects of glucocorticoids (Folkman *et al.*, 1983). In preliminary experiments (not shown), higher concentrations of heparin (60U/mL) were found to inhibit vessel growth. Thus the present optimisation experiment was performed to determine the optimal concentration of heparin required. Rings were cultured as described in **Section 2.3.10.2**, with treatments (Table 2.8) added to rings in 150µL opti-MEM media + 2% FCS (days 0-3) and 5ng/mL VEGF. Exposures were performed in triplicate. Media was added at day 0, and changed on days 3 and 5. Vessels were counted on day 7 only.

2.3.12.3.1 *Heparin optimisation study*

Condition	**Vehicle/Corticosterone**	**Heparin (U/mL)**
Vehicle	0.3% ethanol	-
Vehicle + low heparin	0.3% ethanol	1
Vehicle + high heparin	0.3% ethanol	10
Corticosterone	300nM corticosterone	-
Corticosterone + low heparin	300nM corticosterone	1
Corticosterone + high heparin	300nM corticosterone	10

Table 2.8 - Media conditions for heparin optimisation. Exposures were performed in triplicate. 150µL of media + 2% FCS (days 0-3) + 5ng/mL VEGF were added to each well. Media were added at day 0 and changed on days 3 and 5. Vessels were quantified on day 7.

Aortic rings were cultured in the presence of vehicle or 300nM corticosterone, in media containing 0-10U/mL heparin (Figure 2.7). Increasing heparin concentration reduced vessel number. Adding 1U/mL heparin to aortic rings reduced vessel number in all rings by day 7 and amplified the reduction in vessels in the presence of corticosterone. Increasing the heparin concentration to 10U/mL caused severe

angiostasis in all ring to the degree that the angiostatic effects of corticosterone were slightly masked (61% decrease). Thus, a low concentration of heparin (0.5U/mL) was selected for future studies.

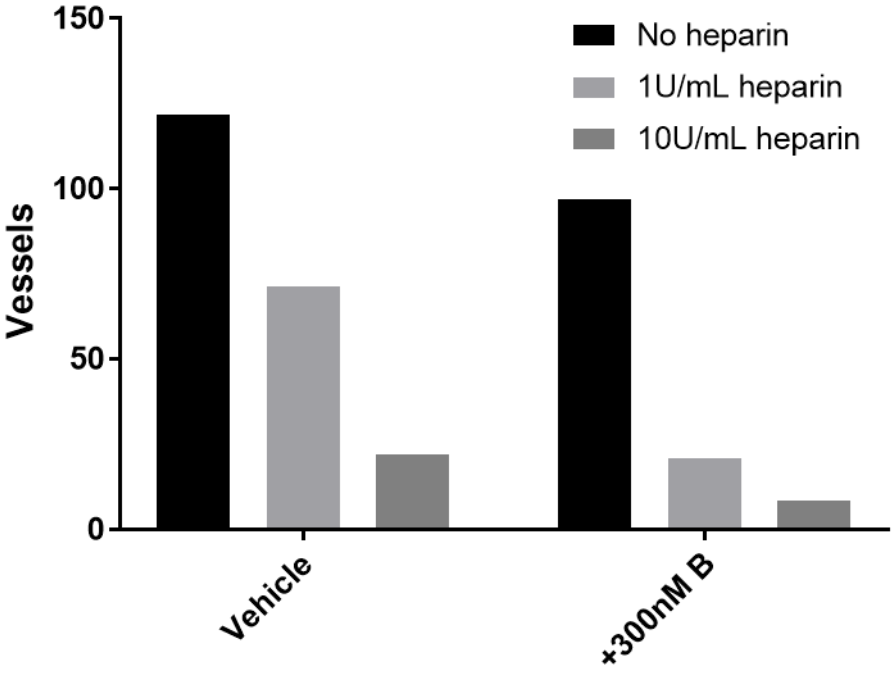

Figure 2.7 - Optimising heparin conditions for glucocorticoid aortic ring assays. A high concentration of heparin in aortic ring medium reduced the number of vessel outgrowths at Day 7, while removing heparin altogether appears to reduce the degree of corticosterone-mediated angiostasis. 1U/mL causes a lesser degree of growth inhibition while still facilitating steroid-mediated angiostasis. N=1, treatments in triplicate.

2.3.13 Cell growth analysis

2.3.13.1 Manual cell counts

Cells were seeded into 6-well plates at a density of 30,000 cells per well (number determined by preliminary experiment), topped up with 2mL media and left to adhere over 12 hours. Once cells were adhered, media was replaced with treatment media (vehicle control and UE2316 at 37.5nM, 75nM, 150nM, 300nM and 600nM). All treatments were in duplicate and each well contained an equal concentration of DMSO (0.6%). After 48 hours cells were trypsinised and pelleted by centrifugation (1000rpm x 5min) then resupended in 1mL media for counting. Counts were performed by haemocytometer - all data were expressed as % of control.

2.3.13.2 Live cell imaging and alamarBlue assay

100µL cells in standard media (charcoal stripped FCS was used in these experiments, **Section 2.3.1.1**) were seeded into 96-well plates (Bio-Greiner) and left for 16 hours to adhere before media was replaced with 100µL of treatment media. Cells were seeded at a density of 10000 cells/mL (SCC-B6-1 and Panc-043) or 5000 cells per well (WT-SCC). All treatments were in sextuplet and all wells contained an equal concentration of ethanol/DMSO (0.6%) as vehicle controls for corticosteroids and UE2316 respectively. Plates were imaged over the subsequent 72 hours (1 image per three hours) using the Incucyte ZOOM Live-cell analysis system (Essen BioScience) and a threshold applied to provide a measure of confluence (Segmentation 0.4, cutoff 400µm). After 72 hours, samples were incubated with 10µl of alamarBlue cell viability dye (Thermo-Fisher) for 3 hours and read by plate reader (Envision Multilabel, Perkin Elmer; filter settings of 560EX nm/590EM. Room temperature) to provide a secondary measure of viable cell number.

2.3.14 Systemic corticosterone manipulation

2.3.14.1 Cell injection

WT-SCC cells were prepared and injected subcutaneously into both flanks of FVB/N mice. Treatments began on the same day as tumour implantation and the final

injections were delivered 24 hours before the cull. Injection volume did not exceed 0.3mL.

2.3.14.2 Tumour development

Tumours were allowed to develop over the subsequent 14 days during which they were measured by callipers every 2-3 days. Measurements were blinded where possible by masking of cage labels and randomisation of cages by a second individual. Mice and diet were weighed and mice checked for any unexpected signs of ill health every 2-3 days.

2.3.14.3 Tissue collection

At the end of the experiment, mice were culled by cervical dislocation and tissues harvested. Blood was collected rapidly from the thoracic cavity using a syringe without a needle and stored in anti-coagulant EDTA-treated tubes (Sarstedt). Plasma was separated from whole blood by centrifugation (2000 RCF x 10 min at 4°C) for storage at -20°C. Tumours were weighed upon removal and halved (one half was snap frozen in liquid nitrogen for storage at -80°C, the other half was fixed in formalin for 24 hours before transfer to 70% ethanol before wax processing). All other required tissues were removed and snap frozen in liquid nitrogen before storage at -80°C.

2.3.15 RNA-sequencing

RNA was sequenced using a combination of paired and single-end RNA-sequencing by GATC Biotech (Constance, Germany).

Bioinformatics analysis was kindly performed by Dr Stuart Aitken. Raw data (fastq files) were processed using Tophat2 (Trapnell *et al.,* 2009), which was used to map reads to the mouse mm10 reference genome. Mapped data (bam files) were then processed using Cuffdiff (Trapnell *et al.,* 2012), which was used to analyse differential gene expression between groups. A Principle Component Analysis (PCA) was performed to assess variance between samples (both between and within groups). DEseq2 (Love *et al.*, 2014) was used for the PCA.

Gene ontology analysis was performed using the Database for Annotation, Visualization and Integrated Discovery (DAVID) v6.8, which uses a modified Fisher Exact test to determine whether the proportion of genes in a given list is significantly associated with a pathway compared to the murine genome.

2.4 Data analysis and statistics

All statistics were performed using Prism software v6/7 (Graphpad). Data are presented as mean ± S.E. Outliers were identified using a Grubbs test and excluded appropriately. All data sets were tested for normality using the Shapiro-Wilk or Kolmogorov-Smirnov tests (dependent on sample size) and analysed appropriately based on the result. Non-parametric data were transformed where possible to allow for the use of parametric tests. Where this was not possible, non-parametric tests were used. Repeated-measures data with 2 or more independent variables were compared using repeated measures 2-way ANOVA, with Tukey's post-hoc test where appropriate. Two independent samples were compared using the independent samples t-test (or Mann-Whitney U test where data had a non-parametric distribution). Three or more independent samples were compared using one-way anova with Tukey's post-hoc test. The Kruskal-Wallis test was used to compare 3 or more independent groups of non-parametric data, with Dunn's post-hoc test used to make specific comparisons. N number refers to the number of animals per group in an experiment, with the exception of cell culture studies, in which N number refers to biological repeats on separate days using the same cell line. A P value of <0.05 was considered significant, a value of 0.05-0.15 was considered a trend.

Chapter 3

11β-HSD1 inhibition and tumour growth

3 11β-HSD1 inhibition and tumour growth

3.1 Introduction

11β-HSD1 catalyses the conversion of inert glucocorticoids (11-dehydrocorticosterone, cortisone) and their active counterparts (corticosterone, cortisol) (Seckl and Walker, 2001). Selective 11β-HSD1 inhibitors have been developed to improve glycaemic control in diabetic patients (Anderson and Walker, 2013) and to improve cognitive function (Sooy *et al.*, 2015). In addition to their beneficial effects on glucose homeostasis and cognition, 11β-HSD1 inhibition and deletion has been shown to increase angiogenesis, an effect that promotes wound healing and recovery after induced myocardial infarction in rodents (Small *et al.*, 2005; McSweeney *et al.*, 2010).

The mechanisms behind this proangiogenic effect remain largely unknown. McSweeney *et al.* (2010) showed that increased recruitment of pro-reparative macrophages preceded enhanced angiogenesis, while Logie *et al.* (2010) found that glucocorticoids induced cytoskeletal changes and increased thrombospondin 1 (TSP-1) expression in cultured endothelial cells. Although promotion of angiogenesis can be beneficial, there is a concern that 11β-HSD1 inhibitors could promote pathological angiogenesis such as that seen in tumour growth and proliferative diabetic retinopathy (PDR).

Investigation of the retina in mice with systemic 11β-HSD1 inhibition/global deletion did not find evidence of enhanced pathological neovascularisation (Davidson *et al.*, 2017), suggesting that it is unlikely to exacerbate PDR. 11β-HSD1 was not present in the retinal vessels, which may explain the lack of effect seen in this model. This does not mean, however, that inhibiting 11β-HSD1 would not increase angiogenesis in other conditions. There is very little in the literature examining the role of 11β-HSD1 specifically in tumours. Liu *et al.* (2016) report that overexpression of the enzyme in hepatocellular carcinoma decreased metastasis, angiogenesis and tumour size in mice via reduced glycolysis, suggesting that increased generation of active glucocorticoids could reduce tumour growth. The present studies used an established murine model of

subcutaneous solid tumour growth in conjunction with UE2316, a novel small molecule inhibitor of murine 11β-HSD1 developed at the University of Edinburgh (Sooy *et al.,* 2015), to investigate this risk.

The tumour cell lines used for these experiments have distinct genetic origins which may influence their response to 11β-HSD1 inhibition. Both SCC cell lines used were generated by using a two-stage DMBA/TPA chemical carcinogenesis protocol (McLean *et al.,* 2004). This protocol primarily targets the *Hras1* gene as an initiating mutation, predominantly in keratinocyte stem cells, while the promotion phase leads to trisomies of chromosomes 6 and 7 and mutations in the *Trp53* gene in mutated cells (Abel *et al.,* 2009). Of note, genetic background powerfully influences susceptibility to skin carcinogenesis; FVB/N mice are more sensitive than C57BL6/J mice to the chemical induction of SCC (Hennings *et al.,* 1993). The PDAC cell line used in these experiments is derived from the KPC mouse, a transgenic model with targeted mutations in the *Kras* and *Trp53* genes leading to the development of invasive PDAC (Hingorani *et al.,* 2005). Prediciting the influence of tumour cell genetics on 11β-HSD1 sensitivity is challenging given the lack of previous studies examining *Ras* mutations in the context of glucocorticoid exposure. The anti-angiogenic effects of glucocorticoids are mediated via the GR (Small *et al.,* 2005), and glucocorticoids cause a reduction in VEGF (Yano *et al.,* 2006) and an increase in the anti-angiogenic glycoprotein TSP-1 (Logie *et al.,* 2010), thus these factors are likely to be of relevance to 11β-HSD1 inhibition. The expression of the glucocorticoid receptor (GR) and mineralocorticoid receptor (MR) and the two 11β-HSD isozymes in tumours may confer varying degrees of sensitivity; high levels of both 11β-HSD1 and GR have been reported in squamous cell carcinomas (SCCs) (Azher *et al.,* 2016), identifying them as a tumour type potentially 'at risk' from 11β-HSD1 inhibition.

Hypotheses

The work described in this chapter addressed the hypotheses that:

- 11β-HSD1 inhibition/deletion will increase vessel density in, and the growth of, subcutaneous murine tumours

- Tumours with higher levels of 11β-HSD1 and GR will be more responsive to 11β-HSD1 inhibition than those with low levels of 11β-HSD1 and GR, showing a more rapid increase in size

Objectives

The specific aims of this work were:

(1) To determine whether inhibition/deletion of 11β-HSD1 increased:

(i) the size of subcutaneous tumours in mice

(ii) vascular density within murine tumours

(iii) mRNA levels of pro-angiogenic factors within murine tumours

(2) To determine whether expression of GR and 11β-HSD1 in tumours predicts sensitivity to 11β-HSD1 inhibition

(3) To determine the tissue distribution of UE2316 delivered via diet in different mouse strains

3.2 Results

3.2.1 11β-HSD1 inhibition enhances WT-SCC tumour growth

To investigate the effect of 11β-HSD1 inhibition on WT-SCC tumour growth, mice were injected with WT-SCC cells and fed either control or UE2316-RM1 diet. In the first of two experimental repeats, WT-SCC cells were injected into FVB/N mice (female, aged 10 weeks) fed either control or UE2316 diet (N=3/group). Tumours were grown for 16 days but began to regress after 11 days, resulting in poor quality tissue that could not be used for downstream analysis. Therefore, a second study was performed (N=6/group) using an identical protocol but with a pre-defined endpoint (day 11 after implantation). Data up to day 11 were pooled and reported as N=9/group (Figure 3.1) with all subsequent downstream analyses performed using tissue from the second study (N=6/group). WT-SCC tumours from UE2316-diet fed animals grew rapidly from day 4 onwards and reached a greater final volume (0.126 ± 0.029 cm^3) than mice fed standard RM-1 diet (day 11, 0.050 ± 0.006cm^3) (Figure 3.1A). UE2316- and control diet fed groups consumed similar quantities of diet (3.58 ± 0.21g RM-1 vs 3.30 ± 0.20g UE2316-RM1) and did not differ in weight throughout the experiment (Figure 3.1B and C). The estimated dosage achieved in the present studies (based on diet consumed per cage per 2-3 days) was 25-30mg/kg/mouse/day.

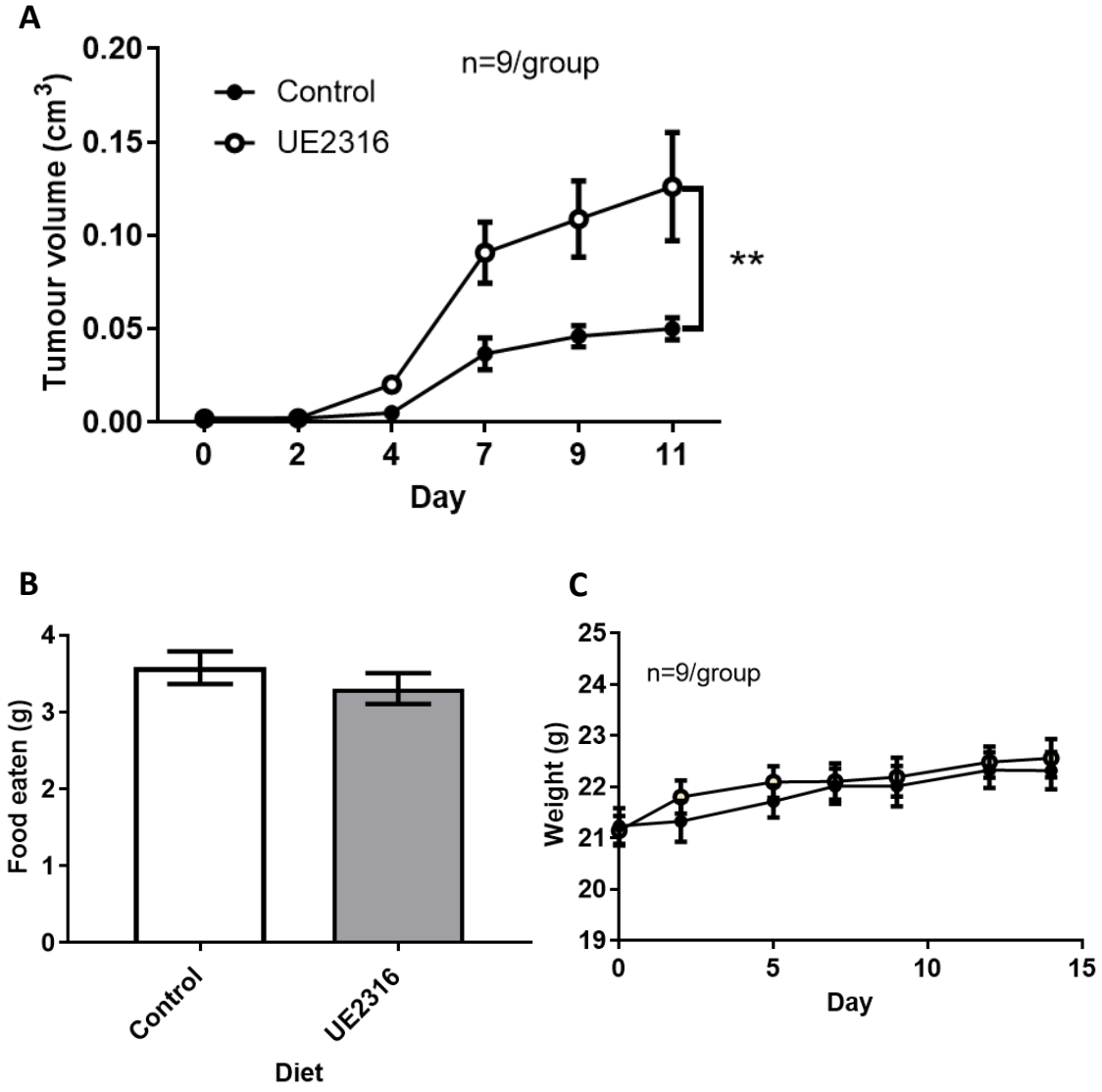

Figure 3.1 – The 11β-HSD1 inhibitor UE2316 enhanced squamous cell carcinoma tumour growth. A) Enhanced tumour growth was apparent from day 4 onwards in UE2316 diet-fed mice injected with the squamous cell carcinoma cell line WT-SCC. B) Mice consumed both UE2316 and control diets in comparable quantities. C) Neither WT-SCC cell injection (day 5) nor UE2316-diet introduction affected mouse weight. N=9/group. ** P<0.01. Data represent mean ± standard error and were compared by 2-Way ANOVA.

3.2.1.1 11β-HSD1 inhibition does not increase vessel density in WT-SCC tumours

To investigate the effect of 11β-HSD1 inhibition on vessels in tumours, experimental WT-SCC tumours were sectioned and stained for CD31/α-SMA-positive structures (Figure 3.2), which were quantified. Vessels staining positive for CD31 only were quantified separately to allow for the proportion of vessels lacking smooth muscle coverage to be quantified, providing an indication of vessel maturity. H+E section shown in Figure 3.2C.

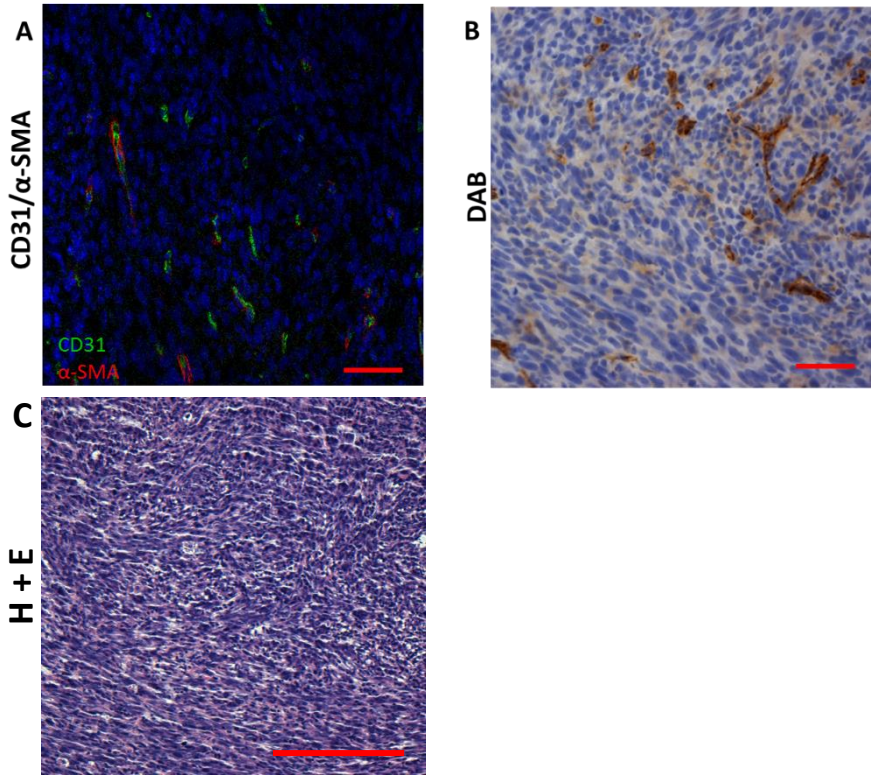

Figure 3.2 – Identification of vessels in WT-SCC tumours. A) Tumour tissue from WT-SCC tumours; endothelial cells are stained green (CD31 visualised with Alexa-Fluor 488) and smooth muscle cells are stained red (α-SMA visualised with Cy3). Nuclei are stained blue (DAPI). Tumours had densely packed nuclei and vessels were typically distinct from one another rather than forming complex branching networks. 200x magnification. Scale bar 50µm. B) CD31 was also visualised with diaminobenzidine (DAB) for Chalkley counts. 200x magnification. Scale bar 50µm.C) Haematoxylin and eosin-stained WT-SCC tumour tissue, demonstrating chaotic tissue organisation and high nuclear-density. 100x magnification. Scale bar 200µm.

The number of blood vessels per field of view did not differ between control (28.6 ± 1.3 vessels/mm^2) and UE2316-treated tumours (30.0 ± 1.9 vessels/mm^2) (Figure 3.3A). The proportion of vessels lacking smooth muscle coverage did not differ between control (47 ± 6%) and UE2316-treated tumours (51 ± 4%) (Figure 3.3B). Vessel number as determined by Chalkley counts did not differ between control (6.1 ± 0.5 counts) and UE2316-treated (6.0 ± 0.6 counts) mice (Figure 3.3C). Vascular hotspots did not differ in vessel number between control (179.4 ± 10.8) and UE2316-treated tumours (190.3 ± 21.7) (Figure 3.3D).

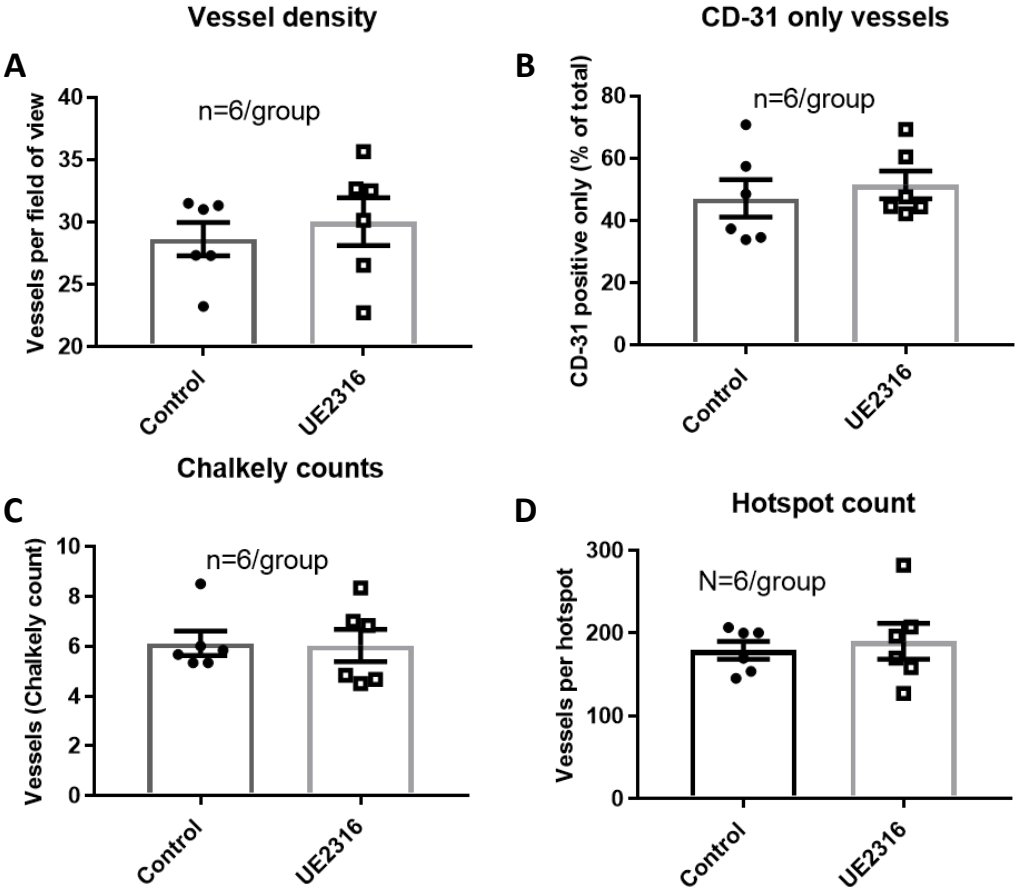

Figure 3.3 – UE2316 does not affect vessel density in WT-SCC tumours. Vessels in WT-SCC tumours from controls and UE2316-treated mice were quantified using multiple methods. A) No difference was seen in manually quantified vessel density between groups. B) There were no differences in the proportion of vessels lacking smooth muscle coverage (CD31 only). Chalkley counts (C) and hotspot quantification (D) were used to confirm vessel density – no differences were identified with either approach. Columns show mean ± standard error. 1 section/tumour, N=6 animals/group. Data compared by independent samples t-test for panels A/B/D, Mann-Whitney U test for Panel C.

3.2.1.2 Vessel density is not a predictor of tumour volume in UE2316-treated tumours

To determine whether vessel number correlated with tumour size, total vessel number per tumour was extrapolated by multiplying vessel density by section area. Total vessel number did not differ between control (1577 ± 458 vessels/section) and UE2316-diet fed mice (2520 ± 615 vessels/section; Figure 3.4A) and did not correlate with tumour size (Figure 3.4B).

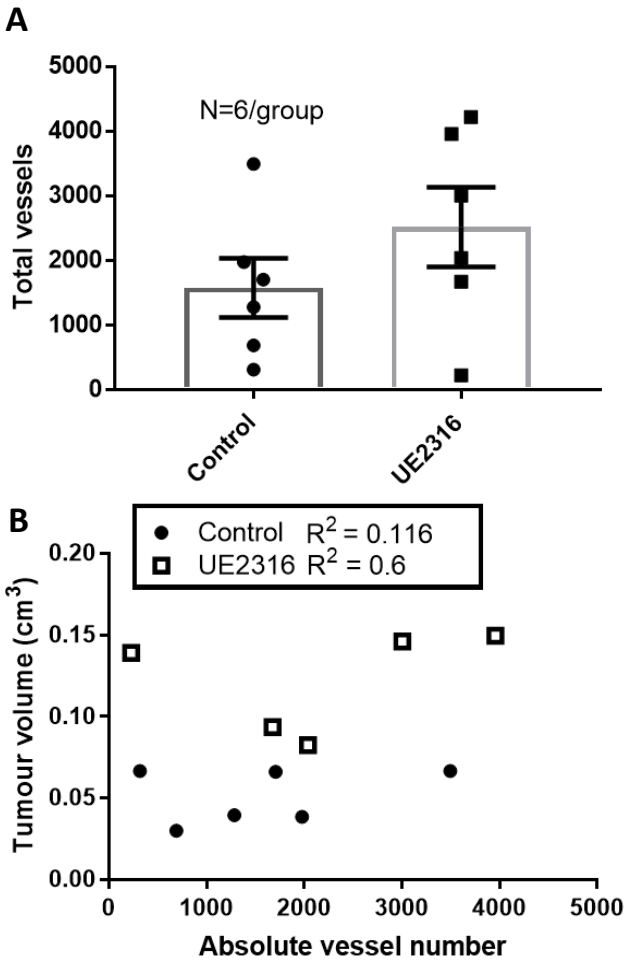

Figure 3.4 – Total vessel number per tumour does not differ significantly between control and UE2316-treated tumours and does not predict tumour volume. A) The total vessel number per tumour section (calculated by multiplying vessel density by section area) did not differ between control and UE2316-treated WT-SCC tumours. Columns represent mean ± standard error. N=6/group; data compared by independent samples t-test. B) No relationship was found between tumour volume and absolute vessel number in either group. 1 section/tumour, N=5-6/group. Data compared by Spearman's rank correlation.

3.2.2 11β-HSD1 inhibition does not affect vessel density during early tumour development

To address the concern that an earlier period of enhanced angiogenesis may have been missed, a short-term WT-SCC tumour study was performed. WT-SCC cells were injected into female FVB/N mice (aged 8 weeks) and tumours taken at the first palpable point (day 4 after injection). Tumour size in the UE2316-treated group did not differ significantly from controls at the day 4 time point (Figure 3.5A). Representative images of control (Figure 3.5B) and UE2316-treated tumours (Figure 3.5C) are shown. Tumours in this study were small enough to allow for complete manual quantification across the tissue section (no randomised fields of view used). Vessel density showed a trend towards being decreased in UE2316-treated tumours (P=0.1089) (Figure 3.5D), while the proportion of vessels lacking α-SMA coverage showed a strong trend towards being increased in UE2316-treated tumours (P=0.0526) (Figure 3.5E). Neither of these results reached significance; power calculations (80% power target) suggested that a sample size of 15/group would detect a difference of this magnitude with the given variance.

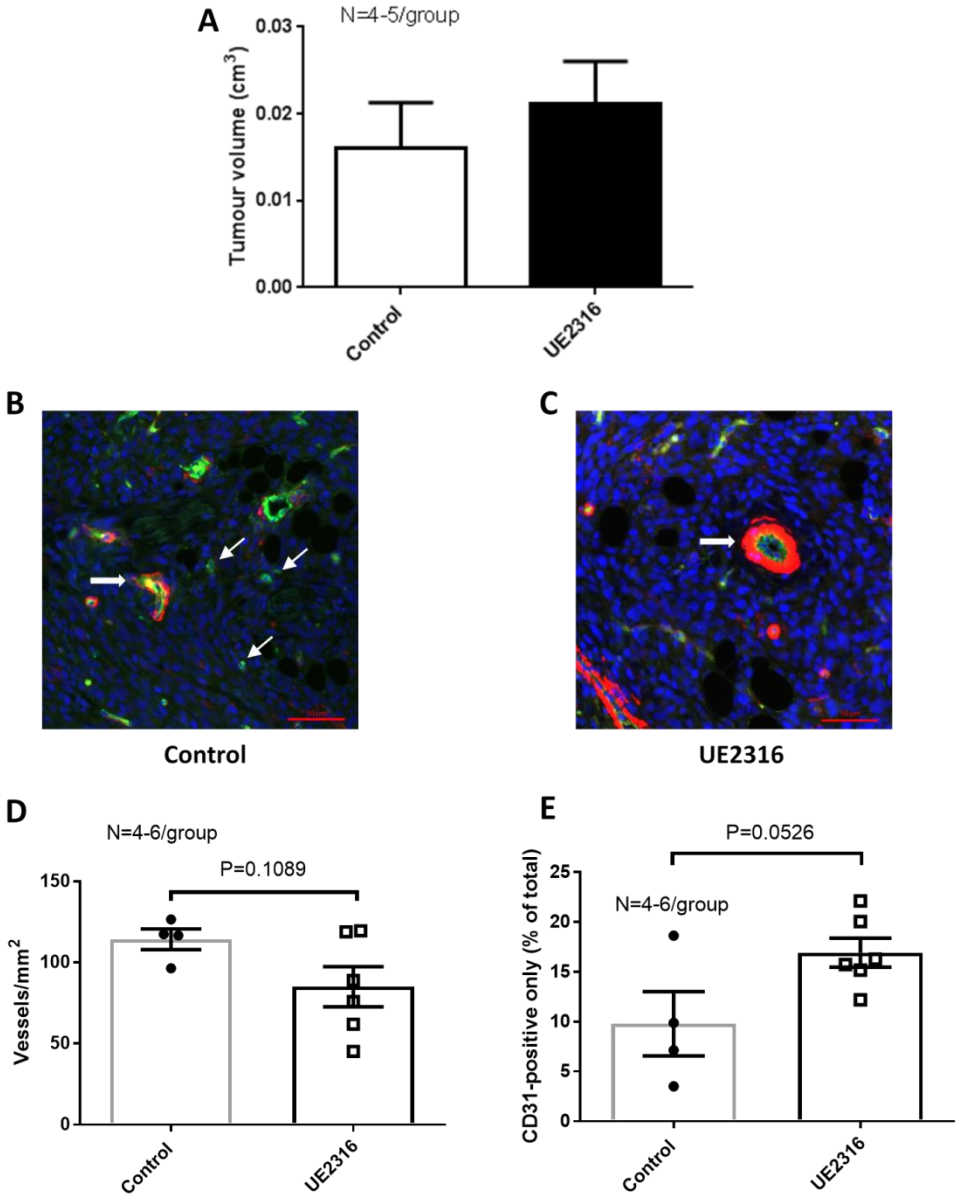

Figure 3.5 – The effect of UE2316 on early vessel density in WT-SCC tumours. A) WT-SCC tumours grown for four days showed no difference in size after UE2316 treatment. Representative images of CD31 (green)/α-smooth muscle actin (SMA; red) co-stained control (C) and UE2316-treated (D) tumours are shown – diagonal white arrows = vessels lacking smooth muscle coverage, horizontal arrows = larger vessels with smooth muscle coverage. The number of vessels in UE2316-treated tumours showed a trend towards being reduced (D), while the number of vessels lacking smooth muscle coverage showed the opposite trend (E). 1 section/tumour. N=4-6 animals/group; Data represent mean ± standard error and were compared by independent samples t-test.

3.2.3 Effect of 11β-HSD1 inhibition on Panc043 tumour size and vessel density

3.2.3.1 11β-HSD1 inhibition does not affect Panc043 tumour growth

The effects of 11β-HSD1 inhibition in an alternative cell line, Panc043, was next investigated. Based on the observation that Panc043 cells formed tumours more rapidly than WT-SCC tumours (A Serrels, personal communication), 0.25 x 10^6 cells/flank were initially injected into C57BL6/J mice (female, aged 10 weeks) fed either control or UE2316 diet (N=6/group), as rapid tumour growth risks ulceration. Palpable tumours formed by day 4 and grew at an exponential rate until day 15 when the experiment was ended due to tumour ulceration. Tumour growth was not affected by UE2316 (Figure 3.6A). Mouse weight remained stable throughout the study and did not differ between groups (Figure 3.6B). Tumours ulcerated before reaching their expected volume (based on previous observations in the lab group). As reducing cell number did not appear to prevent ulceration after two weeks, for future experiments it was decided that 1 million cells/flank would be injected to maximise tumour volume.

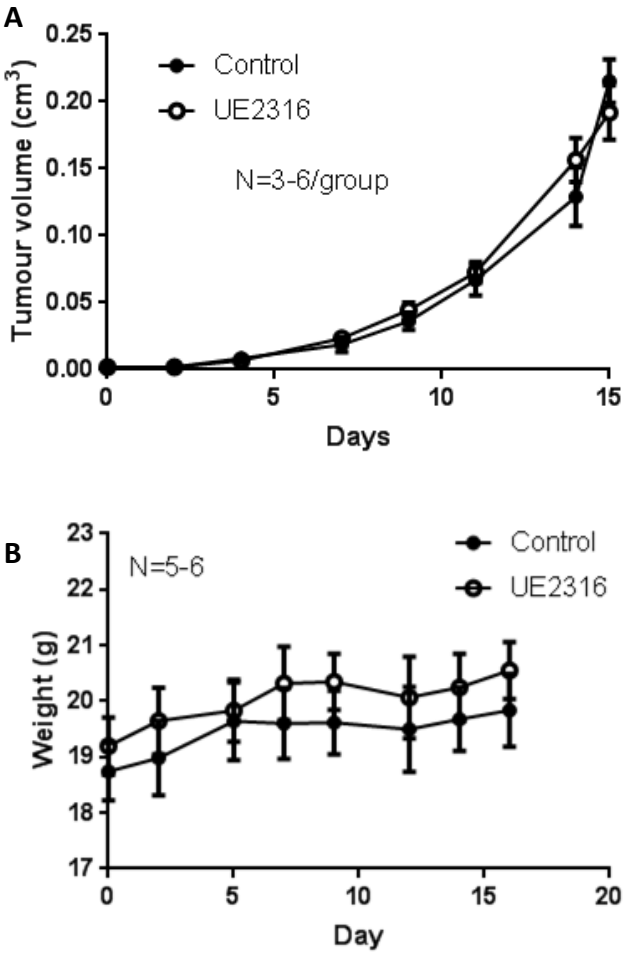

Figure 3.6 – Initial Panc043 tumour growth curve (0.25 x 10^6 cells/flank). A) Pancreatic Ductal Adenocarcinoma (Panc043) tumours grew rapidly between days 4-15 but ulcerated at this point. Administration of UE2316 in the diet (approximately 25-30 mg/kg/mouse/day) did not affect the growth of Panc043 tumours. B) Tumour cell injection and UE2316-diet did not affect mouse weight (first weights taken one day before cell injection). N=3-6/group. Data represent mean ± standard error and were compared by 2-way ANOVA.

In the second study, Panc043 cells (1 x 10^6/flank) were injected into C56BL6/J mice (female, aged 10 weeks) fed either control or UE2316 diet (N=6/group). Tumours grew rapidly and achieved greater volumes than those produced in the initial experiment in a similar timeframe. No differences were seen in the growth dynamics or final (day 14) volume of tumours growing in wild-type mice fed control diet (0.299 ± 0.035 cm^3) or UE2316 diet (0.251 ± 0.044 cm^3) (Figure 3.7A). Mice ate on average less UE2316-diet per day (2.92 ± 0.16 g) than control RM1-diet (3.58 ± 0.12g, P<0.01, Figure 3.7B) but this did not affect mouse weight (Figure 3.7C).

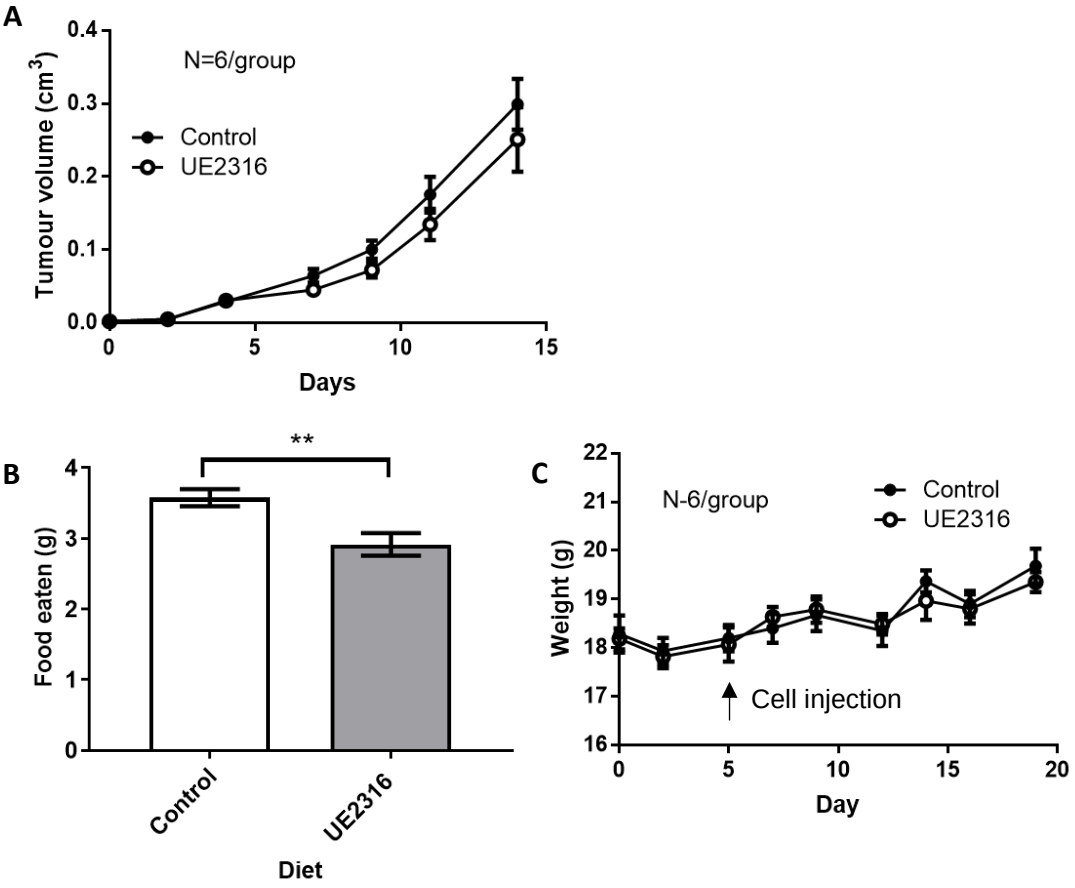

Figure 3.7 – The 11β-HSD1 inhibitor UE2316 does not affect Panc043 tumour growth. A) Administration of UE2316 in diet did not affect the growth of subcutaneously implanted Pancreatic Ductal Adenocarcinoma (Panc043) tumours. B) Mice consumed slightly less UE2316-diet than control RM-1 diet. **P<0.01. Data compared by independent samples t-test. C) Neither Panc043 cell injection (day 5) nor UE2316-diet affected mouse weight, despite the difference in food consumed. N=6/group. Data represent mean ± standard error.

3.2.3.2 **11β-HSD1 deletion does not affect Panc043 tumour growth**

The growth of Panc043 tumours in mice globally deficient in 11β-HSD1 was investigated. Del1 mice (bred on a C57BL6/J background) are homozygous for a deletion of exon 3 of the *hsd11b1* gene (see Zhang *et al.,* (2017)). Genomic DNA isolation was performed on liver samples (WT vs Del1, N=6/group). Mice were genotyped and deletion of the 11β-HSD1 enzyme confirmed (Figure 3.8). Panc043 cells were injected into wildtype C57Bl6/J mice (female, aged 11-13 weeks) fed either control or UE2316 diet, and into Del1 mice on control diet (N=6/group). No differences were seen in the growth dynamics or final (day 16) volume of Panc043 tumours growing in wild-type mice fed control diet (0.623 ± 0.107 cm^3), Del1 mice fed control diet (0.573 ± 0.071 cm^3) or wild-type mice fed UE2316 diet (0.722 ± 0.122 cm^3) (Figure 3.9A). Tumour weights confirmed this finding (Figure 3.9B). Diet did not affect mouse weight but age-matched Del1 mice were found to be significantly heavier than wild-type controls (average weight across experiment - Del1 23.84 ± 0.11g vs control 20.61 ± 0.1g; $P<0.01$), a difference apparent from the experimental onset and throughout the protocol (Figure 3.9C). No differences were seen in the amount of diet consumed between groups (data not shown).

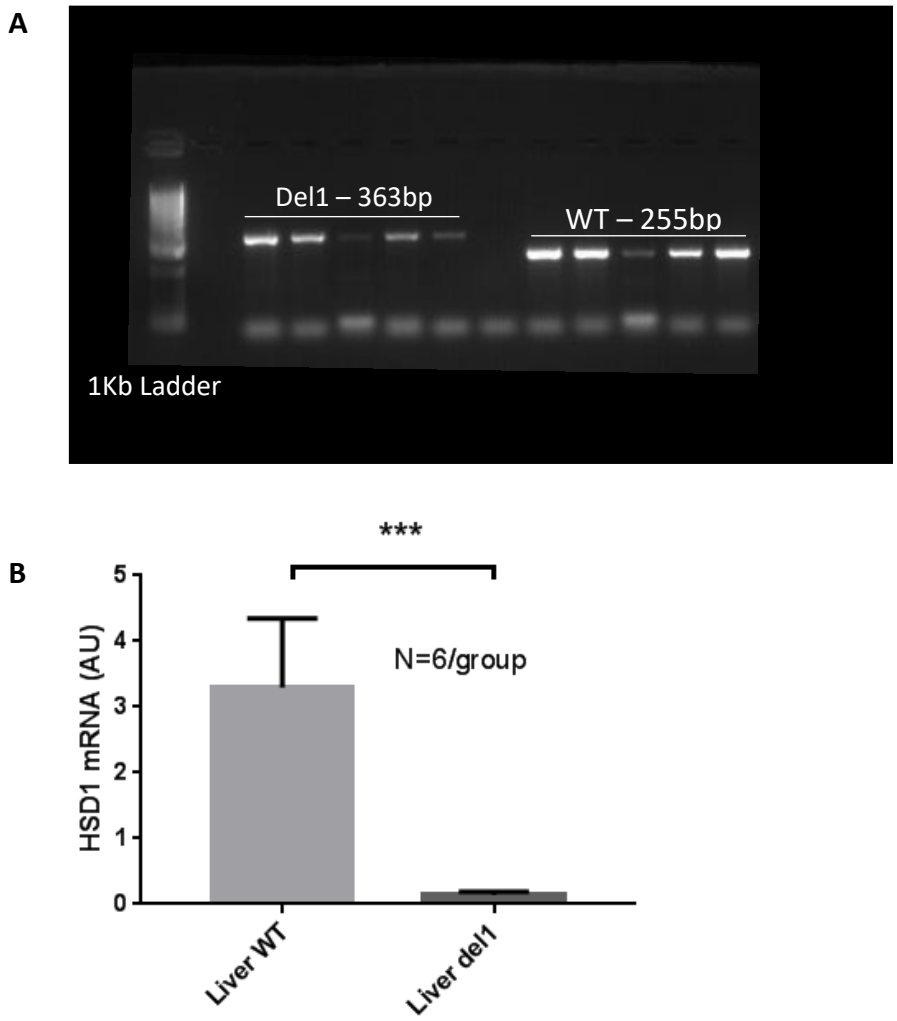

Figure 3.8 – Del1 mice lack 11β-HSD1. A) Genotyping demonstrated the deletion of the 11β-HSD1 gene in Del1 animals. Primers flanking the wildtype (WT) allele produced a 255 base pair (bp) product, while primers flanking the *hsd11b1* knockout allele produced a 363bp product. B) qPCR for 11β-HSD1 in liver from wild-type (WT) and Del1 (11β-HSD1 knockout) mice confirmed genetic deletion of this enzyme. N=6/group; data are mean ± standard error and were compared by independent samples T-test.

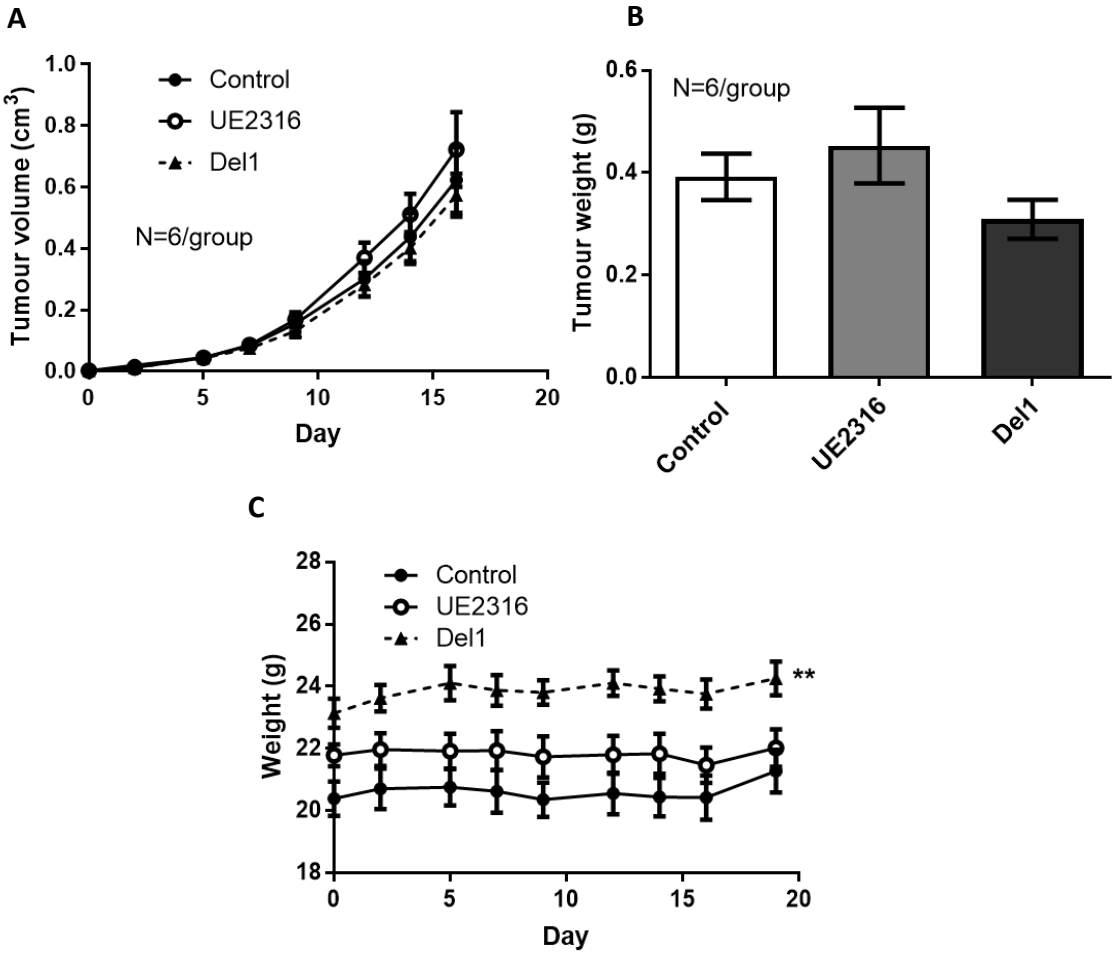

Figure 3.9 – Panc043 tumour growth is unaffected by 11β-HSD1 inhibition or deletion. A) Panc043 cells, a pancreatic ductal adenocarcinoma cell line, grew rapidly over 16 days. Neither administration of an 11β-HSD1 inhibitor (UE2316) in the diet nor genetic deletion of 11β-HSD1 affected tumour growth. B) Tumour weights at day 16 reflected this. N=6/group. P=0.20. Data represent mean ± standard error and were compared by one-way ANOVA. N=6/group. C) Del1 mice were heavier than control and UE2316 diet-fed mice despite age matching. * P<0.01. N=6/group. Data represent mean ± standard error and were compared by repeated measures two-way ANOVA with Tukey's post-hoc test.

3.2.3.3 11β-HSD1 inhibition does not increase vessel density in Panc043 tumours

To determine whether 11β-HSD1 affected vessels in Panc043 tumours, experimental Panc043 tumours (H+E section shown in Figure 3.10A) were sectioned and stained for CD31/α-SMA-positive structures, which were considered vessels and quantified. CD31 Panc043 tumours contained a large number of cells with α-SMA immunoreactivity without associated CD31-positive structures, likely myofibroblasts (Figure 3.10B). The number of blood vessels per field of view did not differ between control (10 ± 1 vessels/mm^2) and UE2316-treated tumours (10 ± 1 vessels/mm^2) (Figure 3.10C). The proportion of vessels lacking smooth muscle coverage did not differ between control (29 ± 4%) and UE2316-treated tumours (26 ± 2%) (Figure 3.10D).

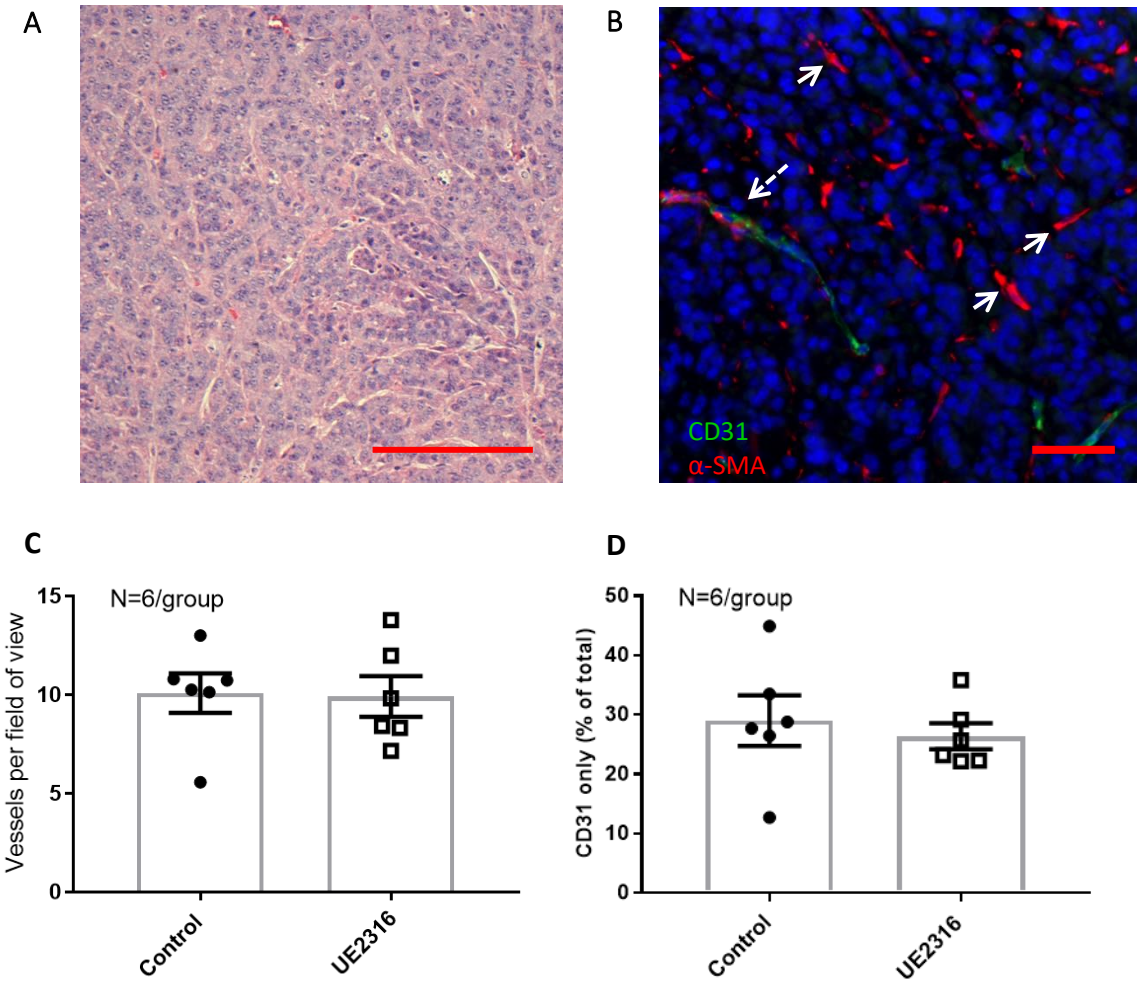

Figure 3.10 – UE2316 does not affect vessel density in Panc043 tumours. A) Haematoxylin and eosin-stained section of control Panc043 tumour tissue. 100x magnification. Scale bar 200µm. B) Panc043 tumour tissue with endothelial cells stained green (CD31 visualised with Alexa-Fluor 488) and smooth muscle cells stained red (α-SMA visualised with Cy3). Nuclei stained blue (DAPI). Solid white arrows = non-vascular α-SMA immunoreactivity, likely in cancer-associated fibroblasts. Dashed white arrow = vessel with clear smooth muscle coating. Panc043 tumours were less vascularised than WT-SCC tumours. 200x magnification. Scale bar 50µm. C) No difference was seen in manually quantified vessel density between tumours from control and UE2316-diet fed mice. D) There were no differences in the proportion of vessels lacking smooth muscle coverage (CD31 only). 1 section/tumour, N=6 animals/group. Data represent mean ± standard error and were compared by independent samples t-test.

3.2.4 Effect of 11β-HSD1 inhibition on SCC-B6-1 tumour size and vessel density

3.2.4.1 11β-HSD1 inhibition or deletion does not affect SCC-B6-1 tumour growth

11β-HSD1 inhibition and deletion were investigated using a second SCC cell line syngeneic on a C57BL6/J background. SCC-B6-1 cells were injected into wildtype C57Bl6/J mice (female, aged 13-14 weeks) fed either control or UE2316 diet, and into Del1 mice globally lacking 11β-HSD1 (N=6/group). SCC-B6-1 cells implanted into C57BL6/J mice ($1x10^6$ cells/flank) grew more slowly than WT-SCC and Panc043 cells, achieving comparable volumes to WT-SCC tumours after 37 days. No significant differences were seen in the growth dynamics or final (day 37) volume of SCC-B6-1 tumours growing in wild-type mice fed control diet (0.221 ± 0.037 cm^3), Del1 mice fed control diet (0.246 ± 0.031 cm^3) or wild-type mice fed UE2316-containing diet (0.289 ± 0.049 cm^3) (Figure 3.11A). A pattern of increased tumour growth in UE2316-treated mice began from day 24 but did not reach significance before the study was ended for reasons of tissue integrity. 3 mice per group were taken to 37 days but tumour tissue at this time-point was unsuitable for further analysis. Subsequently, 6 mice per group were culled at day 28 – the time point at which the initial tumours had begun to show a potential size effect in relation to treatment. Consistent with these data, tumour weights did not differ between groups (Figure 3.11B). The type of diet given to mice did not affect their weight but Del1 mice were found to be significantly heavier than wild-type controls (average weight across experiment - Del1 23.76 ± 0.08g vs control 21.63 ± 0.07g; $P<0.01$), a difference apparent from the experimental onset and throughout (Figure 3.11C). No differences were seen in the amount of diet consumed between groups (data not shown).

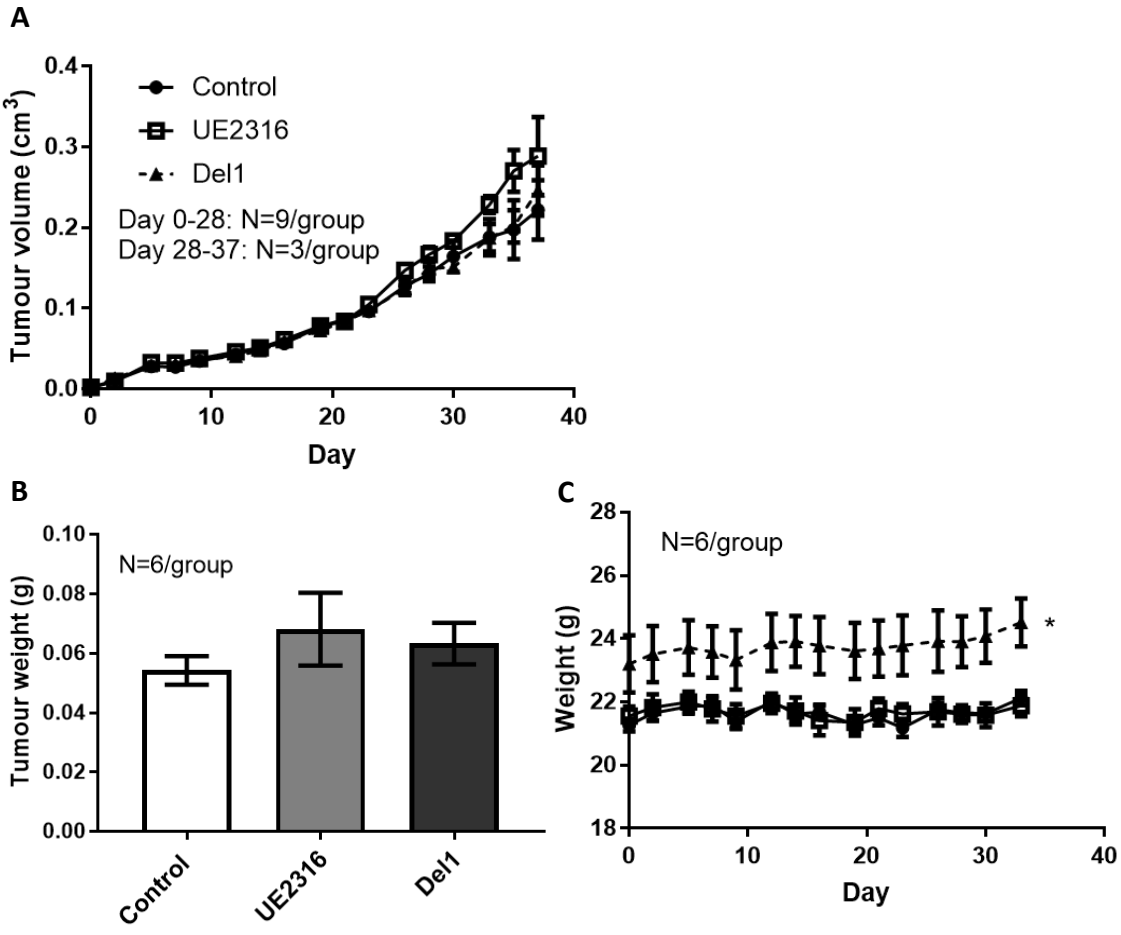

Figure 3.11 – SCC-B6-1 tumour growth is not substantially affected by 11β-HSD1 inhibition or deletion. A) Squamous cell carcinoma cells (SCC-B6-1 cell line) produced tumours that grew more slowly than the other two tumour types (WT-SCC and Panc043) over 4-6 weeks. Administration of UE2316 in the diet, or genetic deletion of 11β-HSD1 did not affect tumour growth. B) Tumour weights at day 28 reflect this lack of effect. C) Del1 mice were heavier than control and UE2316 diet-fed mice despite age matching. * $P<0.05$. Data represent mean ± standard error and were compared by repeated measures two-way ANOVA with Tukey's post-hoc analysis.

3.2.4.2 The effect of 11β-HSD1 inhibition on vessel density in SCC-B6-1 tumours

SCC-B6-1 tumours (H+E image shown in Figure 3.12A) were highly vascularised and contained interconnected vascular network with many branching points (Figure 3.12B). The number of blood vessels per mm^2 did not differ between groups (Figure 3.12C).

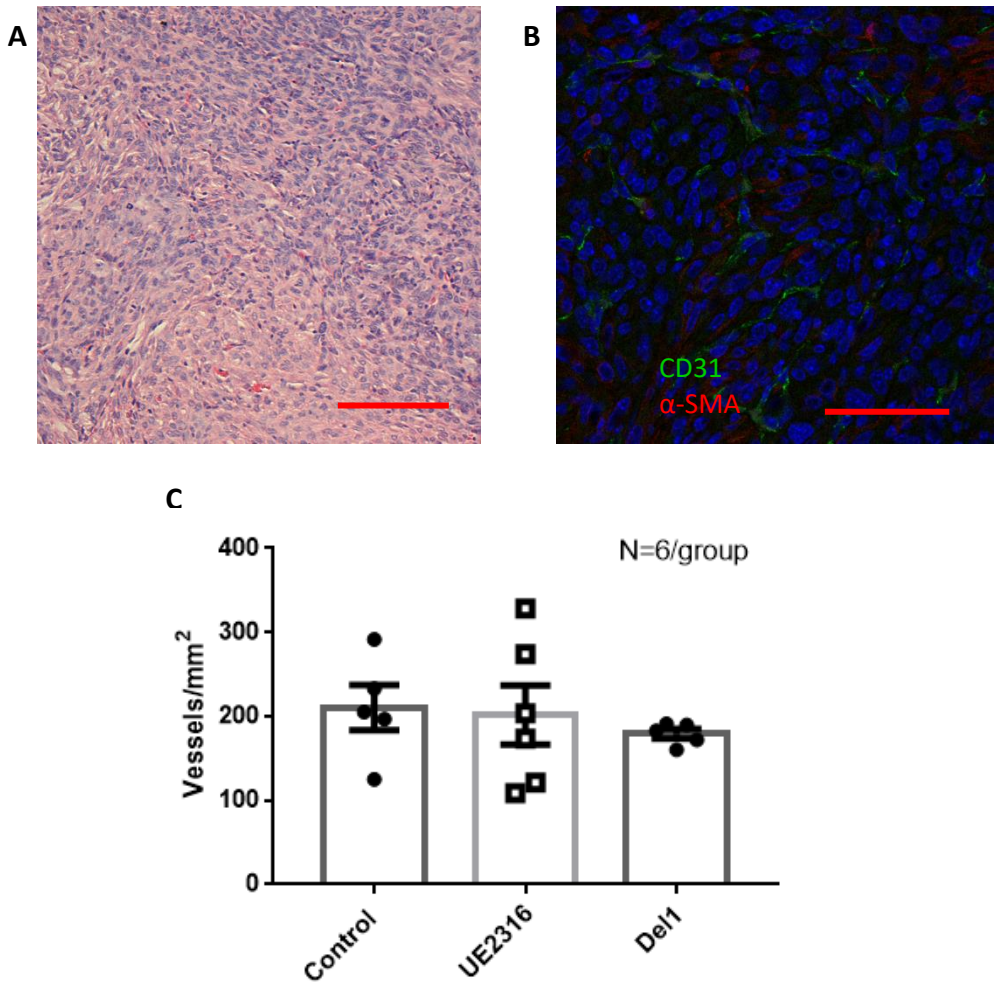

Figure 3.12 – SCC-B6-1 tumour vessels are unaffected by 11β-HSD1 inhibition/deletion. A) Haematoxylin and eosin stained section of SCC-B6-1 tumour. 100x magnification. Scale bar = 200µm. B) Tumour tissue with endothelial cells stained green (CD31 visualised with Alexa-Fluor 488) and smooth muscle cells stained red (α-SMA visualised with Cy3). SCC-B6-1 tumours contained vascular networks that were more interconnected and branching than those seen in WT-SCC and Panc043 tumours. 400x magnification. Scale bar 50µm. B) Manual vessel counts found no differences between tumours from control, UE2316-diet fed, or Del1 mice. 1 section/tumour. N=6 animals/group. Data represent mean ± standard error and were compared by independent samples t-test.

3.2.5 Tumour types have variable vascularity

Pooling control and UE2316-treated tumour vessel density data and grouping by tumour type highlighted the significant (P<0.0001) differences in vessel density between WT-SCC (29.3 ± 1.1 vessels per field of view), Panc043 (10.0 ± 0.7 vessels per field of view) and SCC-B6-1 (19.7 ± 1.5 vessels per field of view) (Figure 3.13).

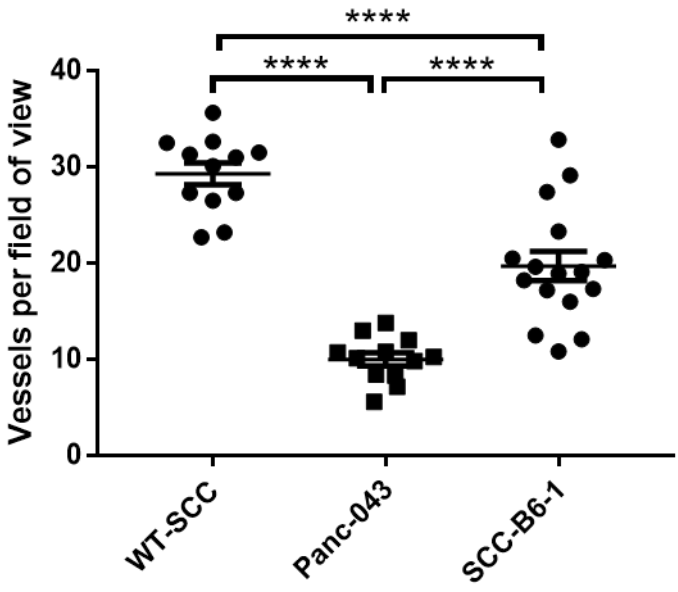

Figure 3.13 – Vascular density differs between tumour types. Vessel density in tumours (control group) varied depending on the cell type used to induce tumour formation. WT-SCC had the highest vessel density, followed by SCC-B6-1 and then Panc043. N=12-17, P<0.0001. Data represent mean ± standard error and were compared by one-way ANOVA with Tukey's post-hoc test.

3.2.6 Effect of 11β-HSD1 inhibition on expression of angiogenic factor mRNA

3.2.6.1 11β-HSD1 inhibition does not affect mRNA levels of known angiogenic factors in WT-SCC tumours

To further determine the influence of UE2316 on angiogenesis, mRNA levels of a selection of angiogenic factors were measured by RT-qPCR in control and UE2316-treated tumours, (N=6/group) and cultured tumour cells (N=6/type). No differences were seen in VEGFa, VEGFR2, IL-6, HIF-1α or TSP-1 mRNA levels between control and UE2316-treated tumours (Figure 3.14). Cellular mRNA levels were lower than tumour levels for all genes. Glucocorticoids have previously been shown to inhibit VEGF signalling, to reduce IL-6 production, and to increase TSP-1 expression, while 11β-HSD1 deletion has been shown to increase HIF-1α expression (Hori *et al.*, 1996; Logie *et al.*, 2010; Michailidou *et al.*, 2012; Wang *et al.*, 2012).

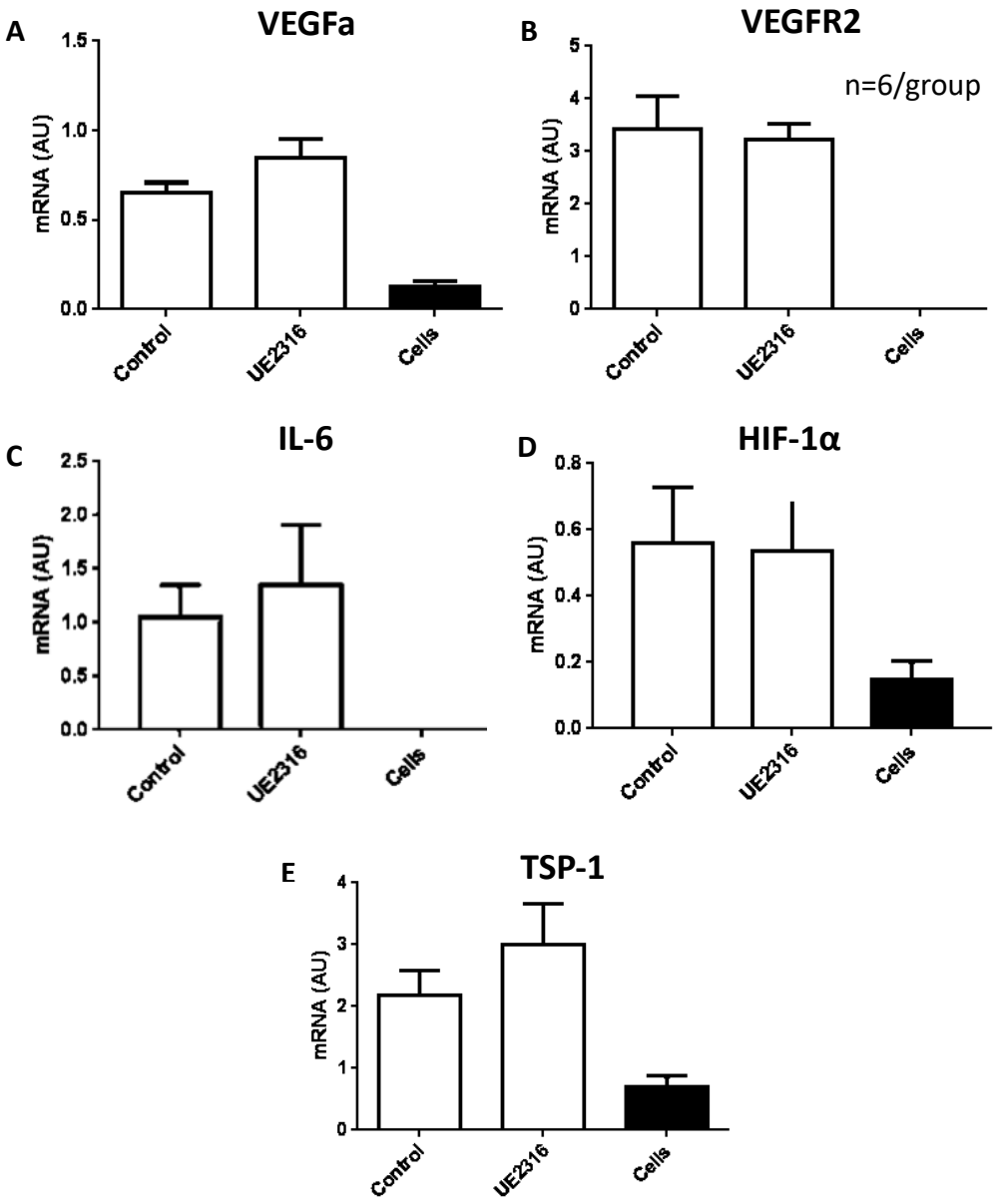

Figure 3.14 – Expression of angiogenic factors in WT-SCC tumours. Control and UE2316 groups indicate WT-SCC tumours from the latter experiment described in section 3.2.1, cells are from the WT-SCC cell line (passage<20). Expression of angiogenic factors in tumour cells was measured to ascertain the possible contribution of host/donor tissues. All genes were normalised to TBP/GAPDH housekeeping genes. No differences were found between tumours from control or UE2316-treated mice in the levels of A) VEGFa; B) VEGFR2; C) IL-6; D) HIF-1α or E) TSP-1. Cellular expression of all genes was lower than in tumours, and VEGFR2 (B) and IL-6 (C) were not detected in cultured cells. Data are mean ± standard error and tumour data were compared by independent samples t-test. N=6/group.

3.2.6.2 **11β-HSD1 inhibition reduces HIF-1α mRNA levels in Panc043 tumours.**

The same investigations were also carried out in Panc043 tumours. HIF-1α mRNA levels were lower ($P<0.05$) in UE2316-treated Panc043 tumours (1.65 ± 0.34, arbitrary units) than in control tumours (0.72 ± 0.17). No differences were detected in VEGFa, VEGFR2 or TSP-1 mRNA levels (Figure 3.15) and IL-6 was not detected in Panc043 cells or tumours. Cellular mRNA levels were lower than tumour levels for all genes.

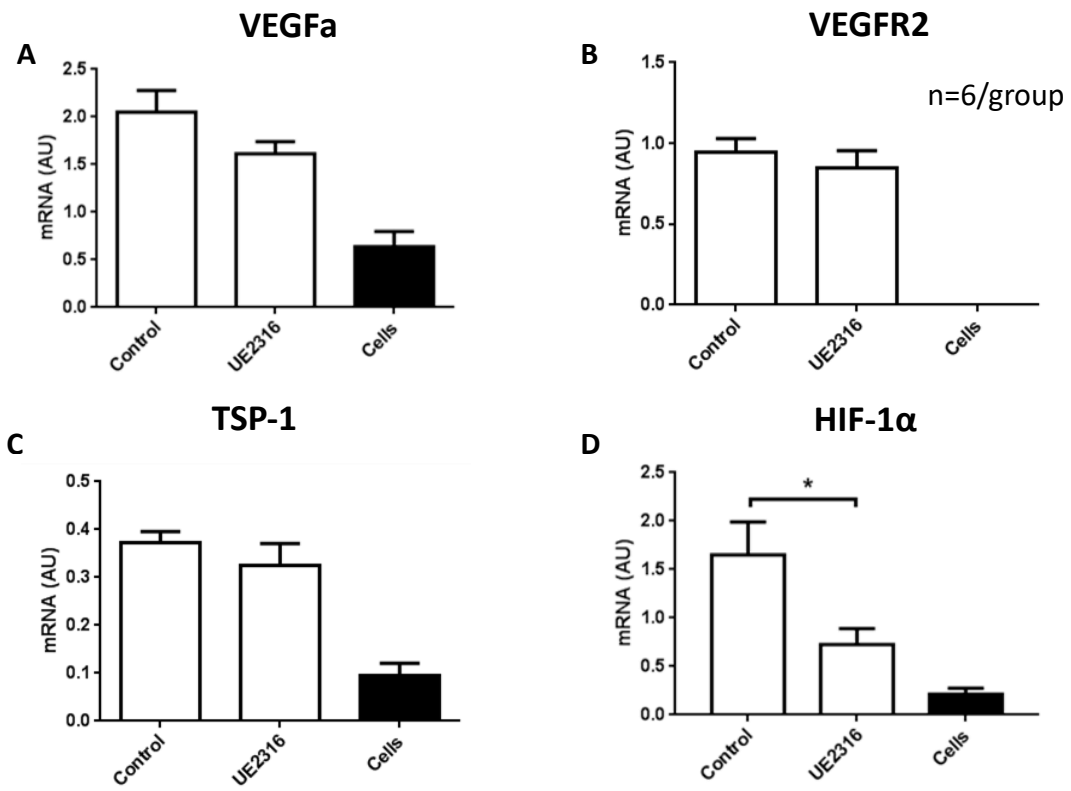

Figure 3.15 – Angiogenic factor expression in Panc043 tumours. Control and UE2316 groups indicate Panc043 tumours from the second experiment described in section 3.2.3.1, cells are Panc043 cell line (passage<20). Expression of angiogenic factors in tumour cells was measured to ascertain the possible contribution of host/donor tissues. All genes were normalised to TBP/GAPDH housekeeping genes. No differences were found between tumours from control or UE2316-treated mice in the levels of A) VEGFa; B) VEGFR2; C) TSP-1. D) HIF-1α was reduced in Panc043 tumours treated with UE2316. * $P<0.05$. Cellular expression of all genes was lower than in tumours, and VEGFR2 (B) was not detected in cultured cells. Data are mean ± standard error and tumour data were compared by independent samples t-test. N=6/group.

3.2.7 Glucocorticoid signalling in tumours

3.2.7.1 Glucocorticoid signalling profile differs between WT-SCC, Panc043 and SCC-B6-1 tumours

The expression of key glucocorticoid receptors and metabolising enzymes was measured in tumours to provide an indication of their potential glucocorticoid sensitivity. GR, MR, 11β-HSD1 and 11β-HSD2 mRNA levels were measured in WT-SCC and Panc043 tumours (control vs UE2316-treated, N=6/group) and SCC-B6-1 tumours (control/UE2316-treated/Del1; N=6/group) and cells. GR was expressed in all tumour and cell types and was lower in UE2316-treated Panc043 tumours (1.47 ± 032) compared to control tumours (0.51 ± 0.06). No change in GR expression was detected between control and UE2316-treated WT-SCC or SCC-B6-1 tumours. Cellular GR mRNA levels were lower than tumour levels (Figure 3.16).

GR was more highly expressed ($P<0.05$) in WT-SCC tumours (1.52 ± 0.12) than in Panc043 (0.31 ± 0.06) and SCC-B6-1 tumours (0.29 ± 0.09) (Figure 3.17A). 11β-HSD1 was more highly expressed ($P<0.05$) in SCC-B6-1 tumours (1.73 ± 0.42) than in WT-SCC (0.11 ± 0.02) and Panc043 tumours (0.0.022 ± 0.003) (Figure 3.17B).

MR mRNA did not differ between Panc043 cells and tumours, and was not detected in other samples (Figure 3.18). 11β-HSD2 mRNA was not detected in any of the cells or tumour types.

11β-HSD1 mRNA was detected in WT-SCC and SCC-B6-1 tumours, and was at the limit of detection for Panc043 tumours (cycles 34-36). 11β-HSD1 levels in WT-SCC tumours were lower in animals receiving UE2316 treatment compared to controls (0.69 ± 0.04 AU vs. 1.57 ± 0.28 AU, $P<0.05$; Figure 3.19A), and 11β-HSD1 levels in SCC-B6-1 tumours were unaffected by UE2316 treatment or genetic deletion of the enzyme in the host tissues (3.19B). Subcutaneous sponge implants (N=4, a kind gift from Dr Holly Stott) and control FVB/N liver (N=12) were also examined as a highly vascularised tissue and a tissue with high 11β-HSD1 expression respectively. 11β-HSD1 levels were similar between WT-SCC tumours (0.156 ± 0.03) and subcutaneously implanted sponges (0.159 ± 0.06), whilst levels in liver were found to be 100-fold higher (15.02 ± 2.51) (Figure 3.20).

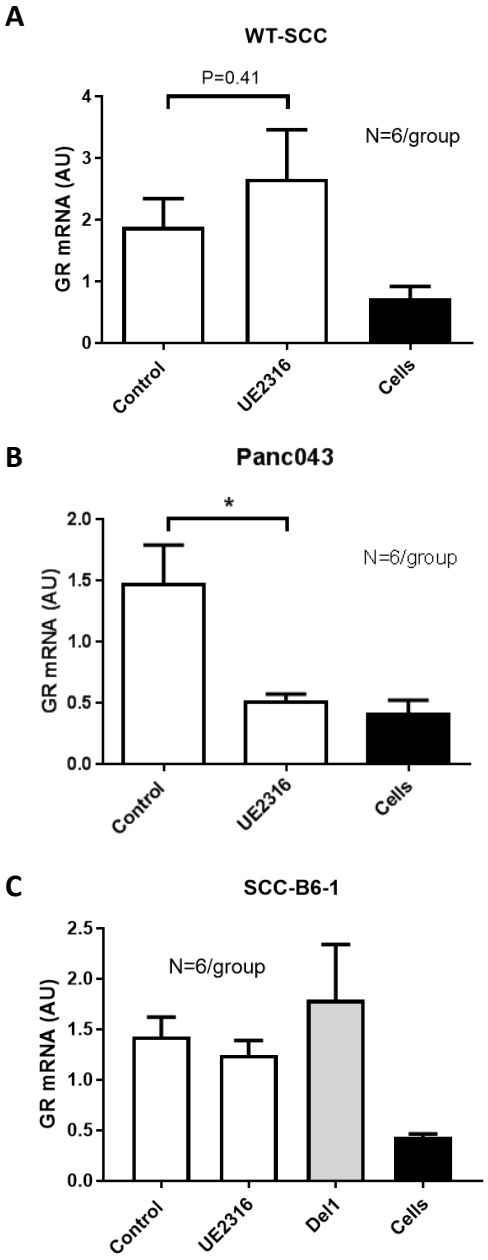

Figure 3.16 – GR mRNA levels in Panc043 tumours are reduced by UE2316 treatment. A) GR expression did not differ significantly between WT-SCC tumours from control and UE2316-treated mice. B) GR expression was lower in UE2316 treated Panc043 tumours compared with controls. * $P<0.05$. Data compared by independent samples t-test, N=6/group. C) GR expression did not differ between control and UE2316-treated SCC-B6-1 tumours, and SCC-B6-1 tumours grown in Del1 mice. Data compared by one-way ANOVA. N=6/group. Data represent mean ± standard error.

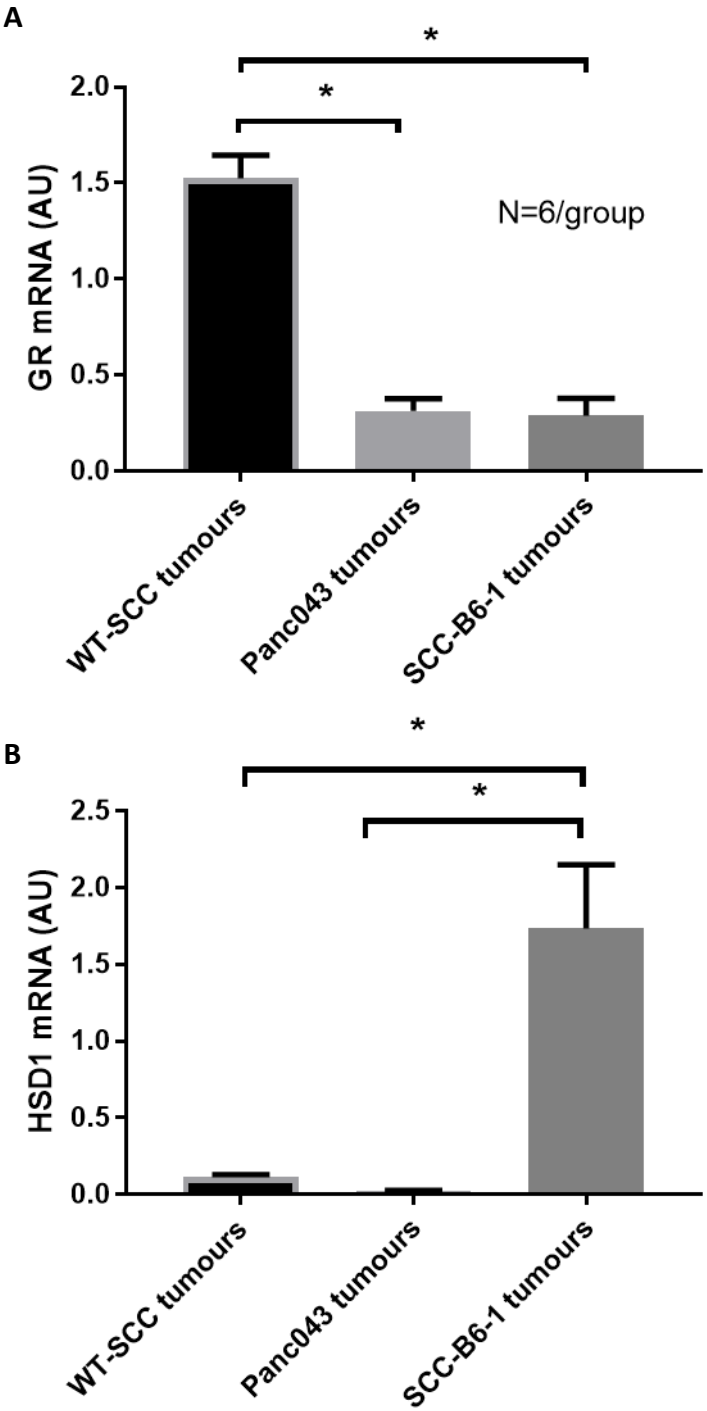

Figure 3.17 - GR and 11β-HSD1 mRNA in different tumour types. A) GR transcript levels were significantly greater in WT-SCC tumours compared to Panc043 and SCC-B6-1 tumours. B) 11β–HSD1 transcript levels were significantly greater in SCC-B6-1 tumours compared to WT-SCC and Panc043 tumours. * $P<0.05$. N=6/group. Data represent mean ± standard error and were compared by one-way ANOVA with Tukey's post-hoc test.

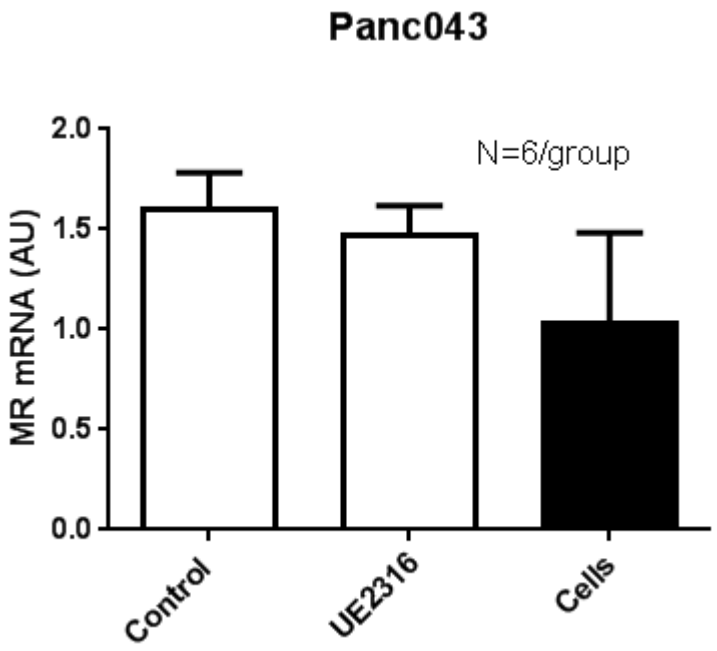

Figure 3.18 - MR mRNA is only detectable in Panc043 tumours. MR mRNA did not differ between Panc043 tumours from control or UE2316-diet fed mice. MR levels were below the limit of detection in both SCC tumour types. N=6/group. Data represent mean ± standard error and were compared by independent samples t-test.

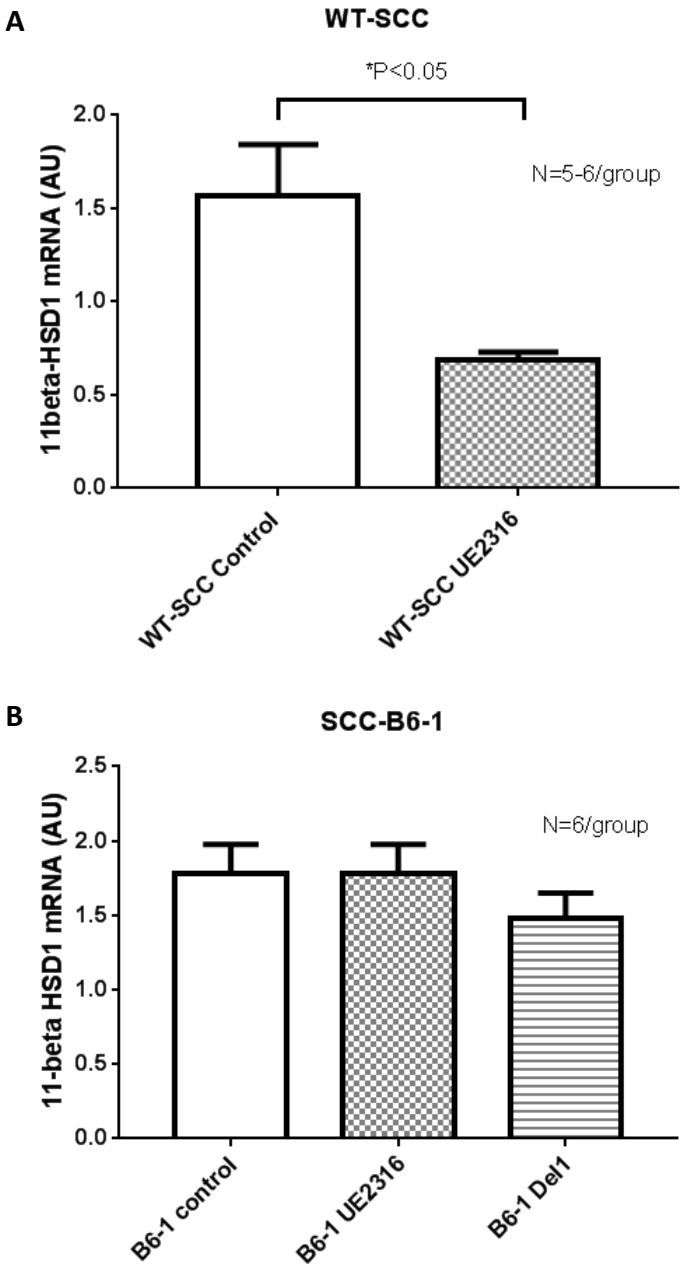

Figure 3.19 – 11β-HSD1 mRNA is expressed in SCC tumours. A) 11β-HSD1 mRNA was lower in WT-SCC tumours from UE2316-diet fed mice vs control diet-fed mice. 11β-HSD1 mRNA was not detected in WT-SCC cells in culture. * P<0.05, data compared by independent samples t-test. N=5-6/group. B) 11β-HSD1 expression in SCC-B6-1 tumours was not affected by UE2316 or 11β-HSD1 deletion (note the injected cells are not from 11β-HSD1 deficient mice). 11β-HSD1 mRNA was not detected in SCC-B6-1 cells in culture. Data represent mean ± standard error and were compared by one-way ANOVA, N=6/group.

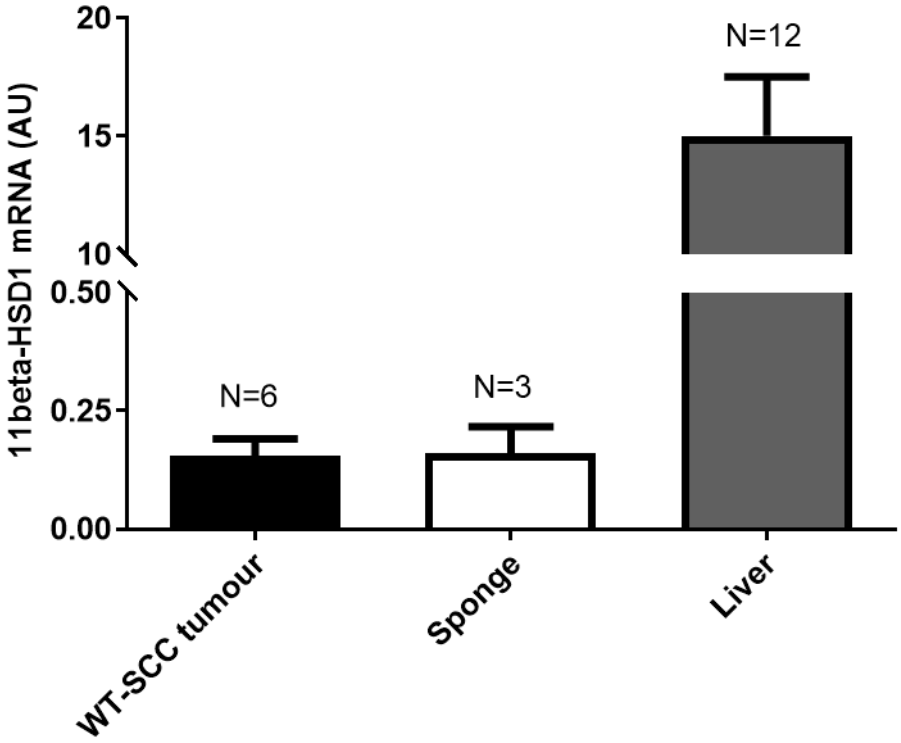

Figure 3.20 - 11β-HSD1 mRNA levels are similar between WT-SCC tumour and subcutaneous sponge. mRNA levels of 11β-HSD1 were similar between WT-SCC tumours and subcutaneous sponges implanted into mice, while both had 100-fold lower levels than in liver. N=6/group. Data represent mean ± standard error.

3.2.7.2 **11β-HSD1 activity differs between tumour types**

11β-HSD1 dehydrogenase activity was measured in control tumours (N=6/tumour type) to determine relative levels of enzyme activity between tumour types. Control liver from FVB/N animals acted as positive control tissue. 11β-HSD1 dehydrogenase activity in WT-SCC tumours was demonstrably lower than that in liver, with 0.5mg/mL [protein] forming product more rapidly than 0.2mg/mL [protein] (Figure 3.21A). A preliminary time course using WT-SCC tumours (0.5mg/mL [protein]) demonstrated that there was a linear relationship between incubation time and steroid conversion between 60 - 120 minutes, thus 90 minutes was selected as an appropriate time point for incubation. Similar experiments (data not shown) were used to optimise conditions for Panc043 and SCC-B6-1 tumours. When comparing 11β-HSD1 dehydrogenase activity between tumour types, SCC-B6-1 tumours showed a considerably higher rate of product formation (1.798 ± 0.204 nmoles/min/mg) than both WT-SCC (0.291 ± 0.054 nmoles/min/mg) and Panc043 (0.038 ± 0.006 nmoles/min/mg) (Figure 3.21B).

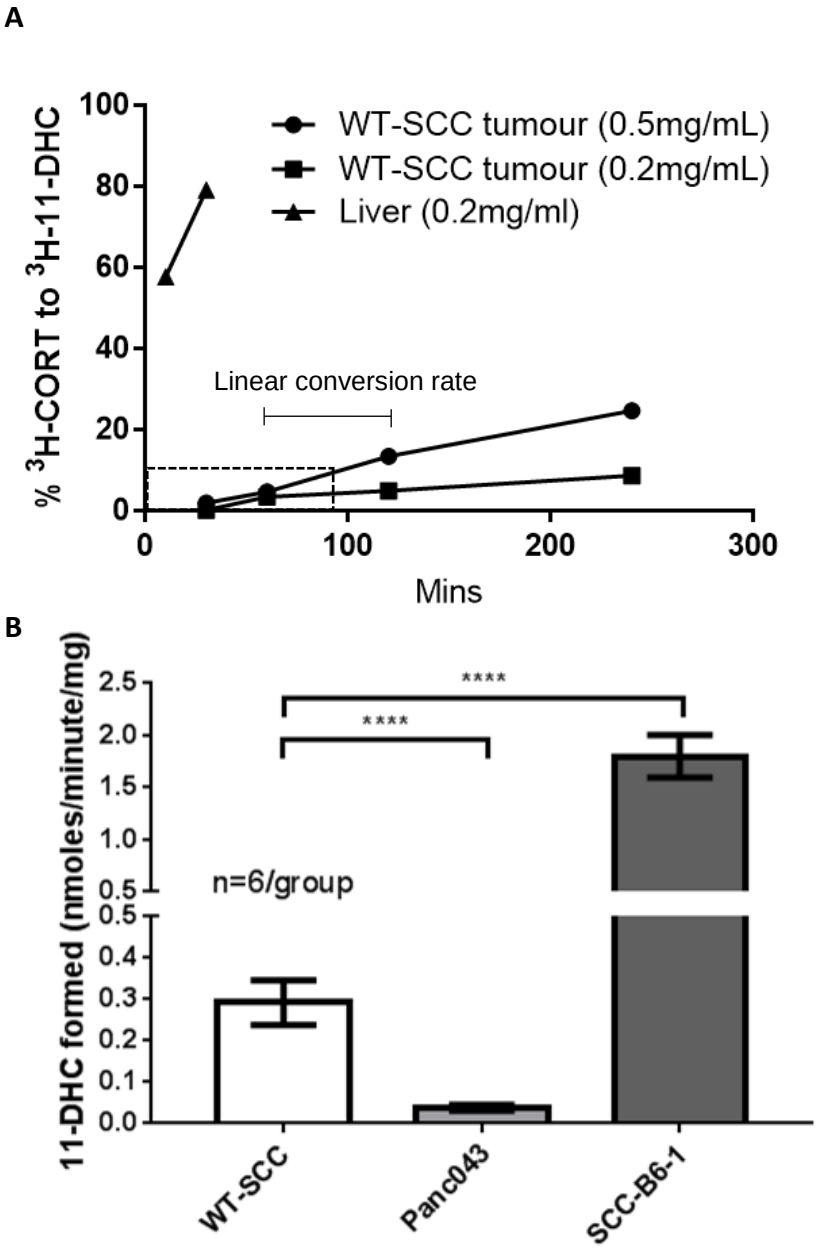

Figure 3.21 - 11β-HSD1 activity varies between tumour types. A) A preliminary time-course experiment established that between 60 - 120 minutes, product conversion was linear, leading to the selection of a 90 minute incubation time at 0.5mg/mL [protein] as the conditions to measure WT-SCC activity. Liver was used as a positive assay control. Negative (protein-free) controls were also run (not shown). B) Comparing enzyme activity between tumour types, SCC-B6-1 tumours had significantly greater 11β-HSD1 dehydrogenase activity than WT-SCC and Panc043 tumours. Experimental controls allowed for the subtraction of background signal. **** $P<0.0001$. N=6/group. Data represent mean ± standard error and were compared by one-way ANOVA with Tukey's post-hoc.

3.2.8 UE2316 levels in tissues of experimental animals

3.2.8.1 UE2316 is detected in FVB/N and C57BL6/J plasma and liver

To determine how much UE2316 delivered via diet had reached the tissues of mice, UE2316 levels were measured in the plasma and in the liver. Plasma from FVB/N mice fed control or UE2316-diet for 9 days (N=5/group) and C57BL6/J mice fed control or UE2316-diet for 19 days (N=5/group) were subject to liquid-liquid extraction. Liver and tumours were used from FVB/N mice (**section 3.2.1.4.1**) and C57BL6/J mice (**section 3.2.1.4.2**). UE2316 levels measured by LC-MS/MS were higher ($P<0.05$) in FVB/N mouse plasma (64.05 ± 30.45 ng/mL) than in C57BL6/J mouse plasma (5.60 ± 2.42 ng/mL) (Figure 3.22A). UE2316 was detectable in the liver of both C57BL6/J mice (130.7ng/g) and FVB/N mice (36.4 ng/g) (Figure 3.22B). UE2316 was not detected in tissues from animals receiving control diet from either strain. Both strains ate the same amount of UE2316-diet (Figure 3.22C). Tumour tissue was too small to allow LC-MS/MS analysis, thus it was not possible to measure UE2316 in extracts from tumours.

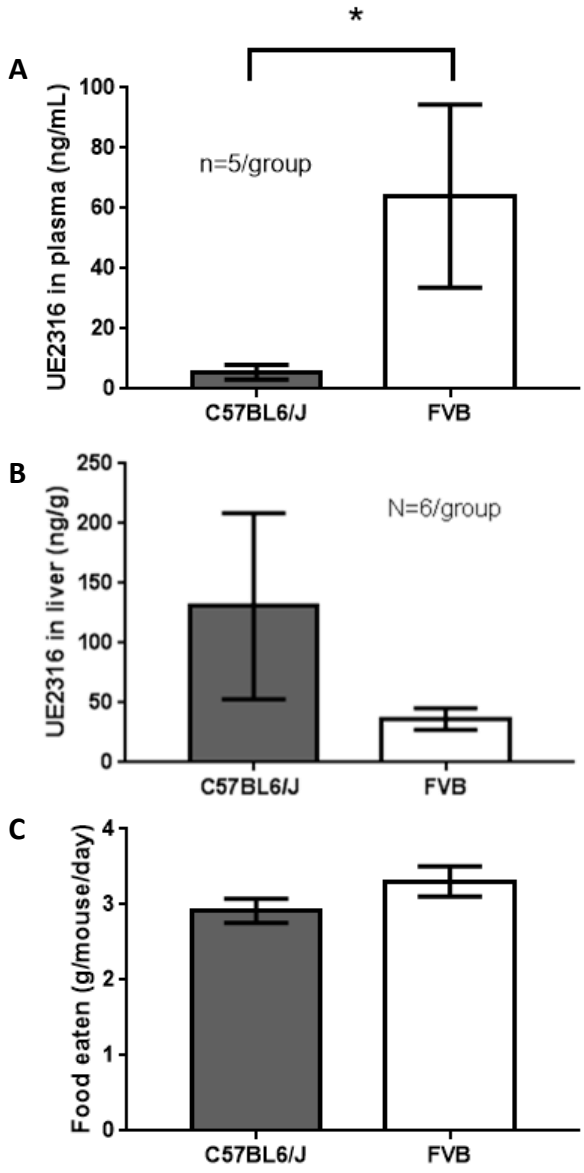

Figure 3.22 - UE2316 is detected in FVB and C57BL6/J mouse plasma and liver. A) LC-MS/MS analysis of plasma from UE2316 diet-fed animals revealed higher levels in FVB/N mice compared to C57BL6/J mice. B) UE2316 was detected in liver tissue from both strains, while the drug was not detected in the liver of untreated animals. C) No strain difference was seen in the amount of UE2316 diet consumed. * $P<0.05$. N=5-6/group. Data represent mean ± standard error and were compared by Mann-Whitney U test for panels A/B and independent samples t-test for panel C.

3.3 Discussion

The studies presented in this chapter addressed the hypothesis that 11β-HSD1 inhibition, or deletion, would decrease local tissue glucocorticoid levels and thus increase the vessel density and subsequent growth of subcutaneous murine tumours. It was further postulated that tumours with higher levels of 11β-HSD1 activity and GR expression would show a more pronounced growth increase in response to 11β-HSD1 inhibition, due to their increased glucocorticoid sensitivity. The data presented support the notion that 11β-HSD1 inhibition can promote tumour growth, as WT-SCC tumours grew more rapidly and reached a larger volume in FVB/N mice fed a diet containing the 11β-HSD1 inhibitor UE2316 than in mice fed a control diet. Enhanced growth after 11β-HSD1 inhibition or deletion was not seen in Panc043 tumours, or in the alternative SCC-B6-1 cell line, suggesting that the risk of enhanced tumour growth may be specific to certain tumour types. SCC-B6-1 tumours exhibited significantly greater levels of 11β-HSD1 activity than both WT-SCC and Panc043 tumours, suggesting that high levels of 11β-HSD1 activity are not predictive of increased growth after inhibition. However, WT-SCC tumours expressed higher levels of GR than either of the non-responsive tumour types, highlighting GR levels as potentially important when assessing sensitivity to 11β-HSD1 inhibition. Crucially, vessel density and angiogenic factor expression were unaltered by 11β-HSD1 inhibition in all tumour types suggesting that an alternative mechanism mediates enhanced growth.

11β-HSD1 inhibition and tumour growth

Subcutaneous injection of WT-SCC or Panc043 cells produced tumours that were large enough for subsequent analysis after 1-2 weeks. In contrast, SCC-B6-1 cells took 5-6 weeks to produce tumour of comparable volumes. Previous studies making use of the WT-SCC cells report tumour volumes of 0.06-0.08cm^3 after 20 days growth *in vivo* (Serrels *et al.,* 2012), suggesting the present studies achieved volumes appropriate to the study duration. Panc043 and SCC-B6-1 tumours are as yet unpublished elsewhere; however volumes achieved were consistent with observations within the lab group (M. Muir, personal communication). 11β-HSD1 inhibition enhanced growth in WT-SCC tumours. This effect was observed across a total of 9 animals per group across two technical repeats. One limitation of the present study was a failure to weigh tumours

from the original WT-SCC study. This parameter was introduced for later studies and added a confirmatory second measurement of tumour growth. The change in tumour size, however, was of sufficient magnitude as to be visually obvious to a secondary observer (M. Muir); thus this limitation is of relatively minor importance.

WT-SCC are syngeneic on an FVB/N background, while the Del1 mice are backcrossed to a C57BL6/J background, rendering the cells non-compatible with the knockout. Panc043 tumours are non-responsive to both inhibition and deletion. SCC-B6-1 cells are an alternative SCC type syngeneic on a C57BL6/J background, but their characteristics differ from WT-SCC in some key respects. The appearance of the WT-SCC cells was spindle-shaped, whereas the SCC-B6-1 cells were cobblestone-like. Spindle-cell carcinomas are a more advanced and highly malignant variant of SCC which become more refractile, invasive and chemotactic (Klein-Santzo *et al.,* 1989; Buchman *et al.,* 1991). This aggressive variant has been termed 'Class B' SCC while the more typical SCC is termed 'Class A' (Wong *et al.,* 2013). Thus the morphology of WT-SCC is indicative of them having undergone the epithelial-mesenchymal-transition after their original generation by DMBA/TPA chemical carcinogenesis and gained a more aggressive and invasive 'Class B' phenotype (Usami *et al.,* 2008; Huang and Balmain, 2014). The growth of SCC-B6-1 cells was considerably less aggressive, more typical of the 'Class A' phenotype. Tumours took around 2-3 times longer to reach sizes comparable to WT-SCC, by which point the tissue integrity was compromised and hindered histological preparation.

The growth-enhancing effect of 11β-HSD1 inhibition could not be replicated using the Del1 mice in the present studies. No significant differences in tumour growth were detected between groups in the SCC-B6-1 studies, although a trend towards increased tumour size following UE2316 administration was apparent between days 28-37; an effect absent in tumours generated in Del1 mice. Power was a likely limitation in this study, but the aforementioned degradation of tumour tissue at later stages limited the usefulness of this experiment and informed the decision to impose a 28 day limit on the length of the study, at which point tumours were intact and could be examined histologically. Given the discrepancy in SCC-B6-1 tumour growth after 11β-HSD1 inhibition compared to deletion, it would be useful to repeat the study with the addition

of a UE2316-treated Del1 mouse group. The use of the inhibitor in global 11β-HSD1 knockout mice would ensure that enzyme activity was absent in both host and donor cell types, as well as addressing any concerns regarding off-target effects.

The only previous study to directly manipulate 11β-HSD1 expression in a solid tumour model demonstrated that 11β-HSD1 overexpression reduced the growth of HCC tumours in Balb/C nude mice (Liu *et al.,* 2016). Overexpression of 11β-HSD1 in this model caused a similarly pronounced alteration in growth which was apparent from a very similar timepoint (3-5 days after cell injection). These and the present findings together support a role for 11β-HSD1 and local glucocorticoid metabolism in regulating tumour growth from an early stage, although important differences between the studies suggest alternative mechanisms may be involved. Different carcinomas were examined in these studies (HCC and SCC), though notably both are derived from tissues in which 11β-HSD1 is known to play a regulatory role (liver and skin) (Tiganuscu *et al.,* 2011; 2013; Terao *et al.,* 2011; 2014; Itoi *et al.,* 2013; Kuo *et al.,* 2015). The use of Balb/C nude, rather than FVB/N, mice also removes the potential influence of the immune system on tumour growth in the study of Liu *et al.*. The use of a murine tumour cell line able to grow in mice with a functional immune system is a considerable strength of the present studies, as 11β-HSD1 deletion reduces T-cell infiltration in some inflammatory models (Wamil *et al.,* 2011; Luo *et al.,* 2012; Kipari *et al.* 2013) and is likely to influence the tumour microenvironment (Kim *et al.,* 2007). Most importantly, Liu *et al.* (2016) saw a significant reduction in tumour angiogenesis (CD31/CD34 staining), attributed to reduced glycolysis, in tumours overexpressing 11β-HSD1 compared to controls. This effect was notably absent from the present study, thus the mechanisms responsible in the HCC model of Liu *et al.* and in the present study models are likely different.

11β-HSD1 inhibition and angiogenesis

Contrary to the hypothesis, both vessel density and the proportion of vessels with smooth muscle coverage were unaltered by 11β-HSD1 inhibition. Small *et al.* (2005) were the first to demonstrate that deletion of 11β-HSD1 could promote angiogenesis *in vivo*. In their studies, 11β-HSD1 KO mice had a greater angiogenic response than their wild-type litter mates across three separate models; subcutaneous sponge

implantation, chronic coronary artery ligation and dermal wound healing. Vessel density in both sponge and dermal wounds was quantified by Chalkley count, an established methodology for use in tumours (Hansen *et al.*, 2000). Chalkley counts were one of three different vessel quantification methods used in the present studies, all of which demonstrated no difference between groups. As well as Chalkley counts, quantification of vessels from both random fields of view and from pre-selected vascular hotspots showed no difference in vessel density after 11β-HSD1 inhibition, demonstrating the robust nature of the observation.

Vessel density has previously proven to be a valid measure of tumour angiogenesis. Yano *et al.* (2006) found that exposing mice to 1μg dexamethasone thrice weekly reduced prostate cancer-derived subcutaneous tumour size and vessel density, quantified using very similar methodology to that used in the present study. Of note, vessel counts in the prostate cancer tumours were considerably lower (30-50 vessels per 0.74mm^2) than counts in WT-SCC tumours (150-200 vessels per 0.74mm^2). While this may reflect a difference in quantification criteria, more likely it suggests that the WT-SCC tumours are a highly vascularised tumour type. Potentially, this may render them less sensitive to angiogenic manipulations, as the sheer magnitude of the angiogenic response could overwhelm any potential influence of altered glucocorticoid levels. This is further supported by the more pronounced difference in vessel density seen in WT-SCC tumours removed at day four compared with those removed at day 11; it is possible that the day four timepoint precedes an intensely pro-angiogenic phase. As this observation did not reach significance, further investigation would be required before conclusions can be drawn. In the present project, alternative lines of investigation were pursued based on results presented in later chapters. Yano *et al.,* (2006) also saw a decrease in VEGF-A mRNA levels corresponding to their reduced vessel density data; in the present study VEGF-A and VEGFR-2 were both unaffected by 11β-HSD1 inhibition, which does not support the original hypothesis.

The main pathological models in which Small *et al.* (2005) saw enhanced angiogenesis were coronary artery ligation and dermal wound healing. Enhanced angiogenesis and recovery post-myocardial infarction has since been demonstrated a number of times, using both 11β-HSD1 knockout mice (McSweeney *et al.*, 2010; White *et al.*, 2015;

Mylonas *et al.* 2017) and the 11β-HSD1 inhibitor UE2316 (McGregor *et al.*, 2014). The reparative response to myocardial infarction is characterised by enhanced neutrophil and macrophage recruitment into the myocardium, a response that is enhanced by 11β-HSD1 inhibition (McSweeney *et al.*, 2010; Mylonas *et al.*, 2017). 11β-HSD1 deficiency also increases acute inflammation in models of arthritis, peritonitis and pleurisy (Coutinho *et al.*, 2012; 2016). This effect is not seen across all disease models; in adipose tissue and atherosclerotic plaques from 11β-HSD1 KO animals, inflammatory and immune cell infiltration is attenuated (Wamil *et al.*, 2011; Kipari *et al.*, 2013). Arguably, the chronic, non-resolving inflammation and hypoxia seen in obese adipose tissue and atheroma is more similar to the tumour microenvironment than ischaemic myocardium, thus mechanistically these models may be of more relevance. Furthermore, angiogenesis after induced myocardial infarction in rodents is a beneficial process and distinct from the aberrant non-resolving hypoxia-driven angiogenesis seen in tumours (Carmeliet, 2003, Chung and Ferrara, 2011).

Panc043 tumours were significantly less vascularised than WT-SCC tumours, an observation in keeping with the literature. Olive *et al.* (2009) report that pancreatic ductal adenocarcinoma (PDAC) specimens are hypovascularised and hypothesise that their vascular architecture limits the perfusion and drug delivery into PDAC. Importantly, the *KrasLSL.G12D/+; p53R172H/+; PdxCretg/+* (KPC) mouse model used by Olive *et al.* (2009) to produce their murine PDAC tumours is the same used to generate the Panc043 cells used in the present study, making these findings highly comparable. PDAC has also been reported to be hypovascularised by groups using contrast-enhanced ultrasound to examine tumour perfusion (Sofuni *et al.*, 2005; Sakamoto *et al.*, 2008) and PDAC does not respond to the anti-angiogenic drug bevacizumab (Van Cutsem *et al.*, 2009), further demonstrating that these tumours are relatively nonangiogenic or that their development is not dependent on angiogenesis. PDAC is also characterised by an abundant desmoplastic stroma comprising mainly α-smooth muscle actin-positive cancer-associated fibroblasts (CAFs) (Özdemir *et al.*, 2014; Öhlund et al., 2017), associated with excessive extracellular matrix (ECM) deposition and increased interstitial fluid pressure which are thought to further inhibit drug delivery (Provenzano *et al.*, 2012; Whatcott *et al.*, 2012). Thus it is possible that

poor perfusion led to compromised delivery of UE2316 into tumours. The present study is limited by the failure to quantify intra-tumour UE2316 levels; insufficient tissue was available to produce a robust result. While reduced perfusion could explain the lack of Panc043 response to UE2316-treament, it cannot explain the lack of response seen in the Del1 mice, suggesting that sensitivity to 11β-HSD1 manipulation is governed by more than just tissue architecture. However, tissue perfusion remains an important consideration as acute enzymatic inhibition may affect tumour growth differently to chronic deletion of 11β-HSD1.

The surprising observation that Del1 mice were significantly heavier than the commercially purchased C57BL6/J mice that formed the control and UE2316 groups, despite age-matching, is difficult to explain. Although not the result of an experimental manipulation (weights differed from the beginning of the study), the difference was apparent across all experiments using the Del1 mice. No differences in the amount of diet consumed by Del1 mice were seen, thus the effect cannot be explained by increased feeding. The previous 11β-HSD1 knockout mice generated in-house did not differ in weight from their wild type litter mates (Kotelevtsev *et al.*, 1997). The current knockout, Del1, has been back-crossed to the C57BL/6OlaHSD substrain (available from the Jackson Laboratory), the same substrain as the commercially purchased mice used in these experiments. Increased body weight is more perplexing still in light of reports that 11β-HSD1 deletion protects against, whereas overexpression promotes, obesity (Stimson and Walker, 2007; Morton *et al.*, 2008; Harno *et al.*, 2013). The difference is thus most likely to have arisen as a result of different housing conditions between in-house lines and commercial lines. The importance of mouse substrain has recently been highlighted as a consideration commonly neglected by researchers (Fontaine and Davis, 2016). Ideally littermate controls would be used for comparison in studies such as this, however as the available Del1 colony was entirely homozygous mutants, age-matched controls of an identical-substrain were selected as the most suitable option.

11β-HSD1 inhibition and angiogenic factor expression

The absence of an effect on vessel number in tumours led to the examination of angiogenic factor expression in tumours, to confirm that a more subtle effect had not

been overlooked. SCC-B6-1 were not included in these studies as the considerable differences seen between WT-SCC and SCC-B6-1 tumour growth limited the usefulness of this comparison. Panc043 tumours were analysed and presented as a non-responsive comparison to the WT-SCC tumours. No differences were seen in expression of VEGFA, VEGFR2 or TSP-1 in WT-SCC or Panc043 tumours. VEGFA and VEGFR2 are central to the process of endothelial cell migration, and are pre-requisites for the coordinated Notch-DLL4 signalling that dictates stalk and tip cell identity (Carmeliet and Jain, 2011). Glucocorticoid-mediated alterations in angiogenesis are often reflected in VEGF mRNA levels (Nauck *et al.,* 1998; Gille *et al.,* 2001; Pufe *et al.,* 2003; Wen *et al.,* 2003; Yano *et al.,* 2006; Michailidou *et al.,* 2012), though a change in VEGF transcript does not always accompany changes in angiogenesis. Hasan *et al.* (2000) found glucocorticoids were able to promote haemangioma regression without an accompanying reduction in VEGF. Logie *et al.,* (2010) also saw no effect of cortisol on VEGFA or VEGFR2 transcript expression in HUVECs, though they did observe a significant increase in the anti-angiogenic glycoprotein TSP-1. Reduced TSP-1 expression and increased 11β-HSD2 signalling were also seen in women with heavy menstrual bleeding (Rae *et al.,* 2009), suggesting this protein may play a mechanistic role in the regulation of angiogenesis by glucocorticoids. 11β-HSD1 knockout mice show increased angiogenesis in models of MI and inflammatory arthritis without an accompanying increase in VEGFA mRNA (McSweeney *et al.,* 2010; Zhang *et al.,* 2017), leading to the proposition that enhanced angiogenesis after 11β-HSD1 deletion is mediated by tissue resident macrophages downstream of VEGF (Zhang *et al.,* 2017).

HIF-1α expression in WT-SCC tumours was unaltered by administration of UE2316, whereas in Panc043 tumours its expression was reduced by UE2316 treatment. This suggests that, despite not affecting tumour growth, 11β-HSD1 inhibition may still be exerting an effect on the tumour microenvironment. Whether this effect is systemic or mediated within the tumour cannot be determined by the present data. The finding that HIF-1α was decreased by UE2316 in Panc043 tumours is at odds with the reduction in HIF-1α and VEGF protein seen in 11β-HSD1 overexpressing HCC tumours (Liu *et al.,* 2016), and, without an associated change in angiogenesis cannot be attributed to reduced hypoxia within the tumour. In keeping with the present observation,

Michalidou *et al.* (2012) observed decreased HIF-1α expression in adipose tissue from 11β-HSD1 knockout mice, likely the result of reduced tissue hypoxia and inflammation. The lack of impact that UE2316 had on Panc043 tumour size suggests that these observations are not of major relevance to tumour progression, but they highlight the myriad influences glucocorticoid manipulation may have on tumour biology. Given the role of HIF-1α in promoting metastasis (Masoud and Li, 2015), such findings may warrant further investigation.

IL-6 is a pro-angiogenic inflammatory cytokine (Gopinathan *et al.,* 2015). In keratinocytes it is regulated by glucocorticoids in a biphasic manner, whereby physiological stress level of cortisol elevate its expression while pharmacological levels suppress it (Bernabé et al., 2011). The angiostatic effects of glucocorticoids have been linked to reduced production of IL-6 *in vivo* (Hori *et al.,* 1996; Hasan *et al.,* 2000). Given that high IL-6 levels are predictive of poor prognosis in squamous cell carcinoma (Duffy *et al.,* 2008) and are seen to be regulated by glucocorticoids in glucocorticoid-sensitive cancers (such as prostate; Nishimura *et al.,* 2001), it was investigated as a potential mechanistic factor; however IL-6 levels did not differ between WT-SCC tumours and transcript could not be detected in Panc043 tumours.

Glucocorticoid sensitivity of different tumour types

A research question for this chapter was whether the glucocorticoid profile of a tumour (11β-HSD1/2, GR and MR levels) was predictive of tumour sensitivity to 11β-HSD1 inhibition. Findings suggest that GR levels may be important, as WT-SCC tumours expressed significantly more GR than either of the other tumour types. The absence of MR transcript from WT-SCC tumours strongly suggests that GR is of more mechanistic importance (notwithstanding the possibility of a systemic mechanism mediated outwith the tumour). The present findings are in agreement with other studies that report SCC express particularly high levels of GR (Budunova *et al.,* 1997; Spiegelman *et al.,* 1997) and lack MR (Suzuki *et al.,* 2000), though data from this chapter did not examine receptor function. As GR levels are a key determinant of tissue sensitivity to glucocorticoid action (Vanderbilt *et al.,* 1987; Lin and Wang, 2016), this suggests that SCC may be a glucocorticoid-sensitive tumour type. GR expression in Panc043 tumours, but not in SCC tumours, was reduced by UE2316 treatment,

additional evidence that 11β-HSD1 inhibition may be altering this tumour type in a manner that does not affect growth. This finding is unexpected; 11β-HSD1 inhibition would be expected to decrease tumour glucocorticoid levels, and glucocorticoids downregulate GR mRNA expression in many tissues including tumours (Rosewicz *et al.,* 1988; Vedeckis *et al.,* 1989; Budunova *et al.,* 1997; Freeman *et al.,* 2004); notable exceptions include some lymphoid cell lines (Eisen *et al.,* 1988). Thus this finding is difficult to interpret without further investigation.

The relevance of absolute enzyme levels is unclear; SCC-B6-1 tumour type expressed large amounts of 11β-HSD1 mRNA and a high degree of activity compared to WT-SCC tumour, but did not respond to 11β-HSD1 inhibition. The cell types expressing 11β-HSD1 within tumours remain to be identified. Understanding cell-specific distribution of this enzyme may clarify the apparent paradox of a tumour with high 11β-HSD1 activity not responding to 11β-HSD1 inhibition. The present data suggest that 11β-HSD1 expression in SCC-B6-1 tumour cells is induced after they are injected into animals, as the Del1-grown tumours had transcript present, despite the gene being deleted in host tissues. Induction of 11β-HSD1 expression may be a consequence of exposure to inflammatory cytokines (Chapman *et al.,* 2013a). The same could theoretically have occurred in the other tumour types, but it is possible that enzyme expression in tumour cells is less important than expression within immune/inflammatory or fibroblast cell populations. The concept that 11β-HSD1 expression is important in a specific subset of cells would somewhat negate the relevance of absolute 11β-HSD1 levels in tumours. From the present data the conclusion is that tumour GR expression within tumours may be predictive of sensitivity to 11β-HSD1 expression, whereas expression of overall tumour 11β-HSD1 is not predictive.

A large number of cancerous tissues express less 11β-HSD1 and more 11β-HSD2 than healthy controls (Takahashi *et al.,* 1998; Bland et al., 1999; Coulter *et al.,* 1999; Cooper et al., 2000; Gingras and Margolin, 2000; Pácha et al., 2002; Dovio et al., 2009; Liu et al., 2016) and several reports suggest this switch enhances cell proliferation (Hundertmark et al., 1997; Koyama and Krozowski, 2001; Woitge *et al.,* 2001; Koyama et al., 2001; Rabbitt *et al.,* 2002). This would suggest that targeting 11β-HSD1

would promote tumour growth. SCC are an exception in that 11β-HSD1 remains detectable while 11β-HSD2 is undetectable (Suzuki *et al.,* 2000; Gronau *et al.,* 2002; Cirillo *et al.,* 2012; Terao *et al.,* 2013). The present findings are in agreement with the literature; 11β-HSD1 was detected in both SCC tumour types at a higher level than in Panc043 tumours (in which 11β-HSD1 levels were at the limit of detection). 11β-HSD2 was undetectable in all tumour types.

11β-HSD1 mRNA levels were reduced by UE2316 in WT-SCC tumours but not in SCC-B6-1 tumours, another potential contributor to the enhanced response seen in WT-SCC tumours. Dexamethasone increases 11β-HSD1 expression in adipose tissue (Balachandran *et al.,* 2008), thus the opposite process may be occurring in tumours, whereby decreased binding of active glucocorticoids to GR reduces 11β-HSD1 expression. The reverse is often true in biology though, with reduced signalling leading to compensatory increased expression of pathway components. Alternatively, the decrease in whole tumour 11β-HSD1 transcript after UE2316 treatment may reflect a change in the relative proportion of 11β-HSD1-positive cell types; data from the current chapter show that vascular cell proportions are not altered by UE2316 and suggest that WT-SCC contribute no or negligible 11β-HSD1 content, thus inflammatory/immune cells and fibroblasts are candidate populations. As 11β-HSD1 expression is also increased by inflammatory stimuli (Sun and Myatt, 2003; Ignatova *et al.,* 2009; Ahasan *et al.,* 2012), reduced 11β-HSD1 expression after UE2316 treatment may also suggest reduced intra-tumour pro-inflammatory signalling. 11β-HSD1 is reduced in conditions that stimulate proliferation of keratinocytes (Terao *et al.,* 2013) so reduced enzyme expression may actually be a consequence of enhanced tumour growth.

Attempts to localise 11β-HSD1 histologically were, unfortunately, unproductive due to problems with the immunohistochemistry technique, specifically, non-specific binding of the 11β-HSD1 antibody in tissues from knockout animals. 11β-HSD1 immunostaining was subsequently abandoned in favour of enzyme transcript and activity measurements, which were reproducible but offered no insight into cellular localisation. No 11β-HSD1 transcript was detected in cultured tumour cells. Key sites of 11β-HSD1 expression in the tumour microenvironment are the vasculature (Walker

et al., 1991; Dover *et al*., 2007), immune and inflammatory cells (Thieringer *et al*., 2001; Gilmour *et al*., 2006), and fibroblasts (Lee *et al*., 2013; Tiganescu *et al*., 2013; Terao *et al*., 2014). Experimental evidence reported in this chapter showed that, whereas 11β-HSD1 expression was low in WT-SCC tumours compared to liver, its expression was very similar in subcutaneous sponge tissue taken from mice 7 days after implantation. Implanted sponges are infiltrated by host vessels, inflammatory cells and stromal cells. Implanted tumour cells form tumours which are similarly populated by host tissues, thus this observation may suggest similar 11β-HSD1-expressing cell populations within WT-SCC tumours. The importance of stromal cells as 11β-HSD1-expressing cells in tumours warrants further investigation, as despite reports (and qualitative observations from the present study) that PDAC express high levels of stromal CAFs (Özdemir *et al*., 2014; Öhlund *et al.,* 2017), Panc043 tumours had negligible 11β-HSD1 activity, suggesting that stromal cells in these tumours do not express large amounts of 11β-HSD1. This would most readily be achieved by fluorescence associated cell sorting of tumour cells.

Delivery of UE2316

For the *in vivo* experiments described in this thesis, UE2316 was delivered via a custom-made RM-1 diet (McGregor *et al.,* 2014; Sooy *et al.,* 2015). Diet-based delivery was selected to avoid the stress associated with other delivery routes (injection/gavage/mini-pump) which could affect circulating glucocorticoids. Mice were given access to diet *ad-libitum* but tissues were also taken as close to 8am as possible so as to capture nadir baseline corticosterone levels. A previous study using the drug-diet delivered an efficacious calculated dosage of 30mg/kg/mouse/day (Sooy *et al.,* 2015). The estimated dosage achieved in the present studies (based on diet consumed per cage per 2-3 days) was 25-30mg/kg/mouse/day, a dose seen to be efficacious in previous studies. UE2316 levels in C57BL6/J mouse plasma were in a similar region to previous measurements that used mini-pump administration of UE2316 (Wheelan *et al.,* 2015). Cobice *et al.* (2013; 2017) have shown that whole brain levels of UE2316 in C57BL6/J mice given 20-25 mg/kg orally (via gavage) fall rapidly from 300-500 ng/g after 1-2 hours to around 50 ng/g after 4-6 hours, demonstrating the fast clearance of the drug. This may explain why plasma UE2316

levels were significantly lower in C57BL6/J animals than in FVB/N animals despite both strains consuming very similar amounts of drug-diet. Liver levels of UE2316 were variable in C57BL6/J mice (50-200 ng/g) and lower but more consistent in FVB/N mice (25-50 ng/g). The time at which mice had last eaten may have affected measured levels and could explain this discrepancy between strains and variability within groups, however strain-specific differences in pharmacokinetics cannot be discounted.

In conclusion, data from this chapter provide evidence that 11β-HSD1 inhibition can promote growth in some models of subcutaneous tumour formation. The sensitivity of tumours formed following injection of WT-SCC may be due to their high GR expression, but high expression of 11β-HSD1 itself is less predictive of a growth response to 11β-HSD1 inhibition. Contrary to the research hypothesis, the mechanism responsible for increased growth does not appear to be increased angiogenesis. UE2316 promotes angiogenesis in a mouse model of myocardial infarction (McGregor *et al.* 2014) but recent evidence suggests that it does not affect angiogenesis in a mouse model of hindlimb ischaemia (J. Wu, personal communication), thus its effects on angiogenesis appear to be context-dependent. No studies have previously examined the effect of a selective 11β-HSD1 inhibitor on an *ex vivo* model of angiogenesis, with previous studies using the non-selective 11β-HSD inhibitor carbenoxolone (Small *et al.*, 2005). If the tumour vasculature is unaffected by 11β-HSD1 inhibition, what is the mechanism? Before examining the different components of the tumour microenvironment, it will be important to directly assess the effect of UE2316 and glucocorticoids on tumour cell proliferation *in vitro*.

Chapter 4

Effects of the 11β-HSD1 inhibitor UE2316 on angiogenesis and tumour cells

4 11β-HSD1 inhibition, angiogenesis and tumour cell division

4.1 Introduction

In the previous chapter, UE2316 increased the growth of WT-SCC tumours but did not affect vessel density or molecular markers of angiogenesis. 11β-HSD1 inhibition has previously been shown to increase angiogenesis in other contexts, including *in vivo* after induced myocardial infarction (Small *et al.*, 2005; McSweeney *et al*., 2010; McGregor *et al.*, 2014; White *et al.*, 2015) and *ex vivo* in the aortic ring assay using the non-selective 11β-HSD inhibitor carbenoxolone and genetic deletion (Small et al., 2005). In tumours, sources are limited but Liu et al. (2016) report that over-expression of 11β-HSD1 in hepatocellular carcinoma decreased tumour angiogenesis and size. Thus, the lack of angiogenic effect observed in the present study was unexpected.

UE2316 is a selective murine 11β-HSD1 inhibitor. The *ex vivo* angiogenic effects of the 11β-HSD1-selective inhibitor UE2316 have never been studied before, with previous studies using the non-selective 11β-HSD inhibitor carbenoxolone. Small *et al.*, (2005) used the aortic ring assay to show that while 11-dehydrocorticosterone (11-DHC) and corticosterone were angiostatic, inhibition using carbenoxolone, or genetic deletion of 11β-HSD1, prevented the angiostatic effects of 11-DHC. These findings suggest that local activation of glucocorticoids promotes angiostasis, however the effects of acute selective 11β-HSD1 inhibition must be determined.

If the enhanced growth effect observed in squamous cell carcinoma (SCC) tumours is not the result of increased angiogenesis, a direct effect on tumour cell proliferation may be responsible. The syngeneic murine solid tumour model generates subcutaneous tumours comprised of donor tumour cells and a tumour microenvironment comprised of invading host cells (predominantly immune, inflammatory and vascular cells). Reports concerning the effects of glucocorticoids on cancer cell lines, including squamous cell carcinoma, are conflicting. The inhibitory effects of glucocorticoids on cell proliferation are well-reported (Azher et al., 2016) but in many solid tumours glucocorticoids induce resistance to chemotherapeutics and promote cell proliferation

(Zhang *et al.,* 2007; Lin and Wang, 2016). The proliferation of healthy keratinocytes is inhibited by locally regenerated glucocorticoids (Terao *et al.,* 2011), though the story in tumour cells is often complicated by increased resistance to glucocorticoid mediated apoptosis (Schlossmacher *et al.,* 2011). Furthermore, corticosteroids have been shown to both increase (Bernabé *et al.,* 2011; Cirillo *et al.,* 2017) and inhibit proliferation (Hofmann *et al.,* 1995) in SCC. Whilst the working hypothesis for these studies predicts the involvement of host cells, an off-target effect of UE2316 on tumour cell growth also cannot be ruled out.

Hypotheses

The work described in this chapter addressed the hypotheses that:

- The 11β-HSD1 inhibitor UE2316 influences angiogenesis and tumour cell proliferation in *ex vivo* and *in vitro* models of these intra-tumour processes

- 11β-HSD1 inhibition/deletion prevents conversion of 11-DHC to corticosterone, thus preventing 11-DHC-mediated angiostasis in the aortic ring assay

- Physiological concentrations of glucocorticoids inhibit SCC cell proliferation

Objectives

The specific aims of this work were:

(1) To determine whether 11-DHC and corticosterone exert angiostatic effects on aortic rings from FVB/N and C57BL6/J mice *ex vivo.*

(2) To determine whether UE2316 selectively inhibits 11-DHC mediated-angiostasis

(3) To determine whether deletion of 11β-HSD1 selectively inhibits 11-DHC mediated-angiostasis

(4) To confirm the inhibitory effect of UE2316 on 11β-HSD1 in intact tissue

(5) To determine whether UE2316 promotes the proliferation of WT-SCC, Panc043 and SCC-B6-1 cells

(6) To determine whether physiological concentrations of corticosterone inhibit the proliferation and viability of WT-SCC, Panc043 and SCC-B6-1 cells

4.2 Results

4.2.1 The effects of 11β-HSD1 inhibition and deletion on aortic ring vessel growth

4.2.1.1 Angiostasis is inhibited by 100-300nM 11-DHC

Before examining the effects of 11β-HSD1 inhibition on aortic rings, an initial experiment was performed to determine an assay appropriate glucocorticoid concentration for inhibiting angiogenesis. A preliminary 11-DHC concentration-response curve was performed, showing that 100 - 300nM 11-DHC significantly reduced vessel number. Aortic rings were harvested from wild-type (WT) C57BL6/J mice (female, aged 10-12 weeks). Experiments included five treatment conditions: vehicle (0.3% ethanol/DMSO); 11-DHC (10nM, 30nM, 100nM, 300nM) - N=10 for all conditions bar 10nM, for which N=8. 300nM was selected for use in future experiments (Figure 4.1). This experiment was performed by Eileen Miller, with data analysis performed by the author.

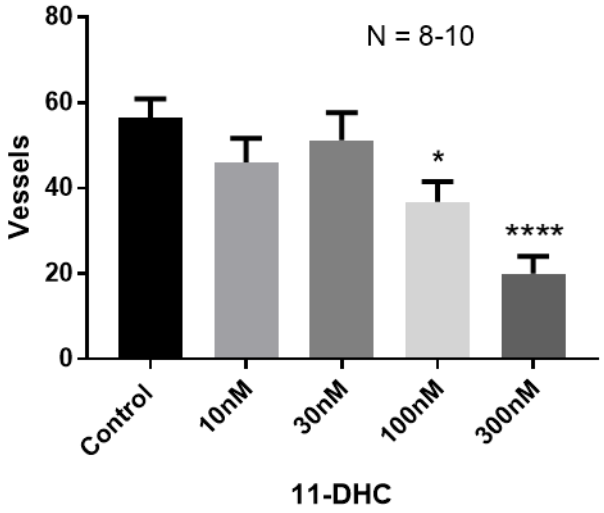

Figure 4.1 – 11-DHC concentration-response curve for *ex vivo* angiogenesis. Aortic rings from wild type C57BL6/J mice were cultured for one week in the presence of varying concentrations of the inactive glucocorticoid 11-dehydrocorticosterone (11-DHC). 300nM caused a marked reduction in vessel number, while 100nM induced mild angiostasis. Lower concentrations had no significant effect. Note that vessel counts are pooled for days 6/7. N=8-10. * P<0.01, **** P<0.0001 vs. control. Data represent mean ± standard error and were compared by one-way ANOVA with Dunnett's post-hoc test.

4.2.1.2 UE2316 did not rescue steroid-mediated angiostasis and reduced outgrowths from aortic rings

4.2.1.2.1 *C57BL6/J mice*

To determine whether UE2316 could prevent corticosteroid-mediated angiostasis, aortic rings from C57BL6/J (female, aged 10-12 weeks, N=8) were cultured in the presence of either vehicle, 300nM 11-DHC or 300nM corticosterone, with or without 300nM UE2316 (Figure 4.2A). Vehicle-treated rings produced 72 ± 14 vessels at day 7 (N=8). Addition of UE2316 alone reduced the number of outgrowths on day 7 (31 ± 7 vessels, $P<0.01$). 11-DHC (20 ± 4 vessels, $P<0.0001$) and corticosterone (9 ± 2 vessels, $P<0.001$) were both angiostatic and UE2316 did not prevent this angiostasis.

4.2.1.2.2 *FVB mice*

To confirm findings in C57BL6/J mice in the FVB/N mice, aortic rings from FVB/N mice (female, aged 10-12 weeks, N=6 mice) were cultured in the presence of either vehicle (0.3% ethanol/DMSO), 300nM 11-DHC or 300nM corticosterone, with or without 300nM UE2316 (Figure 4.2B). Vehicle-treated rings produced 23 ± 5 vessels at day 7 (N=6), fewer than the counts seen in C57BL6/J aortic rings. Addition of UE2316 alone had no effect (23 ± 6 vessels). 11-DHC (1.2 ± 0.8 vessels, $P<0.05$) and corticosterone + UE2316 (0.7 ± 0.2 vessels, $P<0.001$) were both angiostatic.

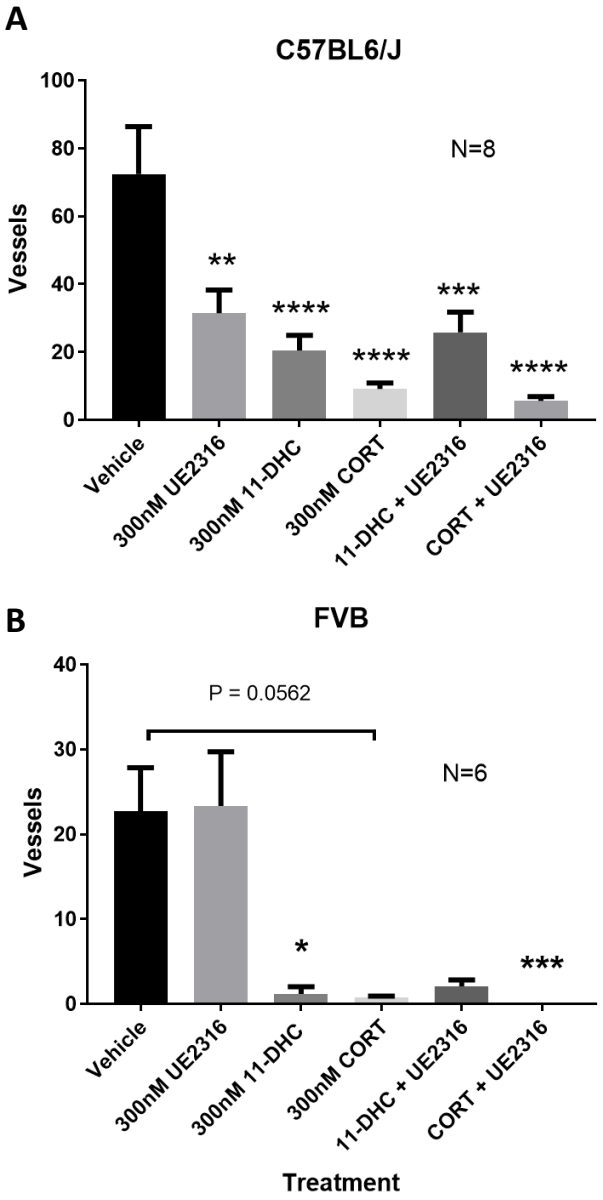

Figure 4.2 - UE2316 did not prevent glucocorticoid-mediated angiostasis. A) In vessels from C57Bl6/J mice, 300nM of the 11β-HSD1 inhibitor UE2316 reduced new vessel outgrowths. 300nM 11-dehydrocorticosterone (11-DHC) or corticosterone potently inhibited angiogenesis, and UE2316 did not affect this inhibition. N=8, data compared by one-way ANOVA with Dunnett's post-hoc test. B) In vessels from FVB mice, the angiostatic effect of UE2316 alone was not apparent. However, UE2316 did not prevent glucocorticoid-mediated angiostasis. Aortic rings from FVB mice showed less vessel growth than C57Bl6/J. * P<0.05, **P<0.01, ***P<0.001, ****P<0.0001. N=6. Data represent mean ± standard error and were compared by Kruskal-Wallis test with Dunn's post-hoc test.

4.2.1.3 Del1 mice were protected from the angiostatic effect of 11-DHC

To determine whether 11β-HSD1 deletion could prevent glucocorticoid-mediated angiostasis, aortic rings from WT C57BL6/J mice (female, 10-12 weeks, N=6) and Del1 mice (homozygous for disruption of *hsd11b1* gene, female, 10-12 weeks, N=4) were cultured in the presence of either vehicle (0.3% ethanol/DMSO), 300nM 11-DHC or 300nM corticosterone (Figure 4.3). Vehicle-treated rings from WT (41 ± 8 vessels) and Del1 mice (74 ± 29 vessels) produced vessels by day 7, with Del mice producing 1.8-fold more vessels than WT mice (non-significant). In WT mice, 11-DHC (10 ± 2 vessels) and corticosterone (10 ± 3 vessels) both caused angiostasis ($P<0.01$). In Del1 mice, only corticosterone was angiostatic (10 ± 5 vessels, $P<0.01$) while 11-DHC had no effect on vessel growth (68 ± 9 vessels). Thus, the lack of 11β-HSD1 in Del1 mice prevents the activation of glucocorticoids and their angiostatic effects, an effect not seen using UE2316.

Representative images from these experiments are summarised in Figure 4.4.

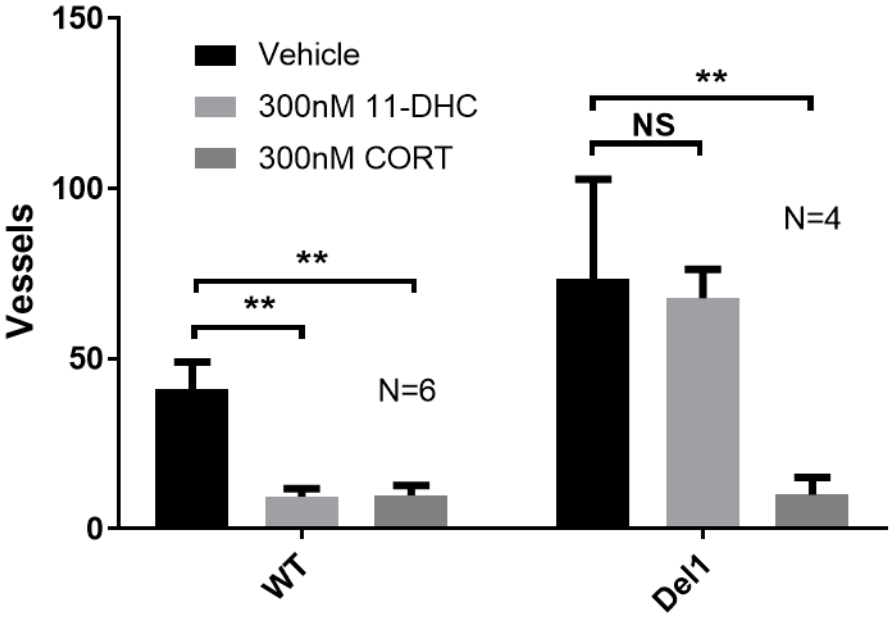

Figure 4.3 - Genetic ablation of 11β-HSD1 prevented 11-DHC-mediated angiostasis. Aortic rings from wildtype mice showed a significant reduction in angiogenesis in the presence of 300nM 11-dehydrocorticosterone (11-DHC) compared to Del1 mice in the presence of 300nM 11-dehydrocorticosterone. 300nM corticosterone inhibited angiogenesis in aortae from both wild-type and Del1 mice. ** $P<0.01$. Data represent mean ± standard error and were compared by one-way ANOVA with Dunnett's post-hoc test. N=6 wild type C57BL6/J mice, N=4 Del1 mice.

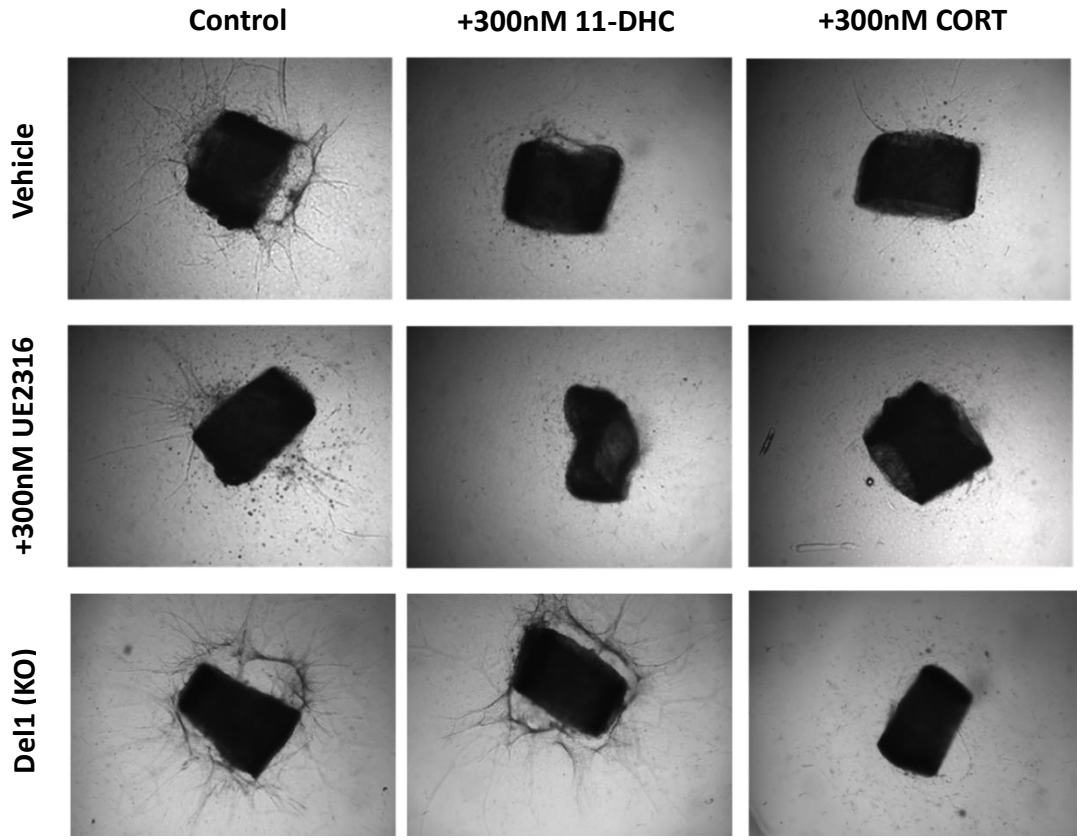

Figure 4.4 - UE2316 is antiangiogenic and did not rescue 11DHC-mediated angiostasis in the same fashion as 11β-HSD1 KO. Representative images of aortic rings from wild-type and Del1 (11β-HSD1 knockout) animals, treated with glucocorticoids and the 11β-HSD1 inhibitor UE2316. Vehicle-treated rings grow similarly in both wild-type and Del1 animals (top and bottom left), while UE2316 causes a moderate reduction in vessel number (middle left). 11-dehydrocorticosterone (11-DHC) and corticosterone potently inhibit angiogenesis in all rings apart from Del1 animals (bottom middle). The addition of UE2316 does not prevent this inhibition (centre).

4.2.2 Effect of UE2316 on 11β-HSD1 activity in intact liver

To confirm the inhibitory effect of UE2316 on 11β-HSD1 activity, an enzyme activity assay was performed using liver from C57BL6/J mice (N=6). 300nM UE2316 inhibited the reduction of ^{3}H-cortisol to ^{3}H-cortisone by 11β-HSD1 in intact liver by 45% (P<0.0001), demonstrating the inhibition of 11β-HSD1 reductase activity (Figure 4.5). Cortisol and cortisone were used as an alternative to 11-DHC and corticosterone in this assay, as they can be commercially purchased as purified steroids, whereas in-house generation of ^{3}H-11-DHC results in the detection of other interfering breakdown products during HPLC analysis. Furthermore, 11-DHC/corticosterone and cortisol/cortisone share very similar enzyme kinetics (Maser *et al.* 2002).

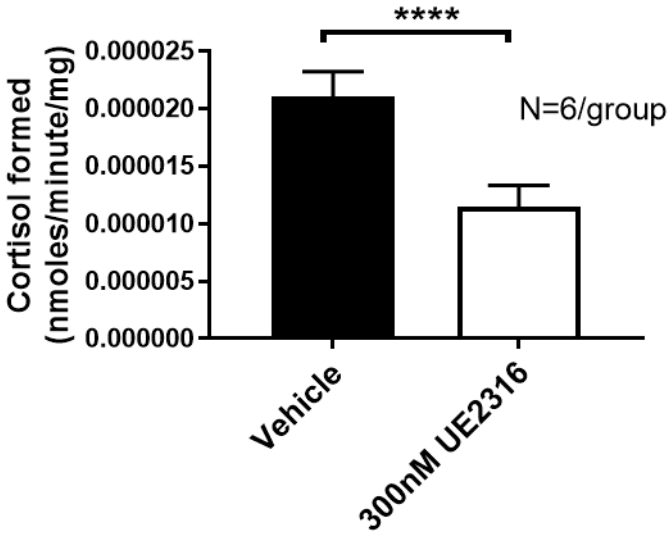

Figure 4.5 - UE2316 inhibits 11β-HSD1 reductase activity in intact tissue. Liver pieces incubated with ^{3}H-cortisone and 300nM of the 11β-HSD1 inhibitor UE2316 were unable to generate as much cortisol over 24 hours as control liver incubated in the absence of UE2316, demonstrating the inhibitory action of the drug. N=6/group, **** P<0.0001. Data represent mean ± standard error and were compared by independent samples t-test.

4.2.3 Effects of UE2316 and glucocorticoids on tumour cells

4.2.3.1 Manual cell counts

To determine the effects of UE2316 on WT-SCC and Panc043 cell proliferation, manual cell counts were performed on cells exposed to the compound for 48 hours. Manual cell counting found no significant effect of UE2316 on absolute cell number across a range of UE2316 concentrations (Figure 4.6). This was true for both cell types examined (WT-SCC and Panc043).

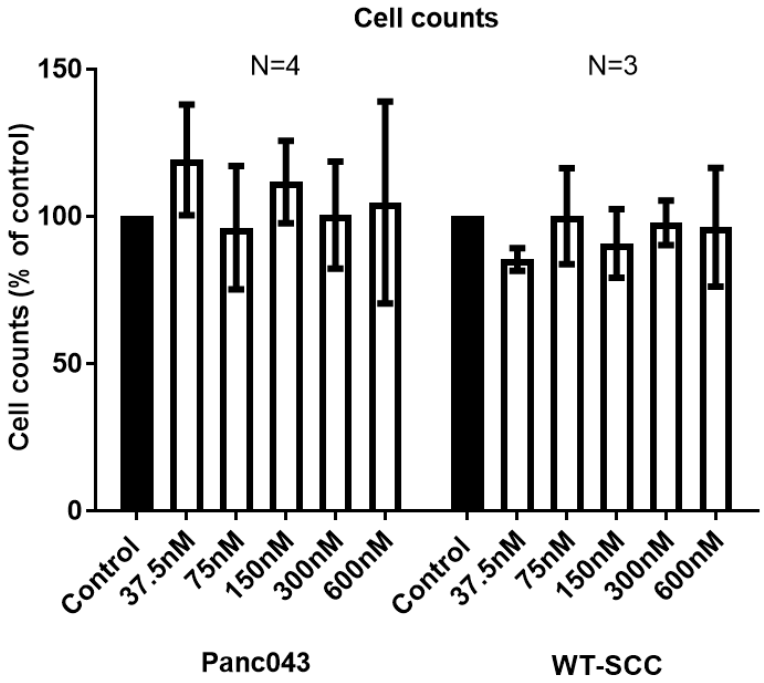

Figure 4.6 – Manual cell counts after exposure of WT-SCC and Panc043 to UE2316. Quantification of cell number found no differences across the UE2316 (11β-HSD1 inhibitor) concentration curve after 48 hours. N=3-4 technical repeats, treatments in duplicate. Data represent mean ± standard error and were compared by one-way ANOVA.

4.2.3.2 **Automated cell confluency analysis**

Cells were also imaged using the Incucyte ZOOM live cell imaging system to investigate the effects of UE2316 and glucocorticoids on tumour cell growth and morphology (Figure 4.7). The pro-apoptotic compound staurosporine (STS; 300nM) was added as a positive assay control.

4.2.3.2.1 *UE2316*

Cell confluence increased steadily over 72 hours. WT-SCC grew more quickly than SCC-B6-1 and Panc043 cells, with both the latter cell lines only reaching approximately 35% of WT-SCC total confluence by 72 hours. Treatments were as follows: vehicle (0.6% ethanol/DMSO); 25nM UE2316; 75nM UE2316; 150nM UE2316; or 300nM UE2316. Addition of increasing concentrations of UE2316 had no effect on the growth of WT-SCC or SCC-B6-1 cells over 72 hours (Figure 4.8A/C), but 150nM and 300nM UE2316 produced a small but significant inhibition of Panc043 growth ($P<0.01$, Figure 4.8B). The cytotoxic staurosporine (STS) prevented growth in all cell types.

Viable cell number after 72 hours was assessed using an alamarBlue assay. UE2316 was not found to affect cell viability in any cell type at any concentration (Figure 4.9).

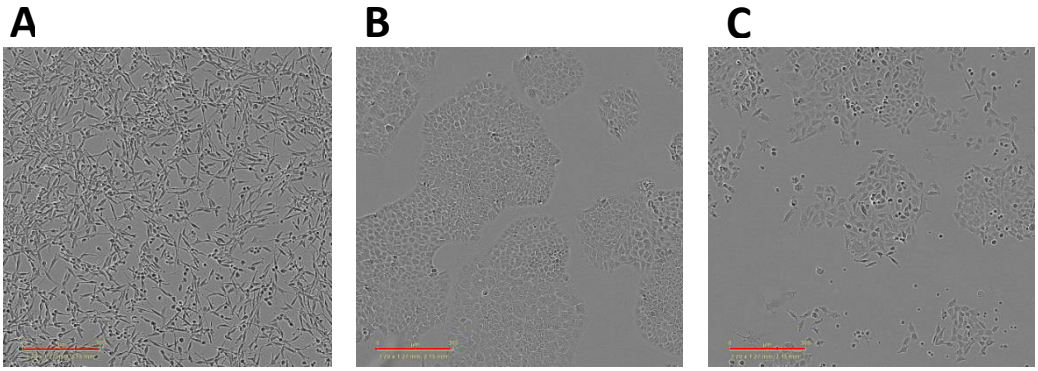

Figure 4.7 - Tumour cells imaged on the Incucyte Zoom live cell imaging system. WT-SCC cells (A) have a spindle-like morphology, while Panc043 (B) and SCC-B6-1 cells (C) have a cobblestone-like morphology. Scale bar = 300μm.

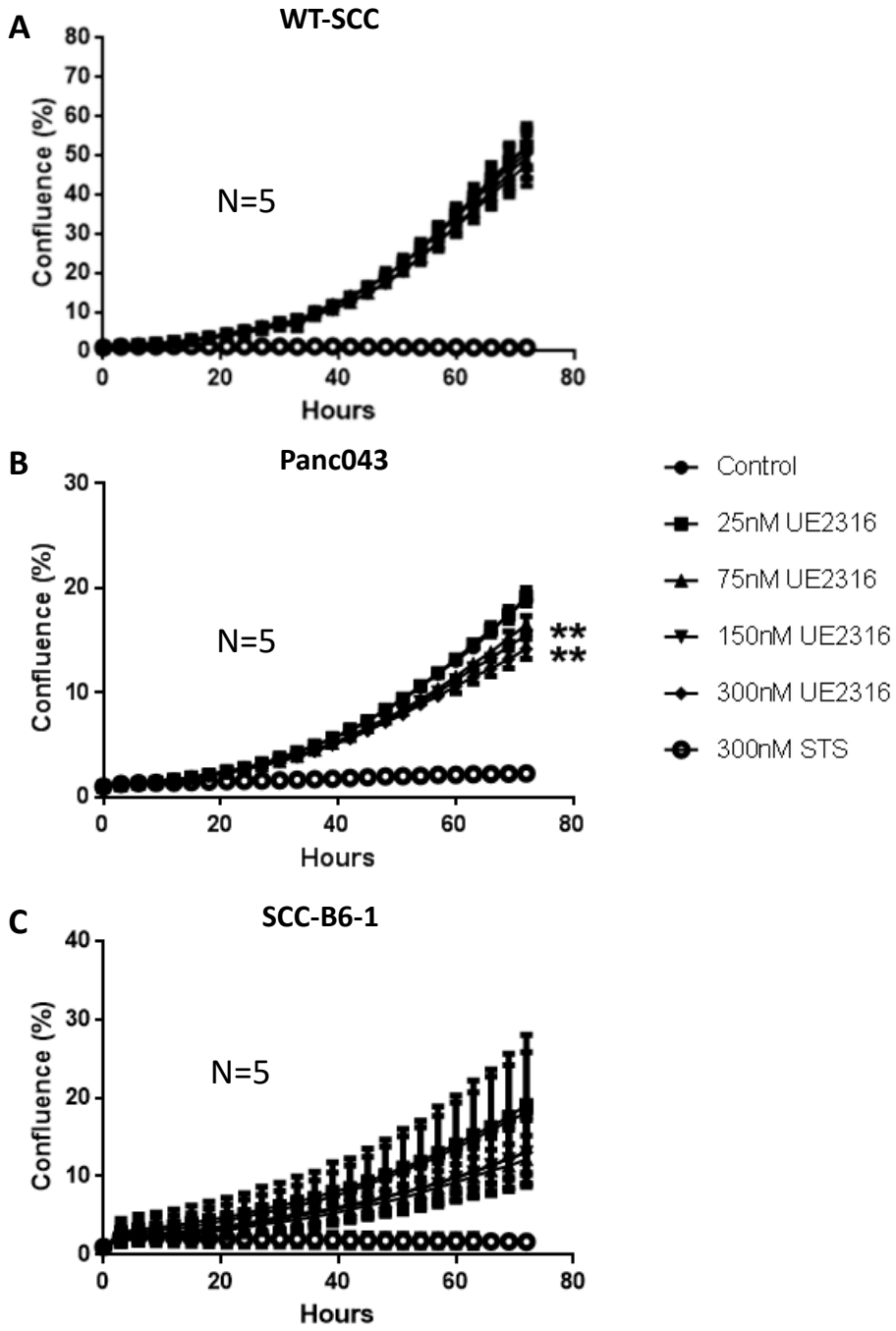

Figure 4.8 - UE2316 selectively reduced Panc043 cell confluence. The confluence of WT-SCC cells (A) and SCC-B6-1 cells (C) imaged over 72 hours using the Incucyte was unaffected by the 11β-HSD1 inhibitor UE2316, however 150nM and 300nM UE2316 caused a small but significant reduction in Panc043 confluence (B). 300nM STS was included in all experiments as a positive assay control (cytotoxic effects). ** $P<0.01$. N=5 (technical repeats, treatments in sextuplet). Data represent mean ± standard error and were compared by 2-way ANOVA with Dunnett's post-hoc test.

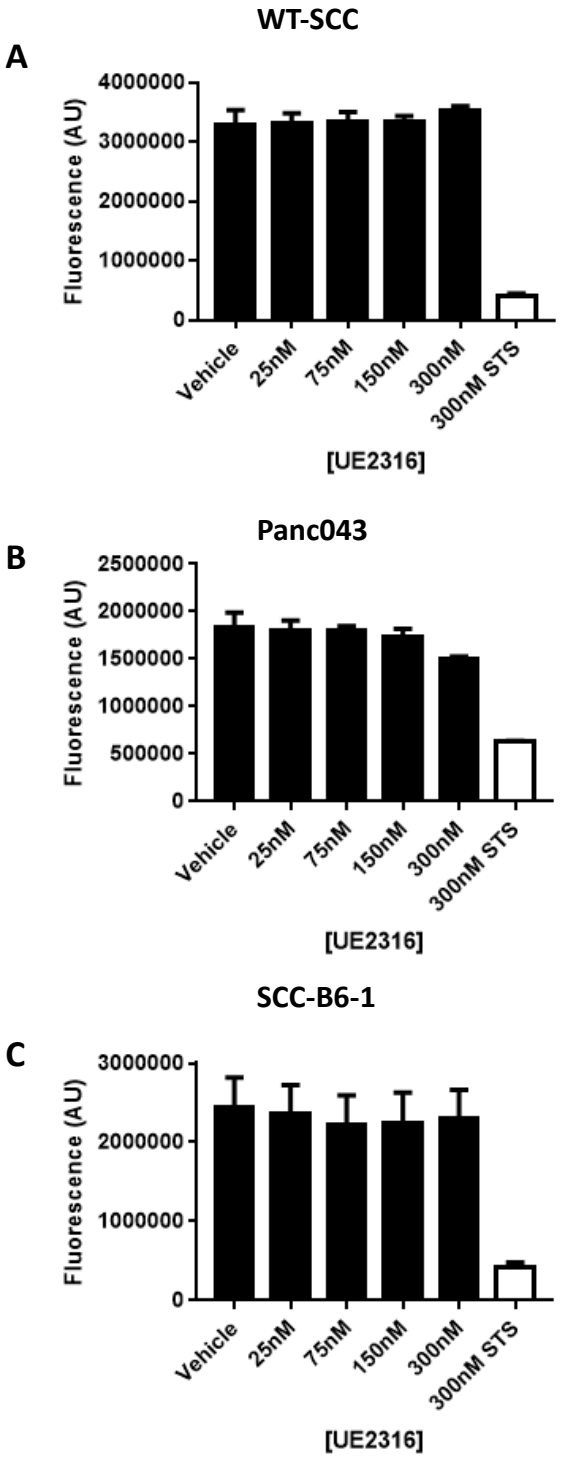

Figure 4.9 - Viable cell number was unaffected by UE2316. Cell viability, as determined by the alamarBlue assay, was unaffected by the addition of the 11β-HSD1 inhibitor UE2316 to WT-SCC (A), Panc043 (B) and SCC-B6-1 cells (C). N=4 (technical repeats, treatments in sextuplet). Data represent mean ± standard error and were compared by one-way ANOVA.

4.2.3.2.2 *Corticosterone*

Treatments (in sextuplet) were added as follows: vehicle (0.6% ethanol/DMSO); 37.5nM corticosterone; 75nM corticosterone; 150nM corticosterone; or 300nM corticosterone. Addition of increasing concentrations of corticosterone had no effect on the growth of WT-SCC or SCC-B6-1 cells over 72 hours (4.10A/C), but 75nM and 600nM corticosterone produced a small but significant inhibition of Panc043 growth ($P<0.05$ and $P<0.01$, respectively, Figure 4.10B). 300nM STS was potently cytotoxic and prevented growth in all cell types.

Viable cell number after 72 hours was assessed using an alamarBlue assay. Corticosterone was not found to affect cell viability in any cell type at any concentration (Figure 4.11).

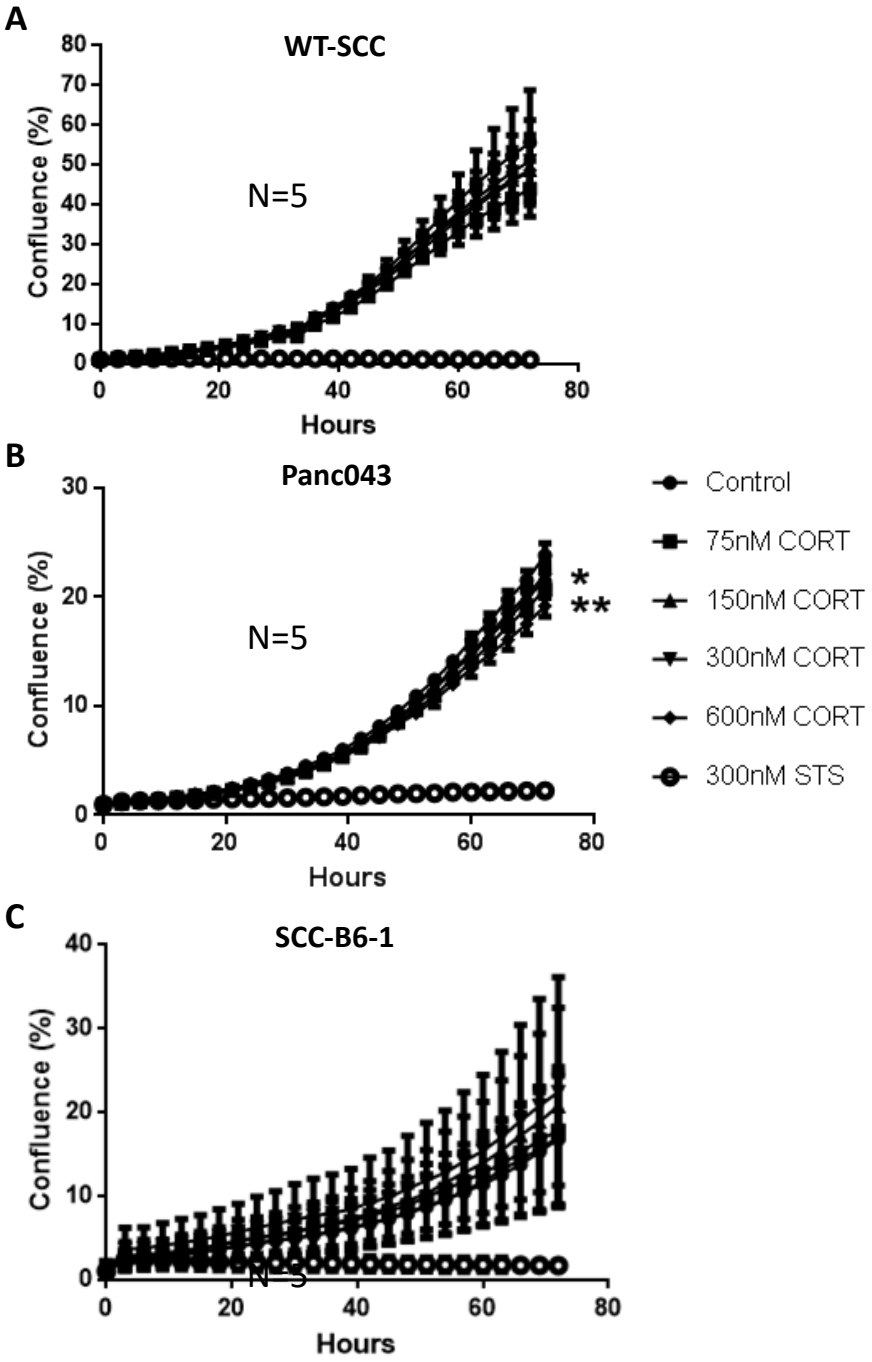

Figure 4.10 – Corticosterone selectively reduces Panc043 cell confluence. The confluence of WT-SCC cells (A) and SCC-B6-1 cells (C) imaged over 72 hours using the Incucyte was unaffected by corticosterone. In contrast, 75nM and 600nM corticosterone caused a small but significant reduction in Panc043 confluence (B). 300nM STS was included in all experiments as a positive assay control (cytotoxic effects). * $P<0.05$, ** $P<0.01$. N=5 (technical repeats, treatments in sextuplet). Data represent mean ± standard error compared by 2-way ANOVA with Dunnett's post-hoc test.

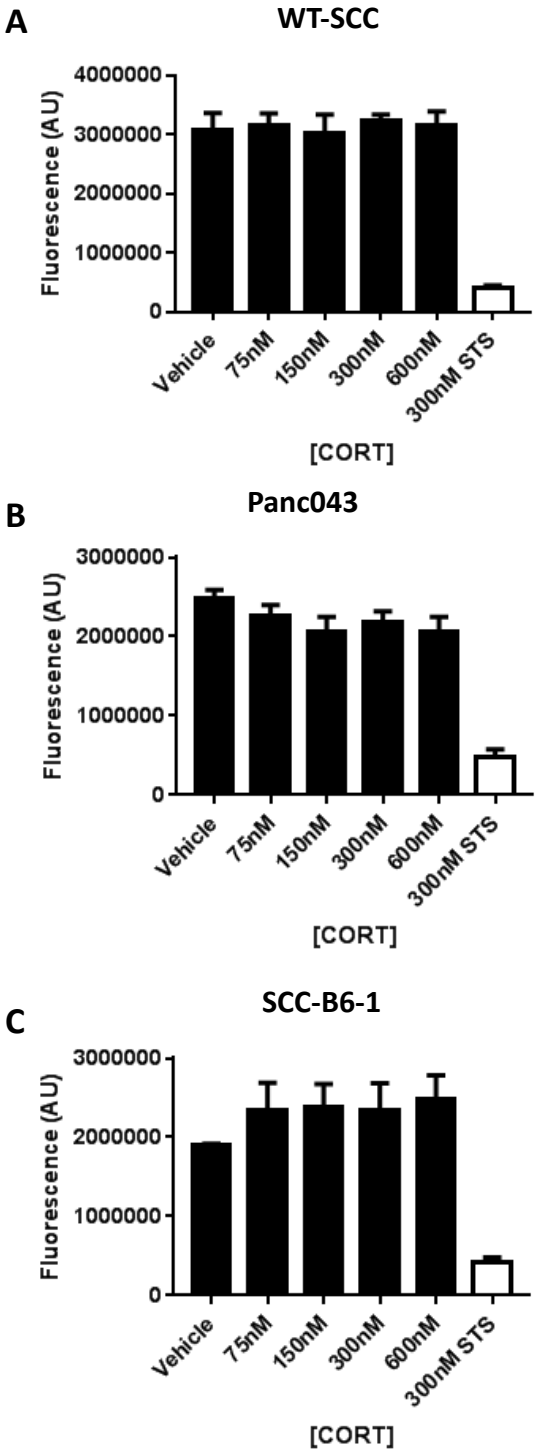

Figure 4.11 - Viable cell number is unaffected by corticosterone. Cell viability, as determined by the alamarBlue assay, was unaffected the addition of corticosterone to WT-SCC (A), Panc043 (B) and SCC-B6-1 cells (C). N=4 (technical repeats, treatments in sextuplet). Data represent mean ± standard error and were compared by one-way ANOVA.

4.3 Discussion

The experiments presented in this chapter addressed the hypothesis that either 11β-HSD1 inhibition (with UE2316) or deletion of 11β-HSD1 would prevent the inhibition of angiogenesis induced by the addition of 11-DHC to the aortic ring assay. Such effects were demonstrated by Small *et al.,* (2005) using a previous 11β-HSD1 knockout mouse model as well as the non-selective 11β-HSD inhibitor carbenoxolone. The effectiveness of UE2316 as an 11β-HSD1 inhibitor was confirmed in liver. Finally, studies were performed to investigate the effects of UE2316 and glucocorticoids on tumour cell proliferation. All three of the experimental tumour cell lines were shown to express negligible 11β-HSD1 transcript, and UE2316 previously has shown no off-target effects during selectivity screening (Yau *et al.,* 2015) thus no off-target effects were anticipated. The literature on glucocorticoids and tumour cell proliferation is complex and, thus, outcomes were more uncertain. The data in this chapter are in agreement with previous findings (Small *et al.,* 2005) in terms of the angiostatic effects of glucocorticoids and the pro-angiogenic effect of 11β-HSD1 deletion; angiogenesis in aortae from Del1 mice was unaffected by the addition of 11-DHC but powerfully inhibited by corticosterone. UE2316 on the other hand did not prevent 11-DHC-mediated angiostasis, and furthermore the drug itself exerted angiostatic effects in the absence of corticosteroids. These findings are unexpected, as studies of reductase activity in liver tissue using identical concentrations of UE2316 found the drug to reduce conversion of inactive to active glucocorticoids by 50%, demonstrating its efficacy *ex vivo*. Furthermore, neither UE2316 nor physiologically-relevant levels of glucocorticoids were seen to affect SCC tumour cell proliferation *in vitro*, indicating that the *in vivo* effect observed is likely mediated by an alternative cell type.

Aortic ring studies

Achieving a balance between substrate and inhibitor concentrations was challenging, as low levels of 11-DHC failed to produce significant angiostasis whereas high concentrations risk displacing the inhibitor. An initial experiment exposing aortic rings to increasing concentrations demonstrated that 300nM 11-DHC was an appropriate concentration to achieve a pronounced angiostatic response. Small *et al.* (2005) saw a

similar degree of angiostasis using 300nM and 600nM 11-DHC, and chose to proceed with 600nM glucocorticoids for their inhibitor experiments. Importantly, both the studies in this chapter and those of Small *et al.* (2005) made use of concentrations far closer to those relevant physiologically, as opposed to the pharmacological doses used by Folkman *et al.* (1983) and others (Hori *et al.*, 1996; Hasan *et al.*, 2000). Both 11-DHC and corticosterone were angiostatic at 300nM, adding further evidence that endogenous glucocorticoids can regulate angiogenesis. Only corticosterone, and not 11-DHC, was able to induce angiostasis in aortae from Del1 mice, emulating the findings of Small *et al.* (2005) and demonstrating that it is the conversion of 11-DHC to corticosterone by 11β-HSD1 that produces the angiostatic effect.

Unexpectedly, UE2316 did not prevent 11-DHC-mediated angiostasis, despite the previous finding (Small *et al.*, 2005) that carbenoxolone prevented 11-DHC-mediated angiostasis, albeit to a lesser degree than enzyme deletion. This led to questions surrounding the effectiveness of the inhibitor under these culture conditions. UE2316 has an IC_{50} of 162nM *in vitro* (Sooy *et al.*, 2010), thus 300nM UE2316 was intended to completely inhibit 11β-HSD1. However, results from the reductase assay performed in cultured liver tissue demonstrated 300nM UE2316 successfully reduced conversion of inactive glucocorticoids by around 50%. Similar findings have been reported in the brain (Wheelan *et al.*, 2015). The reductase assay performed in mouse liver tissue was intended to address the question of compound effectiveness in intact tissue *ex vivo.* Unfortunately, attempts to optimise this assay for use with aortic tissue failed as tissue volumes were too low to detect activity. Nevertheless, it remains possible that residual conversion of 11-DHC to corticosterone may still have been sufficient to induce angiostasis in the aortae treated with both 11-DHC and UE2316. Given the unexpected finding that UE2316 did not prevent 11-DHC-mediated angiostasis, a useful future study would be to expose aortic rings to a UE2316 concentration curve – this would remove the risk of misinterpreting data from single concentration studies.

The above argument still cannot explain one of the most surprising findings from this study; UE2316 itself exerts moderate angiostatic effects in the absence of glucocorticoids. Assay sensitivity is one potential explanation for this finding. Efforts were taken to minimise the levels of heparin in culture medium, as although Folkman

et al. (1983) demonstrated the requirement for heparin in promoting the angiostatic effects of glucocorticoids, its addition did appear to have a detrimental effect on growth and could have contributed to assay sensitivity. Findings in the Del1 mice, however, suggest that the assay was correctly optimised, as addition of 11-DHC here had no effect on growth despite the presence of heparin. If UE2316 does induce anti-angiogenic effects then this warrants further investigation, though data in this chapter only allow for speculation. The present experiments would have benefited from the addition of a UE2316-treatment group in the Del1 aortae to test for an off-target effect; this experiment has since been performed by others in the group using an identical protocol; the anti-angiogenic effect of UE2316 did not occur in mice lacking 11β-HSD1, only in wild-type C57BL6/J aortae (E. Miller and J. Wu, unpublished). These data, in combination with previous reports that UE2316 does not have significant off-target activities (Yau *et al.,* 2015), suggest a previously unreported 11β-HSD1-dependent inhibition of angiogenesis which is glucocorticoid-independent.

Accurate interpretation of these data requires a consideration of the model. The aortic ring assay allows the angiogenic process to be examined in the absence of the paracrine effects of surrounding tissues and the effect of circulating leukocytes (Baker *et al.,* 2011). Unlike cell-based assays of angiogenesis, the aortic ring assay uses intact tissue explants that have not undergone modification by serial passage under culture conditions (Aplin *et al.,* 2008) and involves the development of fully lumenized endothelial tubes which recruit supporting mural cells in a manner far more representative of *in vivo* angiogenesis (Aplin *et al.,* 2008; Baker *et al.,* 2011). Small *et al.* (2005) originally interpreted their observations as evidence for the role of smooth muscle 11β-HSD1 in constraining the angiogenic response during vascular inflammation, on the grounds that the aortic ring assay lacks inflammatory cell involvement. Evidence has since emerged that renders this interpretation problematic. Several studies have demonstrated an important role for tissue-resident macrophages and dendritic cells in the adventitia of aortic explants (Aplin *et al.,* 2006; Gelati *et al.,* 2008), suggesting that the innate immune system remains relevant in this model. Furthermore, White *et al.* (2015) did not see the same pro-angiogenic effects of 11β-HSD1 deletion in the myocardium when the knockout was specifically targeted to smooth-muscle cells. This new information necessitates a reconsideration of the

potential mechanism at work, though this mechanism likely involves the glucocorticoid receptor (GR) rather than the mineralocorticoid receptor (MR) (Small *et al.,* 2005).

Based on the available evidence so far, other 11β-HSD1 expressing cell types of potential importance in this model are cells of the innate immune system (Thieringer *et al.,* 2001; Freeman *et al.,* 2005; Gilmour *et al.,* 2006; Chapman *et al.* 2013b; Coutinho *et al.,* 2016) and fibroblasts (Lee *et al.,* 2013; Tiganescu *et al.,* 2013; Terao *et al.,* 2014). Endothelial cells express little or no 11β-HSD1 (Hadoke *et al.,* 2001; Christy *et al.,* 2003; Rae *et al.,* 2009), although the paracrine influence of other cell types on endothelial cells cannot be excluded in light of the anti-angiogenic effects of glucocorticoids on HUVEC tube-like structure formation (Logie *et al.,* 2010). Interestingly, the most recent studies examining the role of 11β-HSD1 in angiogenesis focus on fibroblasts (Mylonas *et al.,* 2017) and macrophages (Zhang *et al.,* 2017), respectively. An important future study will be to perform the aortic ring assay using the cell-specific 11β-HSD1 knockout animals. For now, it remains difficult to explain why 11β-HSD1 inhibition has the opposite effect on angiogenesis to 11β-HSD1 deletion. The importance of chronic, as opposed to acute, loss of 11β-HSD1 activity may yet prove to be of importance.

The aortic ring assays described above were performed in C57BL6/J mice (OlaHSD substrain), the strain in which Panc043 and SCC-B6-1 tumours were grown. Interestingly, SCC-B6-1 tumours did show a trend towards increased growth that was more pronounced in WT mice fed an 11β-HSD1 inhibitor than in the Del1 mice – this did not reach significance and thus should not be subject to over-interpretation, yet it adds to evidence suggesting that inhibition and deletion of the enzyme may operate via separate mechanisms. The same aortic ring experiments were performed using aortae from FVB mice, as this strain was used for WT-SCC tumour studies. While glucocorticoids were still powerfully angiostatic and UE2316 did not prevent 11-DHC-mediated angiostasis, no anti-angiogenic effect of UE2316 alone was apparent in this model. While this may reflect a genuine strain-difference, more likely it reflects the poor angiogenic potential of FVB/N mice; control rings produced around 30% of the vessel outgrowth seen in control C57BL6/J mice, and their lack of suitability for

assays of angiogenesis has previously been described (Rohan *et al.,* 2000; Zhu *et al.,* 2003; Kim *et al.,* 2013). Thus, rather than resistance to UE2316-mediated angiostasis, outgrowths from these aortae may simply have grown too poorly under control conditions to allow accurate detection of moderate angiostatic effects. In terms of relating findings from the aortic ring assay back to the previous chapter's conclusions, an effect of UE2316 on angiogenesis in the FVB mouse is distinctly absent, adding more weight to the theory that an alternative mechanism is responsible for enhanced tumour growth.

Tumour cell proliferation studies

The original research hypothesis of 11β-HSD1 causing enhanced angiogenesis and promoting tumour growth is not supported by the available evidence. The next potential mechanism to examine was a direct effect of either UE2316 or glucocorticoids on tumour cell proliferation. 11β-HSD1 is rarely expressed in highly-proliferative tumour cell lines (Chapman *et al.,* 2013b) and the cell lines in this chapter were no exception. Therefore, adding UE2316 to cells in culture was performed mainly to confirm the absence of an off-target effect. Three separate methods were used to assess cell growth. Simple cell counting allowed for a direct readout of cell number, while assessment with the incucyte allowed both high-throughput analysis and assessment of cell morphology. The alamarBlue assay provided a tertiary measure to confirm impact on cell viability. No effect of UE2316 on either WT-SCC or SCC-B6-1 cells was seen across a wide range of concentrations (encompassing those detected *in vivo* in plasma in the previous chapter). A subtle but significant reduction in Panc043 confluence in the presence of 150-300nM UE2316 was apparent, though this was not pronounced enough to reach significance in the alamarBlue assay of cell viability and did not appear to alter tumour growth in the previous chapter.

Attention was, thus, turned to glucocorticoids, the effects of which are varied when applied to tumour cells. In androgen-sensitive cancers (breast and prostate), glucocorticoids can suppress tumour cell proliferation, but in many carcinomas glucocorticoids inhibit the apoptotic effects of chemotherapeutics and promote tumour cell proliferation via upregulation of survival factors (reviewed by Lin and Wang, 2016). Many of these studies used high concentrations of dexamethasone, a highly

potent synthetic glucocorticoid which is selective for the GR. While this was relevant to these studies (which were concerned with the use of therapeutic glucocorticoids in conjunction with chemotherapy), the present work is related to manipulation of endogenous glucocorticoids and thus made use of physiologically relevant concentrations of corticosterone (Kotelevtsev *et al*., 1997; Harris *et al*., 2001; Yau *et al*., 2007; Benedetti *et al*., 2012; Gong *et al*., 2015), the naturally occurring murine glucocorticoid. Synthetic glucocorticoids bind the GR with much higher affinity than naturally-occurring corticosteroids (Hollenburg *et al.*, 1985), making direct comparison of studies difficult. Ishiguro *et al.* (2014), for example, found that, while dexamethasone (and several other glucocorticoids) promoted bladder cancer cell growth, corticosterone exhibited only marginal effects. Thus it is perhaps unsurprising that corticosterone was not seen to drastically affect tumour cell proliferation in the present study.

Panc043 cells again appeared to be slightly sensitive to corticosterone exposure, although this was not concentration-dependent and the effect was absent from alamarBlue analysis. Zhang *et al.* (2006a; 2007) report resistance to the cytotoxic effects of chemotherapeutics after exposing numerous pancreatic ductal adenocarcinoma cells to dexamethasone, but inhibition of proliferation has also been reported in pancreatic ductal adenocarcinoma cells (Gower *et al.*, 1994). Evidence from Panc043 tumour growth *in vivo* (Section 3.2.6.2) did suggest that tumours were affected by 11β-HSD1 inhibition (altered GR and HIF-1α signalling); however, this did not alter tumour growth. It is likely, therefore, that the observed mild *in vitro* effects of glucocorticoids are negligible in the *in vivo* situation in which the tumour microenvironment and systemic factors are at play. Similar effects have previously been reported; Shpilberg *et al.* (2015) found that although corticosterone inhibited cell cycle progression in breast cancer cells *in vitro,* co-incubation with conditioned media from adipose tissue overrode this effect. Alternatively, and in light of the effects of UE2316 on Panc043 confluence, it may be that these cells undergo slight morphological changes when stressed by the addition of a treatment *in vitro* (which could affect confluence data).

The absence of a glucocorticoid-mediated effect in either SCC cell line strongly suggests that direct proliferative effects on tumour cells are not the mechanism by which 11β-HSD1 inhibition promotes tumour growth. This finding is not necessarily surprising. A previous study exposing SCC cell lines to glucocorticoids was inconclusive; while exposure to cortisol did promote proliferation in two separate SCC lines, in one line only pharmacological concentrations (1μM) induced this affect, but in the other growth was only enhanced by low physiological concentrations (10nM) (Bernabé *et al.,* 2011). Furthermore, a recent study exposing SCC cell lines to glucocorticoids only found increased invasiveness in one of three cell lines (Cirillo *et al.,* 2017) and of particular note, the more aggressive cell line was non-responsive. The absence of an *in vitro* tumour cell effect implicates other aspects of the tumour microenvironment in the enhanced growth of WT-SCC tumours. Previous studies have also found that although dexamethasone decreased the growth of tumour xenografts *in vivo,* exposing the cancerous cells to dexamethasone *in vitro* had no effect (Crowley *et al.,* 1988; Yano *et al.,* 2006). Determining which component of the WT-SCC tumour microenvironment is sensitive to local glucocorticoid manipulation will be key in determining the risk posed by 11β-HSD1 inhibitors.

In conclusion, closer examination of angiogenesis and tumour cell proliferation has not revealed a clear mechanism of action for UE2316 in promoting WT-SCC tumour growth. As predicted, active glucocorticoids proved angiostatic *ex vivo* and aortae from mice lacking the 11β-HSD1 enzyme were protected from angiostasis after exposure to exogenous 11-DHC. UE2316, however, did not have the expected effect; despite preventing conversion of 11-DHC to corticosterone in liver *ex vivo,* the inhibitor failed to prevent 11-DHC-mediated angiostasis and instead caused moderate angiostasis in the aortic ring assay. Neither UE2316 nor glucocorticoids had drastic effects on tumour cell proliferation, suggesting that direct effects on cell proliferation are unlikely to be responsible for the increased growth seen in UE2316-treated WT-SCC tumours *in vivo*. These findings suggest that UE2316 may be interacting with an alternative component of the tumour microenvironment to influence tumour growth. The recent literature points towards immune and inflammatory cells, as well as fibroblasts. The priority now will be to investigate the wider influence of UE2316 on the tumour microenvironment *in vivo*.

Chapter 5

Mechanism of enhanced WT-SCC tumour growth after 11β-HSD1 inhibition

5 Mechanism of enhanced WT-SCC tumour growth after 11β-HSD1 inhibition

5.1 Introduction

In chapter 3, inhibition of 11β-HSD1 with UE2316 was shown to promote the growth of WT-SCC tumours. In the previous chapter, it was demonstrated that UE2316 did not mimic the effect of 11β-HSD1 deletion on angiogenesis *ex vivo*, despite its ability to inhibit 11β-HSD1 activity in intact tissue. Similarly, neither UE2316 nor physiologically-relevant concentrations of corticosterone directly influenced the proliferative capacity of tumour cells. Key questions remains unanswered – by what mechanism does UE2316 promote WT-SCC tumour growth and why is a response apparent in only one of the three tumour types examined?

Strain-specific differences in the response to UE2316 may influence tumour sensitivity to 11β-HSD1 inhibition. 11β-HSD1 inhibition/deletion decreases tissue-specific glucocorticoid concentrations but the available evidence suggests that 11β-HSD1 inhibitors, including UE2316, do not affect plasma glucocorticoid levels in pre-clinical models or clinical trials (Hermanowski-Vosatka *et al.*, 2005; Harno and White, 2010; Sooy *et al.*, 2010; Coutinho *et al.*, 2016). Furthermore, while conflicting evidence exists surrounding plasma glucocorticoid levels in 11β-HSD1 knockout (KO) animals (Kotelevtsev *et al.*, 1997; Harris *et al.*, 2001), C57BL6/J mice appear to be largely resistant to alterations in HPA axis function (Carter *et al.*, 2009; Harno and White, 2010). This is of great clinical advantage as systemic manipulation of glucocorticoids in humans risks Addisonian crisis or Cushing's syndrome. To the author's knowledge, no studies have previously used 11β-HSD1 inhibitors in FVB/N mice, thus it remains possible that circulating glucocorticoids in this strain may be affected by UE2316.

Tumour type itself is also likely to affect the response to UE2316. The sensitivity and response of tumours to glucocorticoids is highly variable between cancer types, with higher glucocorticoid receptor (GR) expression predictive of greater sensitivity to changing glucocorticoid concentrations (Lin & Wang, 2016). Expression of 11β-HSD1 is often reduced in cancerous tissues compared to their healthy equivalents, and

this can enhance tumour growth (Azher et al., 2016; Liu et al., 2016). Of particular note are studies indicating a role for 11β-HSD1 in constraining the progression of squamous cell carcinoma (SCC) (Terao et al., 2011; 2013; 2014) and increased GR expression in SCC compared to normal skin (Budunova *et al.*, 1997). These reports suggest that SCC are a candidate tumour type for glucocorticoid sensitivity and thus may be at particular risk from 11β-HSD1 inhibitors.

As well as tumour cells and vascular cell types, a variety of immune and inflammatory cells and extracellular matrix producing fibroblasts form the tumour microenvironment (Hanahan and Weinberg, 2011). Over the past 15 years, mounting evidence has highlighted the importance of considering the microenvironment when assessing how best to effectively target cancers. Collagen deposition, for example, may be of relevance in skin cancer (Azher *et al.*, 2016), with remodelling of the extracellular matrix a common component of malignancy (Hompland *et al.*, 2008). 11β-HSD1 amplifies local glucocorticoid concentrations which consequently influences collagen fibril organisation. In aging skin, inhibition of 11β-HSD1 increases collagen density and improves dermal integrity and wound healing (Tiganescu et al., 2013). In adipose tissue, the opposite is true; 11β-HSD1 KO mice show reduced fibrosis (Michailidou et al., 2012). Several methodologies now exist for quantifying collagen in histological sections; as well as conventional picrosirius red staining, techniques like second-harmonic generation imaging allow for label-free high resolution imaging of the fibrillar network in tumours (Hompland *et al*., 2008).

Inflammatory and immune cell types can have powerful effects on tumour progression. The anti-inflammatory and immunosuppressive effects of glucocorticoids are therefore likely to be very relevant when targeting tumour 11β-HSD1. Reducing the regeneration of local glucocorticoids may predict a less constrained inflammatory response and has been suggested as a mechanism in myocardial infarction (McSweeney *et al.*, 2010). Yet the opposite effect has been reported in other inflammatory contexts such as the vasculature (Luo et al., 2012) and adipose tissue (Peng et al., 2016), thus a pro-inflammatory effect of 11β-HSD1 inhibition cannot be assumed. Locally regenerated glucocorticoids produced by SCC cells are able to

inhibit the proliferation of anti-tumour CD8+ T-cells (Cirillo *et al.,* 2017), thus anti-tumour immunity may also be affected by 11β-HSD1 inhibitors.

Hypotheses

The work described in this chapter is intended to address the hypotheses that:

- 11β-HSD1 inhibition/deletion does not affect systemic glucocorticoid levels

- UE2316-responsive WT-SCC tumour growth will increase in response to reduced circulating glucocorticoids

- 11β-HSD1 inhibition alters the tumour microenvironment in a manner that promotes tumour growth

Objectives

The specific aims of this work were:

(1) To confirm the effects of 11βHSD1 inhibition/deletion on circulating glucocorticoids in FVB/N and C57BL6/J mice

(2) To investigate whether reduced glucocorticoid exposure increases WT-SCC tumour growth *in vivo*, and whether glucocorticoid replacement reverses this effect

(3) To use RNA-sequencing to examine the impact of UE2316 on the WT-SCC transcriptome

(4) To determine the impact of 11β-HSD1 inhibition on aspects of the immune/inflammatory cell population and non-cellular fibrillar network of the tumour microenvironment

5.2 Results

5.2.1 Plasma corticosterone was decreased in UE2316-treated FVB/N mice

5.2.1.1 ELISA

To compare plasma corticosterone concentrations between UE2316-diet fed FVB/N mice and control diet-fed FVB/N mice, blood was sampled from female FVB/N mice fed UE2316 or RM-1 diet for 14 days and plasma for analysis by ELISA. FVB/N mice fed UE2316 diet had lower levels of corticosterone than mice fed RM-1 control diet (0.194 ± 0.032 ng/mL vs. 0.715 ± 0.162 ng/mL, $P<0.05$, Figure 5.1).

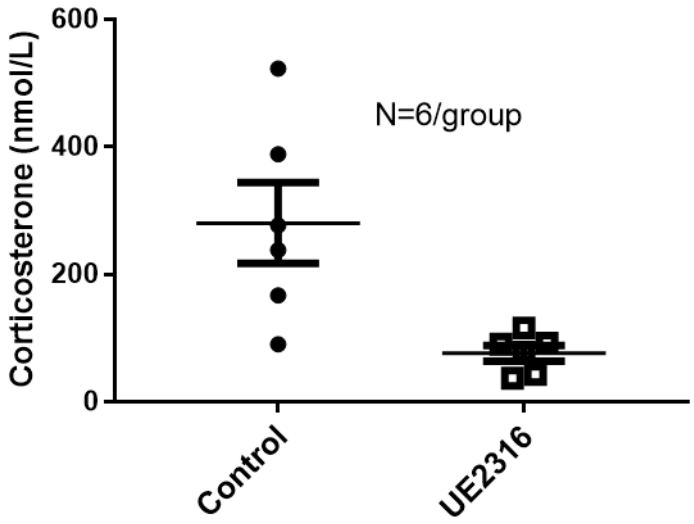

Figure 5.1 - Plasma corticosterone was decreased in UE2316 treated FVB/N mice bearing WT-SCC tumours. Mice fed UE2316-diet showed significantly reduced plasma corticosterone levels compared to mice fed control diet. Symbols represent individual animals. * $P<0.05$. Data are mean ± standard error and were compared by independent samples t-test.

5.2.1.2 **LC-MS/MS**

To confirm the findings of the ELISA, 11-dehydrocorticosterone (11-DHC) and corticosterone were measured in the plasma of FVB/N mice (WT-SCC tumours) and C57Bl6/J mice (Panc043 tumours) by LC-MS/MS. A combination of low plasma yield and technical issues leading to loss of samples necessitated the pooling of FVB/N plasma samples from two experiments in order to achieve sufficient sample volume. FVB/N mice fed UE2316- (n=4) or control diet (n=3) for 9 days were pooled with FVB/N mice fed UE2316 (n=4) or control diet (n=6) for 16 days to give a total sample size of N=7-10/group. All mice underwent identical treatment (implantation of subcutaneous WT-SCC tumours after 5 days on diet), with the only difference being the length of time tumours were left to develop (4 vs 11 days). C57BL6/J plasma was from the second study described in **Section 3.2.3.1** (Panc043 tumours grown for 16 days) and from the 41 day SCC-B6-1 study described in **Section 3.2.4.1.**

11-DHC levels did not differ between RM-1 and UE2316 diet-fed FVB/N or C57BL6/J mice, but were significantly elevated in Del1 mice compared to RM-1 diet fed wild-type (WT) C57BL6/J controls (49.73 ± 20.95 nmol/L vs. 5.83 ± 1.63 nmol/L, $P<0.05$, Figure 5.2A).

Corticosterone levels were reduced in UE2316 diet-fed FVB/N mice compared to RM-1 diet-fed FVB/N mice (56.4 ± 14.8 nmol/L vs. 328.9 ± 84.4 nmol/L, $P<0.01$, Figure 5.2B). Corticosterone levels in C57BL6/J mice were unaffected by both UE2316 and Del1 phenotype.

Glucocorticoids were also measured in the plasma of C57Bl6/J mice implanted with SCC-B6-1 tumours; no differences were seen between treatment groups (Figure 5.3).

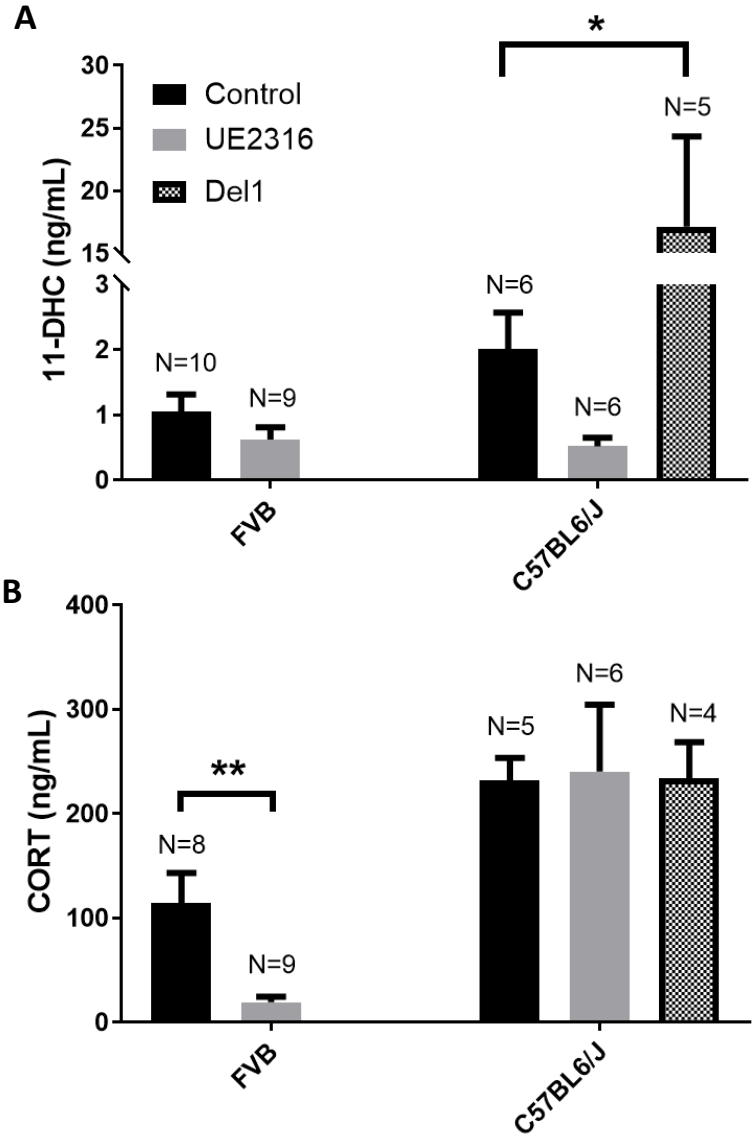

Figure 5.2 – Effects of 11β-HSD1 inhibition or deletion on systemic glucocorticoid levels. A) The 11β-HSD1 inhibitor UE2316 did not significantly alter plasma 11-dehydrocorticosterone (11-DHC) concentrations in either C57BL6/J or FVB/N mice, whereas genetic ablation of 11β-HSD1 (Del1) increased 11-DHC concentrations. * P<0.05. Data represent mean ± standard error and were compared by one-way ANOVA with Dunnett's post-hoc test. B) UE2316 treatment reduced circulating corticosterone in FVB/N animals only, whereas corticosterone concentrations in C57Bl6/J animals were unaffected by inhibitor or Del1 genotype. **=P<0.01. Data represent mean ± standard error and were compared by independent sample t-test.

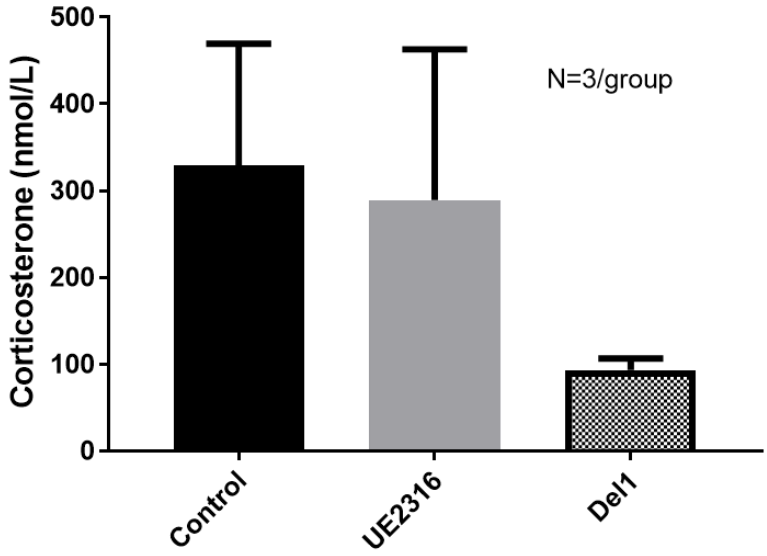

Figure 5.3 – Corticosteroid concentrations in the plasma of C57Bl6/J animals implanted with SCC-B6-1 tumours are not consistently affected by 11β-HSD1 deletion or inhibition. Neither the Del1 genotype nor the 11β-HSD1 inhibitor UE2316 altered plasma corticosterone levels in C57BL6/J animals implanted with the squamous cell carcinoma cell line SCC-B6-1. N=3/group. Data represent mean ± standard error and were compared by one-way ANOVA.

5.2.2 Tumour-bearing does not affect circulating glucocorticoids

Plasma glucocorticoids were compared between tumour and non-tumour bearing animals to assess whether the presence of a subcutaneous tumour affected circulating glucocorticoids in mice. While 11-DHC was below the limit of detection in FVB/N plasma in this experiment, no differences in 11-DHC were found between tumour-bearing and control C57BL6/J mice (Figure 5.4A), and no differences in corticosterone were seen in either strain (Figure 5.4B).

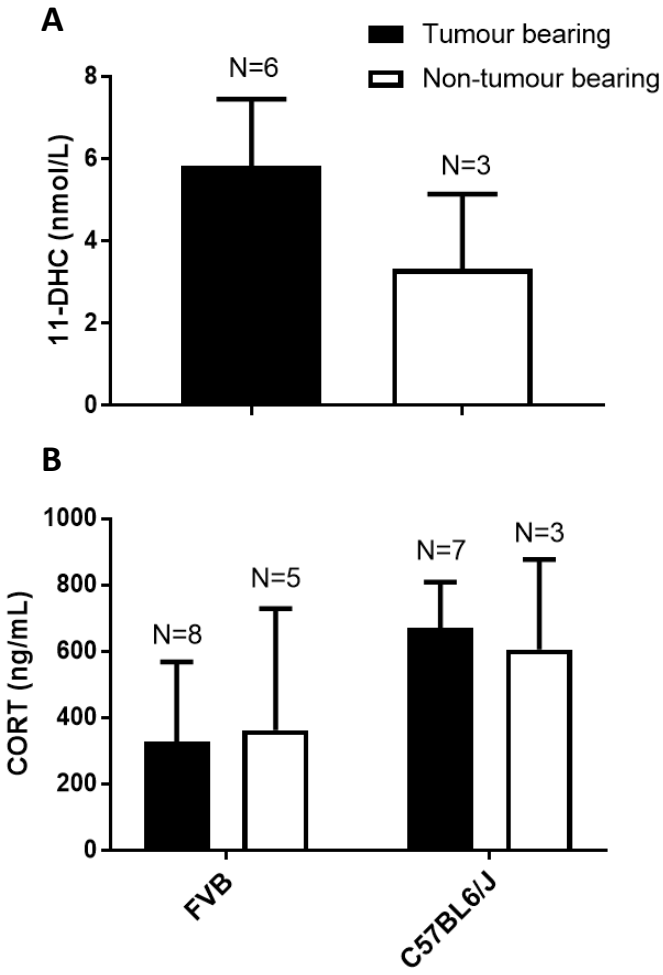

Figure 5.4 - Tumour bearing did not consistently affect circulating glucocorticoids. A) Plasma 11-dehydrocorticosterone (11-DHC) concentrations in C57Bl6/J mice were not significantly altered by pancreatic ductal adenocarcinoma (Panc043) tumour bearing. B) Plasma corticosterone concentrations were not significantly affected by tumour bearing in both FVB/N mice with WT-SCC tumours and C57Bl6/J mice with Panc043 tumours. N=3-8. Data represent mean ± standard error and were compared by independent samples t-test.

5.2.3 UE2316 treatment increases the 11-DHC to corticosterone ratio in liver tissue in FVB/N mice

To investigate whether UE2316 could alter tissue-specific glucocorticoid concentrations, 11-DHC and corticosterone were both measured by LCMS-MS in liver and tumour tissue from FVB/N mice (**Section 3.2.1**) and C57BL6/J mice (**Section 3.2.3.1**). Although trends for increased levels of 11-DHC (Figure 5.5A) and decreased levels of corticosterone (Figure 5.5B) after UE2316 treatment were apparent in FVB/N liver, neither reached significance. Differences in C57BL6/J after UE2316 treatment were less pronounced. When levels were expressed as the ratio of 11-DHC to corticosterone (A:B ratio), FVB/N liver had a significantly ($P<0.0001$) higher proportion of 11-DHC to corticosterone in UE2316 treated mice (0.31 ± 0.03) compared to control mice (0.06 ± 0.01). In C57BL6/J mice, a strong trend towards an increased A:B ratio was apparent ($P = 0.053$) but this did not reach significance (Figure 5.5C). Tumour tissue quantities were too small to accurately detect glucocorticoids.

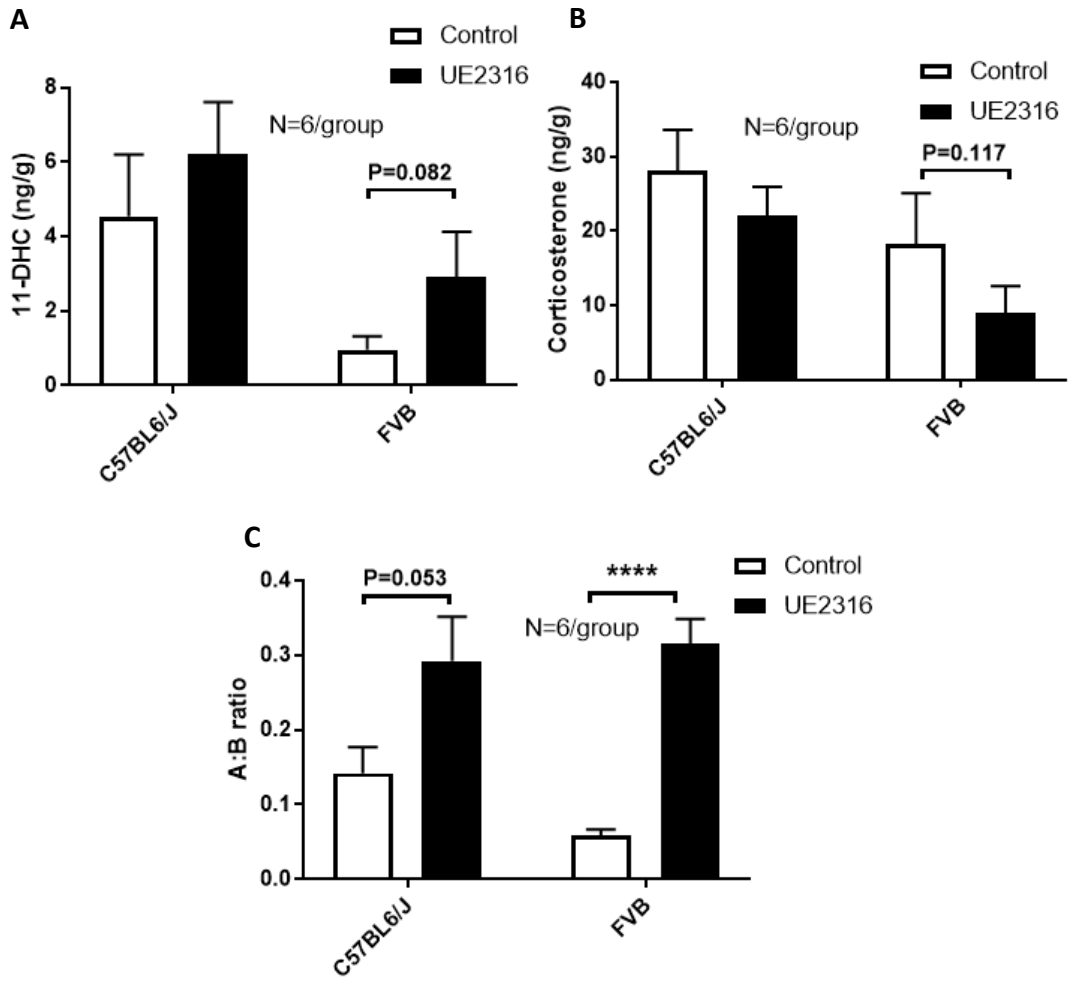

Figure 5.5 – UE2316 increases ratio of 11-DHC to corticosterone in FVB/N liver. A) 11-dehydrocorticosterone (11=-DHC; Kendall's compound 'A') levels did not differ between livers from control and UE2316-treated C57BL6/J mice, but there was a trend towards increased 11-DHC in the livers from UE2316-treated FVB/N mice compared to controls. B) Corticosterone (Kendall's compound 'B') levels did not differ in livers from control and UE2316-treated C57BL6/J mice, but there was a trend towards decreased corticosterone in the livers from UE2316-treated FVB/N mice compared to controls. C) The A:B ratio in livers from UE2316-treated C57BL6/J mice showed a strong trend towards being increased compared to controls. In FVB/N mice, this increase achieved significance. N=6/group. Data are mean ± standard error and were compared by independent samples t-test.

5.2.4 Systemic manipulation of glucocorticoids *in vivo*

5.2.4.1 Systemic manipulation of glucocorticoids did not affect WT-SCC tumour growth

This study was performed on FVB/N mice (N=6/group) to determine whether altered circulating glucocorticoid levels influenced WT-SCC tumour growth. One group received daily intraperitoneal (i.p.) injections of saline (0.1mL/10g body weight), one group received daily i.p. injections of metyrapone (100mg/kg, prepared as described in **Section 2.1.3.3**) to inhibit adrenal 11β-hydroxylase and hence glucocorticoid synthesis and a third group received daily i.p. metyrapone injections (100 mg/kg) and corticosterone in drinking water (25 μg/mL) to replace endogenous glucocorticoids.

Neither metyrapone nor metyrapone with corticosterone replacement altered WT-SCC tumour growth (Figure 5.6A), final tumour weight (Figure 5.6B), or mouse weight (Figure 5.6C) when compared to tumours from control mice. Small but significant changes in some organ weights were observed between groups; heart weights were higher (117.4 ± 6.7 mg vs 96.7 ± 1.8 mg, $P<0.05$) and spleen weights decreased (111.3 ± 9.0 mg vs. 145.2 mg, $P<0.05$) in mice receiving glucocorticoid compared with vehicle-treated controls (Figure 5.7A and E). Kidney weights were slightly higher in metyrapone-treated mice compared with vehicle-treated controls (142.7 ± 3.4 mg vs. 133.6 ± 0.97mg, $P<0.05$, Figure 5.7B). Adrenal and thymus weights were similar between groups (Figure 5.7C/D).

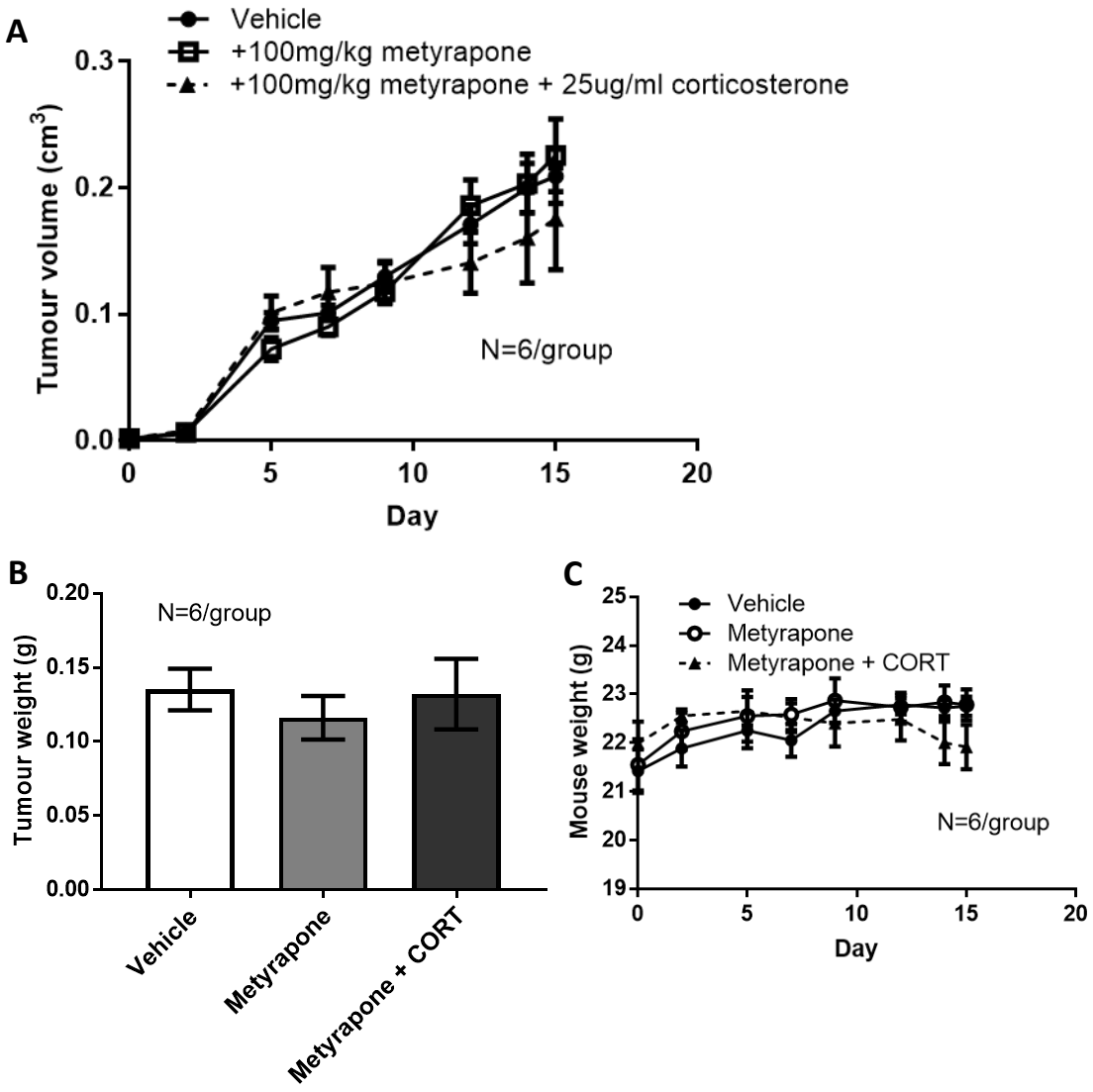

Figure 5.6 – WT-SCC tumour growth was unaffected by metyrapone or metyrapone with corticosterone replacement. A) 100mg/kg metyrapone (i.p.) daily did not affect squamous cell carcinoma (WT-SCC) tumour growth compared to vehicle (saline). Addition of corticosterone to drinking water (25µg/mL) alongside metyrapone treatment (100mg/kg, i.p.) to replace systemic glucocorticoids also had no effect on tumour growth. Data compared by repeated measures two-way ANOVA. B) Final (day 15) tumour weight was unaffected by either metyrapone or metyrapone with corticosterone. Data compared by one-way ANOVA. C) Mouse weight was unaffected by either metyrapone or metyrapone with corticosterone. Data compared by repeated measures two-way ANOVA. N=6/group. All data are mean ± standard error.

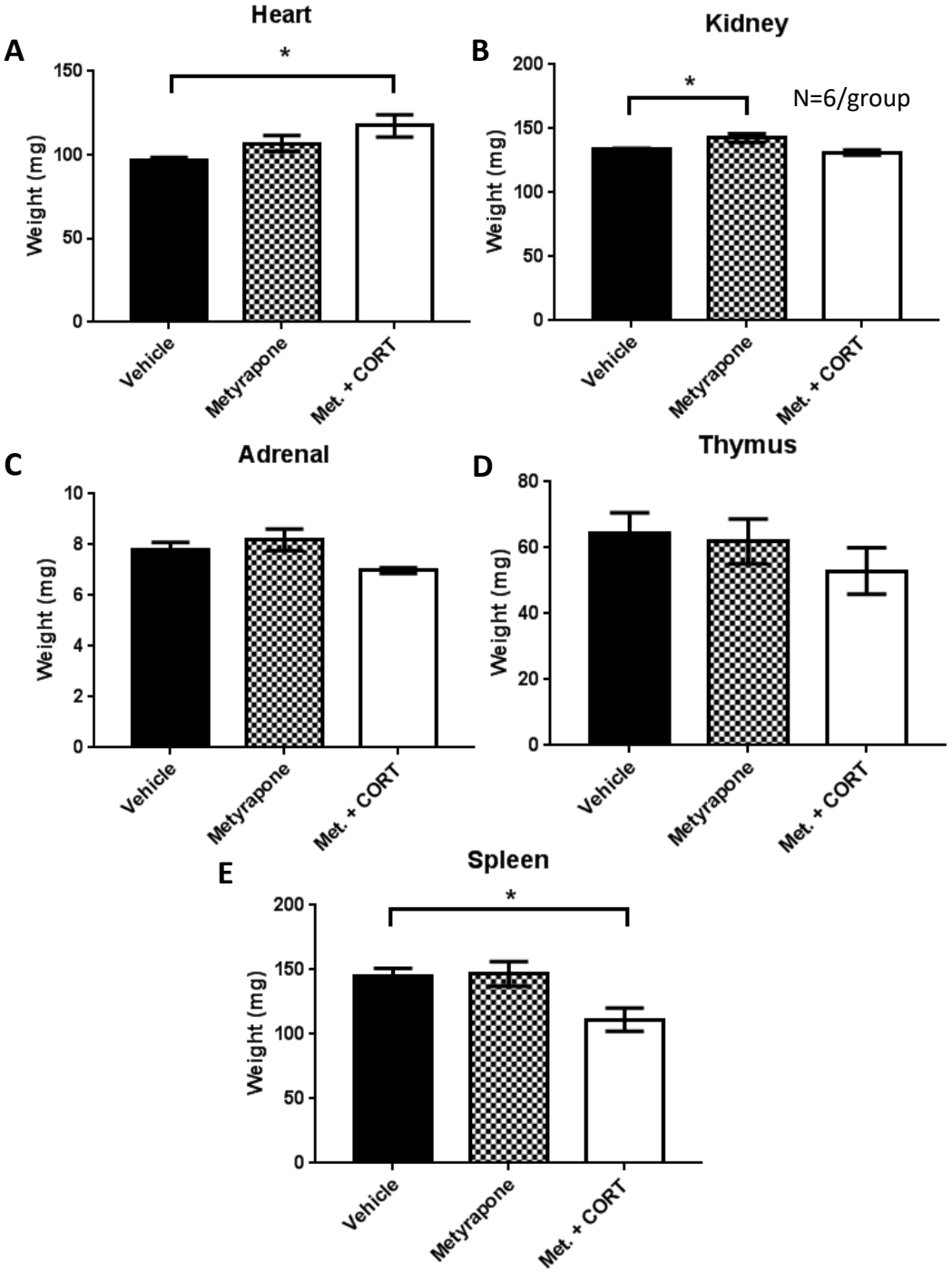

Figure 5.7 – Effects of metyrapone with/without corticosterone on glucocorticoid sensitive organ weights. A) Heart weight was increased in the mice treated with metyrapone daily (100mg/kg, i.p.) and corticosterone (25µg/mL in drinking water). B) Kidney weight was increased in the mice treated with metyrapone daily. C) Adrenal and D) Thymus weights were unaffected by either treatment. E) Spleen weight was decreased in the mice treated with metyrapone and corticosterone. N=6/group. * $P<0.05$. Data are mean ± standard error and were compared by one-way ANOVA with Dunnett's post-hoc test.

5.2.4.2 Effect of metyrapone and corticosterone replacement on plasma glucocorticoids

The corticosterone synthesis inhibitor metyrapone did not significantly alter circulating 11-DHC levels in mice injected daily (100mg/kg). Mice injected with the same dose of metyrapone and given access to corticosterone in drinking water (25µg/mL) had elevated levels of circulating 11-DHC compared to metyrapone-treated mice (10.95 ± 1.76 nmol/L vs. 3.40 ± 1.03 nmol/L, $P<0.05$, Figure 5.8A). Circulating corticosterone levels were not significantly affected by either metyrapone or metyrapone with corticosterone in drinking water (Figure 5.8B).

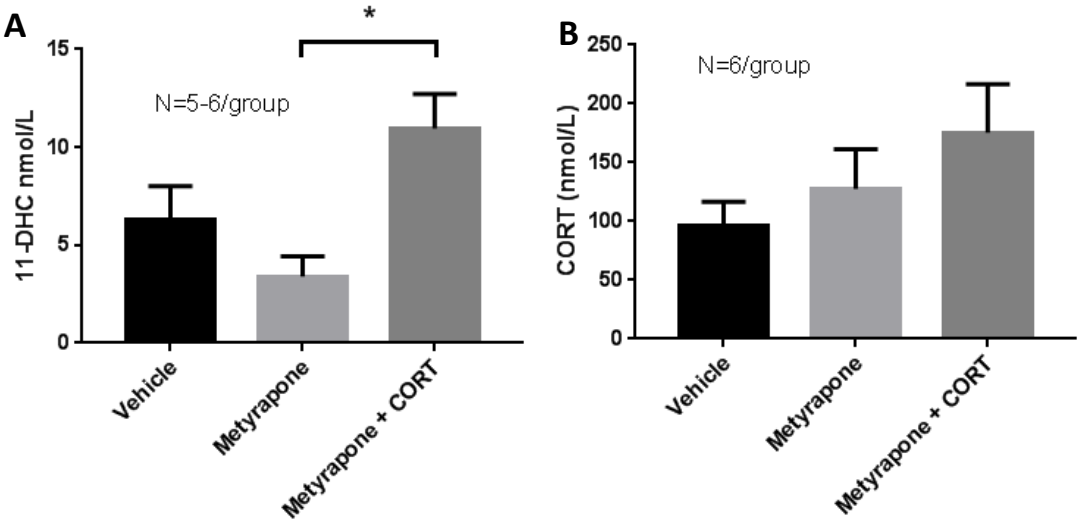

Figure 5.8 – Metyrapone was ineffective in inhibiting adrenal glucocorticoid synthesis. A) 11-dehydrocorticosterone (11-DHC) levels were increased in the metyrapone (100mg/kg/day) + corticosterone (25µg/mL in drinking water) group compared to the metyrapone (100mg/kg) group. *$P<0.05$. B) Corticosterone levels were not significantly altered by metyrapone or metyrapone + corticosterone. Glucocorticoid levels measured by liquid chromatography tandem-mass spectrometry. N=5-6/group. Data are mean ± standard error and were compared by one-way ANOVA with Tukey's post-hoc test.

5.2.5 Cell proliferation in tumours

5.2.5.1 Slide scanner analysis

To determine whether inhibition of 11β-HSD1 with UE2316 affected cell proliferation *in vivo* in tumours, proliferation marker Ki67 was quantified in WT-SCC tumours from control or UE2316 diet-fed wildtype mice and Panc043 and SCC-B6-1 tumours from control or UE2316 diet-fed wildtype mice or control diet-fed Del1 mice (N=6/group). ImageJ thresholding and quantification of whole tissue images from the slide scanner revealed no significant differences in Ki67 % area between tumours from control, UE2316-treated or Del1 mice, across all three tumour types (Figure 5.9).

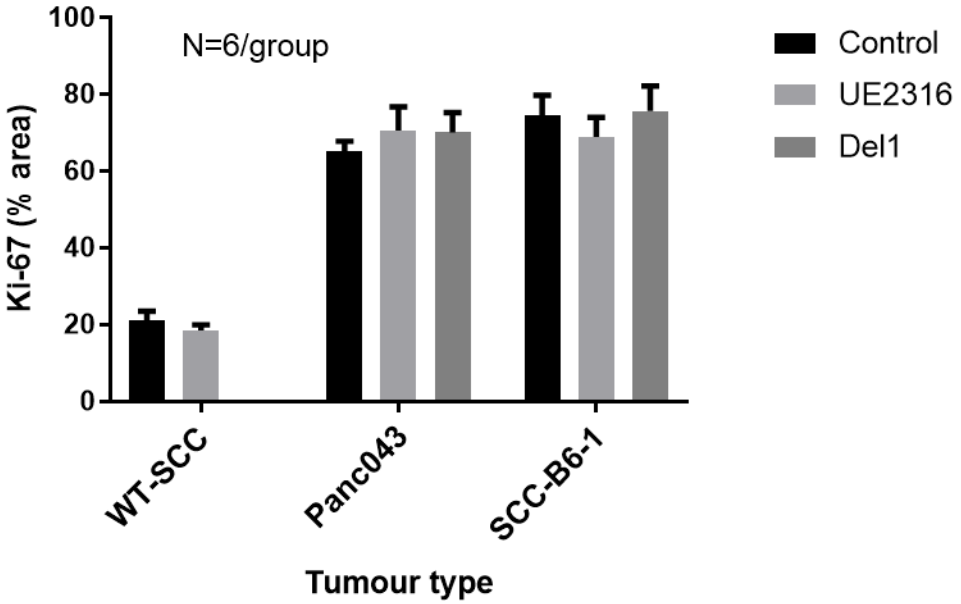

Figure 5.9 – UE2316 and 11β-HSD1 deletion do not affect Ki67 % area in any of the three tumour types. ImageJ was used to threshold and quantify whole sections from each tumour type stained with the cell proliferation marker Ki67 and imaged on the slide scanner. Data are expressed as % stain area. Squamous cell carcinoma tumour (WT-SCC) data were compared by independent samples t-test, Panc043 and SCC-B6-1 tumour data were compared by one-way ANOVA. N=6/group. Data are mean ± standard error.

5.2.5.2 **Hotspot quantification**

5.2.5.2.1 *WT-SCC*

As a secondary method of quantification, hotspots from Ki67-stained tumours were identified and quantified. Representative images from control (Figure 5.10A) and UE2316-treated tumours (Figure 5.10B) demonstrate the strong nuclear signal produced. Immunoreactivity was apparent across the tumour but concentrated in distinct proliferative hotspots. No difference in DAPI-positive nuclei per mm^2 was seen between control and UE2316 WT-SCC tumours (Figure 5.10C), demonstrating an equal cell density between treatment groups. Quantification of Ki67-positive cell nuclei staining revealed a trend towards reduced proliferation in UE2316-treated tumours as compared to control tumours (16.64 ± 0.97 % vs 22.16 ± 2.64 %, P=0.077), though this did not reach significance (Figure 5.10D). A power calculation suggests a sample size of 11/group would detect a difference of this magnitude with the given variance (80% power).

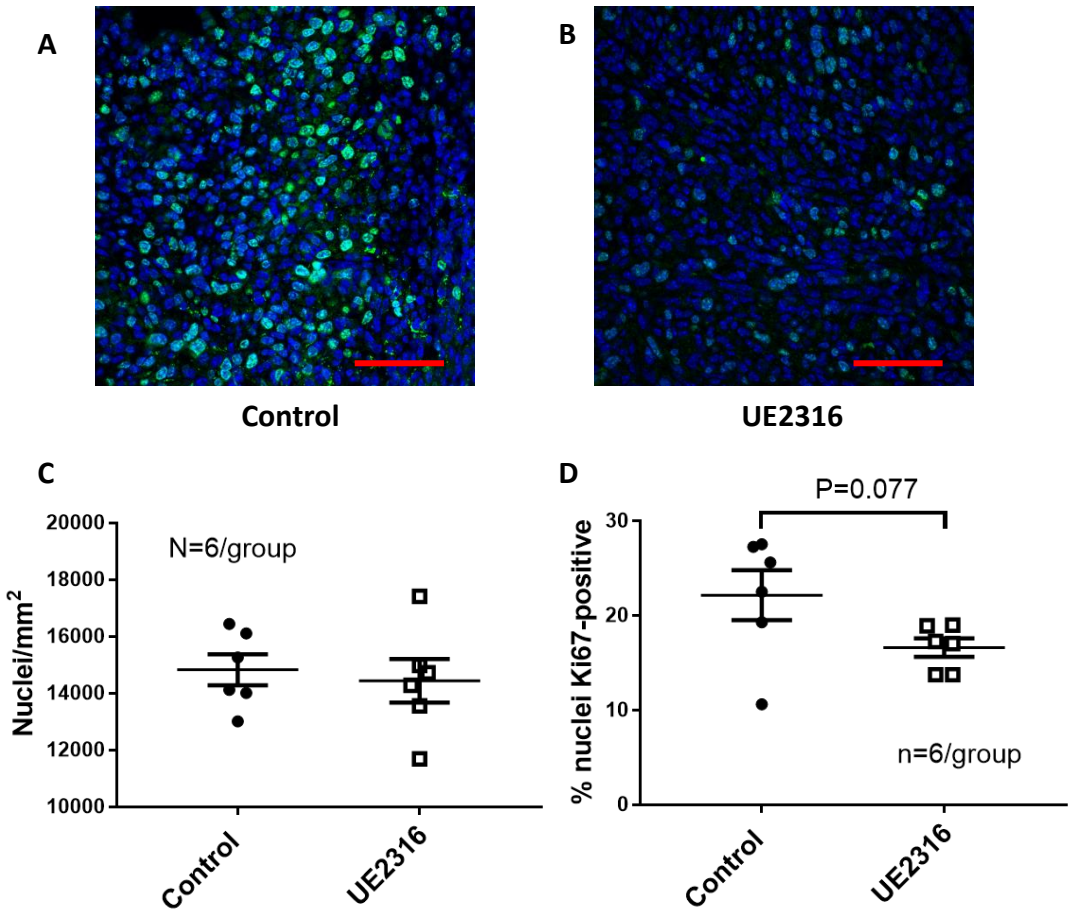

Figure 5.10 - End-stage UE2316-treated WT-SCC tumours showed a trend towards reduced proliferation. Representative images of hotspots from Ki67-stained squamous cell carcinoma (WT-SCC) tumours from control (A) and UE2316 treated (B) mice are shown. Hotspots were typically near the periphery of the tumour. Scale bar = 50µm. C) Nuclear density between control and UE2316-treated tumours was unaltered. D) The proportion of cells staining positive for proliferation marker Ki67 showed a trend towards being reduced in tumours from UE2316-treated mice but this did not reach significance. N=6/group. Data represent mean ± standard error are were compared by independent samples t-test.

5.2.5.2.2 *Panc043 and SCC-B6-01*

Ki67 staining of Panc043 and SCC-B6-1 tumours showed no differences or trends between control tumours, UE2316-treated tumours and tumours from Del1 mice in terms of end-stage cell proliferation (Figure 5.11).

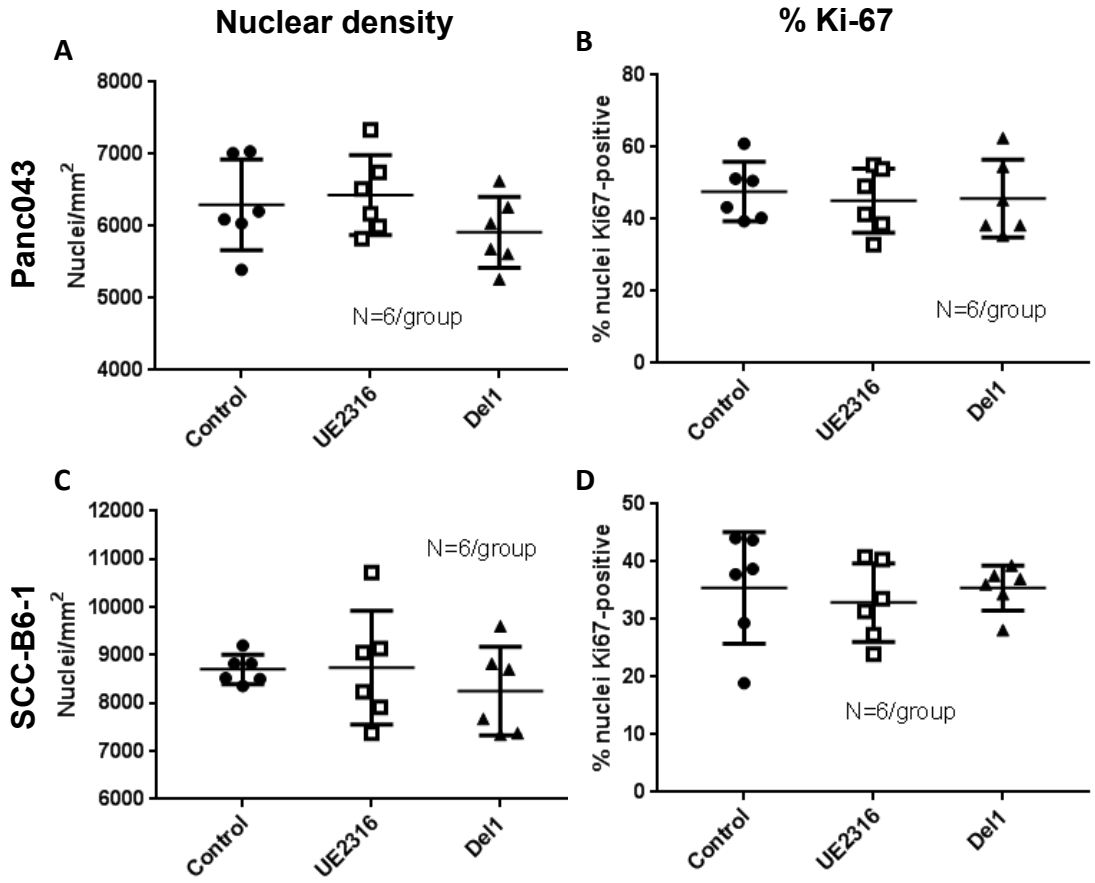

Figure 5.11 – UE2316 and 11β-HSD1 deletion do not affect cell proliferation in end-stage Panc043 and SCC B6-1 tumours. Panc043 (A) and SCC-B6-1 (C) tumour nuclear density is unaffected by UE2316 treatment and 11β-HSD1 deletion (Del1 mice). The percentage of cells staining positive for Ki67 was also unaffected by either condition in both Panc043 (B) and SCC-B6-1 (D) tumours. N=6/group, data represent mean ± standard error and were compared by one-way ANOVA.

5.2.6 RNA-sequencing in WT-SCC tumours

5.2.6.1 Principal component analysis (PCA)

To gain further insight into the mechanism behind the enhanced growth seen in WT-SCC tumours after UE2316 treatment, RNA-sequencing was performed on WT-SCC samples (day 11 timepoint, Section 3.2.1). The average number of reads obtained from control samples was 45 million and from UE2316 samples was 42 million. Tophat2 was used to map an average of 43 million control reads and 41 million UE2316 reads to the mouse mm10 reference genome. The average concordant pair alignment rate was 86% across the entire sample.

Control samples are coded as CON1-6 and UE2316-treated tumours as T1-6. PCA showed that samples subjected to single-end sequencing rather than paired-end sequencing (CON4 and T5) were separated along the first principle component, likely a processing effect. PCA also showed a further UE2316-treated tumour (T4) to be an outlier (Figure 5.12A). Samples CON4/T4/T5 were therefore excluded from further analysis. Repeat PCA showed a split in the control samples along the first principle component CON1/2/3 vs CON5/6 (Figure 5.12B). Consequently, differential gene expression was assessed between samples CON1/2/3/5/6 vs. T1/2/3/6 but genes also found to be significantly different within the control group were excluded from Gene Ontology (GO) analysis.

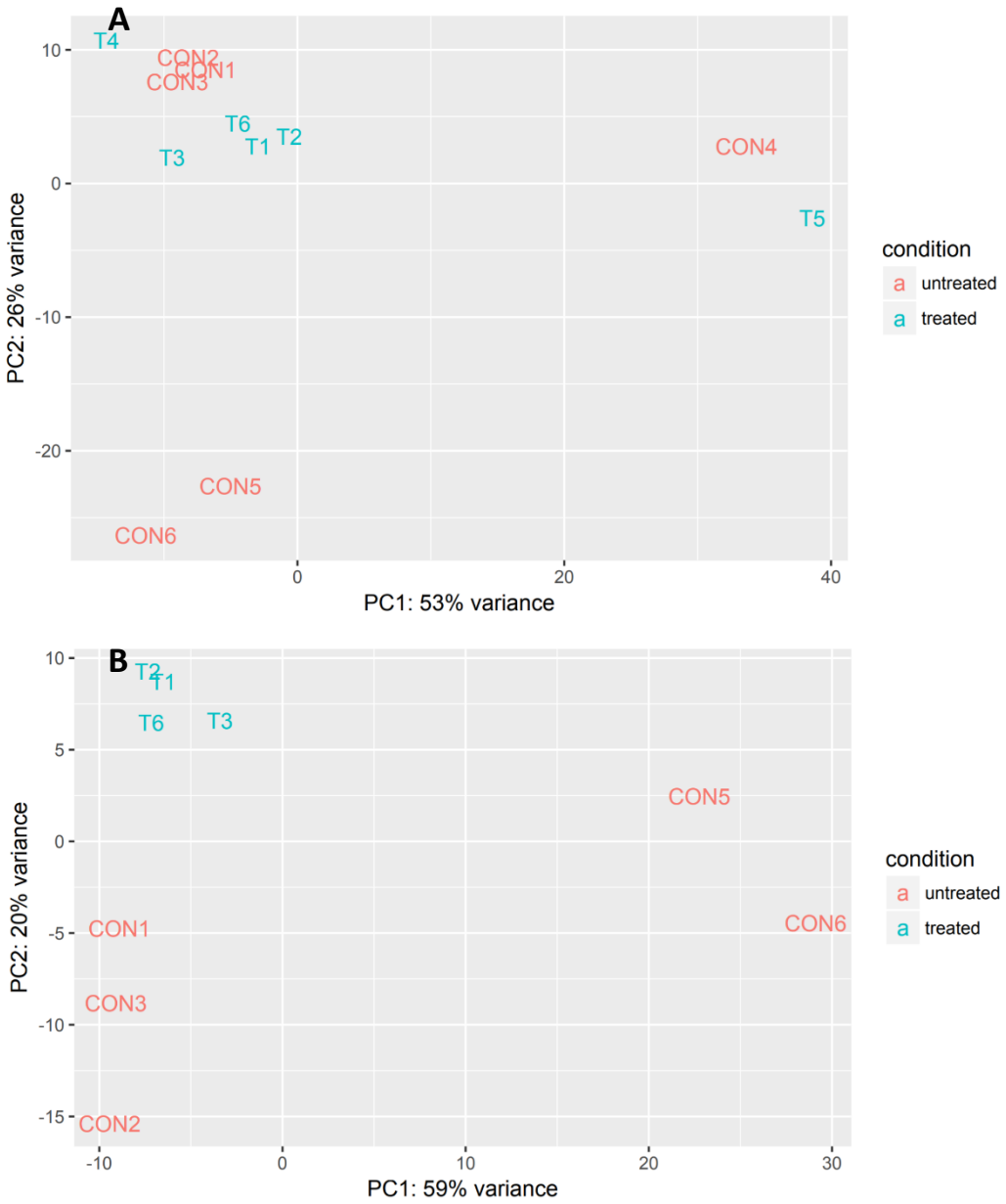

Figure 5.12 - Principal component analysis of RNA-sequencing data. A) Principal Component Analysis (PCA) showed that samples sequenced using a single-end protocol (CON4/T5) were outliers, as was T4, necessitating their exclusion. B) Repeat PCA of the samples revealed a split within the control group. To maintain sample size rather than excluding further data, only genes shown to differ significantly between T1/2/3/6 and C1/2/3/5/6, but not between C1/2/3 and C5/6, were included in subsequent gene ontology analysis.

5.2.6.2 Gene Ontology Enrichment analysis

Genes found to be differentially expressed between groups were fed into the Database for Annotation, Visualization and Integrated Discovery (DAVID) v6.8 (Huang *et al.*, 2008). Whilst data presented here are derived using this tool, it is important to note that near identical results were achieved using similar GO databases, for example AmiGO (Carbon et al., 2009) accessed via the GO website using data from the GO consortium (Ashburner et al., 2000). Significantly relevant ($P<0.05$) biological processes are listed in Table 5.1.

Genes associated with the inflammatory response, immune response and collagen fibril organisation (as identified by DAVID) and their relative expression in UE2316-treated tumours (as identified by RNA-seq) are shown in Figures 5.13-5.15 respectively. These particular processes were selected based on their q-values from GO analysis, and also their mechanistic relevance to the 11β-HSD1 inhibition literature – further investigations pertaining to these processes are described below.

Process	**q-value**
Inflammatory response	2.76E-08
Cellular response to interferon-beta	4.08E-07
Positive regulation of gene expression	2.73E-04
Immune response	6.21E-04
Response to lipopolysaccharide	9.91E-04
Positive regulation of cell migration	0.00134
Chemokine-mediated signalling pathway	0.00375
Cellular response to interferon-γ	0.003808
Negative regulation of osteoblast differentiation	0.00345

Chemotaxis	0.007944
Collagen fibril organization	0.007565
Defence response to virus	0.007221
Positive regulation of apoptotic process	0.008123
Circadian rhythm	0.00936
Osteoblast differentiation	0.014029
Negative regulation of cell migration	0.028646
Cell adhesion	0.042488
Ossification	0.042287
Immune system process	0.047532
Positive regulation of osteoblast differentiation	0.046155
Defence response to protozoan	0.045956

Table 5.1 - Gene ontology analysis of RNA-seq data demonstrates importance of immune response. Gene Ontology (GO) analysis was performed using the Database for Annotation, Visualization and Integrated Discovery (DAVID) v6.8. Significance is expressed using the p-value corrected for multiple hypothesis testing using the Benjamini-Hochberg method (q-value). The listed biological processes were found to be significant ($q<0.05$).

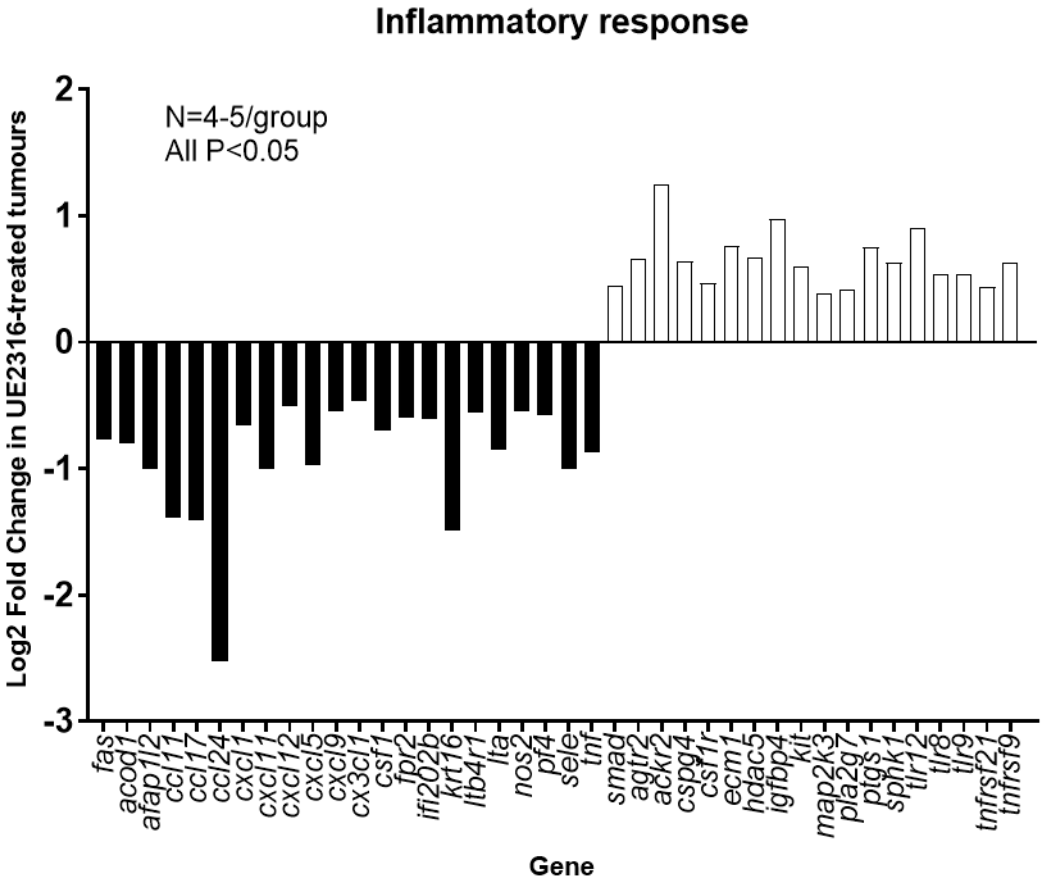

Figure 5.13 – 'Inflammatory response' genes identified by Gene Ontology analysis. These differentially expressed genes were identified as being related to the inflammatory response by Gene Ontology analysis. Note that mRNA coding for a large number of pro-inflammatory cytokines are reduced after UE2316 treatment, while cytokine receptors and toll-like receptor transcript is increased. N=4-5/group. A modified Fisher Exact test was used to determine whether the proportion of genes in a given list was significantly associated with a biological process compared to the murine genome: $P<0.05$ for all the above. Data represent mean values.

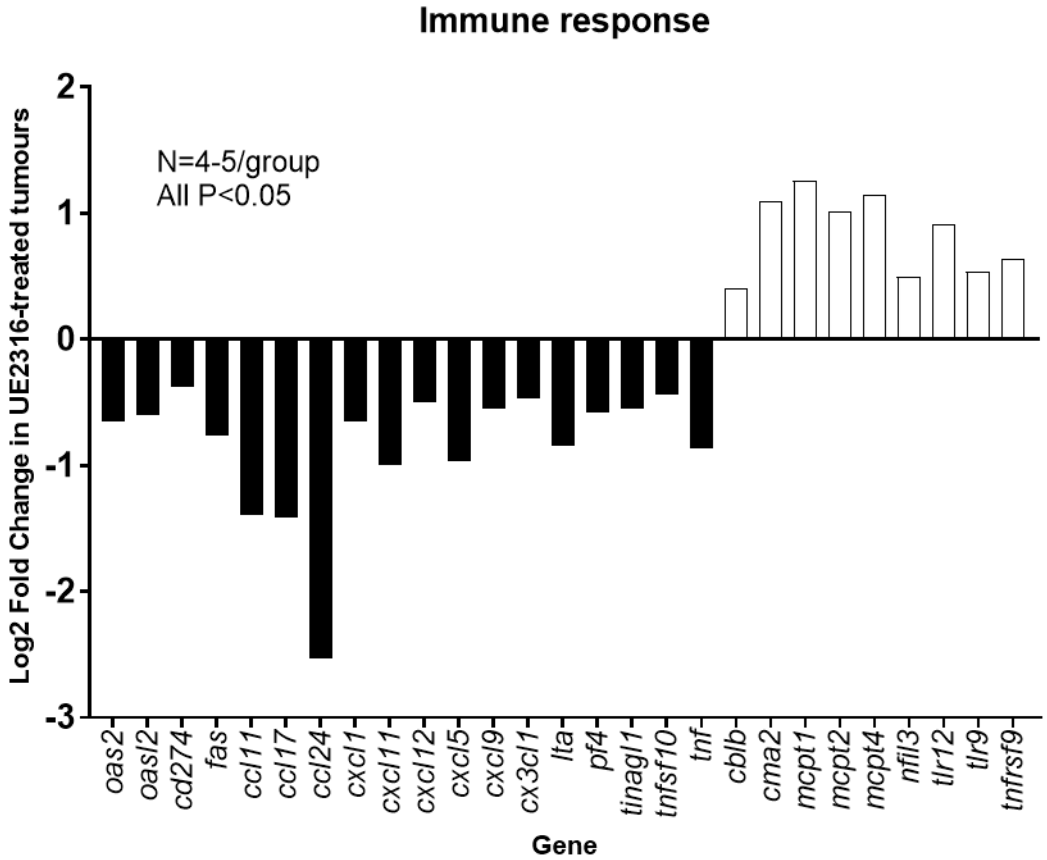

Figure 5.14 – 'Immune response' genes identified by Gene Ontology analysis. These differentially expressed genes were identified as being related to the immune response by Gene Ontology analysis. Note that mRNA coding for a large number of pro-inflammatory cytokines are reduced after UE2316 treatment, while toll-like receptor and mast cell protease transcript is increased. N=4-5/group. A modified Fisher Exact test was used to determine whether the proportion of genes in a given list was significantly associated with a biological process compared to the murine genome: $P<0.05$ for all the above. Data represent mean values.

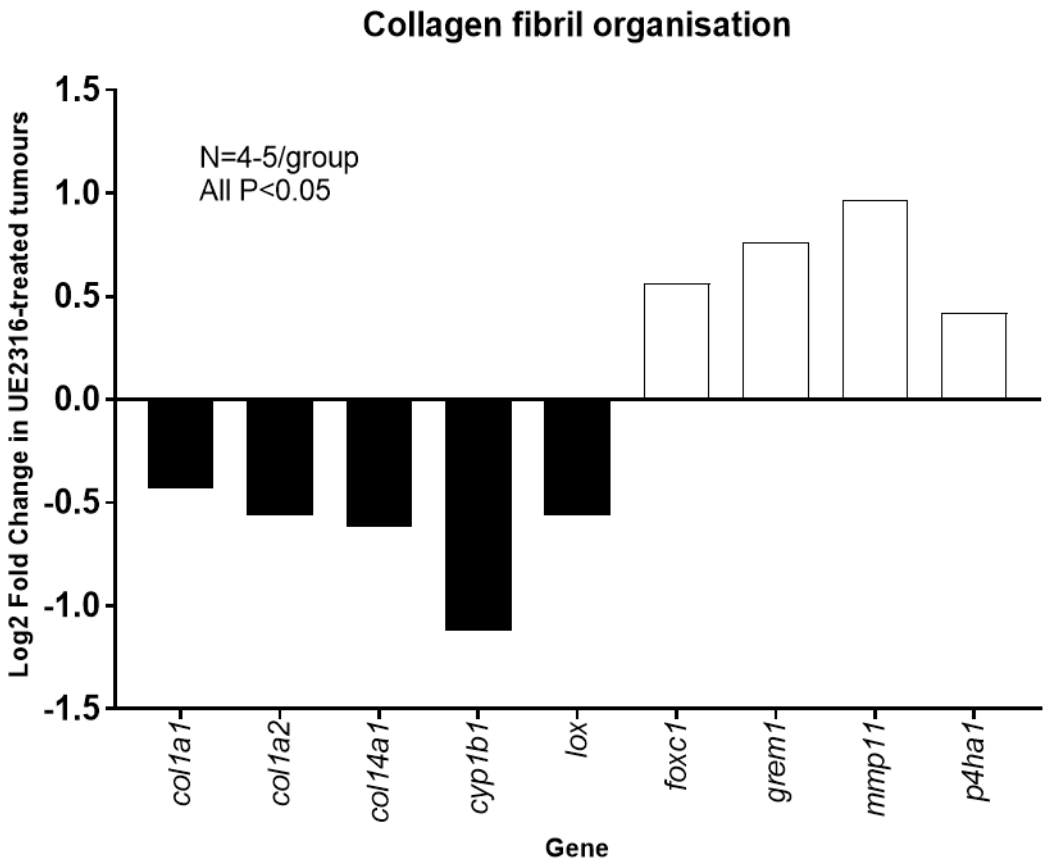

Figure 5.15 – 'Collagen fibril organisation' genes identified by Gene Ontology analysis. These differentially expressed genes were identified as being related to the inflammatory process by Gene Ontology analysis. N=4-5/group. A modified Fisher Exact test was used to determine whether the proportion of genes in a given list was significantly associated with a biological process compared to the murine genome: P<0.05 for all the above. Data represent mean values

5.2.7 Validation of RNA-sequencing by RT-qPCR

A selection of key differentially expressed genes were assessed by RT-qPCR to determine the validity of the RNA-sequencing data. The genes of interest and their associated RNA-sequencing data are listed in Table 5.2. Validated genes with their expression reduced by UE2316 treatment were: Type 1 collagen (COL1A1); chemokine (C-X-C motif) ligand 9 (CXCL9); colony stimulating factor 1 (CSF1); platelet factor 4 (PF4); fas cell surface death receptor (FAS); signal transducer and activator of transcription 2 (STAT2); C-C motif chemokine ligand 11 (CCL11); nitric oxide synthase (inducible) (NOS2); arginase 1 (ARG1); and 11β-HSD1 (HSD11B1). Validated genes with their expression increased by UE2316 treatment were: tumour necrosis factor receptor superfamily, member 23 (TNFRSF23); integrin alpha-10 (ITGA10) ($P<0.05$ control vs. UE2316; Figure 5.16A). To confirm the specificity of the RNA sequencing, genes from similar pathways not found to be significant by RNA sequencing were also compared between groups using RT-qPCR. Chemokine (C-X-C motif) ligand 2 (CXCL2) and interleukin-6 (IL6), both pro-inflammatory cytokines, were selected and found not to differ between control and UE2316-treated WT-SCC tumours (Figure 5.16A).

Genes that could not be validated (non-significant) were: decorin (DCN); tumour necrosis factor receptor superfamily, member 9 (TNFRSF9, $P=0.12$); tumour necrosis factor receptor superfamily, member 21 (TNFRSF21); tumour necrosis factor (TNF, $P=0.10$); alpha smooth muscle actin (ACTA2); toll-like receptor 9 (TLR9, $P=0.14$); angiopoietin-like protein 2 (ANGPTL2); chondroitin sulfate proteoglycan 4 precursor (CSPG4) (Figure 5.16B).

Gene	Control (FPKM)	UE2316 (FPKM)	Log2 Fold-change	q-value
Enriched in UE2316 tumours				
Tlr9	5.92963	8.6073	0.537619	0.0112153
Itga10	26.2958	51.8496	0.979502	0.00211442
Dcn	538.249	722.191	0.424106	0.024116
Angptl2	145.96	218.175	0.579917	0.00211442
Cspg4	34.3593	53.7223	0.64482	0.00211442
Reduced in UE2316 tumours				
Ccl24	3.08241	0.533999	-2.52915	0.00712227
Wnt11	0.813976	0.286914	-1.50437	0.0399818
Ccl17	6.82636	2.56146	-1.41415	0.0112153
Ccl11	26.0511	9.93497	-1.39076	0.00211442
Cxcl11	41.6018	20.7693	-1.0022	0.0230463
Cxcl5	44.3702	22.6915	-0.967439	0.00211442
Tnf	8.77976	4.80803	-0.868736	0.00211442
Acod1	19.6915	11.3465	-0.795329	0.00211442
Fas	12.934	7.59826	-0.767429	0.00211442
Csf1	67.5942	41.5673	-0.701449	0.00211442
Pf4	34.6935	23.2396	-0.578079	0.0356906
Cxcl9	211.537	144.709	-0.547754	0.00211442

Cxcl12	47.8659	33.7732	-0.503119	0.00211442
Cx3cl1	66.6268	48.2425	-0.465796	0.0124766
Arg1	128.306	92.6027	-0.470468	0.00211442
Stat2	46.327	34.9967	-0.404637	0.0112153
Acta2	30.5468	9.32152	-1.71238	0.00211442

Table 5.2 – Selected differentially expressed genes of interest. The listed differentially expressed genes play key roles in a range of the biological processes identified by Gene Ontology analysis and thus are likely to be important mediators of the effects of UE2316 in squamous cell carcinoma (WT-SCC) tumours.

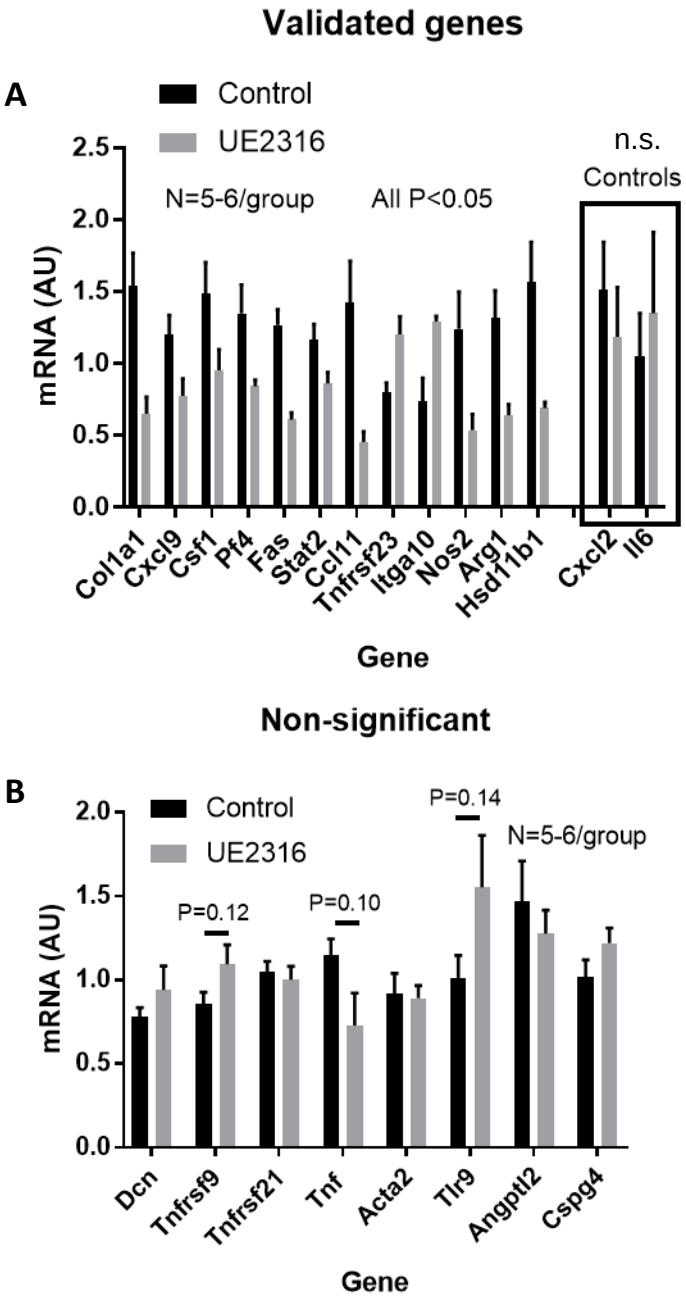

Figure 5.16 – Validation of RNA-sequencing genes by RT-PCR. cDNA generated from WT-SCC tumours grow in control and UE2316-diet-fed mice was subjected to RT-qPCR to confirm the RNA-sequencing data. An array of key genes was examined. A) Genes confirmed to significantly differ ($P<0.05$) between groups include type I collagen, 11β-HSD1 and several cytokines related to immune and inflammatory processes. The box on the right highlights genes that did not differ between groups in either the RNA sequencing or RT-qPCR analysis. B) Some genes failed to match the RNA-sequencing data, though several still showed a trend towards the expected change. N=5-6/group. Data are mean ± standard error and were compared by independent samples t-test.

5.2.8 CD3 immunoreactivity in WT-SCC tumour was not affected by UE2316 treatment

To quantify infiltrating T-cells, WT-SCC tumours from control vs UE2316-diet-fed mice (N=5/group) were stained for CD3-positive cells. The antibody produced a stain which was concentrated at the periphery of the tumour, usually very pronounced at one border (Figure 5.17A/B). A higher magnification image is shown in Figure 5.17C. There was no significant difference in CD3-positive area in tumours from RM-1 and UE2316 diet-fed mice, assessed either across whole tissue sections (Figure 5.17E) or using hotspot quantification (Figure 5.17F).

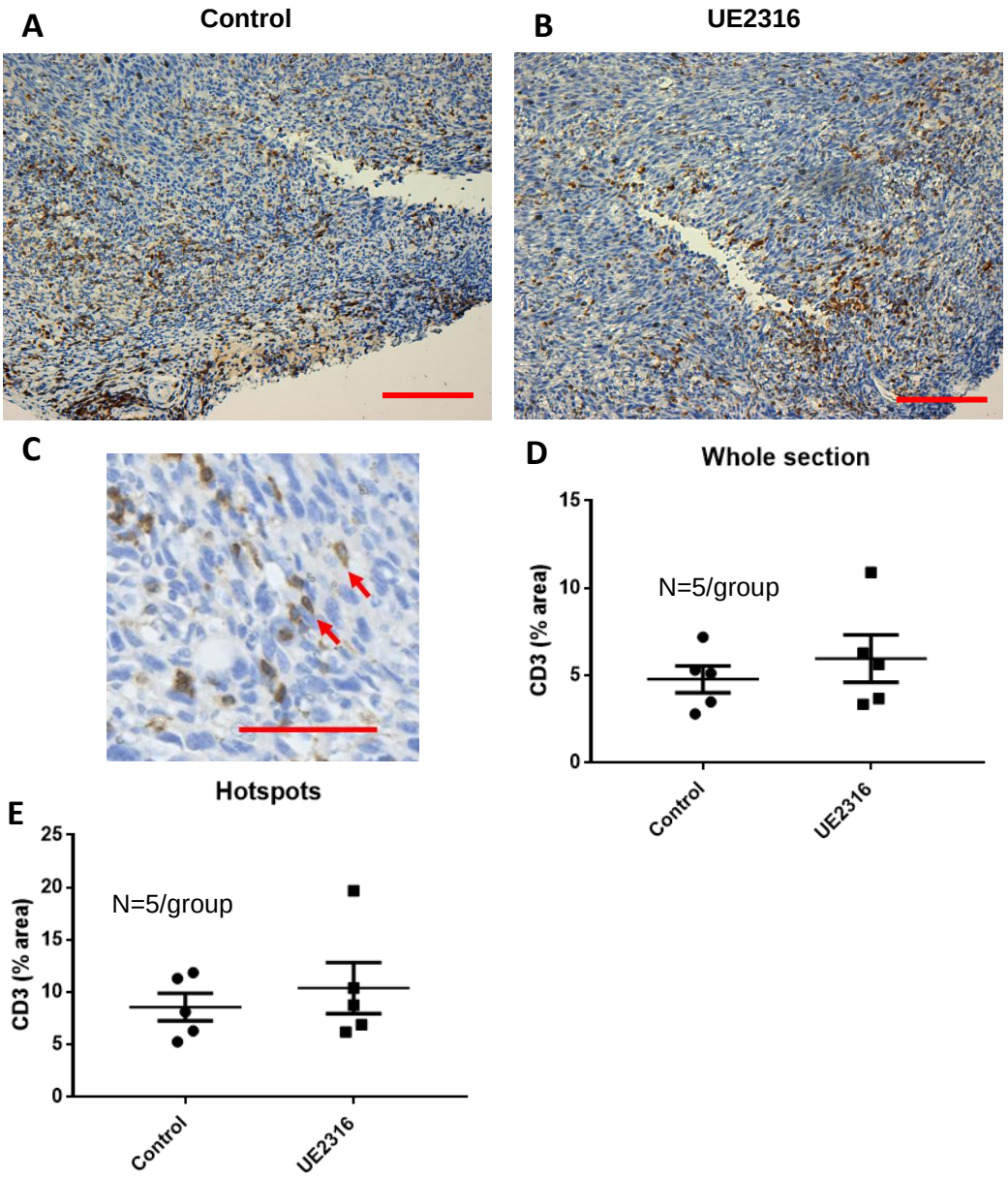

Figure 5.17 – CD3-positive cell number in WT-SCC tumours was unaffected by 11β-HSD1 inhibitor (UE2316) administration. Representative images of CD3-stained control (A) and UE2316-treated (B) squamous cell carcinoma (WT-SCC). DAB immunoreactivity shown in brown and haematoxylin-counterstained nuclei in blue. CD3 signal was usually strongest along one border of the tumour. C) 200x magnification image showing perinuclear cytoplasmic localisation of CD3 (red arrows). Scale bar = 50µm. Immunostaining found no difference in CD3-positive stain area between WT-SCC tumours from control and UE2316-treated mice, assessed by either whole section analysis (D) or hotspot analysis (E). Data represent mean ± standard error and were compared by independent samples t-test, N=5/group.

5.2.9 F4/80 immunoreactivity in WT-SCC tumours was not affected by UE2316 treatment

To quantify inflammatory cell content, WT-SCC tumours from control vs UE2316-diet-fed mice (N=6/group) were stained for F4/80-positive cells. The antibody produced a cytoplasmic stain, present across the tumour but concentrated at the tumour periphery and in regions near the centre of the tumour. There was no significant difference in F4/80-positive area in tumours from RM-1 and UE2316 diet-fed mouse, despite an apparent slight decrease in UE2316-treated tumours (Figure 5.18).

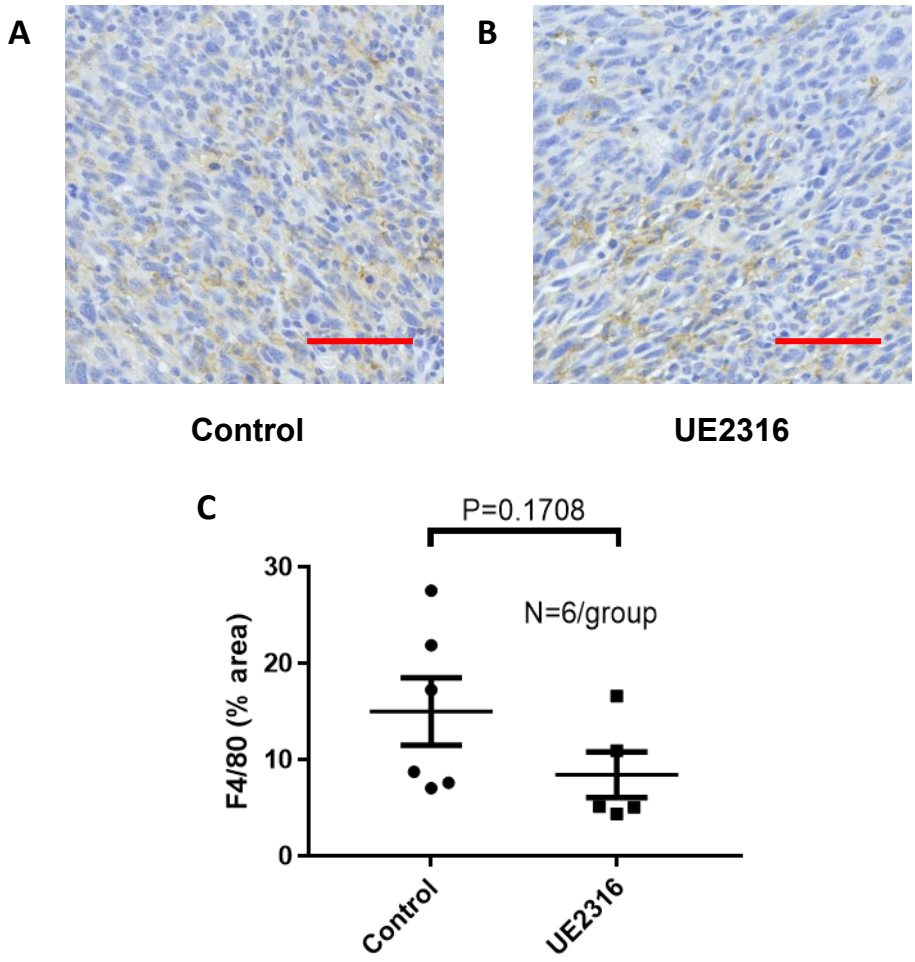

Figure 5.18 - F4/80 positive cell number in WT-SCC tumours was unaffected by 11β-HSD1 inhibitor (UE2316) administration. Representative images of squamous cell carcinoma (WT-SCC) tumours from control (A) and UE2316-treated (B) mice are shown, with DAB immunoreactivity shown in brown and haematoxylin-counterstained nuclei in blue. C) Immunostaining did not reveal a difference in F4/80-positive stain area between tumour from control and UE2316-treated mice. N=6/group. Data are mean ± standard error and were compared by independent samples t-test. Scale bar = 50µm.

5.2.10 Effects of UE2316 on fibrosis in tumours

5.2.10.1 UE2316 decreased type I collagen mRNA in WT-SCC tumours

After the observation that Type I collagen mRNA was decreased in WT-SCC tumours from UE2316-diet fed mice compared to control-diet fed mice (RNA-sequencing), expression was also examined in Panc043 tumours, where it did not differ between groups (1.54 ± 0.23 AU vs. 0.65 ± 0.12 AU, P<0.01, Figure 5.19).

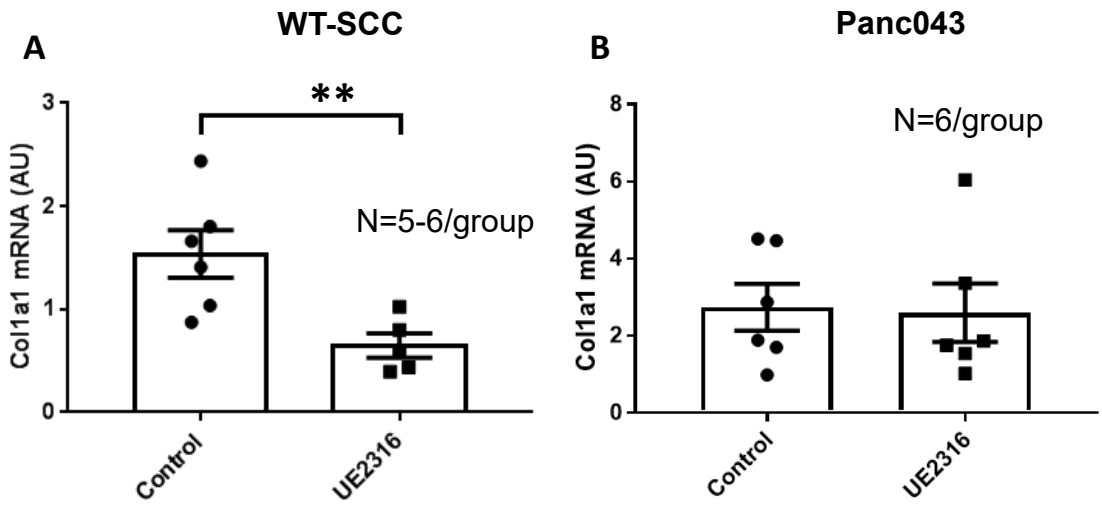

Figure 5.19 - Col1a1 mRNA was decreased in WT-SCC tumours, but not Panc043 tumour, by 11β-HSD1 inhibitor (UE2316) administration. A) Col1a1 mRNA expression was decreased in squamous cell carcinoma (WT-SCC) tumours from UE2316-treated mice compared to control mice, an effect that was not seen in Pancreatic Ductal Adenocarcinoma (Panc043) tumours (B). * P<0.01. N=5-6/group. Data are mean ± standard error and were compared by independent samples t-test.

5.2.10.2 Second Harmonic Generation imaging shows reduced type I collagen content in UE2316 WT-SCC tumours

To determine whether tumour collagen deposition was altered at the protein level by 11β-HSD1 inhibition, picrosirius red staining was performed to quantify collagen protein content in WT-SCC tumours from control and UE2316 diet-fed mice (N=6/group). Quantification of stain % area failed to detect a difference (Figure 5.20). To visualise Type-I collagen specifically, Second Harmonic Generation (SHG) microscopy was performed by Dr Martin Lee on WT-SCC tumours (N=6/group), Panc043 tumours (N=3/group) and SCC-B6-1 tumours (Day 28 N=6/group, Day 41 N=3/group). Automatic quantification of % collagen area from SHG images revealed a reduced amount of type I collagen in tumours from mice fed UE2316-diet (9.78 ± 0.84%) compared to tumours from mice fed normal diet (3.85 ± 0.56%, $P<0.001$, Figure 5.21).

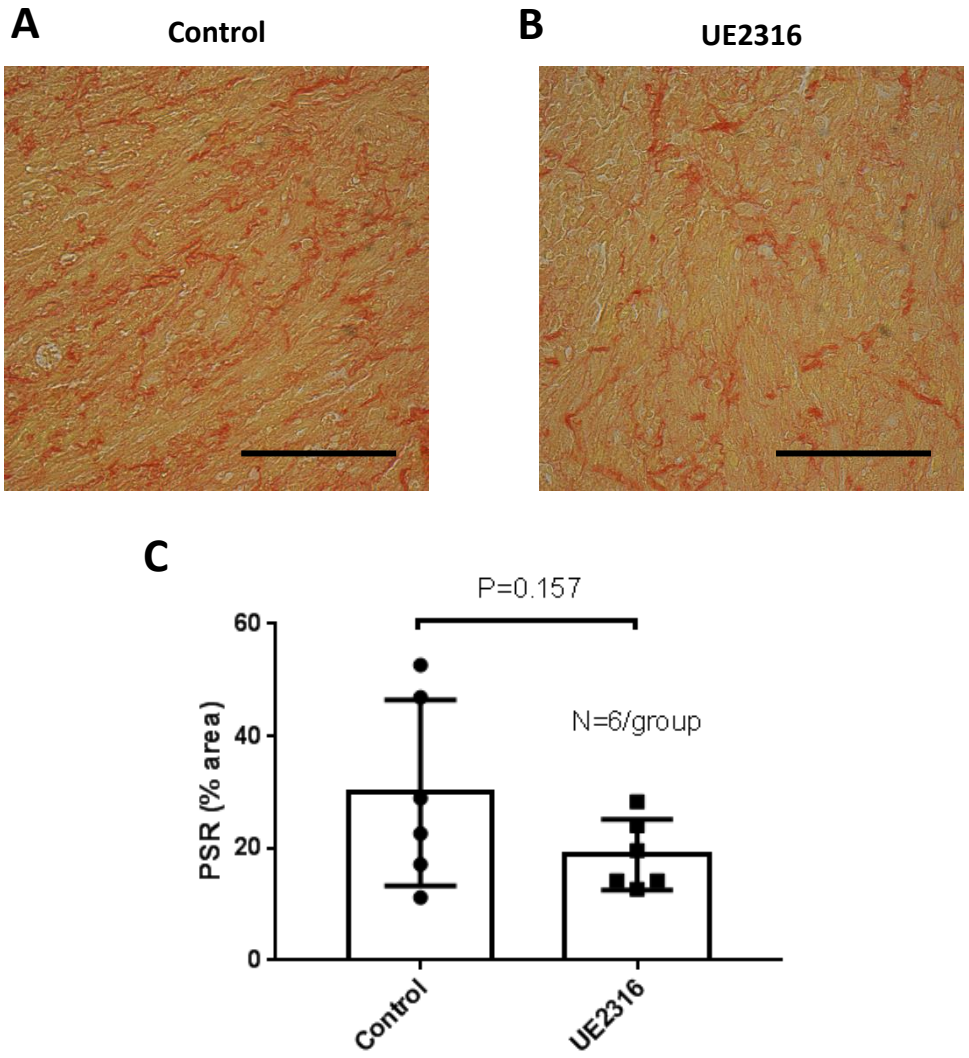

Figure 5.20 - Total collagen content does not differ significantly between WT-SCC tumours from control and UE2316-treated mice. A) Picrosirius red (PSR) images showed total collagen content in squamous cell carcinoma (WT-SCC) tumours from control (A) and UE2316-treated (B) mice. Scale bar = 100µm. B) UE2316-treated tumours, showed an apparent trend toward decreased collagen deposition, though this did not reach significance. N=6/group. Data represent mean ± standard error and were compared by independent samples t-test.

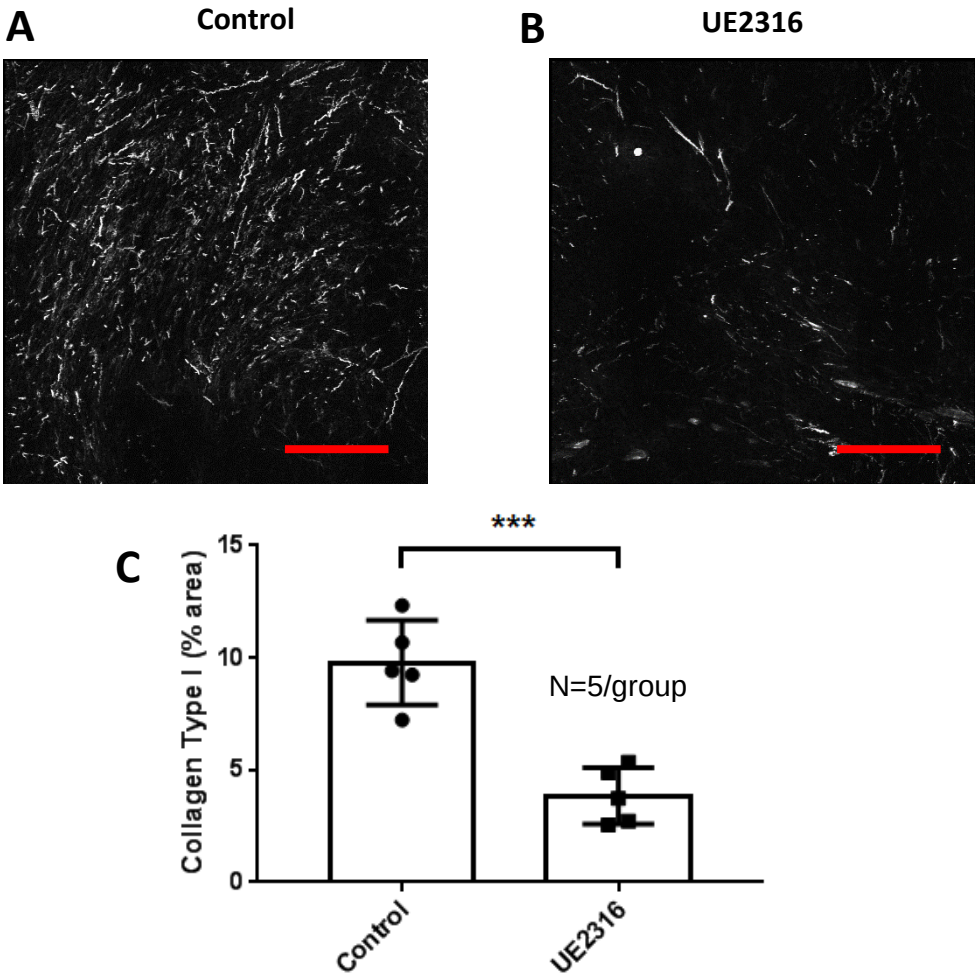

Figure 5.21 – Type I collagen is reduced in WT-SCC tumours from UE2316- treated mice. Second Harmonic Generation imaging showed that type I collagen (white signal) is reduced in WT-SCC tumours from UE2316-treated mice (B) as compared to tumours from control mice (A). Scale bar = 100µm. B) Type I collagen was reduced in tumours from UE2316-treated mice. *** P<0.001. N=5/group. Data represent mean ± standard error and were compared by independent samples t-test.

5.2.10.3 Second Harmonic Generation imaging shows increased type I collagen content in SCC-B6-1 tumours from UE2316-treated, but not del1, mice

SCC-B6-1 tumours grown in C57BL6/J mice fed either control or UE2316-diet, and Del1 animals, were also examined using SHG imaging to determine whether an effect on collagen was likely to relate to tumour growth. SCC-B6-1 tumours grown to day 28 (N=6/group) were sectioned and imaged using SHG – tissue from tumours grown to day 41 was too degraded for useful analysis. Automatic quantification revealed higher levels of type I collagen in SCC-B6-1 tumours from UE2316-treated mice compared with tumours from age-matched control mice (2.92 ± 0.72% vs. 6.38 ± 1.82%, P<0.01, Figure 5.22). The collagen content of SCC-B6-1 tumours from Del1 mice did not differ significantly from controls.

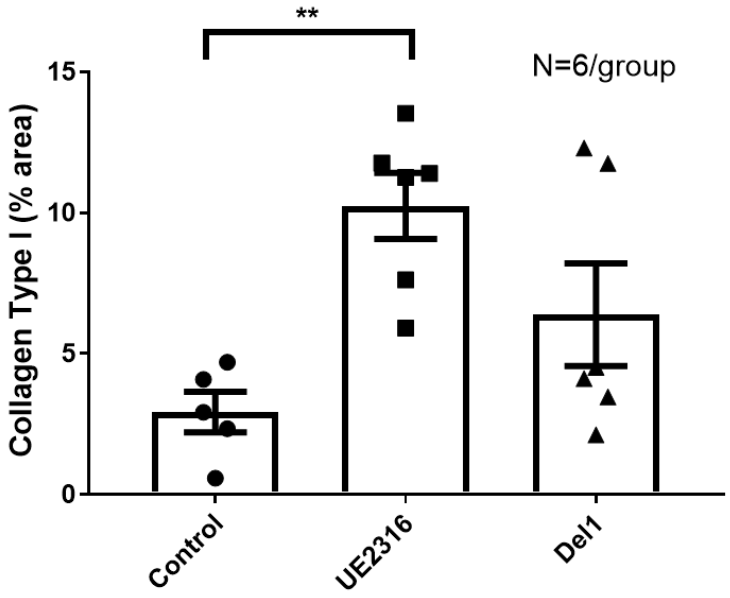

Figure 5.22 – Levels of type I collagen in SCC-B6-1 tumours were increased by 11β-HSD1 inhibition (UE2316) but not by 11β-HSD1 deletion (Del1). Type I collagen, automatically quantified from Second Harmonic Generation (SHG) images, was increased in SCC-B6-1 tumours from the day 28 time point from UE2316-treated mice. SCC-B6-1 tumours from Del1 mice did not differ from control tumours. ** = P<0.01. N=5-6/group. Data represent mean ± standard error and were compared by one way ANOVA with Dunnett's post-hoc test.

5.2.10.4 11β-HSD1 inhibition and deletion do not affect collagen content in Panc043 tumours

Type I collagen content in Panc043 tumours did not differ between groups (Figure 5.23).

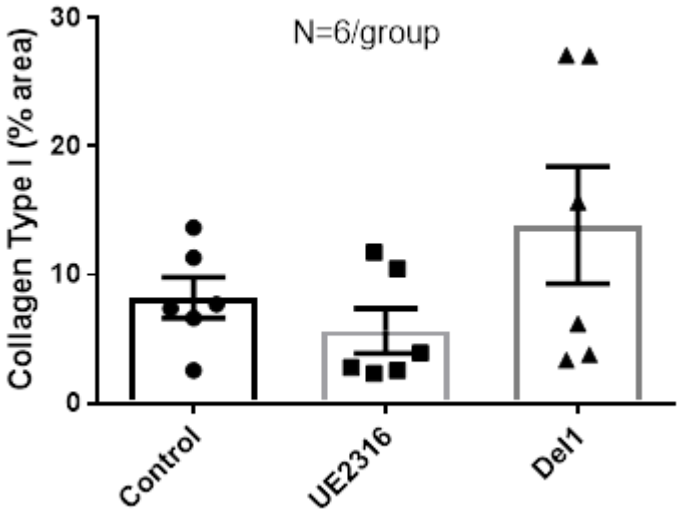

Figure 5.23 - Panc043 collagen type I is not affected by UE2316 or 11β-HSD1 deletion. A) Type I collagen, automatically quantified from SHG images, was not affected in either Pancreatic Ductal Adenocarcinoma (Panc043) tumours grown in UE2316-treated mice or those grown in Del1 mice compared to those grown in control mice. N=6/group. Data represent mean ± standard error and were compared by one-way ANOVA.

5.3 Discussion

The experiments described in this chapter tested three hypotheses; that 11β-HSD1 inhibition and deletion would not affect circulating glucocorticoid levels in mice; that UE2316-responsive WT-SCC tumour growth would increase in response to reduced circulating glucocorticoids; and that the enhanced WT-SCC growth seen after 11β-HSD1 inhibition would be associated with altered signalling between cells of the tumour microenvironment, likely fibroblasts and/or immune/inflammatory cells. Data presented led to the rejection of the first hypothesis; while circulating glucocorticoids in C57BL6/J mice were unaffected by UE2316 treatment, FVB/N mice showed a significant decrease in circulating corticosterone, suggesting a potential systemic effect. Corticosterone levels did not differ between wild-type and Del1 mice, but 11-DHC levels were increased in the transgenic animals. Attempts to determine whether UE2316-responsive WT-SCC tumour growth would increase in response to reduced circulating glucocorticoids were unfortunately unsuccessful, as the adrenal glucocorticoid synthesis inhibitor metyrapone failed to reduce systemic corticosterone levels in FVB/N mice. The second hypothesis thus remains unaddressed. RNA-sequencing data supports the third hypothesis; GO analysis and subsequent qPCR highlighted changes in immune and inflammatory signalling pathways in UE2316-treated WT-SCC tumours, although histological analysis did not reveal differences in the extent of either F4/80- or CD3-positive cells in these tumours compared to controls. Collagen fibril organisation was also identified by GO analysis as an altered process in UE2316-treated tumours, a finding that was validated by SHG imaging which detected a decrease in type I collagen in UE2316-treated WT-SCC tumours.

In vivo glucocorticoids

It was originally predicted that neither UE2316 treatment nor 11β-HSD1 deletion would affect circulating glucocorticoid levels in mice. When 11β-HSD1 inhibitors were initially recognised as a prospective treatment for type 2 diabetes, questions arose surrounding their safety with regards to HPA axis function. The concern was that the reduction in tissue-specific cortisol regeneration after 11β-HSD1 inhibition would reduce negative feedback to the HPA axis and result in increased cortisol release by the adrenals. However, data generated using preclinical mouse models has not shown

a significant effect on basal circulating corticosterone levels using the selective 11β-HSD1 inhibitors compound 544 (Hermanowski-Vosatka *et al.,* 2005), compound L-750 (Luo *et al.,* 2012) or UE2316 (Sooy *et al.,* 2010; Coutinho *et al.,* 2016) in C57BL6/J mice. A number of clinical trials have also reported no alteration in circulating glucocorticoids after treatment with 11β-HSD1 inhibitors (reviewed by Harno and White, 2010; Anderson and Walker, 2013), suggesting that compensatory activation of the HPA axis acts only to restore normal levels of plasma glucocorticoids in response to increased cortisol/corticosterone clearance.

In agreement with the literature (Sooy *et al.,* 2010; Coutinho *et al.,* 2016), the present studies did not detect a significant difference in circulating corticosterone or 11-DHC after UE2316 administration in C57BL6/J mice. In FVB/N mice, however, UE2316 induced a significant decrease in circulating corticosterone, which was detected via two separate assays. This unexpected finding suggests reduced HPA axis activity after 11β-HSD1 inhibition. One possible explanation for this finding is that the HPA axis of FVB/N mice are particularly sensitive to disruption of 11β-HSD1, potentially due to the importance of the enzyme at central negative feedback sites. Evidence for this theory is limited as FVB/N mice, whilst ideal for use in tumour studies (Huang and Balmain, 2014), are rarely used for studies of HPA axis activity. FVB/N mice are mentioned in the literature as being particularly sensitive to glucocorticoid-induced bone loss (Thiele *et al.,* 2014), and in work performed as part of this chapter showed immediate signs of temporary mild sedation and hyperphagia after receiving 100mg/kg metyrapone, a dose not reported to cause such effects in other strains. Strain-specific differences in the response of the HPA axis to 11β-HSD1 deletion have previously been reported; Carter *et al.* (2009) and Kotelevtsev *et al.* (1997) both report increased corticosterone levels in 11β-HSD1 KO mice bred on a 129/MF1 background compared to wild-type animals; the present evidence suggests FVB/N mice may also be a sensitive strain, and calls into question the role of genetic variation in determining patient response to 11β-HSD1 inhibitors.

An alternative explanation for the reduced circulating corticosterone in UE2316-treated FVB/N mice concerns animal handling and corticosterone clearance; although every effort was made to capture nadir corticosterone levels, it is likely that handling

of animals resulted in induction of the stress response. As 11β-HSD1 inhibitor-fed mice will have developed more rapid corticosterone clearance, it may be that the reported reduction in corticosterone levels reflects a more rapid return to baseline levels in UE2316-treated animals. Indeed, Sarabdjitsingh *et al.* (2014) report that stressed UE2316-treated C57BL6/J mice have significantly reduced plasma corticosterone compared to vehicle-treated controls, supporting this theory. That being said, the same method of plasma collection was used in UE2316-treated C57BL6/J animals and Del1 animals in the present studies, neither of which showed altered corticosterone levels. Thus even if the finding is the result of rapid corticosterone clearance and animal handling, FVB/N mice still show enhanced sensitivity and this could potentially influence tumour sensitivity to 11β-HSD1 inhibition. The same argument becomes relevant in relation to the data on liver-specific glucocorticoid levels; in FVB/N liver, changes in all three parameters after UE2316 treatment (11-DHC levels, corticosterone levels and 11-DHC:corticosterone ratio) were more pronounced than in C57BL6/J mice, suggesting an enhanced sensitivity of FVB/N mice to glucocorticoid manipulation. Importantly, these liver data also demonstrate the effectiveness of UE2316 in preventing conversion of 11-DHC to corticsterone *in vivo*. It is an unfortunate limitation of the study that levels could not be shown in tumours; very small quantities of tissue obtained from the tumour studies meant that LC-MS/MS could not achieve the sensitivity required to measure corticosterone and 11-DHC accurately. Attempts to use state-of-the-art mass spectrometry imaging methods also proved unsuccessful but have previously been effective in demonstrating the effectiveness of UE2316 in altering brain glucocorticoid levels (Cobice *et al.*, 2013; 2017). Further optimisation of these mass spectrometry methods will provide greater insight into tumour steroid intracrinology.

Although not statistically significant, 11-DHC levels appear to be decreased by UE2316 treatment in both C57BL6/J and FVB/N animals. Given the relatively small sample size in this study, it is important to appreciate the possibility of a type 2 error. If UE2316 does indeed reduce circulating 11-DHC levels, it may be indicative of an off-target effect on adrenal glucocorticoid synthesis, which may also explain the reduced corticosterone levels in FVB/N plasma. Repetition of the study with an increased sample size would be required to fully address this possibility.

In Del1 animals, corticosterone levels were not seen to differ from those in wild-type animals, while 11-DHC levels were increased around 10-fold compared to wild-type controls. These are the first reported plasma glucocorticoid levels in the Del1 mouse, with previous papers from the group having made use of an older KO mouse which exhibited some residual enzyme expression. The present corticosterone findings are in keeping with several other studies which did not see an effect on corticosterone in KO animals on a C57BL6/J background (Kotelevtsev *et al.,* 1997; Carter *et al.,* 2005; Harno and White, 2010). 11-DHC levels are less frequently reported, although Harris *et al.* (2001) do report an increase in 11-DHC in the previous 11β-HSD1 KO mouse. These findings suggest that 11β-HSD1 deletion in the Del1 mouse prevents the conversion of 11-DHC to corticosterone, resulting in accumulation of 11-DHC. While this increase in 11-DHC is apparent in the plasma, the HPA axis appears to be able to compensate for the increased clearance of corticosterone, presumably by increased release of CRH and ACTH to stimulate enhanced adrenal glucocorticoid synthesis.

A key hypothesis that the present chapter unfortunately was unable to address was that inhibiting adrenal glucocorticoid synthesis would enhance WT-SCC tumour growth, and this effect could be reversed by glucocorticoid replacement. This experiment, had it been successful, would have provided support for the inference that alterations in active glucocorticoid exposure were responsible for the enhanced growth phenotype displayed by WT-SCC tumours treated with UE2316. Insufficient inhibition of adrenal glucocorticoid synthesis is likely the main reason the experiment failed. Considerations of animal welfare necessitated a limit in the number of intraperitoneal injections that could be administered to mice. The initial plan had been to co-administer metyrapone, an 11β-hydroxylase inhibitor, in combination with aminoglutethamide, a P450 enzyme inhibitor that prevents the conversion of cholesterol to pregnenolone. This dual administration would have offered more complete inhibition and prevented the accumulation of the precursor deoxycorticosterone which can occur with metyrapone alone. Unfortunately, a common solvent in which both drugs were soluble could not be found, leading to the decision to use metyrapone alone in these studies. While metyrapone may have caused subtle alterations in circulating 11-DHC levels, these did not reach statistical significance and, critically, corticosterone levels were not reduced by metyrapone.

Compensatory activation of the HPA axis appears to have been able to overcome the effects of metyrapone treatment alone, as the only significant difference in circulating glucocorticoids detected was an increase in plasma 11-DHC in the mice given metyrapone in combination with corticosterone replacement (potentially due to inhibition of 11β-HSD1 by metyrapone). If time allowed, a repeat of this study using surgical adrenalectomy (prohibited in these experiments by the terms of the Home Office Project Licence) would provide far more useful data; the data generated here are invalidated by the methodological limitations.

Cell proliferation in tumours

Ki67 staining of tumours revealed a small (~5%) decrease in proliferating cells in UE2316-treated WT-SCC tumours that fell slightly short of statistical significance (P=0.077), likely due to lack of power. Imaging parameters (gain/digital offset) for these experiments were optimised using negative experimental controls (secondary antibody only, no primary), with levels set below the threshold of background fluorescence. Strict optimisation of imaging parameters is important given that alteration of these parameters is subject to investigator bias and could influence the statistical outcome of image analysis. Given the trend observed in the data, it is necessary to note that alternative imaging parameters may have achieved true statistical significance.

The relevance of this observation is unclear, as it was only apparent when examining proliferative hotspots and not the entire tumour section. Whilst the underpowered nature of the study limits the interpretation, this observation could suggest a decrease in the proliferation of a particular cell type in the tumour microenvironment, localised to certain regions of the tumour. Hotspots were typically found near the tumour border rather than the centre of the tumour, suggesting that infiltrating host cells (fibroblasts, immune cells, inflammatory cells) may have been more prevalent. Key future studies would involve the optimisation of co-stains for specific cell populations that could identify not only the proportion of proliferating cells, but also the type. Importantly, this effect was completely absent from the both the SCC-B6-1 and the Panc043 tumours, indicating it could be of relevance to the enhanced growth phenotype observed in WT-SCC tumours.

Immune and inflammatory signalling in tumours

RNA sequencing of WT-SCC tumours and subsequent GO analysis identified a number of prospective mechanistic pathways which may have contributed to the enhanced growth seen after 11β-HSD1 inhibition. Immune and inflammatory responses feature heavily in the GO analysis list of significantly altered biological processes. WT-SCC tumours from UE2316-treated mice showed reduced expression of a range of pro-inflammatory cytokine and chemokine genes, including members of the CCL, CXCL, CX3CL and TNF families, and CSF1. These changes were accompanied by an increase in the expression of several members of the TLR and TNFRSF families, and CSF1R, suggesting reduced pro-inflammatory ligand binding. Furthermore, expression of a number of interferon-γ (IFN-γ) inducible genes was reduced in tumours from UE2316-treated animals, including some CXCL chemokines, OAS2 and OASL2, members of the interferon inducible protein (IFI) family, lymphotoxin-alpha (LTA) and NOS2. As TLR activation can stimulate the production of IFNs, interleukins and TNF by myeloid and lymphoid cells (Chapman *et al.*, 2013a), the evidence overwhelmingly points towards reduced inflammatory and immune cell signalling within tumours from UE2316-treated mice. Unfortunately, not all of the differentially expressed genes selected for validation achieved significance when compared by qPCR. Despite this, the majority of genes tested were validated and many of the changes appear to be specific to certain pathways, thus failure to validate all of the genes does not detract from the overwhelming evidence that intra-tumour immune and inflammatory signalling is significantly disrupted by UE2316. The reduced expression of CCL and CXCL chemokines would predict reduced migration of eosinophils, neutrophils and T-cells into tumours. The reduced expression of 11β-HSD1 itself after UE2316 treatment is indicative of reduced immune/inflammatory cell infiltration and activation as the enzyme is expressed in macrophages and lymphocytes (Chapman *et al.* 2013b) and upregulated by immune cell activation, including TNF and IL1 stimulation (Hardy *et al.*, 2006; Ahasan *et al.*, 2012).

The overriding message to emerge from the RNA sequencing data is that UE2316 treatment leads to a dampening of the innate immune response in WT-SCC tumours. Determining the cell types responsible for this effect will be a focus of future work.

11β-HSD1 is expressed in the mast cells (Coutinho *et al.,* 2013) and macrophages (Thieringer *et al.,* 2001) that are responsible for the initial release of pro-inflammatory mediators during an immune response. Expression of chymase 2 (CMA2) and mast cell proteases (MCPT) 1, 2 and 4 were all increased in tumours from UE2316-treated mice, suggesting increased mast cell degranulation. Coutinho *et al.* (2013) demonstrated that 11β-HSD1 deficiency reduces the activation threshold of mast cells and increases the rate of piecemeal degranulation, a slower form of degranulation associated with chronic inflammation. The pro-inflammatory mediators released by mast cells recruit eosinophils and neutrophils to the site of inflammation, though a decrease in the expression of CXCL chemokines, Formyl Peptide Receptor 2 (FPR2), TNF and Platelet Factor 4 (PF4) all suggest reduced neutrophil recruitment. Blocking 11β-HSD1 during acute inflammation results in more severe acute inflammation after myocardial infarct (McSweeney *et al.,* 2010; White *et al.,* 2015; Mylonas *et al.,* 2017) and during pleural inflammation, arthritis and sterile peritonitis (Coutinho *et al.,* 2012). The situation examined in these tumours, however, is not likely to represent the acute inflammatory phase, as transcript data are taken from tumours that have been developing over 11 days; thus conclusions cannot be drawn regarding the acute inflammation. As inflammation progresses towards resolution, mononuclear cells become the predominant cell type (Chapman *et al.,* 2009). The failure of inflammation to resolve results in chronic inflammatory environments such as those seen in arthritis and atherosclerosis. In tumours from UE2316-treated mice, reduced expression of CCL chemokines, FPR2, CSF1, TNF, PLA2G7 and CD274 all suggest reduced macrophage infiltration and activity, and a dampened anti-tumour inflammatory response.

11β-HSD1 inhibition and anti-tumour immunosurveillance

The role of inflammation in tumour progression is controversial in that it can both promote tumour progression (via stimulation of angiogenesis for instance) but also inhibit tumour progression (via anti-tumour immunosurveillance). Manipulation of physiological glucocorticoids may well affect anti-tumour immunity; for example, in a model of colorectal cancer, generation of endogenous glucocorticoids prevented anti-tumour immunity (Sidler *et al.,* 2011) and physiological levels of corticosterone also

limit the effectiveness of immunotherapy in pancreatic cancer (Flint *et al.* 2016). Furthermore, Cirillo *et al.* (2017) recently demonstrated that glucocorticoids in conditioned media from SCC cells inhibited the proliferation of anti-tumour CD8+ T-cells via binding at the GR (this effect was abolished by the addition of GR antagonist RU486). In the present model, 11β-HSD1 inhibition appears to decrease inflammation whilst enhancing tumour growth, raising the intriguing possibility that UE2316 dampens the anti-tumour immune response. Transcriptomic data suggest a decrease in IFN-γ signalling in WT-SCC tumours from UE2316 treated mice. IFN-γ, released by NK cells and cytotoxic T-cells, is able to destroy tumour cells and prevent tumour progression as part of the ant-tumour immune response (Dighe *et al.,* 1994; Kaplan *et al.,* 1998; Shankaran *et al.,* 2001; Girardi *et al.,* 2001; Kim *et al.* 2007). Several further factors associated with anti-tumour immunity are altered in the present study. FAS has previously been shown to reduce the number of myeloid-derived suppressor cells MDSCs) in the tumour microenvironment (Sinha *et al.,* 2011). These cells express KIT (Murdoch *et al.* 2008) so reduced FAS and increased KIT ligand (Murdoch *et al.,* 2008) in tumours from UE2316-treated mice could, therefore, result in increased MDSC number and activation in the tumour microenvironment. These MDSCs are known to suppress anti-tumour function of T-cells and NK cells and thus promote tumour progression (Sica and Bronte, 2007; Murdoch *et al.,* 2008). The evidence is mixed though, as MDSCs are associated with increased ARG1 and NOS2 expression, both of which are in fact decreased in tumours from UE2316-treated mice (at least at the transcript level). The reduced expression of CXCL12 and CXCL5 in tumours from UE2316-treated mice would also be predicted to reduce MDSC infiltration. Glucocorticoids have previously been shown to increase the induction of MDSCs in mice (Varga *et al.,* 2008), thus it may follow that 11β-HSD1 inhibition would reduce their migration into tumours. TNF and LTA have both previously been considered as effective promoters of a beneficial anti-tumour immune response in melanoma (Schrama *et al.,* 2001; Drutskaya *et al.,* 2010), thus their reduced expression supports the theory of reduced anti-tumour immunity. Factors known to negatively regulate T-cell function, such as CBLB (Lutz-Nicoladoni *et al.,* 2015), are also increased in tumours from UE2316-treated mice. Reduced CSF-1 in tumours treated with UE2316 could also inhibit the differentiation of tumour suppressing dendritic cells (Menetrier-

Caux *et al.,* 1998). The complexity of immunosurveillance is increased in SCC by the interactions of the epimmunome (factors released by the epithelial tumour cells themselves rather than myeloid cells), and the fact that subtle alterations in one or two cytokines can cause a switch in the SCC inflammatory profile from a pro- to an anti-tumour environment (Huang and Balmain, 2014). Glucocorticoids are known to affect the epimmunome (Stojadinovic *et al*., 2006; Sanchis *et al*., 2012; Itoi *et al.,* 2013) and, likewise, SCC cells may produce endogenous glucocorticoids that prevent anti-tumour T-cell behaviour via a paracrine mechanism (Cirillo *et al.,* 2017). In summary, deducing the exact cellular mechanisms at work will require more in-depth study at the protein and cellular level, but this work provides substantial evidence that factors relating to anti-tumour immunity are affected by 11β-HSD1 inhibition. Deducing the mechanisms and confirming intra-tumour glucocorticoid levels will prove vital in assessing the risk posed by these inhibitors in SCC.

11β-HSD1 inhibition in chronic inflammatory conditions

The notion that 11β-HSD1 inhibition may have differential effects based on whether inflammation is acute or chronic may be pivotal to understanding the effects of UE2316 in WT-SCC tumours. Obesity is a chronic inflammatory condition, and the way in which adipose tissue from models of obesity responds to 11β-HSD1 deletion shares some similarities with the response of WT-SCC tumours to UE2316. Wamil *et al.* (2011) studied the effects of 11β-HSD1 deletion in obesity and found that a number of similar cytokines (including members of the CCL, CXCL and TNF families) were decreased in adipose tissue from high-fat diet-fed 11β-HSD1 KO mice compared to wild-type controls. Furthermore, adipose tissue from 11β-HSD1 KO animals showed decreased CD8+ T-cell infiltration and macrophage infiltration. Michailidou *et al.* (2012) built upon the aforementioned work on 11β-HSD1 deficiency in obese mice and found increased angiogenesis in adipose tissue from 11β-HSD1 KO animals. The present study identified no such change. This could be due to the highly angiogenic nature of the tumour microenvironment, which potentially masked subtle changes in angiogenic factors. RNA-sequencing did identify a subtle increase in CSPG4 expression in UE2316-treated tumours, which is known to be expressed in pericytes (Raza *et al.,* 2010). Thus it may be that more detailed examination of tumour vessel

function would identify subtle differences. Alternatively, it may be that the changes in inflammatory and immune cell content, and the altered fibrosis, exerted a powerful influence on tumour cell proliferation and survival, and angiogenesis is less relevant in this model. The lack of differences seen in vessel smooth muscle cell coverage after UE2316 treatment supports the latter theory.

Further similarities are seen in another chronic inflammatory context: atherosclerosis. 11β-HSD1 deletion reduces macrophage and T-cell infiltration into plaques (Kipari *et al.,* 2013). Several of the key gene expression changes seen in the present study have also been seen in atherosclerotic plaques after 11β-HSD1 inhibition (Luo *et al.,* 2012), including reductions in interleukins, toll-like receptors, STAT family members, and several chemokines. Interestingly, when gene expression was profiled specifically within the vascular smooth muscle cell and macrophage populations from within whole aortic samples, reduced expression of pro-inflammatory mediators was still apparent in 11β-HSD1 deficient samples (Luo *et al.,* 2012). This finding could perhaps imply that, as well as reduced inflammatory cell infiltration into tumours, these inflammatory cells may also be less active in the production of pro-inflammatory mediators.

CXCL chemokines are induced by IFN-γ and TNF signalling which corresponds with the reduced TNF expression identified by RNA-seq (disappointingly qPCR did not validate TNF). CXCL signalling, as well as playing a role in tumour progression, has also been linked to atherosclerosis in which it does not promote neutrophil infiltration (as in acute inflammation) but rather exerts a beneficial effect by preventing macrophage foam cell accumulation in plaques (Rouselle *et al.,* 2013). 11β-HSD1 inhibition similarly prevents foam cell formation *in vivo* (Garcia *et al.,* 2013). Several 11β-HSD1 inhibitors, and genetic deletion of the enzyme, improve atherosclerosis by reducing plaque formation (reviewed in Hadoke *et al.,* 2013). Garcia *et al.* (2013) examined gene expression in peritoneal macrophages from 11β-HSD1 KO mice and noted attenuation of the inflammatory state compared to wild-type macrophages, including reduced chemokine signalling. Release of TNF from 11β-HSD1 KO macrophages was reduced by 30% compared to control macrophages. Importantly, bone marrow transplantation studies demonstrated that it was the 11β-HSD1

deficiency in myeloid cells that was important in reducing plaque formation (Garcia *et al.,* 2013; Kipari *et al.,* 2013). This suggests that inflammatory cells may also be responsible for reduced TNF expression in tumours, and thus important in tumour progression. TLR expression was decreased in the study by Garcia *et al.* (2013), whereas in the present study, expression was increased and accompanied by a decrease in ACOD1 (a negative regulator of TLR expression). It is interesting to note the involvement of the TLRs in both studies, despite their opposing expression in the different models.

Many of the observed effects of 11β-HSD1 inhibition (for example reduced interleukin, IFN, and TNF expression) mimic the reported anti-inflammatory and immunosuppressive effects of glucocorticoids (Sapolsky *et al.,* 2000; Coutinho and Chapman, 2011), which occur as a result of binding at the GR (Cronstein *et al.,* 1992; Cirillo *et al.,* 2017). As 11β-HSD1 inhibition ought to reduce local glucocorticoid levels, this may seem counterintuitive. Yet there are several examples of physiologically relevant concentrations of glucocorticoids promoting, rather than reducing, inflammation. Barber *et al.* (1993) report that pre-treatment with glucocorticoids increased TNF-α and IL-6 release into the plasma of mice treated with lipopolysaccharide (LPS). Furthermore, low concentrations of corticosterone (500-1000nM) enhanced T-cell growth *in vitro* (Weigers *et al.* 1993; 1994; 1995) and *in vivo* (Wiegers *et al.* 1993). This effect is thought to be mediated via activation of the MR in immune and inflammatory cells (Wiegers *et al.,* 1993; Sapolsky *et al.* 2000) and the same mechanism has been proposed for anti-inflammatory effects of 11β-HSD1 inhibition in atherosclerotic plaques (Luo *et al.,* 2012). MR and GR are both expressed in macrophages (Barish *et al.,* 2005; Lim *et al.,* 2007), while only the 11β-HSD1 (and not the 11β-HSD2) isozyme is expressed (Gilmour *et al.,* 2006; Usher *et al.,* 2010; Chapman *et al.,* 2013a). Thus corticosterone binding at either receptor could be relevant to the effect seen in the present studies. MR antagonism also reduces pro-inflammatory cytokine levels (including TNF) in obese adipose tissue (Guo *et al.,* 2008) and polarises macrophages towards an M2 phenotype whilst reducing fibrosis in models of cardiac hypertrophy and stroke (Usher *et al.,* 2010; Frieler *et al.,* 2011). While this evidence could explain why 11β-HSD1 inhibition exerts anti-inflammatory effects, MR was undetectable in WT-SCC tumours. Furthermore, Lim *et al.* (2007)

found that while low concentrations of corticosterone (100 pM) enhanced pro-inflammatory cytokine production by macrophages, high concentrations (1µM) were potently anti-inflammatory (similar results were seen by Itoi *et al.* (2013) after exposing keratinocytes to glucocorticoids). Only deletion of GR abrogated the pro-inflammatory response of macrophages to glucocorticoids, while MR deletion had little effect (Lim *et al.*, 2007). GR blockade also prevented the anti-proliferative effect of tumour-derived glucocorticoids on T-cell proliferation in the study by Cirillo *et al.* (2017). Thus, GR likely remains the more important receptor in the solid tumour model. Studies using selective MR and GR inhibitors will be required to more comprehensively address this question.

CD3 staining in the present study did not detect a difference between WT-SCC tumours from control and UE2316-treated mice However, CD3 is a general T cell marker and fluorescence associated cell sorting (FACS) is required to determine more subtle alterations in specific T-cell populations. The perinuclear localisation of CD3 in many of the WT-SCC tumour cells may even suggest immature thymocytes (Swerdlow *et al.*, 1988) in which CD3 has not yet been translocated to the cell surface; an avenue for future investigation. Likewise, F4/80 staining did not reveal a marked difference between treatment groups in our study, yet key markers of macrophage polarisation were altered (see below), suggesting a more subtle effect of 11β-HSD1 inhibition on tumour inflammation, possibly on macrophage polarisation states. Accelerated switching of macrophages from an M1 to an M2 phenotype in 11β-HSD1 deficient tissues is reported in the acute inflammatory context of myocardial infarction (McSweeney *et al.*, 2010) but was not seen *in vitro* (Gilmour *et al.*, 2006; Zhang *et al.*, 2007) or in adipose tissue *in vivo* (Wamil *et al.*, 2006). Determining the polarisation state of macrophages from the RNA sequencing data is difficult due to conflicting expression of transcripts. UE2316 appears to have reduced IFN-γ signalling and TLR activation in WT-SCC tumours, and this would be predicted to polarise macrophages towards an M2 phenotype. Comparing the present RNA-seq data with previously published data on macrophage polarisation gene profiles (Martinez *et al.*, 2006), a number of changes did suggest M2 polarisation (decreased expression of NOS2, CXCL9, OASL2, HSD11B1, FAS, TNF, CXCL11, and CCL11), yet several contradictory findings were also apparent (decreased expression of ARG1, platelet-

derived growth factor A (PDGF-A), macrophage scavenger receptor 1 (MSR1), LTA, CCL17 and CCL24). As transcripts from whole tumours were analysed, altered expression could reflect alternative cell populations infiltrating tumours, as opposed to change in polarisation state. A good case in point is the reduced 11β-HSD1 expression seen in WT-SCC tumours after UE2316 treatment; M1 polarised macrophages increase their 11β-HSD1 expression while expression is unaffected by M2 polarisation (Chapman *et al.,* 2013a), so this finding may indicate increased M2 polarisation. However, this reduced expression may also reflect a reduced number of macrophages, dendritic cells, neutrophils, mast cells or activated T-cells in these tumours, as all of these cell types express 11β-HSD1 (Freeman *et al.,* 2005; Zhang *et al.,* 2005; Chapman *et al.,* 2013a; Coutinho *et al.,* 2016). Isolation of tumour-associated macrophages by FACS and subsequent analysis is required if a more firm conclusion is to be reached.

11β-HSD1 deficiency has also been studied in several non-cardiometabolic chronic inflammatory conditions, including peritonitis and arthritis. 11β-HSD1 deficient mice showed delayed clearance of apoptotic neutrophils (Gilmour *et al.,* 2006), earlier onset and delayed resolution of inflammation in models of arthritis and sterile peritonitis (Coutinho *et al.* 2012). These effects are thought to be at least partially due to 11β-HSD1 deletion in macrophages (Zhang *et al.,* 2012), which promotes angiogenesis and contributes to pathology in arthritis (Jackson *et al.,* 1997). By contrast, the selective 11β-HSD1 inhibitor BVT-2733 improved symptoms of collagen-induced arthritis by reducing the expression of pro-inflammatory cytokines, including TNF, IL-1β and IL6, and reducing inflammatory cell infiltration into joints (Zhang *et al.,* 2013). The beneficial effects of 11β-HSD1 inhibition in the synovium have been linked to reduced glucocorticoid action in synovial fibroblasts and osteoclasts (Hardy *et al.,* 2012; 2013) resulting in a net reduction in damaging inflammation (Hardy *et al.,* 2013). Thus there is a fascinating degree of crossover between these chronic inflammatory conditions and the findings in the solid tumour model; 11β-HSD1 in immune and inflammatory cells, and often fibroblasts, appears to be central to all of these models.

<u>11β-HSD1 inhibition, fibroblasts and the extracellular matrix</u>

Thus far the present findings in solid tumours exhibit many similarities to chronic inflammatory cardiometabolic disorders; namely obesity and atherosclerosis. Mechanistically, fewer similarities are apparent between solid tumours and the acute inflammatory setting of the infarcted myocardium. That said, similar pathways do appear to be affected although apparently in the opposite direction depending on setting. Mylonas *et al.* (2017) recently showed that deletion of 11β-HSD1 from a subset of cardiac fibroblasts enriched for the enzyme results in the increased release of CXCL2 and 5, which subsequently recruit more neutrophils to the infarct and promote recovery. CXCL5 is reduced in WT-SCC tumours in which 11β-HSD1 has been inhibited. This discussion has thus far focussed on the role of immune and inflammatory cells in promoting tumour growth, yet cancer-associated fibroblasts (CAFs) and extracellular matrix (ECM) deposition can also heavily influence tumour progression.

Mice in the present studies were given UE2316 for 5 days before tumour cells were injected, thus 11β-HSD1 inhibition and its associated effects on inflammation will have been present from the onset of tumour formation. Previously, depletion of macrophages before the point of injury has been shown to ameliorate fibrosis (Duffield *et al.*, 2005). Duffield *et al.* (2005) used a model of liver injury to show that during the initial stages of inflammation, M2 macrophages dominate and maintain a resident population of myofibroblasts (which are mechanistically very similar to activated CAFs), which promote fibrosis. With decreasing levels of pro-inflammatory mediators (the recovery phase of inflammation), a subset of ECM-degrading macrophages becomes predominant (M1 phenotype). In the UE2316-treatment group in the WT-SCC model, and in previous studies of 11β-HSD1-deficient adipose tissue (Michailidou *et al.*, 2012), fibrosis and pro-inflammatory signalling are reduced; findings somewhat at odds with the expected effects of 11β-HSD1 inhibition on fibrosis. Yet in SCC-B6-1 tumours, the opposite effect was seen; UE2316 promoted fibrosis compared to tumours from control mice. Thus, this conclusion cannot be applied universally to the solid tumour microenvironment and likely depends on tumour type. Differences in the response of Class A and B SCC tumours to inflammation are well documented (Wong *et al.*, 2013; Huang and Balmain, 2014), so it is perhaps not surprising that UE2316 exerts alternative effects in WT-SCC and

SCC-B6-1. Focus will remain on the WT-SCC tumours due to their altered growth phenotype.

The reduced fibrosis seen in WT-SCC tumours was also found in obese adipose tissue from 11β-HSD1 KO animals, which showed decreased fibrosis and alpha-smooth muscle actin expression, suggesting reduced fibroblast numbers. In WT-SCC tumours, Type I collagen, detected using SHG imaging, was significantly reduced. This result is consistent with the reduced Col1a1 and Col1a2 expression and the increased matrix metalloprotease 11 expression reported in UE2316-treated tumours. Likewise, alpha-smooth muscle actin was identified by RNA-seq as having reduced expression in tumours from UE2316-treated mice; though this finding could not be validated, making it difficult to conclude whether this reflects reduced fibroblast content.

Although direct quantification of fibroblasts in WT-SCC was not performed in the present study, several factors suggest that CAF activation and possibly number is reduced by UE2316-treatment. Reduced fibrosis and reduced expression of COL1A1, COL1A2, COL14A1, stromal-cell derived factor 1 (SDF-1) and LOX are all suggestive of reduced fibroblast activity (Harper and Sainson. 2013; Fang *et al.*, 2014). The possible reduced alpha-SMA (expressed by activated CAFs: Özdemir *et al*., 2014) in UE2316-treated tumours would also suggest reduced fibroblast number. CAFs can promote anti-tumour immune cell infiltration into tumours (Harper and Sainson, 2014; Özdemir *et al.* 2014), providing a link between the potentially dampened anti-tumour immune response seen in WT-SCC tumours treated with UE2316 and the reduced fibrosis observed. Inflammatory cells are also able to recruit fibroblasts into SCC tumours (Coussens *et al.,* 1999) and this enhanced recruitment can promote SCC growth suppression via the deposition of a fibrotic ECM that constrains tumour cell proliferation and invasiveness (Willhauck *et al.,* 2006; Cretu and Brooks, 2007). Collagen itself is able to interact with the immune and inflammatory cells of the tumour microenvironment (Fang *et al.,* 2014), and reducing collagen has been shown to predict poor prognosis in SCC (Baba *et al.,* 2008). Whilst this is in keeping with observations from the present study, the decrease in fibrosis is unexpected given previous studies of 11β-HSD1 inhibition showing enhanced fibroblast proliferation and fibrosis in skin (Tiganesu *et al.,* 2013; Terao *et al.,* 2014) and given the inhibitory

effects of glucocorticoids on collagen deposition (Maragoudakis et al., 1989; Morgan *et al.,* 2014). The tumour microenvironment is of course a very different situation from healthy skin and enhanced fibrosis was seen in obese adipose tissue (Michailidou *et al.,* 2012), arguably a more similar chronic inflammatory environment. It is possible that 11β-HSD1 inhibition dampens the inflammatory response, leading to reduced activation and migration of pro-inflammatory CAFs (Erez *et al.,* 2010) into the tumour which further dampens the anti-tumour immune response and leads to an underdeveloped ECM conducive to tumour growth. Disappointingly, attempts to quantify fibroblasts in this study were unsuccessful due to the expression of vimentin in SCC cells (Klein-Szanto *et al.,* 1989; Huang and Balmain, 2014).

In summary, inhibition of 11β-HSD1 in WT-SCC tumours dampens immune and inflammatory signalling within the tumour microenvironment, likely leading to the reduced activation of CAFs and the reduced deposition of type I collagen. These factors, in combination, promote WT-SCC growth. The effects of physiological glucocorticoid manipulation may relate to pro-inflammatory effects of MR, as well as GR, activation in inflammatory and immune cells. Future studies must focus on more detailed dissection of the tumour immune and inflammatory microenvironment using FACs, more detailed IHC studies to determine the exact cell types involved, and the use of selective receptor inhibitors to determine the relevant pathways.

Chapter 6

Conclusions and future work

6 Conclusions and future work

6.1 Aims revisited

The work presented in this thesis addressed the hypothesis that 11β-HSD1 inhibition promotes tumour angiogenesis and, consequently, enhances solid tumour growth. The need for this research arose from concerns surrounding the pro-angiogenic effects of reduced 11β-HSD1 activity, which are apparent in models of myocardial infarction (Small *et al.,* 2005; McSweeney *et al.,* 2010; McGregor *et al.,* 2014; White *et al.,* 2015; Mylonas *et al.,* 2017), obesity (Michailidou *et al.,* 2012), inflammatory arthritis (Zhang *et al.,* 2017) and tumour growth (Liu *et al.,* 2016). Increased tumour growth via enhanced angiogenesis would present a significant adverse effect of clinical 11β-HSD1 inhibitors, which were originally designed to treat type II diabetes (Anderson and Walker, 2013) and have also shown promise in the treatment of Alzheimer's disease (Webster *et al.,* 2017). Given the findings of the present experiments, it is important to draw conclusions in relation to the primary research aims.

The first research aim was to determine whether pharmacological inhibition or genetic ablation of 11β-HSD1 would promote tumour growth and angiogenesis in murine models of squamous cell carcinoma (SCC) and pancreatic ductal adenocarcinoma (PDAC). It was shown that only one of the tested SCC cell lines (WT-SCC) produced tumours that grew more quickly in response to 11β-HSD1 inhibition, while the other two cell lines examined (SCC-B6-1 and Panc043) grew normally, both in wild-type mice fed an 11β-HSD1 inhibitor and in Del1 mice genetically deficient for the enzyme. Unexpectedly, no evidence of increased angiogenesis in any tumour type was seen, strongly suggesting that an alternative mechanism was responsible for increased SCC growth. The second research aim was to determine the effects of pharmacological 11β-HSD1 inhibition and exogenous glucocorticoids on *ex vivo* angiogenesis, and *in vitro* tumour cell growth. As has been seen previously (Small *et al.,* 2005), active glucocorticoids were potently anti-angiogenic *ex vivo.* In the present experiments, only genetic deletion, not inhibition, of 11β-HSD1 was able to prevent this angiostasis. As neither glucocorticoids nor the 11β-HSD1 inhibitor UE2316 drastically affected tumour cell growth, attention was turned to other components of the tumour

microenvironment. The third and final research aim was to determine the effects of 11β-HSD1 inhibition on the tumour microenvironment and to investigate mechanisms by which glucocorticoid manipulation might influence tumour growth. Inhibition of 11β-HSD1 led to reduced expression of a range of pro-inflammatory cytokines and chemokines in WT-SCC tumours, suggesting a significant dampening of immune and inflammatory signalling in these tumours. Type I collagen deposition in WT-SCC tumours was also reduced by 11β-HSD1 inhibition; determining the degree to which altered immune signalling and collagen deposition are linked may provide an important mechanistic insight into the enhanced tumour growth.

6.1.1 11β-HSD1 inhibition can promote squamous cell carcinoma growth

One of the most important conclusions to be drawn from this work is that 11β-HSD1 inhibitors can promote growth in some types of murine SCC. The finding that SCC in particular is sensitive to 11β-HSD1 inhibition is not entirely surprising, given the atypical expression of the 11β-HSDs in this cancer type. Upon progression to malignancy, healthy tissues typically show decreased 11β-HSD1 expression and increased 11β-HSD2 expression, a pathological 'switch' thought to promote tumour growth (Rabbitt *et al.,* 2003b). This switch is absent in SCC, with many studies (including the present) detecting only the type 1 isozyme in SCC samples (Gronau *et al.,* 2002; Terao *et al.,* 2013), though low levels of 11β-HSD2 expression have been reported (Cirillo *et al.,* 2017). This unusual 11β-HSD expression profile, combined with the known importance of 11β-HSD1 in skin homeostasis (Cirillo and Prime, 2011), has led to an increased focus being placed on local glucocorticoid metabolism in SCC (reviewed by Azher *et al.,* 2016).

Incidences of skin cancer are increasing; healthcare data from the United States suggest that cases of non-melanoma skin cancers (including SCC) have doubled between 1994 and 2006 (Donaldson and Coldiron, 2011). Non-melanoma skin cancers are the most common cancer in the world, accounting for 80% of all skin cancers, with incidences outweighing all other cancers combined (Garcovich *et al.,* 2017). SCC specifically is a disease of advanced age, with a mean age of 70 years at diagnosis and more than 80% of cases occurring in the elderly. Over the past three decades, incidence

of SCC in the elderly has increased dramatically due to cumulative ultraviolet-exposure and an aging population (Leiter *et al.,* 2014). Given the promise that 11β-HSD1 inhibitors have shown in treating diseases of the elderly, such as type II diabetes (Anderson and Walker, 2013) and more recently Alzheimer's disease (Sooy *et al.,* 2010; 2015; Yau *et al.,* 2015; Webster *et al.,* 2017), the prospect that they could promote SCC growth is concerning. A further concern is the evidence identifying chronic wounds (which are associated with type II diabetes) as a risk factor for SCC (Belbasis *et al.,* 2016), though to date there is little evidence suggesting a direct association between diabetes and SCC. 11β-HSD1 activity is also increased in the skin of older individuals, potentially further increasing their sensitivity to 11β-HSD1 inhibitors (Tiganescu *et al.,* 2013). Thus, diligence is advisable when proceeding with clinical trials, with long-term monitoring of patients for SCC recommended.

Further research to determine the mechanism responsible for enhanced SCC growth after 11β-HSD1 inhibition will hopefully provide answers to several key questions.

<u>How much of a threat do 11β-HSD1 inhibitors pose in promoting human SCC?</u>

The present experiments found increased tumour growth using a murine model of SCC, implanting cultured murine WT-SCC cells into female FVB/N mice. Female mice were used to allow for group housing as FVB/N males are prone to fighting when group housed (Thiele *et al.,* 2014). The influence of the oestrus cycle was not examined in these studies, though previous studies in mice suggest that corticosterone levels are not drastically affected (Malisch *et al.,* 2008; Gong *et al.,* 2015). A murine cell line was selected for use in conjunction with an immunocompetent mouse strain to allow investigation surrounding the influence of the immune system on tumour growth. This is a significant strength in that it provides *in vivo* conditions more comparable to the clinical situation in which patients are unlikely to be immunodeficient. Yet the effects of 11β-HSD1 inhibition were only seen in one of the two SCC lines examined; SCC-B6-1 cells did not respond to inhibition or deletion of 11β-HSD1 in C57BL6/J mice. This could be due to the different characteristics of the tumour type, but could also be due to strain-specific differences; plasma and liver glucocorticoid levels in FVB/N mice appeared to show increased sensitivity to 11β-HSD1 inhibition compared to C57BL6/J mice. The reduction in circulating

corticosterone seen in UE2316-diet-fed FVB/N mice may suggest that these mice also had an increased net reduction in intratumour corticosterone levels compared to tumours grown in C57BL6/J mice, and this could explain the growth-enhancing effect of UE2316 on WT-SCC tumours that was not seen in SCC-B6-1 or Panc043 tumours. Until the influence of strain has been fully examined, it is difficult to draw firm conclusions regarding the degree of clinical risk. Genetic variation in glucocorticoid sensitivity is known to exist in humans, due in part to polymorphisms in the *HSD11B1* and *GR* genes (Edwards *et al.*, 1988; Stewart *et al.*, 1988; reviewed extensively by Quax *et al.*, 2013). Older females are a group particularly associated with both increased glucocorticoid sensitivity (Heuser *et al.*, 1994) and Alzheimer's disease (Viña and Lloret, 2010), emphasising the need for particular vigilance when monitoring this prospective patient group.

If it is the features of the tumour type that determine SCC sensitivity to 11β-HSD1, then this has important implications. 11β-HSD1 inhibition only promoted the growth of WT-SCC tumours, a tumour type displaying features characteristic of a 'Class B' SCC, including spindle-cell morphology, increased invasiveness and aggressive growth (Wong *et al.*, 2013; Huang and Balmain, 2014). These tumours arise via an alternative pathway to classical 'Class A' SCCs, and are known to depend less on an inflammatory stimulus for their formation (Wong *et al.*, 2013). If indeed Class B SCC is more sensitive to 11β-HSD1 inhibition, then measuring the impact of 11β-HSD1 inhibition on number of metastases will be important (Wong *et al.* (2013) described a method for achieving this), as these tumours grow aggressively. Metastatic SCC has a 10-year survival rate of less than 20% and metastasis vastly worsens prognosis.

The question of whether host or donor 11β-HSD1 is more important in the tumour microenvironment remains unresolved. UE2316 will have inhibited 11β-HSD1 activity in both host cells and donor tumour cells, while experiments in the Del1 mice will only have inhibited host 11β-HSD1. Given that 11β-HSD1 mRNA was detected in Del1-grown SCC-B6-1 tumours, the induction of 11β-HSD1 expression after injection of tumour cells cannot be ruled out. To address this problem, future studies must focus on generating SCC lines similar to WT-SCC (and responsive to UE2316) but syngeneic on a C57BL6/J background. This is difficult to achieve given the

increased sensitivity of the FVB/N strain to skin carcinogenesis (Hennings *et al.*, 1993). Additionally, the investigation of both classes of SCC in the FVB/N model would provide further insight into tumour-specific differences in sensitivity to 11β-HSD1 inhibition. Ideally, the generation of an 11β-HSD1-deficient FVB/N line would allow comparison of acute inhibition and chronic deletion of 11β-HSD1. Developing such a model may pose less of a challenge given the advent of CRISPR/Cas9 gene-editing technology.

Are other tumour types at risk from 11β-HSD1 inhibition?

Growth of PDAC tumours (Panc043) was unaffected by 11β-HSD1 deletion and inhibition, demonstrating that these inhibitors do not pose a universal risk to tumour growth. While it is unfeasible to consider examining every tumour type, it is important to use the present findings to anticipate which other tumour types may be sensitive to 11β-HSD1 inhibition. Glucocorticoid therapy has shown some benefit in prostate (Yano *et al.*, 2006; Sahu *et al.*, 2013) and breast cancer (Karmakar *et al.*, 2013; Lin and Wang, 2016). Colorectal cancer also shows an unusual system of local glucocorticoid regulation (Sidler *et al.*, 2011; Cirillo *et al.*, 2017), including increased 11β-HSD1 expression compared to healthy tissue (Žbánková *et al.*, 2004). These three cancers are candidate tumour types for future investigations. Azher *et al.* (2016) recently compiled a list of cancers exhibiting dysregulated glucocorticoid signalling, and found that small lung cell carcinoma commonly displays reduced glucocorticoid receptor (GR) expression or function. Given that the tumour responsive to 11β-HSD1 inhibition in the present work displayed more GR than non-responsive tumour types, this may suggest that cancers expressing lower GR are less at risk. Blocking GR with RU486 or using cell-specific knockdown of GR in mice implanted with WT-SCC cells will be important for determining the importance of GR in regulating WT-SCC tumour growth.

6.1.2 The anti-inflammatory effects of 11β-HSD1 inhibition in some solid tumours may promote their growth

The original hypothesis for this thesis was that 11β-HSD1 inhibition would enhance angiogenesis and this would promote increased tumour growth. Yet, no evidence for

increased angiogenesis in tumours was found. Instead, RNA-sequencing data suggested that administration of UE2316 had reduced inflammatory and immune signalling in WT-SCC tumours. Second harmonic generation (SHG) imaging also demonstrated a significant reduction in type I collagen deposition in WT-SCC tumours from mice treated with UE2316. Although the present experiments have not established a causal relationship between these findings and the increased growth seen in UE2316-treated tumours, Gene Ontology (GO) analysis highlighted the relevance of these processes (7 of the top 10 significantly associated biological processes were related to immune and inflammatory cell signalling) – it appears that some of the most profound effects of 11β-HSD1 inhibition in SCC involve altered immune and inflammatory signalling. In light of the complex interplay between the immune and inflammatory cells, fibroblasts, and the extracellular matrix (ECM) of the tumour microenvironment, it is likely that the reduced immune and inflammatory signalling and altered ECM seen in tumours after UE2316 treatment are related. Indeed, determining the specific effects of 11β-HSD1 inhibition on the interaction between these components of the tumour microenvironment will be the first key step in identifying the mechanism of increased growth.

Three firm conclusions can be drawn thus far. These are that WT-SCC tumours from mice treated with UE2316 show: reduced expression of pro-inflammatory cytokines and chemokines; reduced type I collagen deposition, and; increased growth. As discussed in chapter 5, many of the observations in the solid tumour model are similar to those seen after 11β-HSD1 inhibition or deletion in models of obesity (Wamil *et al.,* 2011; Michailidou *et al.,* 2012), atherosclerosis (Luo *et al.,* 2012; Garcia *et al.,* 2013; Kiparie *et al.,* 2013) and arthritis (Zhang *et al.,* 2013). These chronically hypoxic and non-resolving pathological inflammatory situations are similar in many respects to the tumour microenvironment. It is very interesting to note that macrophages, T-cells and fibroblasts are all involved to some extent in each of these models. Other cell types do have an important role to play in these models (adipocytes in obesity for example, or osteocytes in arthritis). However, interaction with mesenchymal, lymphoid and myeloid cells is mechanistically integral to the effects of 11β-HSD1 deficiency in each situation. Even in models in which 11β-HSD1 deficiency promotes inflammation, the same applies; 11β-HSD1 inhibition (and thus reduced glucocorticoid binding at the

GR) in cardiac fibroblasts is thought to increase their expression of pro-inflammatory cytokines, promoting neutrophil recruitment, and subsequently improving recovery after myocardial infarction (Mylonas *et al.*, 2017). Likewise, Zhang *et al.* (2017) recently demonstrated that 11β-HSD1 deficiency in macrophages specifically promotes inflammatory angiogenesis. Thus, it appears increasingly important to examine the role of 11β-HSD1 in these cell types if the full potential of 11β-HSD1 inhibitors is to be realised, particularly in chronic inflammatory situations where inhibitors may be anti-inflammatory or immunosuppressive.

Sapolsky *et al.* (2000) offer an interesting interpretation of the opposing effects glucocorticoids can exert upon inflammation and immunity. They propose that the immunosuppressive and anti-inflammatory effects caused by high 'stressed' glucocorticoid concentrations (or exploited clinically) are acting to constrain an anticipated inflammatory response (such as that seen during acute myocardial infarction), while basal levels of glucocorticoids may act permissively to promote inflammation at lower concentrations (Barber *et al.*, 1993, Weigers *et al.*, 1993; 1994; 1995; Lim *et al.*, 2007). Thus, in a chronic inflammatory situation, it can perhaps be argued that low level endogenous glucocorticoid production is permissive in allowing the low-level inflammation characteristic of tumours, atheroma, obesity or arthritis. Inhibiting the generation of these permissive glucocorticoids thus exerts anti-inflammatory effects.

<u>By what mechanism does 11β-HSD1 inhibition promote tumour growth?</u>

The present work has not fully answered the question of mechanism, but has provided sufficient evidence to allow for the generation of a hypothesis. A proposed mechanism of enhanced growth in SCC is outlined in Figure 6.1. 11β-HSD1 inhibition in macrophages and fibroblasts dampens inflammatory signalling via reduced glucocorticoid binding at the GR, reducing reciprocal stimulation between these cell populations and decreasing the recruitment of anti-tumour cytotoxic T-cells and other tumour-suppressing cell types (natural killer cells, for example) (Coussens *et al.*, 1999; Schrama *et al.*, 2001; Drutskaya *et al.*, 2010; Harper and Sainson, 2014; Özdemir *et al.* 2014). Furthermore, the reduced activation and/or recruitment of fibroblasts leads to impaired ECM deposition and thus removes the tumour-constraining influence of

the fibrotic scaffold (Willhauck *et al.,* 2006; Cretu and Brooks, 2007). The reduced anti-tumour immunity and growth-restraining ECM deposition combine to promote rapid SCC growth. This model is overly simplistic in that it presents tumour cells as passive players, whereas in reality they are likely to be active participants in the inflammatory process. Given that pro-inflammatory cytokines can induce 11β-HSD1 in cells (Chapman *et al.,* 2013b), and 11β-HSD1 expression was seen in SCC-B6-1 tumours implanted into Del1 mice, a possible role for tumour cell 11β-HSD1 cannot be excluded. A recent paper by Cirillo *et al.* (2017) concluded by postulating that cortisol generated by 11β-HSD1 in malignant keratinocytes could lead to tumour suppression via alterations to the fibroblast secretome, a hypothesis not dissimilar to that described here. Given the evidence available, this model seems a sensible starting point for further investigation.

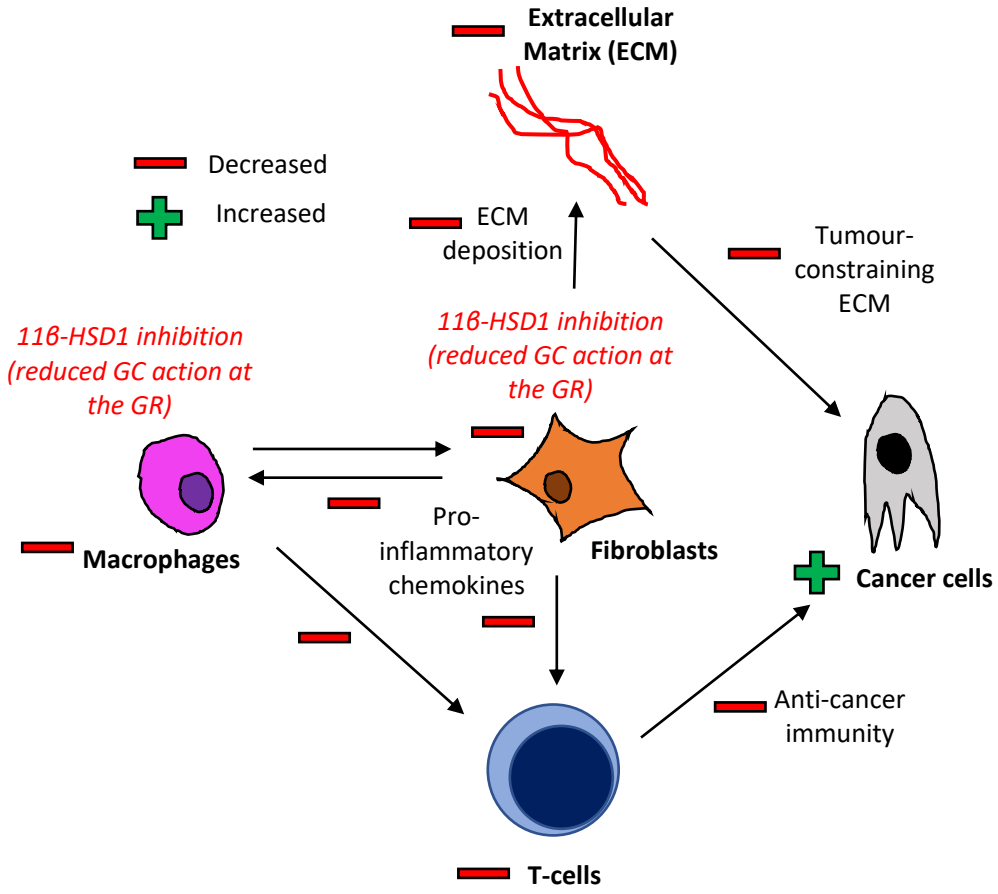

Figure 6.1 – Proposed mechanism of enhanced SCC tumour growth. 11β-HSD1 inhibition in macrophages and cancer-associated fibroblasts leads to reduced glucocorticoid (GC) binding at the glucocorticoid receptor (GR), resulting in reduced reciprocal pro-inflammatory signalling, and consequently leading to reduced anti-tumour T-cell recruitment to the tumour microenvironment. Reduced fibroblast recruitment/activation also reduces the deposition of tumour-constraining extracellular matrix (ECM) deposition. These factors combine to promote rapid squamous cell carcinoma (SCC) growth.

Questions for the future

The proposed mechanism presents several questions which must form the basis of future work.

- Does 11β-HSD1 inhibition lead to reduced inflammatory and immune cell and fibroblast recruitment to the tumour microenvironment?

Although RNA-sequencing and SHG data strongly suggest this may be the case, only by performing Fluorescence Associated Cell Sorting (FACS) and immunohistochemical staining can the true effects of 11β-HSD1 inhibition on the microenvironment be ascertained.

- Which cells in the tumour express 11β-HSD1?

Previous evidence points towards expression of 11β-HSD1 in macrophages, fibroblasts and vascular cell types. However, it will be important to determine whether tumour cells themselves also begin to express the enzyme once implanted into mice (possibly as a result of inflammatory cytokine exposure). This will require more elegant immunohistochemical techniques. Another approach may be to label 11β-HSD1 with green fluorescent protein (GFP) and sort cells on the basis of GFP expression. Exposing cultured WT-SCC tumour cells to inflammatory cytokines and measuring 11β-HSD1 expression will also help to address this question.

- Are tissue glucocorticoid levels altered by UE2316?

An unfortunate limitation of the present experiments was failure to demonstrate tumour-specific glucocorticoid concentrations in animals given the 11β-HSD1 inhibitor UE2316. The optimisation of mass spectrometry imaging techniques such as MALDI (Cobice *et al.*, 2013; 2017) are the best approach to this problem. Determining the distribution of steroid throughout tumours will also provide insight into the cell types in which enzyme inhibition is most important.

6.2 Concluding remarks

The work presented in this thesis has added to the rich literature already surrounding 11β-HSD1. In the three decades since its discovery, this enzyme has been shown to play a part in many of the most serious diseases that scientists are striving to understand. The promise of 11β-HSD1 inhibitors has already been shown in clinical trials for type II diabetes and Alzheimer's disease, but preclinical data suggests that they have much more to offer in terms of treating chronic inflammatory conditions. Yet, as with any new therapy, caution must always be exercised. The importance of this message is highlighted by the discoveries made in SCC. The process of demonstrating that 11β-HSD1 inhibitors can promote SCC tumour growth has been an interesting one; the discovery that the original pro-angiogenic hypothesis needed to be rejected, but that an entirely separate mechanism was still able to promote tumour growth, is a perfect example of how science can sometimes both frustrate and fascinate in equal measure.

The effects of 11β-HSD1 inhibition in SCC add to the mounting evidence that reducing local glucocorticoid regeneration can have profoundly different effects depending on the inflammatory context. Inhibition of 11β-HSD1 in chronic inflammatory situations seems to reduce this inflammation. While this may be possible to exploit for clinical benefit, it is vital to remain vigilant of the threat of increased tumour growth moving forward.

References

Abel, E. L., Angel, J. M., Kiguchi, K. and DiGiovanni, J. (2009), 'Multi-stage chemical carcinogenesis in mouse skin: Fundamentals and applications', *Nature Protocols*, 4(9), pp. 1350-1362. doi: 10.1038/nprot.2009.120.

Abramsson, A., Lindblom, P. and Betsholtz, C. (2003) 'Endothelial and nonendothelial sources of PDGF-B regulate pericyte recruitment and influence vascular pattern formation in tumors', *Journal of Clinical Investigation*, 112(8), pp. 1142–1151. doi: 10.1172/JCI18549.

Alberts, P., Engblom, L., Edling, N., Forggren, M., Klingström, G., Larrson, C., Rönquist-Nii, Y., Ohman, B. and Abrahmsén, L. (2002) 'Selective inhibition of 11β-hydroxysteroid dehydrogenase type 1 decreases blood glucose concentrations in hyperglycaemic mice', *Diabetologia*. 45(11), pp. 1528–1532. doi: 10.1007/s00125-002-0959-6.

Adams, R. H. and Alitalo, K. (2007) 'Molecular regulation of angiogenesis and lymphangiogenesis', *Nature Reviews Molecular Cell Biology*, 8(6), pp. 464–478. doi: 10.1038/nrm2183.

Adler, G. K. and Williams, G. H. (2007) 'Aldosterone: villain or protector?', *Hypertension*, 50(1), pp. 31-2.

Ahasan, M. M., Hardy, R., Jones, C., Kaur, K., Nanus, D., Juarez, M., Morgan, S. A., Hassan-Smith, Z., Bénézech, C., Caamaño, J. H., Hewison, M., Lavery, G., Rabbitt, E. H., Clark, A. R., Filer, A., Buckley, C. D., Raza, K., Stewart, P. M. and Cooper, M. S. (2012) 'Inflammatory regulation of glucocorticoid metabolism in mesenchymal stromal cells.', *Arthritis and Rheumatism*, 64(7), pp. 2404–13. doi: 10.1002/art.34414.

Alam, M. & Désirée, R. (2001), 'Cutaneous Squamous-Cell Carcinoma', *New England Journal of Medicine*, 344, pp. 975-983. doi: 10.1056/NEJM200103293441306

Alberts, P., Nilsson, C., Selen, G., Engblom, L. O. M., Edling, N. H. M., Norling, S., Klingström, G., Larsson, C., Forsgren, M., Ashkzari, M., Nilsson, C. E., Fiedler, M., Bergqvist, E., Ohman, B., Björkstrand, E. and Abrahmsen, L. B. (2003) 'Selective Inhibition of 11β-Hydroxysteroid Dehydrogenase Type 1 Improves Hepatic Insulin Sensitivity in Hyperglycemic Mice Strains', *Endocrinology*, 144(11), pp. 4755–4762. doi: 10.1210/en.2003-0344.

Albiston, A. L., Obeyesekere, V. R., Smith, R. E. and Krozowski, Z. S. (1994) 'Cloning and tissue distribution of the human 11 beta-hydroxysteroid dehydrogenase type 2 enzyme.', *Molecular and Cellular Endocrinology*, 105(2), pp. R11-7.

Amelung, D., Hübener, H. J., Roka, L. And Meyerheim, G. (1953) 'Conversion of cortisone to compound F', *The Journal of Clinical Endocrinology & Metabolism*, 13(9), pp. 1125–1126. doi: 10.1210/jcem-13-9-1125.

Anderson, A. and Walker, B. R. (2013) '11 beta-HSD1 Inhibitors for the Treatment of Type 2 Diabetes and Cardiovascular Disease', *Drugs*, 73(13), pp. 1385–1393. doi: 10.1007/s40265-013-0112-5.

Andrews, R. C. and Walker, B. R. (1999) 'Glucocorticoids and insulin resistance: old hormones, new targets', *Clinical Science*, 96(5), pp. 513–23.

Aplin, A. C., Gelati, M., Fogel, E., Carnevale, E. & Nicosia, R. F. (2006), Angiopoietin-1 and vascular endothelial growth factor induce expression of inflammatory cytokines before angiogenesis', *Physiological Genomics, 27, pp.* 20-28. doi: 10.1152/physiolgenomics.00048.2006.

Aplin, A. C., Fogel, E., Zorzi, P. and Nicosia, R. F. (2008) 'The aortic ring model of angiogenesis', *Methods in Enzymology*, 443, pp. 119–36. doi: 10.1016/S0076-6879(08)02007-7.

Arima, S., Kohagura, K., Xu, H.-L., Sugawara, A., Uruno, A., Satoh, F., Takeuchi, K. and Ito, S. (2004) 'Endothelium-Derived Nitric Oxide Modulates Vascular Action of Aldosterone in Renal Arteriole', *Hypertension*, 43(2).

Arriza, J. L., Weinberger, C., Cerelli, G., Glaser, T. M., Handelin, B. L., Housman, D. E. and Evans, R. M. (1987) 'Cloning of human mineralocorticoid receptor complementary DNA: structural and functional kinship with the glucocorticoid receptor', *Science*, 237(4812), pp. 268–75.

Arroyo, A. G. and Iruela-Arispe, M. L. (2010) 'Extracellular matrix, inflammation, and the angiogenic response', *Cardiovascular Research*, 86(2), pp. 226–235. doi: 10.1093/cvr/cvq049.

Ashburner, M., Ball, C. A., Blake, J. A., Botstein, D., Butler, H., Cherry, J. M., Davis, A. P., Dolinski, K., Dwight, S. S., Eppig, J. T., Harris, M. A., Hill, D. P., Issel-Tarver, L., Kasarskis, A., Lewis, S., Matese, J. C., Richardson, J. E., Ringwald, M., Rubin, G. M. & Sherlock, G. (2000). 'Gene Ontology: tool for the unification of biology'. *Nature Genetics*, 25(1), pp. 25–29. doi.org/10.1038/75556

Atanasov, A. G., Nashev, L. G., Gelman, L., Legeza, B., Sack, R., Portmann, R. and Odermatt, A. (2008) 'Direct protein-protein interaction of 11β-hydroxysteroid dehydrogenase type 1 and hexose-6-phosphate dehydrogenase in the endoplasmic reticulum lumen', *Biochimica et Biophysica Acta (BBA) - Molecular Cell Research*, 1783(8), pp. 1536–1543. doi: 10.1016/j.bbamcr.2008.03.001.

Augustin, H. G., Young Koh, G., Thurston, G. and Alitalo, K. (2009) 'Control of vascular morphogenesis and homeostasis through the angiopoietin–Tie system', *Nature Reviews Molecular Cell Biology*, 10(3), pp. 165–177. doi: 10.1038/nrm2639.

Azher, S., Azami, O., Amato, C., McCullough, M., Celentano, A. and Cirillo, N. (2016) 'The Non-Conventional Effects of Glucocorticoids in Cancer', *Journal of Cellular Physiology*, 231(11), pp. 2368–73. doi: 10.1002/jcp.25408.

Baba, Y., Iyama, K.-I. Ikeda, K., Ishikawa, S., Hayashi, N., Miyanari, N., Sado, Y., Ninomiya, Y. & Baba, H. (2008), 'The Expression of Type IV Collagen α6 Chain Is Related to the Prognosis in Patients with Esophageal Squamous Cell Carcinoma', *Annals of Surgical Oncology*, 15(2), pp. 555-565.

Baeriswyl, V. and Christofori, G. (2009) 'The angiogenic switch in carcinogenesis', *Seminars in Cancer Biology*, 19(5), pp. 329–337. doi: 10.1016/j.semcancer.2009.05.003.

Baker, M., Robinson, S. D., Lechertier, T., Barber, P. R., Tavora, B., D'Amico, G., Jones, D. T., Vojnovic, B. & Hobdivala-Dilke, K. (2011), 'Use of the mouse aortic ring assay to study angiogenesis', *Nature Protocols*, 7(1), pp. 89-104. doi:10.1038/nprot.2011.435.

Balachandran, A., Guan, H., Sellan, M., van Uum, S. and Yang, K. (2008) 'Insulin and Dexamethasone Dynamically Regulate Adipocyte 11β-Hydroxysteroid Dehydrogenase Type 1', *Endocrinology*, 149(8), pp. 4069–4079. doi: 10.1210/en.2008-0088.

Baluk, P., Morikawa, S., Haskell, A., Mancuso, M. and McDonald, D. M. (2003) 'Abnormalities of basement membrane on blood vessels and endothelial sprouts in tumors', *The American Journal of Pathology*, 163(5), pp. 1801–15. doi: 10.1016/S0002-9440(10)63540-7.

Barber, A. E., Coyle, S. M., Marano, M. A., Fischer, E., Calvano, S. E., Fong, Y., Moldawer, L. L. and Lowry, S. F. (1993) 'Glucocorticoid therapy alters hormonal and cytokine responses to endotoxin in man.', *Journal of Immunology*, 150(5), pp. 1999–2006.

Barish, G. D., Downes, M., Alaynick, W. A., Yu, R. T., Ocampo, C. B., Bookout, A. L., Mangelsdorf, D. J. and Evans, R. M. (2005) 'A Nuclear Receptor Atlas: Macrophage Activation', *Molecular Endocrinology*, 19(10), pp. 2466–2477. doi: 10.1210/me.2004-0529.

Belbasis, L., Stefanaki, I., Stratigos, A. J. & Evangelou, E. (2016), 'Non-genetic risk factors for cutaneous melanoma and keratinocyte skin cancers: An umbrella review of meta-analyses', *Journal of Dermatological Science,* 84(3), pp. 330-339. doi: 10.1016/j.jdermsci.2016.09.003.

Benedetti, M., Merino, R., Kusuda, R., Ravanelli, M. I., Cadetti, F., dos Santos, P., Zanon, S. and Lucas, G. (2012) 'Plasma corticosterone levels in mouse models of pain', *European Journal of Pain*, 16(6), pp. 803–815. doi: 10.1002/j.1532-2149.2011.00066.x.

Benedetti, S., Pirola, B., Poliani, P. L., Cajola, L., Pollo, B., Bagnati, R., Magrassi, L., Tunici, P. and Finocchiaro, G. (2003) 'Dexamethasone inhibits the anti-tumor effect of interleukin 4 on rat experimental gliomas', *Gene Therapy*, 10(2), pp. 188–192. doi: 10.1038/sj.gt.3301863.

Benediktsson, R., Yau, J. L., Low, S., Brett, L. P., Cooke, B. E., Edwards, C. R. and Seckl, J. R. (1992) '11 beta-Hydroxysteroid dehydrogenase in the rat ovary: high expression in the oocyte.', *The Journal of Endocrinology*, 135(1), pp. 53–8. doi: 10.1677/JOE.0.1350053.

Benedito, R., Roca, C., Sörensen, I., Adams, S., Gossler, A., Fruttiger, M. and Adams, R. H. (2009) 'The Notch Ligands Dll4 and Jagged1 Have Opposing Effects on Angiogenesis', *Cell*, 137(6), pp. 1124–1135. doi: 10.1016/j.cell.2009.03.025.

Bergers, G., Song, S., Meyer-Morse, N., Bergsland, E. and Hanahan, D. (2003) 'Benefits of targeting both pericytes and endothelial cells in the tumor vasculature with kinase inhibitors', *Journal of Clinical Investigation*, 111(9), pp. 1287–1295. doi: 10.1172/JCI17929.

Bergman, A. M., Pinedo, H. M. and Peters, G. J. (2001) 'Steroids affect collateral sensitivity to gemcitabine of multidrug-resistant human lung cancer cells', *European Journal of Pharmacology*, 416(1–2), pp. 19–24.

Berk, B. C., Gordon, J. B. and Alexander, R. W. (1991) 'Pharmacologic roles of heparin and glucocorticoids to prevent restenosis after coronary angioplasty', *Journal of the American College of Cardiology*, 17(6 Suppl B), p. 111B–117B.

Berk, B. C., Vallega, G., Griendling, K. K., Gordon, J. B., Cragoe, E. J., Canessa, M. and Alexander, R. W. (1988) 'Effects of glucocorticoids on Na+/H+ exchange and growth in cultured vascular smooth muscle cells', *Journal of Cellular Physiology*, 137(3), pp. 391–401. doi: 10.1002/jcp.1041370302.

Bernabé, D. G., Tamae, A. C., Biasoli, É. R. and Oliveira, S. H. P. (2011) 'Stress hormones increase cell proliferation and regulates interleukin-6 secretion in human oral squamous cell carcinoma cells', *Brain, Behavior, and Immunity*, 25(3), pp. 574–583. doi: 10.1016/j.bbi.2010.12.012.

Berthiaume, M., Laplante, M., Festuccia, W., Gélinas, Y., Poulin, S., Lalonde, J., Joanisse, D. R., Thieringer, R. and Deshaies, Y. (2007) 'Depot-Specific Modulation of Rat Intraabdominal Adipose Tissue Lipid Metabolism by Pharmacological Inhibition of 11?-Hydroxysteroid Dehydrogenase Type 1', *Endocrinology*, 148(5), pp. 2391–2397. doi: 10.1210/en.2006-1199.

Bertini, R., Bianchi, M. and Ghezzi, P. (1988) 'Adrenalectomy sensitizes mice to the lethal effects of interleukin 1 and tumor necrosis factor', *The Journal of Experimental Medicine*, 167(5), pp. 1708–12.

Best, R., Nelson, S. M. and Walker, B. R. (1997) 'Dexamethasone and 11-dehydrodexamethasone as tools to investigate the isozymes of 11 beta-hydroxysteroid dehydrogenase in vitro and in vivo', *The Journal of Endocrinology*, 153(1), pp. 41–8.

Bland, R., Worker, C. A., Noble, B. S., Eyre, L. J., Bujalska, I. J., Sheppard, M. C., Stewart, P. M. and Hewison, M. (1999) 'Characterization of 11beta-hydroxysteroid dehydrogenase activity and corticosteroid receptor expression in human osteosarcoma cell lines.', *The Journal of Endocrinology*, 161(3), pp. 455–64.

Blasco, M. A. (2005) 'Telomeres and human disease: ageing, cancer and beyond', *Nature Reviews Genetics*, 6(8), pp. 611–622. doi: 10.1038/nrg1656.

Boucher, E., Provost, P. R. & Tremblay, Y. (2014) 'Ontogeny of adrenal-like glucocorticoid synthesis pathway of a 20α-hydroxysteroid dehydrogenase in the mouse lung', *BMC Research Notes*, 1(7), pp. 119. doi: 10.1186/1756-0500-7-119.

Brem, A. S., Bina, R. B., King, T. C. and Morris, D. J. (1998) 'Localization of 2 11 beta-OH steroid dehydrogenase isoforms in aortic endothelial cells', *Hypertension*, 31(1), pp. 459–462.

Brem, A. S., Bina, R. B., King, T. and Morris, D. J. (1995) 'Bidirectional activity of 11 beta-hydroxysteroid dehydrogenase in vascular smooth muscle cells', *Steroids*, 60(5), pp. 406–10.

Briassoulis, G., Damjanovic, S., Xekouki, P., Lefebvre, H. and Stratakis, C. A. (2011) 'The glucocorticoid receptor and its expression in the anterior pituitary and the adrenal cortex: a source of variation in hypothalamic-pituitary-adrenal axis function; implications for pituitary and adrenal tumors', *Endocrine Practice*, 17(6), pp. 941–8. doi: 10.4158/EP11061.RA.

Briet, M. and Schiffrin, E. L. (2010) 'Aldosterone: effects on the kidney and cardiovascular system', *Nature Reviews Nephrology*, 6(5), pp. 261–273. doi: 10.1038/nrneph.2010.30.

Brooks, P. C., Silletti, S., von Schalscha, T. L., Friedlander, M. and Cheresh, D. A. (1998) 'Disruption of Angiogenesis by PEX, a Noncatalytic Metalloproteinase Fragment with Integrin Binding Activity', *Cell*, 92(3), pp. 391–400. doi: 10.1016/S0092-8674(00)80931-9.

Buchmann, A., Ruggeri, B., Klein-Szanto, A. J. P. & Balmain, A. (1991), 'Progression of Squamous Carcinoma Cells to Spindle Carcinomas of Mouse Skin Is Associated with an Imbalance of H-*ras* Alleles on Chromosome 7', *Cancer Research*, 51, pp. 4097-4101.

Budunova, I. V, Carbajal, S., Kang, H., Viaje, A. and Slaga, T. J. (1997) 'Altered glucocorticoid receptor expression and function during mouse skin carcinogenesis', *Molecular Carcinogenesis*, 18(3), pp. 177–85.

Bujalska, I. J., Kumar, S. and Stewart, P. M. (1997) 'Does central obesity reflect "Cushing's disease of the omentum?', *The Lancet*, 349(9060), pp. 1210–1213. doi: 10.1016/S0140-6736(96)11222-8.

Burton, P. J., Krozowski, Z. S. and Waddell, B. J. (1998) 'Immunolocalization of 11β-Hydroxysteroid Dehydrogenase Types 1 and 2 in Rat Uterus: Variation Across the Estrous Cycle and Regulation by Estrogen and Progesterone 1', *Endocrinology*, 139(1), pp. 376–382. doi: 10.1210/endo.139.1.5692.

Cai, T. Q., Wong, B. M., Mundt, S. S., Thieringer, R., Wright, S. D. and Hermanowski-Vosatka, A. (2001) 'Induction of 11 beta-hydroxysteroid dehydrogenase type 1 but not-2 in human aortic smooth muscle cells by inflammatory stimuli', *Journal of Steroid Biochemistry and Molecular Biology*, 77(2–3), pp. 117–122. doi: 10.1016/s0960-0760(01)00041-3.

Carbon, S., Ireland, A., Mungall, C. J., Shu, S., Marshall, B., & Lewis, S. (2009). AmiGO: online access to ontology and annotation data. *Bioinformatics Applications Note*, 25(2), pp. 288–28910. doi: 10.1093/bioinformatics/btn615.

Carmeliet, P. (2000) ‘Mechanisms of angiogenesis and arteriogenesis’, *Nature Medicine*, 6(4), pp. 389–395. doi: 10.1038/74651.

Carmeliet, P. (2003) ‘Angiogenesis in health and disease’, *Nature Medicine*, 9(6), pp. 653–660. doi: 10.1038/nm0603-653.

Carmeliet, P. (2005a) ‘Angiogenesis in life, disease and medicine’, *Nature*, 438(7070), pp. 932–936. doi: 10.1038/nature04478.

Carmeliet, P. (2005b) ‘VEGF as a key mediator of angiogenesis in cancer’, *Oncology*, 69 Suppl 3(Suppl. 3), pp. 4–10. doi: 10.1159/000088478.

Carmeliet, P., Ferreira, V., Breier, G., Pollefeyt, S., Kieckens, L., Gertsenstein, M., Fahrig, M., Vandenhoeck, A., Harpal, K., Eberhardt, C., Declercq, C., Pawling, J., Moons, L., Collen, D., Risau, W. and Nagy, A. (1996) ‘Abnormal blood vessel development and lethality in embryos lacking a single VEGF allele’, *Nature*, 380(6573), pp. 435–439. doi: 10.1038/380435a0.

Carmeliet, P. and Jain, R. K. (2011) ‘Molecular mechanisms and clinical applications of angiogenesis’, *Nature*, 473(7347), pp. 298–307. doi: 10.1038/nature10144.

Carmeliet, P. and Jain, R. K. (2011) ‘Principles and mechanisms of vessel normalization for cancer and other angiogenic diseases’, *Nature Reviews Drug Discovery*, 10(6), pp. 417–427. doi: 10.1038/nrd3455.

Carmeliet, P., Lampugnani, M. G., Moons, L., Breviario, F., Compernolle, V., Bono, F., Balconi, G., Spagnuolo, R., Oosthuyse, B., Dewerchin, M., Zanetti, A., Angellilo, A., Mattot, V., Nuyens, D., Lutgens, E., Clotman, F., de Ruiter, M. C., Gittenberger-de Groot, A., Poelmann, R., Lupu, F., Herbert, J. M., Collen, D. and Dejana, E. (1999) ‘Targeted deficiency or cytosolic truncation of the VE-cadherin gene in mice impairs VEGF-mediated endothelial survival and angiogenesis.’, *Cell*, 98(2), pp. 147–57.

Carter, R. N., Paterson, J. M., Tworowska, U., Stenvers, D. J., Mullins, J. J., Seckl, J. R., & Holmes, M. C. (2009). ‘Hypothalamic-pituitary-adrenal axis abnormalities in response to deletion of 11beta-HSD1 is strain-dependent’. *Journal of Neuroendocrinology*, 21(11), 879–87. doi.org/10.1111/j.1365-2826.2009.01899.x

Cavallaro, U. and Dejana, E. (2011) ‘Adhesion molecule signalling: not always a sticky business’, *Nature Reviews Molecular Cell Biology*, 12(3), pp. 189–197. doi: 10.1038/nrm3068.

Cerami, E., Gao, J., Dogrusoz, U., Gross, B. E., Sumer, S. O., Aksoy, B. A,, Jacobsen, A., Byrne, C. J., Heuer, M. L., Larsson, E., Antipin, Y., Reva, B., Goldberg, A. P., Sander, C. and Schultz, N. (2012), ‘The cBio cancer genomics portal: an open platform for exploring multidimensional cancer genomics data’. *Cancer Discovery*, 2(5), pp. 401-404. doi: 10.1158/2159-8290.CD-12-0095.

Chan, S. and Debono, M. (2010) ‘Replication of cortisol circadian rhythm: new advances in hydrocortisone replacement therapy’, *Therapeutic Advances in Endocrinology and Metabolism*, 1(3), pp. 129–38. doi: 10.1177/2042018810380214.

Chapman, K. E., Coutinho, A. E., Gray, M., Gilmour, J. S., Savill, J. S. and Seckl, J. R. (2009) ‘The role and regulation of 11β-hydroxysteroid dehydrogenase type 1 in the inflammatory response’, *Molecular and Cellular Endocrinology*, 301(1), pp. 123–131. doi: 10.1016/j.mce.2008.09.031.

Chapman, K. E., Coutinho, A. E., Zhang, Z., Kipari, T., Savill, J. S. and Seckl, J. R. (2013a) ‘Changing glucocorticoid action: 11β-hydroxysteroid dehydrogenase type 1 in acute and chronic

inflammation', *The Journal of Steroid Biochemistry and Molecular Biology. , 137(100),* pp. 82–92. doi: 10.1016/j.jsbmb.2013.02.002.

Chapman, K. E, Holmes, M. and Seckl, J. (2013b) '11β-hydroxysteroid dehydrogenases: intracellular gate-keepers of tissue glucocorticoid action', *Physiological Reviews*, 93(3), pp. 1139–206. doi: 10.1152/physrev.00020.2012.

Choi, E.-H., Demerjian, M., Crumrine, D., Brown, B. E., Mauro, T., Elias, P. M. and Feingold, K. R. (2006) 'Glucocorticoid blockade reverses psychological stress-induced abnormalities in epidermal structure and function', *AJP: Regulatory, Integrative and Comparative Physiology*, 291(6), pp. R1657–R1662. doi: 10.1152/ajpregu.00010.2006.

Christy, C., Hadoke, P. W. F., Paterson, J. M., Mullins, J. J., Seckl, J. R. and Walker, B. R. (2003) '11 beta-hydroxysteroid dehydrogenase type 2 in mouse aorta - Localization and influence on response to glucocorticoids', *Hypertension*. 42(4), pp. 580–587. doi: 10.1161/01.hyp.0000088855.06598.5b.

Chung, A. S. and Ferrara, N. (2011) 'Developmental and Pathological Angiogenesis', *Annual Review of Cell and Developmental Biology*, 27(1), pp. 563–584. doi: 10.1146/annurev-cellbio-092910-154002.

Cirillo, N., Hassona, Y., Pignatelli, M., Gasparoto, T. H., Morgan, D. J. and Prime, S. S. (2012) 'Characterization of a Novel Oral Glucocorticoid System and Its Possible Role in Disease', *Journal of Dental Research*, 91(1), pp. 97–103. doi: 10.1177/0022034511427909.

Cirillo, N., Morgan, D. J., Pedicillo, M. C., Celentano, A., Lo Muzio, L., McCullough, M. J. & Prime, S. S. (2017), 'Characterisation of the cancer-associated glucocorticoid system: key role of 11β-hydroxysteroid dehydrogenase type 2', *British Journal of Cancer,* 117(7), pp. 984-993. doi: 10.1038/bjc.2017.243.

Cirillo, N. and Prime, S. S. (2011) 'Keratinocytes synthesize and activate cortisol', *Journal of Cellular Biochemistry*, 112(6), pp. 1499–1505. doi: 10.1002/jcb.23081.

Clem, B., Telang, S., Clem, A., Yalcin, A., Meier, J., Simmons, A., Rasku, M. A., Arumugam, S., Dean, W. L., Eaton, J., Lane, A., Trent, J. O. and Chesney, J. (2008) 'Small-molecule inhibition of 6-phosphofructo-2-kinase activity suppresses glycolytic flux and tumor growth', *Molecular Cancer Therapeutics*, 7(1), pp. 110–120. doi: 10.1158/1535-7163.MCT-07-0482.

Cobice, D. F., Mackay, L., Goodwin, R. J. A., McBride, A., Langbridge-Smith, P. R., Webster, S. P., Walker, B. R. & Andrew, R. (2013) 'Mass Spectrometry Imaging for Dissecting Steroid Intracrinology within Target Tissues', *Analytical Chemistry,* 85(23), pp. 11576-11584. doi: 10.1021/ac402777k.

Cobice, D. F., Livingstone, D. E. W., McBride, A., MacKay, C. L., Walker, B. R., Webster, S. P. & Andrew, R. (2017) 'Quantification of 11b-hydroxysteroid dehydrogenase 1 kinetics and pharmacodynamic effects of inhibitors in brain using mass spectrometry imaging and stable-isotope tracers in mice', *Biochemical Pharmacology,* 148, pp. 88-99. doi: 10.1016/j.bcp.2017.12.013

Coffelt, S. B., Lewis, C. E., Naldini, L., Brown, J. M., Ferrara, N. and De Palma, M. (2010) 'Elusive Identities and Overlapping Phenotypes of Proangiogenic Myeloid Cells in Tumors', *The American Journal of Pathology,* 176(4), pp. 1564–1576. doi: 10.2353/ajpath.2010.090786.

Condon, J., Gosden, C., Gardener, D., Nickson, P., Hewison, M., Howie, A. J. and Stewart, P. M. (1998) 'Expression of Type 2 11β-Hydroxysteroid Dehydrogenase and Corticosteroid Hormone Receptors in Early Human Fetal Life 1', *The Journal of Clinical Endocrinology & Metabolism*, 83(12), pp. 4490–4497. doi: 10.1210/jcem.83.12.5302.

Conn, J. W., Rovner, D. R. and Cohen, E. L. (1968) 'Licorice-Induced Pseudoaldosteronism', *JAMA*, 205(7), p. 492. doi: 10.1001/jama.1968.03140330034006.

Cooper, M. S., Rabbitt, E. H., Goddard, P. E., Bartlett, W. A., Hewison, M. and Stewart, P. M. (2002) 'Osteoblastic 11β-Hydroxysteroid Dehydrogenase Type 1 Activity Increases With Age and Glucocorticoid Exposure', *Journal of Bone and Mineral Research*, 17(6), pp. 979–986. doi: 10.1359/jbmr.2002.17.6.979.

Cooper, M. S., Walker, E. A., Bland, R., Fraser, W. D., Hewison, M. and Stewart, P. M. (2000) 'Expression and functional consequences of 11beta-hydroxysteroid dehydrogenase activity in human bone', *Bone*, 27(3), pp. 375–81.

Corada, M., Nyqvist, D., Orsenigo, F., Caprini, A., Giampietro, C., Taketo, M. M., Iruela-Arispe, M. L., Adams, R. H. and Dejana, E. (2010) 'The Wnt/β-Catenin Pathway Modulates Vascular Remodeling and Specification by Upregulating Dll4/Notch Signaling', *Developmental Cell*, 18(6), pp. 938–949. doi: 10.1016/j.devcel.2010.05.006.

Coulter, C. L., Smith, R. E., Stowasser, M., Sasano, H., Krozowski, Z. S. and Gordon, R. D. (1999) 'Expression of 11β-hydroxysteroid dehydrogenase type 2 (11βHSD-2) in the developing human adrenal gland and human adrenal cortical carcinoma and adenoma', *Molecular and Cellular Endocrinology*, 154(1–2), pp. 71–77. doi: 10.1016/S0303-7207(99)00077-5.

Coussens, L. M., Raymond, W. W., Bergers, G., Laig-Webster, M., Behrendtsen, O., Werb, Z., Caughey, G. H. and Hanahan, D. (1999) 'Inflammatory mast cells up-regulate angiogenesis during squamous epithelial carcinogenesis', *Genes & Development*, 13(11), pp. 1382–97.

Coutinho, A. E., Brown, J. K., Yang, F., Brownstein, D. G., Gray, M., Seckl, J. R., Savill, J. S. and Chapman, K. E. (2013) 'Mast cells express 11β-hydroxysteroid dehydrogenase type 1: a role in restraining mast cell degranulation', *Plos ONE*, 8(1), p. e54640. doi: 10.1371/journal.pone.0054640.

Coutinho, A. E. and Chapman, K. E. (2011) 'The anti-inflammatory and immunosuppressive effects of glucocorticoids, recent developments and mechanistic insights', *Molecular and Cellular Endocrinology*, 335(1), pp. 2–13. doi: 10.1016/j.mce.2010.04.005.

Coutinho, A. E., Gray, M., Brownstein, D. G., Salter, D. M., Sawatzky, D. A., Clay, S., Gilmour, J. S., Seckl, J. R., Savill, J. S. and Chapman, K. E. (2012) '11β-Hydroxysteroid dehydrogenase type 1, but not type 2, deficiency worsens acute inflammation and experimental arthritis in mice.', *Endocrinology*, 153(1), pp. 234–40. doi: 10.1210/en.2011-1398.

Coutinho, A. E., Kipari, T. M. J., Zhang, Z., Esteves, C. L., Lucas, C. D., Gilmour, J. S., Webster, S. P., Walker, B. R., Hughes, J., Savill, J. S., Seckl, J. R., Rossi, A. G. and Chapman, K. E. (2016) '11β-Hydroxysteroid Dehydrogenase type 1 is expressed in neutrophils and restrains an inflammatory response in male mice.', *Endocrinology*, 157(7):2928-36. doi: 10.1210/en.2016-1118.

Cretu, A. and Brooks, P. C. (2007) 'Impact of the non-cellular tumor microenvironment on metastasis: Potential therapeutic and imaging opportunities', *Journal of Cellular Physiology*, 213(2), pp. 391–402. doi: 10.1002/jcp.21222.

Cronstein, B. N., Kimmel, S. C., Levin, R. I., Martiniuk, F. and Weissmann, G. (1992) 'A mechanism for the antiinflammatory effects of corticosteroids: the glucocorticoid receptor regulates leukocyte adhesion to endothelial cells and expression of endothelial-leukocyte adhesion molecule 1 and intercellular adhesion molecule 1.', *Proceedings of the National Academy of Sciences of the United States of America*, 89(21), pp. 9991–5.

Crowley, P., Lai, N. Y., De Young, N., Pearce, P., Funder, J. W. and Gill, P. G. (1988) 'Inhibition of growth of B16 melanoma by glucocorticoids does not result directly from receptor-mediated inhibition of tumour cells.', *Oncology*, 45(4), pp. 331–5.

Curnow, K. M., Tusie-Luna, M.-T., Pascoe, L., Natarajan, R., Gu, J.-L., Nadler, J. L. and White, P. C. (1991) 'The Product of the CYP11B2 Gene Is Required for Aldosterone Biosynthesis in the Human Adrenal Cortex', *Molecular Endocrinology*, 5(10), pp. 1513–1522. doi: 10.1210/mend-5-10-1513.

Dailey, J. W. and Westfall, T. C. (1978) 'Effects of adrenalectomy and adrenal steroids on norepinephrine synthesis and monoamine oxidase activity', *European Journal of Pharmacology*, 48(4), pp. 383–391. doi: 10.1016/0014-2999(78)90165-6.

Dallman, M. F., la Fleur, S. E., Pecoraro, N. C., Gomez, F., Houshyar, H. and Akana, S. F. (2004) 'Minireview: Glucocorticoids—Food Intake, Abdominal Obesity, and Wealthy Nations in 2004', *Endocrinology*, 145(6), pp. 2633–2638. doi: 10.1210/en.2004-0037.

Davidson, C. T., Dover, A. R., McVicar, C. M., Megaw, R., Glenn, J. V., Hadoke, P. W. F., Stitt, A. W. and Walker, B. R. (2017) 'Inhibition or deletion of 11β-HSD1 does not increase angiogenesis in ischemic retinopathy', *Diabetes & Metabolism*. doi: 10.1016/j.diabet.2016.12.001.

Dayan, F., Mazure, N. M., Brahimi-Horn, M. C. and Pouysségur, J. (2008) 'A dialogue between the hypoxia-inducible factor and the tumor microenvironment', *Cancer Microenvironment*, 1(1), pp. 53–68. doi: 10.1007/s12307-008-0006-3.

De Bock, K., Georgiadou, M., Schoors, S., Kuchnio, A., Wong, B. W., Cantelmo, A. R., Quaegebeur, A., Ghesquière, B., Cauwenberghs, S., Eelen, G., Phng, L.-K., Betz, I., Tembuyser, B., Brepoels, K., Welti, J., Geudens, I., Segura, I., Cruys, B., Bifari, F., Decimo, I., Blanco, R., Wyns, S., Vangindertael, J., Rocha, S., Collins, R. T., Munck, S., Daelemans, D., Imamura, H., Devlieger, R., Rider, M., Van Veldhoven, P. P., Schuit, F., Bartrons, R., Hofkens, J., Fraisl, P., Telang, S., DeBerardinis, R. J., Schoonjans, L., Vinckier, S., Chesney, J., Gerhardt, H., Dewerchin, M. and Carmeliet, P. (2013) 'Role of PFKFB3-Driven Glycolysis in Vessel Sprouting', *Cell*, 154(3), pp. 651–663. doi: 10.1016/j.cell.2013.06.037.

De Palma, M., Murdoch, C., Venneri, M. A., Naldini, L. and Lewis, C. E. (2007) 'Tie2-expressing monocytes: regulation of tumor angiogenesis and therapeutic implications'. *Trends in Immunology*, 28(12), pp. 519-24. doi: 10.1016/j.it.2007.09.004.

De Palma, M., Venneri, M. A., Galli, R., Sergi, L. S., Politi, L. S., Sampaolesi, M. and Naldini, L. (2005) 'Tie2 identifies a hematopoietic lineage of proangiogenic monocytes required for tumor vessel formation and a mesenchymal population of pericyte progenitors', *Cancer Cell*, 8(3), pp. 211–226. doi: 10.1016/j.ccr.2005.08.002.

De Weever, O., Demetter, P., Mareel, M. & Bracke, M. (2008), 'Stomal myofibroblasts are drivers of invasive cancer growth', *International Journal of Cancer,* 123(10), pp. 2229-38. doi: 10.1002/ijc.23925.

De Wever, O., Van Bockstal, M., Mareel, M., Hendrix, A. and Bracke, M. (2014) 'Carcinoma-associated fibroblasts provide operational flexibility in metastasis', *Seminars in Cancer Biology*, 25, pp. 33–46. doi: 10.1016/j.semcancer.2013.12.009.

Debono, M., Ghobadi, C., Rostami-Hodjegan, A., Huatan, H., Campbell, M. J., Newell-Price, J., Darzy, K., Merke, D. P., Arlt, W. and Ross, R. J. (2009) 'Modified-Release Hydrocortisone to Provide Circadian Cortisol Profiles', *The Journal of Clinical Endocrinology & Metabolism*, 94(5), pp. 1548–1554. doi: 10.1210/jc.2008-2380.

DeNardo, D. G., Andreu, P. and Coussens, L. M. (2010) 'Interactions between lymphocytes and myeloid cells regulate pro- versus anti-tumor immunity', *Cancer and Metastasis Reviews*, 29(2), pp. 309–316. doi: 10.1007/s10555-010-9223-6.

Dermond, O. and Ruegg, C. (2001) 'Inhibition of tumor angiogenesis by non-steroidal anti-inflammatory drugs: emerging mechanisms and therapeutic perspectives', *Drug Resistance Updates*, 4(5), pp. 314–321. doi: 10.1054/drup.2001.0219.

Dhawan, L., Liu, B., Blaxall, B. C. and Taubman, M. B. (2007) 'A Novel Role for the Glucocorticoid Receptor in the Regulation of Monocyte Chemoattractant Protein-1 mRNA Stability', *Journal of Biological Chemistry*, 282(14), pp. 10146–10152. doi: 10.1074/jbc.M605925200.

Diederich, S., Scholz, T., Eigendorff, E., Bumke-Vogt, C., Quinkler, M., Exner, P., Pfeiffer, A., Oelkers, W. and Bähr, V. (2004) 'Pharmacodynamics and Pharmacokinetics of Synthetic Mineralocorticoids and Glucocorticoids: Receptor Transactivation and Prereceptor Metabolism by 11β-hydroxysteroid-dehydrogenases', *Hormone and Metabolic Research*, 36(6), pp. 423–429. doi: 10.1055/s-2004-814578.

Dighe, A. S., Richards, E., Old, L. J. and Schreiber, R. D. (1994) 'Enhanced in vivo growth and resistance to rejection of tumor cells expressing dominant negative IFNγ receptors', *Immunity*, 1(6), pp. 447–456. doi: 10.1016/1074-7613(94)90087-6.

Donaldson, M. R. & Coldiron, B. M. (2011), 'No end in sight: the skin cancer epidemic continues', *Seminars in Cutaneous Medicine and Surgery*, 30(1), pp. 3-5, doi: 10.1016/j.sder.2011.01.002.

Dover, A. R., Hadoke, P. W. F., Macdonald, L. J., Miller, E., Newby, D. E. and Walker, B. R. (2007) 'Intravascular glucocorticoid metabolism during inflammation and injury in mice', *Endocrinology*, 148(1), pp. 166–172. doi: 10.1210/en.2006-0996.

Dovio, A., Sartori, M. L., De Francia, S., Mussino, S., Perotti, P., Saba, L., Abbadessa, G., Racca, S. and Angeli, A. (2009) 'Differential expression of determinants of glucocorticoid sensitivity in androgen-dependent and androgen-independent human prostate cancer cell lines', *The Journal of Steroid Biochemistry and Molecular Biology*, 116(1–2), pp. 29–36. doi: 10.1016/j.jsbmb.2009.04.007.

Drutskaya, M. S., Efimov, G.A., Kruglov, A.A., Kuprash, D.V., Nedospasov, S. A. (2010), 'Tumor necrosis factor, lymphotoxin and cancer', *IUBMB Life*, 62(4), pps 283-9. doi: 10.1002/iub.309.

Ducloux, D., Carron, P. L., Racadot, E., Rebibou, J. M., Bresson-Vautrin, C., Saint-Hillier, Y. and Chalopin, J. M. (1998) 'CD4 lymphocytopenia in long-term renal transplant recipients', *Transplantation Proceedings*, 30(6), pp. 2859–60.

Duffield, J. S., Forbes, S. J., Constandinou, C. M., Clay, S., Partolina, M., Vuthoori, S., Wu, S., Lang, R. & Iredale, J. P. (2005), 'Selective depletion of macrophages reveals distinct, opposing roles during liver injury and repair', *Journal of Clinical Investigation*, 115(1), pp. 56-65. doi: 10.1172/JCI22675.

Duffy, S. A., Taylor, J. M. G., Terrell, J. E., Islam, M., Li, Y., Fowler, K. E., Wolf, G. T. and Teknos, T. N. (2008) 'Interleukin-6 predicts recurrence and survival among head and neck cancer patients', *Cancer*, 113(4), pp. 750–757. doi: 10.1002/cncr.23615.

Dumont, N., Liu, B., Defilippis, R. A., Chang, H., Rabban, J. T., Karnezis, A. N., Tjoe, J. A., Marx, J., Parvin, B. and Tlsty, T. D. (2013) 'Breast fibroblasts modulate early dissemination, tumorigenesis, and metastasis through alteration of extracellular matrix characteristics.', *Neoplasia*, 15(3), pp. 249–62.

Dyer, L. and Patterson, C. (2010) 'Development of the Endothelium: An Emphasis on Heterogeneity', *Seminars in Thrombosis and Hemostasis*, 36(3), pp. 227–235. doi: 10.1055/s-0030-1253446.

Eble, J. A. and Niland, S. (2009) 'The extracellular matrix of blood vessels', *Current Pharmaceutical Design*, 15(12), pp. 1385–400.

Ebos, J. M. L., Lee, C. R., Cruz-Munoz, W., Bjarnason, G. A., Christensen, J. G. and Kerbel, R. S. (2009) 'Accelerated Metastasis after Short-Term Treatment with a Potent Inhibitor of Tumor Angiogenesis', *Cancer Cell*, 15(3), pp. 232–239. doi: 10.1016/j.ccr.2009.01.021.

Edwards, C. R. W, Stewart, P. M., Burt, D., Brett, L., McIntyre, M. A., Sutanto, W. S., de Kloet, E. R. and Monder, C. (1988) 'Localisation of 11 beta-hydroxysteroid dehydrogenase--tissue specific protector of the mineralocorticoid receptor.', *The Lancet*, 2(8618), pp. 986–9.

Edwards, C. R. W., Benediktsson, R., Lindsay, R. S. and Seckl, J. R. (1993) 'Dysfunction of placental glucocorticoid barrier - link between fetal environment and adult hypertension', *The Lancet*, 341(8841), pp. 355–357. doi: 10.1016/0140-6736(93)90148-a.

Eelen, G., Cruys, B., Welti, J., De Bock, K. and Carmeliet, P. (2013) 'Control of vessel sprouting by genetic and metabolic determinants', *Trends in Endocrinology and Metabolism*, 24(12), pp. 589–596. doi: 10.1016/j.tem.2013.08.006.

Eelen, G., de Zeeuw, P., Simons, M. and Carmeliet, P. (2015) 'Endothelial Cell Metabolism in Normal and Diseased Vasculature', *Circulation Research*, 116(7), pp. 1231–1244. doi: 10.1161/CIRCRESAHA.116.302855.

Eikel, D., Vavrek, M., Smith, S., Bason, C., Yeh, S., Korfmacher, W. A. & Henion, J. D., (2011), 'Liquid extraction surface analysis mass spectrometry (LESA-MS) as a novel profiling tool for drug distribution and metabolism analysis: the terfenadine example', *Rapid Communications in Mass Spectrometry*, 25(23), pp. 3587-96. doi: 10.1002/rcm.5274.

Eilken, H. M. and Adams, R. H. (2010) 'Dynamics of endothelial cell behavior in sprouting angiogenesis', *Current Opinion in Cell Biology*, 22(5), pp. 617–625. doi: 10.1016/j.ceb.2010.08.010.

Eisen, L. P., Elsasser, M. S. & Harmon, J. M., (1988), 'Positive regulation of the glucocorticoid receptor in human T-cells sensitive to the cytolytic effects of glucocorticoids', *Journal of Biological Chemistry*, 263, pp. 12044-12048.

Ema, M., Taya, S., Yokotani, N., Sogawa, K., Matsuda, Y. and Fujii-Kuriyama, Y. (1997) 'A novel bHLH-PAS factor with close sequence similarity to hypoxia-inducible factor 1alpha regulates the VEGF expression and is potentially involved in lung and vascular development.', *Proceedings of the National Academy of Sciences of the United States of America*, 94(9), pp. 4273–8.

Engeli, S., Böhnke, J., Feldpausch, M., Gorzelniak, K., Heintze, U., Janke, J., Luft, F. C. and Sharma, A. M. (2004) 'Regulation of 11β-HSD Genes in Human Adipose Tissue: Influence of Central Obesity and Weight Loss', *Obesity Research*, 12(1), pp. 9–17. doi: 10.1038/oby.2004.3.

Erez, N., Truitt, M., Olson, P., Hanahan, D. and Hanahan, D. (2010) 'Cancer-Associated Fibroblasts Are Activated in Incipient Neoplasia to Orchestrate Tumor-Promoting Inflammation in an NF-κB-Dependent Manner', *Cancer Cell*, 17(2), pp. 135–147. doi: 10.1016/j.ccr.2009.12.041.

Euvrard, S., Kanitakis, J. and Claudy, A. (2003) 'Skin Cancers after Organ Transplantation', *New England Journal of Medicine*, 348(17), pp. 1681–1691. doi: 10.1056/NEJMra022137.

Falcón, B. L., Hashizume, H., Koumoutsakos, P., Chou, J., Bready, J. V., Coxon, A., Oliner, J. D. and McDonald, D. M. (2009) 'Contrasting Actions of Selective Inhibitors of Angiopoietin-1 and Angiopoietin-2 on the Normalization of Tumor Blood Vessels', *The American Journal of Pathology*, 175(5), pp. 2159–2170. doi: 10.2353/ajpath.2009.090391.

Fang, M.m Yuan, J., Peng, C & Li, Y. (2014), 'Collagen as a double-edged sword in tumor progression', *Tumor Biology*, 35, pp. 2871-2882. doi: 10.1007/s13277-013-1511-7.

Fang, S. and Salven, P. (2011) 'Stem cells in tumor angiogenesis', *Journal of Molecular and Cellular Cardiology*, 50(2), pp. 290–295. doi: 10.1016/j.yjmcc.2010.10.024.

Fearon, D. T. (2017) 'Immune-Suppressing Cellular Elements of the Tumor Microenvironment', *Annual Review of Cancer Biology*, 1(1), pp. 241–255. doi: 10.1146/annurev-cancerbio-050216-034359.

Feng, Z., Liu, L., Zhang, C., Zheng, T., Wang, J., Lin, M., Zhao, Y., Wang, X., Levine, A. J. and Hu, W. (2012) 'Chronic restraint stress attenuates p53 function and promotes tumorigenesis', *Proceedings of the National Academy of Sciences of the United States of America*, 109(18), pp. 7013–8. doi: 10.1073/pnas.1203930109.

Ferrara, N. (2009) 'VEGF-A: a critical regulator of blood vessel growth', *European Cytokine Network*, 20(4), pp. 158–163. doi: 10.1684/ecn.2009.0170.

Ferrara, N., Carver-Moore, K., Chen, H., Dowd, M., Lu, L., O'Shea, K. S., Powell-Braxton, L., Hillan, K. J. and Moore, M. W. (1996) 'Heterozygous embryonic lethality induced by targeted inactivation of the VEGF gene', *Nature*, 380(6573), pp. 439–442. doi: 10.1038/380439a0.

Fischbach, F. T. & Dunning, M. B., (2009), *Manual of Laboratory and Diagnostic Tests*, 8th edn, Lippincott Williams and Wilkins, Philadelphia.

Flier, J. S., Underhill, L. H. and Dvorak, H. F. (1986) 'Tumors: Wounds That Do Not Heal', *New England Journal of Medicine*, 315(26), pp. 1650–1659. doi: 10.1056/NEJM198612253152606.

Flint, T. R., Fearon, D. T. and Janowitz, T. (2017) 'Connecting the Metabolic and Immune Responses to Cancer', *Trends in Molecular Medicine*, 23(5), pp. 451–464. doi: 10.1016/j.molmed.2017.03.001.

Flint, T. R., Janowitz, T., Connell, C. M., Roberts, E. W., Denton, A. E., Coll, A. P., Jodrell, D. I. and Fearon, D. T. (2016) 'Tumor-Induced IL-6 Reprograms Host Metabolism to Suppress Anti-tumor Immunity', *Cell Metabolism*, 24(5), pp. 672–684. doi: 10.1016/j.cmet.2016.10.010.

Folkman, J. (1972) 'anti-angiogenesis - new concept for therapy of solid tumors', *Annals of Surgery*, 175(3), p. 409-. doi: 10.1097/00000658-197203000-00014.

Folkman, J. (1995) 'Angiogenesis in cancer, vascular, rheumatoid and other disease', *Nature Medicine*, 1(1), pp. 27–31.

Folkman, J. (2001) 'Angiogenesis-dependent diseases', *Seminars in Oncology*, 28(6), pp. 536–542. doi: 10.1053/sonc.2001.29543.

Folkman, J. and Ingber, D. E. (1987) 'Angiostatic steroids. Method of discovery and mechanism of action', *Annals of Surgery*, 206(3), pp. 374–383. doi: 10.1097/00000658-198709000-00016.

Folkman, J., Langer, R., Linhardt, R., Haudenschild, C. and Taylor, S. (1983) 'Angiogenesis inhibition and tumor regression caused by heparin or a heparin fragment in the presence of cortisone', *Science*, 221(4612), pp. 719–725. doi: 10.1126/science.6192498.

Folkman, J., Watson, K., Ingber, D. and Hanahan, D. (1989) 'Induction of angiogenesis during the transition from hyperplasia to neoplasia', *Nature*, 339(6219), pp. 58–61. doi: 10.1038/339058a0.

Fong, G. H., Zhang, L., Bryce, D. M. and Peng, J. (1999) 'Increased hemangioblast commitment, not vascular disorganization, is the primary defect in flt-1 knock-out mice', *Development*, 126(13), pp. 3015–25.

Fontaine, D. A & Davis, D. B. (2016) 'Attention to Background Strain Is Essential for Metabolic Research: C57BL/6 and the International Knockout Mouse Consortium', *Diabetes*, 65(1), pp.25-33. doi: 10.2337/db15-0982.

Fraccarollo, D., Berger, S., Galuppo, P., Kneitz, S., Hein, L., Schütz, G., Frantz, S., Ertl, G. and Bauersachs, J. (2011) 'Deletion of Cardiomyocyte Mineralocorticoid Receptor Ameliorates Adverse Remodeling After Myocardial Infarction', *Circulation*, 123(4), pp. 400-8.

Francavilla, C., Maddaluno, L. & Cavallaro, U. (2009) 'The functional role of cell adhesion molecules in tumor angiogenesis', *Seminars in Cancer Biology*, 19(5), pp. 298-309. doi: 10.1016/j.semcancer.2009.05.004.

Freeman, A. I., Munn, H. L., Lyons, V., Dammermann, A., Seckl, J. R. & Chapman, K. E. (2004), 'Glucocorticoid down-regulation of rat glucocorticoid receptor does not involve differential promoter regulation'. *Journal of Endocrinology*, 183, pp. 365–374.

Freeman, L., Hewison, M., Hughes, S. V, Evans, K. N., Hardie, D., Means, T. K. and Chakraverty, R. (2005) 'Expression of 11 -hydroxysteroid dehydrogenase type 1 permits regulation of glucocorticoid bioavailability by human dendritic cells', *Blood*, 106(6), pp. 2042–2049. doi: 10.1182/blood-2005-01-0186.

Frieler, R.A., Meng, H., Duan, S. Z., Berger, S., Schütz, G., He, Y., Xi, G., Wang, M. M. & Mortensen, R.M. (2011), 'Myeloid-specific deletion of the mineralocorticoid receptor reduces infarct volume and alters inflammation during cerebral ischemia', *Stroke*, 42(1), pp. 179-85. doi: 10.1161/STROKEAHA.110.598441.

Funder, J. W. (2005) 'RALES, EPHESUS and redox', *The Journal of Steroid Biochemistry and Molecular Biology*, 93(2), pp. 121–125. doi: 10.1016/j.jsbmb.2004.12.010.

Funder, J. W., Pearce, P. T., Smith, R. and Smith, A. I. (1988) 'Mineralocorticoid action: target tissue specificity is enzyme, not receptor, mediated', *Science*, 242(4878), pp. 583–5.

Mac Gabhann, F., Qutub, A. A., Annex, B. H. and Popel, A. S. (2010) 'Systems biology of pro-angiogenic therapies targeting the VEGF system', *Wiley Interdisciplinary Reviews-Systems Biology and Medicine*, 2(6), pp. 694–707. doi: 10.1002/wsbm.92.

Gaengel, K., Genove, G., Armulik, A. and Betsholtz, C. (2009) 'Endothelial-Mural Cell Signaling in Vascular Development and Angiogenesis', *Arteriosclerosis, Thrombosis, and Vascular Biology*, 29(5), pp. 630–638. doi: 10.1161/ATVBAHA.107.161521.

Gale, N. W. and Yancopoulos, G. D. (1999) 'Growth factors acting via endothelial cell-specific receptor tyrosine kinases: VEGFs, angiopoietins, and ephrins in vascular development', *Genes & Development*. 13(9), pp. 1055–66.

Galosy, R. A., Clarke, L. K., Vasko, M. R. and Crawford, I. L. (1981) 'Neurophysiology and neuropharmacology of cardiovascular regulation and stress', *Neuroscience and Biobehavioral Reviews*, 5(1), pp. 137–75.

Garcia, R. A., Search, D. J., Lupisella, J. A., Ostrowski, J., Guan, B., Chen, J., Yang, W. P., Truong, A., He, A. Q., Zhang, R. G., Yan, M. J., Hellings, S. E., Gargalovic, P. S., Ryan, C. S., Watson, L. M., Langish, R. A., Shipkova, P. A., Carson, N. L., Taylor, J. R., Yang, R., Psaltis, G. C., Harrity, T. W., Robl, J. A. and Gordon, D. A. (2013) '11 beta-Hydroxysteroid Dehydrogenase Type 1 Gene Knockout Attenuates Atherosclerosis and In Vivo Foam Cell Formation in Hyperlipidemic apoE(-/-) Mice', *Plos ONE*, 8(2), p. 15. doi: 10.1371/journal.pone.0053192.

Garcovich, S., Colloca, G., Sollena, P., Andrea, B., Balducci, L., Cho, W. C., Bernabei, R. & Peris, K. (2017), 'Skin Cancer Epidemics in the Elderly as An Emerging Issue in Geriatric Oncology', *Aging and Disease*, 8(5), pp. 643-661. doi: 10.14336/AD.2017.0503.

Gassler, N., Zhang, C., Wenger, T., Schnabel, P. A., Dienemann, H., Debatin, K.-M., Mattern, J. and Herr, I. (2005) 'Dexamethasone-induced cisplatin and gemcitabine resistance in lung carcinoma samples treated ex vivo', *British Journal of Cancer*, 92(6), pp. 1084–8. doi: 10.1038/sj.bjc.6602453.

Ge, R.-S., Hardy, D. O., Catterall, J. F. and Hardy, M. P. (1997) 'Developmental Changes in Glucocorticoid Receptor and 11β-Hydroxysteroid Dehydrogenase Oxidative and Reductive Activities in Rat Leydig Cells 1', *Endocrinology*, 138(12), pp. 5089–5095. doi: 10.1210/endo.138.12.5614.

Gelati, M., Aplin, A. C., Fogel, E., Smith, K. D. & Nicosia, R. F. (2008), 'The angiogenic response of the aorta to injury and inflammatory cytokines requires macrophages', *Journal of Immunology*, 181(8), pp. 5711-9.

Gille, J., Reisinger, K., Westphal-Varghese, B. & Kaufmann, R. (2001), 'Decreased mRNA stability as a mechanism of glucocorticoid-mediated inhibition of vascular endothelial growth factor gene expression by cultured keratinocytes'. *Journal of Investigative Dermatology*. 117(6):1581–1587. doi: 10.1046/j.0022-202x.2001.01573.x.

Gilmour, J. S., Coutinho, A. E., Cailhier, J.-F., Man, T. Y., Clay, M., Thomas, G., Harris, H. J., Mullins, J. J., Seckl, J. R., Savill, J. S. and Chapman, K. E. (2006) 'Local amplification of glucocorticoids by 11 beta-hydroxysteroid dehydrogenase type 1 promotes macrophage phagocytosis of apoptotic leukocytes.', *Journal of Immunology*, 176(12), pp. 7605–11.

Gingras, M.-C. and Margolin, J. F. (2000) 'Differential expression of multiple unexpected genes during U937 cell and macrophage differentiation detected by suppressive subtractive hybridization', *Experimental Hematology*, 28(3), p. 350. doi: 10.1016/S0301-472X(00)00149-1.

Girardi, M., Oppenheim, D. E., Steele, C. R., Lewis, J. M., Glusac, E., Filler, R., Hobby, P., Sutton, B., Tigelaar, R. E. and Hayday, A. C. (2001) 'Regulation of Cutaneous Malignancy by γδ T Cells', *Science*, 294(5542).

Glover, M. T., Deeks, J. J., Raftery, M. J., Cunningham, J. and Leigh, I. M. (1997) 'Immunosuppression and risk of non-melanoma skin cancer in renal transplant recipients', *The Lancet*, 349(9049), p. 398. doi: 10.1016/S0140-6736(97)80015-3.

Goel, S., Wong, A. H. K. and Jain, R. K. (2012) 'Vascular Normalization as a Therapeutic Strategy for Malignant and Nonmalignant Disease', *Cold Spring Harbor Perspectives in Medicine*, 2(3), p. 24. doi: 10.1101/cshperspect.a006486.

Goncharova, E. A., Billington, C. K., Irani, C., Vorotnikov, A. V., Tkachuk, V. A., Penn, R. B., Krymskaya, V. P. and Panettieri, R. A. (2003) 'Cyclic AMP-Mobilizing Agents and Glucocorticoids Modulate Human Smooth Muscle Cell Migration', *American Journal of Respiratory Cell and Molecular Biology*, 29(1), pp. 19–27. doi: 10.1165/rcmb.2002-0254OC.

Gong, S., Miao, Y.-L., Jiao, G.-Z., Sun, M.-J., Li, H., Lin, J., Luo, M.-J. and Tan, J.-H. (2015) 'Dynamics and correlation of serum cortisol and corticosterone under different physiological or stressful conditions in mice', *Plos ONE*, 10(2), p. e0117503. doi: 10.1371/journal.pone.0117503.

Goodwin, J. E. and Geller, D. S. (2012) 'Glucocorticoid-induced hypertension', *Pediatric Nephrology*, 27(7), pp. 1059–1066. doi: 10.1007/s00467-011-1928-4.

Gopinathan, G., Milagre, Pearce, O. M. T., Reynolds, L. E., Hodivala-Dilke, K., Leinster, D. A., Zhong, H., Hollingsworth, R. E., Thompson, R., Whiteford, J. R. & Balkwill, F. (2015), 'Interleukin-6 stimulate defective angiogenesis', *Cancer Research*, 75(15), pp. 3098-3107. doi: 10.1158/0008-5472.CAN-15-1227.

Gordon, C. B., Li, D. G., Stagg, C. A., Manson, P. and Udelsman, R. (1994) 'Impaired wound healing in Cushing's syndrome: the role of heat shock proteins', *Surgery*, 116(6), pp. 1082–7.

Gordon, O., He, Z. H., Gilon, D., Gruener, S., Pietranico-Cole, S., Oppenheim, A. and Keshet, E. (2014) 'A Transgenic Platform for Testing Drugs Intended for Reversal of Cardiac Remodeling Identifies a Novel 11 beta HSD1 Inhibitor Rescuing Hypertrophy Independently of Re-Vascularization', *Plos ONE*, 9(3), p. 11. doi: 10.1371/journal.pone.0092869.

Gorman, A. M., Hirt, U. A., Orrenius, S. and Ceccatelli, S. (2000) 'Dexamethasone pre-treatment interferes with apoptotic death in glioma cells', *Neuroscience*, 96(2), pp. 417–25.

Gower, W.R. Jr, Risch, R. M., Godellas, C. V., Fabri, P. J. (1994), 'HPAC, a new human glucocorticoid-sensitive pancreatic ductal adenocarcinoma cell line', *In Vitro Cellular and Developmental Biology*, 30A(3), 151-61.

Gridley, T. (2010) 'Notch Signaling in the Vasculature', *Current Topics in Developmental Biology*, pp. 277–309. doi: 10.1016/S0070-2153(10)92009-7.

Grivennikov, S. I., Greten, F. R. and Karin, M. (2010) 'Immunity, inflammation, and cancer', *Cell*, 140(6), pp. 883–99. doi: 10.1016/j.cell.2010.01.025.

Gronau, S., Koenig Greger, D., Jerg, M. and Riechelmann, H. (2002) '11beta-Hydroxysteroid dehydrogenase 1 expression in squamous cell carcinomas of the head and neck', *Clinical Otolaryngology and Allied Sciences*, 27(6), pp. 453–457. doi: 10.1046/j.1365-2273.2002.00609.x.

Gündisch, S., Boeckeler, E., Behrends, U., Amtmann, E., Ehrhardt, H. and Jeremias, I. (2012) 'Glucocorticoids augment survival and proliferation of tumor cells', *Anticancer Research*, 32(10), pp. 4251–61.

Guo, C., Ricchiuti, V., Lian, B. Q., Yao, T. M., Coutinho, P., Romero, J. R., Li, J., Williams, G. H. and Adler, G. K. (2008) 'Mineralocorticoid Receptor Blockade Reverses Obesity-Related Changes in Expression of Adiponectin, Peroxisome Proliferator-Activated Receptor- , and Proinflammatory Adipokines', *Circulation*, 117(17), pp. 2253–2261. doi: 10.1161/CIRCULATIONAHA.107.748640.

Hadoke, P. W. F., Christy, C., Kotelevtsev, Y. V, Williams, B. C., Kenyon, C. J., Seckl, J. R., Mullins, J. J. and Walker, B. R. (2001) 'Endothelial cell dysfunction in mice after transgenic knockout of type 2, but not type 1, 11 beta-hydromysteroid dehydrogenase', *Circulation*, 104(23), pp. 2832–2837. doi: 10.1161/hc4801.100077.

Hadoke, P. W. F., Macdonald, L., Logie, J. J., Small, G. R., Dover, a. R. and Walker, B. R. (2006) 'Intra-vascular glucocorticoid metabolism as a modulator of vascular structure and function', *Cellular and Molecular Life Sciences*, 63(5), pp. 565–578. doi: 10.1007/s00018-005-5427-2.

Hadoke, P. W. F., Kipari, T., Seckl, J. R. & Chapman, K. E. (2013), 'Modulation of 11β-Hydroxysteroid Dehydrogenase as a Strategy to Reduce Vascular Inflammation', *Current Atherosclerosis Reports,* 15(5), pp. 320. doi: 10.1007/s11883-013-0320-1.

Hagendoorn, J., Tong, R., Fukumura, D., Lin, Q., Lobo, J., Padera, T. P., Xu, L., Kucherlapati, R. and Jain, R. K. (2006) 'Onset of Abnormal Blood and Lymphatic Vessel Function and Interstitial Hypertension in Early Stages of Carcinogenesis', *Cancer Research*, 66(7), pp. 3360–3364. doi: 10.1158/0008-5472.CAN-05-2655.

Hammami, M. M. and Siiteri, P. K. (1991) 'Regulation of 11 β -Hydroxysteroid Dehydrogenase Activity in Human Skin Fibroblasts: Enzymatic Modulation of Glucocorticoid Action', *The Journal of Clinical Endocrinology & Metabolism*, 73(2), pp. 326–334. doi: 10.1210/jcem-73-2-326.

Hanahan, D. and Coussens, L. M. (2012) 'Accessories to the Crime: Functions of Cells Recruited to the Tumor Microenvironment', *Cancer Cell*, 21(3), pp. 309–322. doi: 10.1016/j.ccr.2012.02.022.

Hanahan, D. and Folkman, J. (1996) 'Patterns and emerging mechanisms of the angiogenic switch during tumorigenesis', *Cell*, 86(3), pp. 353–64.

Hanahan, D. and Weinberg, R. A. (2000) 'The hallmarks of cancer', *Cell*, 100(1), pp. 57–70.

Hanahan, D. and Weinberg, R. A. (2011) 'Hallmarks of Cancer: The Next Generation', *Cell*, 144(5), pp. 646–674. doi: 10.1016/j.cell.2011.02.013.

Handa, M., Kondo, K., Suzuki, H. and Saruta, T. (1984) 'Dexamethasone Hypertension in Rats: Role of Prostaglandins and Pressor Sensitivity to Norepinephrine'. *Hypertension*, 6, pp. 236-241.

Hansen, S., Grabau, D. A., Sørensen, F. B., Bak, M., Vach, W. & Rose, C. (2000), 'The prognostic value of angiogenesis by Chalkley counting in a confirmatory study design on 836 breast cancer patients', *Clinical Cancer Research,* 6(1), pp. 139-146.

Hardy, R., Juarez, M., Naylor, A., Tu, J., Rabbitt, E. H., Filer, A., Stewart, P. M., Buckley, C. D., Raza, K & Cooper, M. S. (2012), 'Synovial DKK1 expression is regulated by local glucocorticoid metabolism in inflammatory arthritis', *Arthritis Research and Therapy,* 14(5), pp. R226. doi: 10.1186/ar4065.

Hardy, R. S., Seibel, M. J. & Cooper, M. S. (2013), 'Targeting 11β-hydroxysteroid dehydrogenases: a novel approach to manipulating local glucocorticoid levels with implications for rheumatic disease', *Current Opinion in Pharmacology,* 13(3), pp. 440-4. doi: 10.1016/j.coph.2013.03.003.

Harno, E., & White, A. (2010). Will treating diabetes with 11β-HSD1 inhibitors affect the HPA axis?, *Trends in Endocrinology and Metabolism*, 21(10), pp. 619–27. doi.org/10.1016/j.tem.2010.06.004.

Harno, E., Cottrell, E. C., Yu, A., DeSchoolmeester, J., Gutierrez, P. M., Denn, M., Swales, J. G., Goldberg, F. W., Bohlooly-Y, M., Andersén, H., Wild, M. J., Turnbull, A. V., Leighton, B. & White, A. (2013), '11β-Hydroxysteroid Dehydrogenase Type 1 (11β-HSD1) Inhibitors Still Improve Metabolic Phenotype in Male 11β-HSD1 Knockout Mice Suggesting Off-Target Mechanisms', *Endocrinology,* 154(12), pp. 4580-4593. doi: 10.1210/en.2013-1613.

Harper, J. and Sainson, R. C. A. (2014) 'Regulation of the anti-tumour immune response by cancer-associated fibroblasts', *Seminars in Cancer Biology*, 25, pp. 69–77. doi: 10.1016/j.semcancer.2013.12.005.

Harris, H. J., Kotelevtsev, Y., Mullins, J. J., Seckl, J. R. and Holmes, M. C. (2001) 'Intracellular regeneration of glucocorticoids by 11 beta-hydroxysteroid dehydrogenase (11 beta-HSD1)

plays a key role in regulation of the hypothalamic-pituitary-adrenal axis: Analysis of 11 beta-HSD-1-deficient mice', *Endocrinology*, 142(1), pp. 114–120. doi: 10.1210/en.142.1.114.

Hasan, Q., Tan, S. T., Gush, J., Peters, S. G. and Davis, P. F. (2000) 'Steroid therapy of a proliferating hemangioma: Histochemical and molecular changes', *Pediatrics*, 105(1), pp. 117–121. doi: 10.1542/peds.105.1.117.

Heikkilä, K., Ebrahim, S. and Lawlor, D. A. (2008) 'Systematic review of the association between circulating interleukin-6 (IL-6) and cancer', *European Journal of Cancer*, 44(7), pp. 937–945. doi: 10.1016/j.ejca.2008.02.047.

Hench, P. S. And Kendall, E. C. (1949) 'The effect of a hormone of the adrenal cortex (17-hydroxy-11-dehydrocorticosterone; compound E) and of pituitary adrenocorticotropic hormone on rheumatoid arthritis', *Proceedings of the staff meetings. Mayo Clinic*, 24(8), pp. 181–97.

Hendrix, M. J. C., Seftor, E. A., Hess, A. R. and Seftor, R. E. B. (2003) 'Angiogenesis: Vasculogenic mimicry and tumour-cell plasticity: lessons from melanoma', *Nature Reviews Cancer*, 3(6), pp. 411–421. doi: 10.1038/nrc1092.

Hennings, H., Glick, A. B., Lowry, D. T., Krsmanovic, L. S., Sly, L. M. & Yuspa, S. H. (1993), 'FVB/N mice: an inbred strain sensitive to the chemical induction of squamous cell carcinomas in the skin', *Carcinogenesis*, 14(11), pp. 2353-8.

Hermanowski-Vosatka, A., Balkovec, J. M., Cheng, K., Chen, H. Y., Hernandez, M., Koo, G. C., Le Grand, C. B., Li, Z. H., Metzger, J. M., Mundt, S. S., Noonan, H., Nunes, C. N., Olson, S. H., Pikounis, B., Ren, N., Robertson, N., Schaeffer, J. M., Shah, K., Springer, M. S., Strack, A. M., Strowski, M., Wu, K., Wu, T. J., Xiao, J. Y., Zhang, B. B., Wright, S. D. and Thieringer, R. (2005) '11 beta-HSD1 inhibition ameliorates metabolic syndrome and prevents progression of atherosclerosis in mice', *Journal of Experimental Medicine*, 202(4), pp. 517–527. doi: 10.1084/jem.20050119.

Hess, A. R., Seftor, E. A., Gruman, L. M., Kinch, M. S., Seftor, R. E. B. and Hendrix, M. J. C. (2006) 'VE-cadherin regulates EphA2 in aggressive melanoma cells through a novel signaling pathway: Implications for vasculogenic mimicry', *Cancer Biology & Therapy*, 5(2), pp. 228–233. doi: 10.4161/cbt.5.2.2510.

Heuser, I. J., Gotthardt, U., Schweiger, U., Schmider, J., Lammers, C. H., Dettling, M. & Holsboer, F. (1994), 'Age-associated changes of pituitary-adrenocortical hormone regulation in humans: importance of gender', *Neurobiology of Aging*, 15(2), pp. 227-31.

Hingorani, S. R., Wang, L., Multani, A. S., Combs, C., Deramaudt, T. B., Hruban, R. H., Rustgi, A. K., Chang, S. and Tuveson, D. A. (2005), 'Trp53R172H and KrasG12D cooperate to promote chromosomal instability and widely metastatic pancreatic ductal adenocarcinoma in mice', *Cancer Cell*, 7(5), pp. 469-483. doi: 10.1016/j.ccr.2005.04.023.

Hofmann, J., Kaiser, U., Maasberg, M., & Havemann, K. (1995). 'Glucocorticoid receptors and growth inhibitory effects of dexamethasone in human lung cancer cell lines'. *European Journal of Cancer*, 31A(12), 2053–8.

Hollenberg, S. M., Weinberger, C., Ong, E. S., Cerelli, G., Oro, A., Lebo, R., Thompson, E. B., Rosenfeld, M. G. and Evans, R. M. (1985) 'Primary structure and expression of a functional human glucocorticoid receptor cDNA.', *Nature*, 318(6047), pp. 635–41.

Hompland, T., Erikson, A., Lindgren, M., Lindmo, T., & de Lange Davies, C. (2008). Second-harmonic generation in collagen as a potential cancer diagnostic parameter. *Journal of Biomedical Optics*, 13(5), 54050. doi.org/10.1117/1.2983664.

Hori, Y., Hu, D. E., Yasui, K., Smither, R. L., Gresham, G. A. and Fan, T. P. D. (1996) 'Differential effects of angiostatic steroids and dexamethasone on angiogenesis and cytokine levels in rat sponge implants', *British Journal of Pharmacology*, 118(7), pp. 1584–1591.

Hou, L., Kim, J. J., Woo, Y. J. and Huang, N. F. (2016) 'Stem cell-based therapies to promote angiogenesis in ischemic cardiovascular disease', *American Journal of Physiology - Heart and Circulatory Physiology*, 310(4).

Huang, P. Y. & Balmain, A. (2014), 'Modeling Cutaneous Squamous Carcinoma Development in the Mouse', *Cold Spring Harbour Perspectives in Medicine*, 4(9), a013623. doi: 10.1101/cshperspect.a013623.

Huang, D. W., Sherman, B. T., & Lempicki, R. A. (2008). Systematic and integrative analysis of large gene lists using DAVID bioinformatics resources. *Nature Protocols*, 4(1), pp. 44–57. doi.org/10.1038/nprot.2008.211.

Hundertmark, S., Bühler, H., Rudolf, M., Weitzel, H. K. and Ragosch, V. (1997) 'Inhibition of 11 beta-hydroxysteroid dehydrogenase activity enhances the antiproliferative effect of glucocorticosteroids on MCF-7 and ZR-75-1 breast cancer cells', *The Journal of Endocrinology*, 155(1), pp. 171–80.

Ignatova, I. D., Kostadinova, R. M., Goldring, C. E., Nawrocki, A. R., Frey, F. J. and Frey, B. M. (2009) 'Tumor necrosis factor-α upregulates 11β-hydroxysteroid dehydrogenase type 1 expression by CCAAT/enhancer binding protein-β in HepG2 cells', *American Journal of Physiology - Endocrinology and Metabolism*, 296(2).

Inaba, H. and Pui, C.-H. (2010) 'Glucocorticoid use in acute lymphoblastic leukaemia', *The Lancet*. Oncology. NIH Public Access, 11(11), pp. 1096–106. doi: 10.1016/S1470-2045(10)70114-5.

Inoue, H., Umesono, K., Nishimori, T., Hirata, Y. and Tanabe, T. (1999) 'Glucocorticoid-Mediated Suppression of the Promoter Activity of the Cyclooxygenase-2 Gene Is Modulated by Expression of Its Receptor in Vascular Endothelial Cells', *Biochemical and Biophysical Research Communications*, 254(2), pp. 292–298. doi: 10.1006/bbrc.1998.9939.

Iqbal, J., Macdonald, L. J., Low, L., Seckl, J. R., Yau, C. W., Walker, B. R. and Hadoke, P. W. F. (2012) 'Contribution of Endogenous Glucocorticoids and Their Intravascular Metabolism by 11 beta-HSDs to Postangioplasty Neointimal Proliferation in Mice', *Endocrinology*, 153(12), pp. 5896–5905. doi: 10.1210/en.2012-1481.

Ishiguro, H., Kawahara, T., Zheng, Y., Kashiwagi, E., Li, Y. & Miyamoto, H. (2014), 'Differential regulation of bladder cancer growth by various glucocorticoids: corticosterone and prednisone inhibit cell invasion without promoting cell proliferation or reducing cisplatin cytotoxicity', *Cancer Chemotherapy and Pharmacology*, 74(2), pp 249-255.

Isner, J. M. (2002) 'Myocardial gene therapy', *Nature*, 415(6868), pp. 234–239. doi: 10.1038/415234a.

Itoi, S., Terao, M., Murota, H. and Katayama, I. (2013) '11β-Hydroxysteroid dehydrogenase 1 contributes to the pro-inflammatory response of keratinocytes', *Biochemical and Biophysical Research Communications*, 440(2), pp. 265–270. doi: 10.1016/j.bbrc.2013.09.065.

Iyer, N. V, Kotch, L. E., Agani, F., Leung, S. W., Laughner, E., Wenger, R. H., Gassmann, M., Gearhart, J. D., Lawler, A. M., Yu, A. Y. and Semenza, G. L. (1998) 'Cellular and developmental control of O2 homeostasis by hypoxia-inducible factor 1 alpha.', *Genes & Development*, 12(2), pp. 149–62.

Jain, R. K. (2003) 'Molecular regulation of vessel maturation', *Nature Medicine*, 9(6), pp. 685–693. doi: 10.1038/nm0603-685.

Jain, R. K., Duda, D. G., Clark, J. W. and Loeffler, J. S. (2006) 'Lessons from phase III clinical trials on anti-VEGF therapy for cancer', *Nature Clinical Practice Oncology*, 3(1), pp. 24–40. doi: 10.1038/ncponc0403.

Jackson, J. R., Seed, M. P., Kircher, C. H., Willoughby, D. A. & Winkler, J. D. (1997), 'The codependence of angiogenesis and chronic inflammation', *FASEB Journal*, 11(6), pp. 457-65.

Jakobsson, L., Franco, C. A., Bentley, K., Collins, R. T., Ponsioen, B., Aspalter, I. M., Rosewell, I., Busse, M., Thurston, G., Medvinsky, A., Schulte-Merker, S. and Gerhardt, H. (2010) 'Endothelial cells dynamically compete for the tip cell position during angiogenic sprouting', *Nature Cell Biology*, 12(10), pp. 943–953. doi: 10.1038/ncb2103.

Jamieson, P. M., Chapman, K. E., Edwards, C. R. and Seckl, J. R. (1995) '11 beta-hydroxysteroid dehydrogenase is an exclusive 11 beta- reductase in primary cultures of rat hepatocytes: effect of physicochemical and hormonal manipulations.', *Endocrinology*, 136(11), pp. 4754–4761. doi: 10.1210/endo.136.11.7588203.

Jeansson, M., Gawlik, A., Anderson, G., Li, C., Kerjaschki, D., Henkelman, M. and Quaggin, S. E. (2011) 'Angiopoietin-1 is essential in mouse vasculature during development and in response to injury', *Journal of Clinical Investigation*, 121(6), pp. 2278–2289. doi: 10.1172/JCI46322.

Jobe, N. P., Rösel, D., Dvořánková, B., Kodet, O., Lacina, L., Mateu, R., Smetana, K. and Brábek, J. (2016) 'Simultaneous blocking of IL-6 and IL-8 is sufficient to fully inhibit CAF-induced human melanoma cell invasiveness', *Histochemistry and Cell Biology*, 146(2), pp. 205–217. doi: 10.1007/s00418-016-1433-8.

Joffe, H. V. and Adler, G. K. (2005) 'Effect of Aldosterone and Mineralocorticoid Receptor Blockade on Vascular Inflammation', *Heart Failure Reviews*. Kluwer Academic Publishers, 10(1), pp. 31–37. doi: 10.1007/s10741-005-2346-0.

Jung, C., Greco, S., Nguyen, H. H. T., Ho, J. T., Lewis, J. G., Torpy, D. J. and Inder, W. J. (2014) 'Plasma, salivary and urinary cortisol levels following physiological and stress doses of hydrocortisone in normal volunteers', *BMC Endocrine Disorders*, 14, p. 91. doi: 10.1186/1472-6823-14-91.

Kalluri, R. (2016) 'The biology and function of fibroblasts in cancer', *Nature Reviews Cancer*, 16(9), pp. 582–598. doi: 10.1038/nrc.2016.73.

Kamradt, M. C., Mohideen, N., Krueger, E., Walter, S. and Vaughan, A. T. (2000) 'Inhibition of radiation-induced apoptosis by dexamethasone in cervical carcinoma cell lines depends upon increased HPV E6/E7, *British Journal of Cancer*, 82(10), pp. 1709–1716. doi: 10.1054/bjoc.2000.1114.

Kaplan, D. H., Shankaran, V., Dighe, A. S., Stockert, E., Aguet, M., Old, L. J. and Schreiber, R. D. (1998) 'Demonstration of an interferon gamma-dependent tumor surveillance system in immunocompetent mice.', *Proceedings of the National Academy of Sciences of the United States of America*, 95(13), pp. 7556–61.

Karmakar, S., Jin, Y. and Nagaich, A. K. (2013) 'Interaction of Glucocorticoid Receptor (GR) with Estrogen Receptor (ER) α and Activator Protein 1 (AP1) in Dexamethasone-mediated Interference of ERα Activity', *Journal of Biological Chemistry*, 288(33), pp. 24020–24034. doi: 10.1074/jbc.M113.473819.

Karnoub, A. E., Dash, A. B., Vo, A. P., Sullivan, A., Brooks, M. W., Bell, G. W., Richardson, A. L., Polyak, K., Tubo, R. and Weinberg, R. A. (2007) 'Mesenchymal stem cells within tumour stroma promote breast cancer metastasis', *Nature*, 449(7162), pp. 557–563. doi: 10.1038/nature06188.

Kennedy, B. and Ziegler, M. G. (1991) 'Cardiac epinephrine synthesis. Regulation by a glucocorticoid', *Circulation*, 84(2).

Kennedy, D., Pignatelli, M., Hassona, Y., Prime, S. S. and Cirillo, N. (2015) 'The Role of the Glucocorticoid System in Anchorage- independence during Progression of Squamous Cell Carcinoma', *American Journal of Oral Medicine*, 1(1), pp. 8–19. doi: 10.7726/ajom.2015.1003.

Kim, R., Emi, M. and Tanabe, K. (2007) 'Cancer immunoediting from immune surveillance to immune escape', *Immunology*, 121(1), pp. 1–14. doi: 10.1111/j.1365-2567.2007.02587.x.

Kim, D.-H., Gutierrez-Aguilar, R., Kim, H.-J., Woods, S. C. and Seeley, R. J. (2013) 'Increased adipose tissue hypoxia and capacity for angiogenesis and inflammation in young diet-sensitive C57 mice compared with diet-resistant FVB mice.', *International Journal of Obesity*, 37(6), pp. 853–60. doi: 10.1038/ijo.2012.141.

Kipari, T., Hadoke, P. W. F., Iqbal, J., Man, T. Y., Miller, E., Coutinho, A. E., Zhang, Z. G., Sullivan, K. M., Mitic, T., Livingstone, D. E. W., Schrecker, C., Samuel, K., White, C. I., Bouhlel, M. A., Chinetti-Gbaguidi, G., Staels, B., Andrew, R., Walker, B. R., Savill, J. S., Chapman, K. E. and Seckl, J. R. (2013) '11 beta-hydroxysteroid dehydrogenase type 1 deficiency in bone marrow-derived cells reduces atherosclerosis', *The FASEB Journal*, 27(4), pp. 1519–1531. doi: 10.1096/fj.12-219105.

Klein-Szanto, A. J., Larcher, F., Bonfil, R. D. & Conti, C. J. (1989), 'Multistage chemical carcinogenesis protocols produce spindle cell carcinomas of the mouse skin', *Carcinogenesis*; 10(11), pp. 2169-72.

Koh, Y. J., Kim, H.-Z., Hwang, S.-I., Lee, J. E., Oh, N., Jung, K., Kim, M., Kim, K. E., Kim, H., Lim, N.-K., Jeon, C.-J., Lee, G. M., Jeon, B. H., Nam, D.-H., Sung, H. K., Nagy, A., Yoo, O. J. and Koh, G. Y. (2010) 'Double Antiangiogenic Protein, DAAP, Targeting VEGF-A and Angiopoietins in Tumor Angiogenesis, Metastasis, and Vascular Leakage', *Cancer Cell*, 18(2), pp. 171–184. doi: 10.1016/j.ccr.2010.07.001.

Korbonits, M., Bujalska, I., Shimojo, M., Nobes, J., Jordan, S., Grossman, A. B. and Stewart, P. M. (2001) 'Expression of 11β-Hydroxysteroid Dehydrogenase Isoenzymes in the Human Pituitary: Induction of the Type 2 Enzyme in Corticotropinomas and Other Pituitary Tumors', *The Journal of Clinical Endocrinology & Metabolism*, 86(6), pp. 2728–2733. doi: 10.1210/jcem.86.6.7563.

Kornel, L., Ramsay, C., Kanamarlapudi, N., Travers, T. and Packer, W. (1982) 'Evidence for the presence in arterial walls of intracellular-molecular mechanism for action of mineralocorticoids', *Clinical and Experimental Hypertension. Part A, Theory and practice*, 4(9–10), pp. 1561–82.

Kotelevtsev, Y., Holmes, M. C., Burchell, a, Houston, P. M., Schmoll, D., Jamieson, P., Best, R., Brown, R., Edwards, C. R., Seckl, J. R. and Mullins, J. J. (1997) '11Beta-Hydroxysteroid Dehydrogenase Type 1 Knockout Mice Show Attenuated Glucocorticoid-Inducible Responses and Resist Hyperglycemia on Obesity or Stress.', *Proceedings of the National Academy of Sciences of the United States of America*, 94(26), pp. 14924–14929. doi: 10.1073/pnas.94.26.14924.

Koyama, K. and Krozowski, Z. (2001) 'Modulation of 11 beta-hydroxysteroid dehydrogenase type 2 activity in Ishikawa cells is associated with changes in cellular proliferation', *Molecular and Cellular Endocrinology*, 183(1–2), pp. 165–70.

Koyama, K., Myles, K., Smith, R. and Krozowski, Z. (2001) 'Expression of the 11beta-hydroxysteroid dehydrogenase type II enzyme in breast tumors and modulation of activity and cell growth in

PMC42 cells', *The Journal of Steroid Biochemistry and Molecular Biology*, 76(1–5), pp. 153–9.

Krozowski, Z. S. and Funder, J. W. (1983) 'Renal mineralocorticoid receptors and hippocampal corticosterone-binding species have identical intrinsic steroid specificity', *Proceedings of the National Academy of Sciences of the United States of America*, 80(19), pp. 6056–60.

Kuhweide, R., van Damme, J. and Ceuppens, J. L. (1990) 'Tumor necrosis factor-α and interleukin 6 synergistically induce T cell growth', *European Journal of Immunology*, 20(5), pp. 1019–1025. doi: 10.1002/eji.1830200511.

Kuo, T., McQueen, A., Chen, T.-C. and Wang, J.-C. (2015) 'Regulation of Glucose Homeostasis by Glucocorticoids', in *Glucocorticoid Signaling*. Springer, pp. 99–126. doi: 10.1007/978-1-4939-2895-8_5.

Lakshmi, V. And Monder, C. (1988) 'Purification and Characterization of the Corticosteroid 1lβ-Dehydrogenase Component of the Rat Liver 1lβ-Hydroxysteroid Dehydrogenase Complex', *Endocrinology*, 123(5), pp. 2390–2398. doi: 10.1210/endo-123-5-2390.

Lakshmi, V., Sakai, R. R., Mcewen, B. S. And Monder, C. (1991) 'Regional Distribution of 1 β-Hydroxysteroid Dehydrogenase in Rat Brain', *Endocrinology*, 128(4), pp. 1741–1748. doi: 10.1210/endo-128-4-1741.

Lavery, G. G., Walker, E. A., Draper, N., Jeyasuria, P., Marcos, J., Shackleton, C. H. L., Parker, K. L., White, P. C. and Stewart, P. M. (2006) 'Hexose-6-phosphate Dehydrogenase Knock-out Mice Lack 11beta-Hydroxysteroid Dehydrogenase Type 1-mediated Glucocorticoid Generation', *Journal of Biological Chemistry*, 281(10), pp. 6546–6551. doi: 10.1074/jbc.M512635200.

Leckie, C. M., Welberg, L. A. and Seckl, J. R. (1998) '11beta-hydroxysteroid dehydrogenase is a predominant reductase in intact rat Leydig cells', *The Journal of Endocrinology*, 159(2), pp. 233–8.

Lee, J. H., Gao, Z. and Ye, J. (2013) 'Regulation of 11β-HSD1 expression during adipose tissue expansion by hypoxia through different activities of NF-κB and HIF-1α.', American journal of physiology. *Endocrinology and Metabolism*, 304(10), pp. E1035-41. doi: 10.1152/ajpendo.00029.2013.

Lee, S., Chen, T. T., Barber, C. L., Jordan, M. C., Murdock, J., Desai, S., Ferrara, N., Nagy, A., Roos, K. P. and Iruela-Arispe, M. L. (2007) 'Autocrine VEGF Signaling Is Required for Vascular Homeostasis', *Cell*, 130(4), pp. 691–703. doi: 10.1016/j.cell.2007.06.054.

Leiter, U., Eigentler, T. & Garbe, C. (2014), 'Epidemiology of skin cancer', *Advances in Experimental Medicine and Biology*, 810, pp. 120-40.

Leonard, M. O., Godson, C., Brady, H. R. and Taylor, C. T. (2005) 'Potentiation of glucocorticoid activity in hypoxia through induction of the glucocorticoid receptor', *Journal of immunology*, 174(4), pp. 2250–7.

Less, J. R., Posner, M. C., Skalak, T. C., Wolmark, N. and Jain, R. K. (1997) 'Geometric resistance and microvascular network architecture of human colorectal carcinoma.', *Microcirculation*, 4(1), pp. 25–33.

Lewis, J. G., Bagley, C. J., Elder, P. A., Bachmann, A. W. and Torpy, D. J. (2005) 'Plasma free cortisol fraction reflects levels of functioning corticosteroid-binding globulin', *Clinica Chimica Acta*, 359(1), pp. 189–194. doi: 10.1016/j.cccn.2005.03.044.

Lim, H.-Y., Müller, N., Herold, M. J., van den Brandt, J. and Reichardt, H. M. (2007) 'Glucocorticoids exert opposing effects on macrophage function dependent on their concentration.', *Immunology*, 122(1), pp. 47–53. doi: 10.1111/j.1365-2567.2007.02611.x.

Lin, A. Y., Ai, Z., Lee, S.-C., Bajcsy, P., Pe'er, J., Leach, L., Maniotis, A. J. and Folberg, R. (2007) 'Comparing vasculogenic mimicry with endothelial cell-lined vessels: techniques for 3D reconstruction and quantitative analysis of tissue components from archival paraffin blocks.', *Applied Immunohistochemistry & Molecular Morphology : AIMM*, 15(1), pp. 113–9.

Lin, K.-T. and Wang, L.-H. (2016) 'New dimension of glucocorticoids in cancer treatment', *Steroids*, 111, pp. 84–88. doi: 10.1016/j.steroids.2016.02.019.

Lin, K.-T., Yeh, Y.-M., Chuang, C.-M., Yang, S. Y., Chang, J.-W., Sun, S.-P., Wang, Y.-S., Chao, K.-C. and Wang, L.-H. (2015) 'Glucocorticoids mediate induction of microRNA-708 to suppress ovarian cancer metastasis through targeting Rap1B', *Nature Communications*, 6, p. 5917. doi: 10.1038/ncomms6917.

Liu, G., Liu, M., Wei, J., Huang, H., Zhang, Y., Zhao, J., Xiao, L., Wu, N., Zheng, L. and Lin, X. (2014) 'CS5931, a Novel Polypeptide in Ciona savignyi, Represses Angiogenesis via Inhibiting Vascular Endothelial Growth Factor (VEGF) and Matrix Metalloproteinases (MMPs)', *Marine Drugs*, 12(3), pp. 1530–1544. doi: 10.3390/md12031530.

Liu, S. L., Schmuck, S., Chorazcyzewski, J. Z., Gros, R. and Feldman, R. D. (2003) 'Aldosterone Regulates Vascular Reactivity', *Circulation*, 108(19).

Liu, X., Tan, X., Xia, M., Wu, C., Song, J., Wu, J., Laurence, A., Xie, Q., Zhang, M., Liang, H., Zhang, B. and Chen, X. (2016) 'Loss of 11βHSD1 enhances glycolysis, facilitates intrahepatic metastasis, and indicates poor prognosis in hepatocellular carcinoma', *Oncotarget*, 7(2). Pp. 2038-53.

Liu, Y. Q., Cousin, J. M., Hughes, J., Van Damme, J., Seckl, J. R., Haslett, C., Dransfield, I., Savill, J. and Rossi, A. G. (1999) 'Glucocorticoids promote nonphlogistic phagocytosis of apoptotic leukocytes', *Journal of Immunology*, 162(6), pp. 3639–3646.

Lloyd, D. J., Helmering, J., Cordover, D., Bowsman, M., Chen, M., Hale, C., Fordstrom, P., Zhou, M., Wang, M., Kaufman, S. A. and Véniant, M. M. (2009) 'Antidiabetic effects of 11β-HSD1 inhibition in a mouse model of combined diabetes, dyslipidaemia and atherosclerosis', *Diabetes, Obesity and Metabolism*, 11(7), pp. 688–699. doi: 10.1111/j.1463-1326.2009.01034.x.

Logie, J. J., Ali, S., Marshall, K. M., Heck, M. M. S., Walker, B. R. and Hadoke, P. W. F. (2010) 'Glucocorticoid-mediated inhibition of angiogenic changes in human endothelial cells is not caused by reductions in cell proliferation or migration', *PloS ONE, 5(12)*, p. e14476. doi: 10.1371/journal.pone.0014476.

Lombès, M., Oblin, M. E., Gasc, J. M., Baulieu, E. E., Farman, N. and Bonvalet, J. P. (1992) 'Immunohistochemical and biochemical evidence for a cardiovascular mineralocorticoid receptor.', *Circulation Research*, 71(3), pp. 503–10.

Longenecker, J. P., Kilty, L. A. and Johnson, L. K. (1982) 'Glucocorticoid influence on growth of vascular wall cells in culture', *Journal of Cellular Physiology*, 113(2), pp. 197–202. doi: 10.1002/jcp.1041130203.

Longenecker, J. P., Kilty, L. A. and Johnson, L. K. (1984) 'Glucocorticoid inhibition of vascular smooth-muscle cell-proliferation - influence of homologous extracellular-matrix and serum mitogens', *Journal of Cell Biology*, 98(2), pp. 534–540. doi: 10.1083/jcb.98.2.534.

Lother, A., Berger, S., Gilsbach, R., Rosner, S., Ecke, A., Barreto, F., Bauersachs, J., Schutz, G. and Hein, L. (2011) 'Ablation of Mineralocorticoid Receptors in Myocytes But Not in Fibroblasts Preserves Cardiac Function', *Hypertension*, 57(4), pp. 746–754. doi: 10.1161/HYPERTENSIONAHA.110.163287.

Love, M. I., Huber, W. and Anders, S. (2014), 'Moderated estimation of fold change and dispersion for RNA-seq data with DESeq2.', *Genome Biology*, 15, p. 550. doi: 10.1186/s13059-014-0550-8.

Low, S. C., Chapman, K. E., Edwards, C. R., Wells, T., Robinson, I. C. and Seckl, J. R. (1994) 'Sexual dimorphism of hepatic 11 beta-hydroxysteroid dehydrogenase in the rat: the role of growth hormone patterns', *The Journal of Endocrinology*, 143(3), pp. 541–8.

Luo, M. J., Thieringer, R., Springer, M. S., Wright, S. D., Hermanowski-Vosatka, A., Plump, A., Balkovec, J. M., Cheng, K., Ding, G. J., Kawka, D. W., Koo, G. C., Le Grand, C. B., Luo, Q., Maletic, M. M., Malkowitz, L., Shah, K., Singer, I., Waddell, S. T., Wu, K. K., Yuan, J., Zhu, J., Stepaniants, S., Yang, X., Yee Lum, P. and Wang, I.-M. (2012) '11β-HSD1 inhibition reduces atherosclerosis in mice by altering proinflammatory gene expression in the vasculature'. *Physiological Genomics*, 45, pp. 47-57.

Luttun, A., Carmeliet, G. and Carmeliet, P. (2002) 'Vascular progenitors: from biology to treatment', *Trends in Cardiovascular Medicine*, 12(2), pp. 88–96.

Lutz-Nicoladoni, C., Wolf, D. & Sopper, S. (2015), 'Modulation of Immune Cell Functions by the E3 Ligase Cbl-b', *Frontiers in Oncology*, 5, pp. 58, doi: 10.3389/fonc.2015.00058.

Luu-The, V., Pelletier, G. and Labrie, F. (2005) 'Quantitative appreciation of steroidogenic gene expression in mouse tissues: new roles for type 2 5α-reductase, 20α-hydroxysteroid dehydrogenase and estrogen sulfotransferase', *The Journal of Steroid Biochemistry and Molecular Biology*, 93(2–5), pp. 269–276. doi: 10.1016/j.jsbmb.2005.01.003.

Majmundar, A. J., Wong, W. J. and Simon, M. C. (2010) 'Hypoxia-Inducible Factors and the Response to Hypoxic Stress', *Molecular Cell*, 40(2), pp. 294–309. doi: 10.1016/j.molcel.2010.09.022.

Malisch, J. L., Breuner, C. W., Gomes, F. R., Chappell, M. A. and Garland Jr, T. (2008) 'Circadian pattern of total and free corticosterone concentrations, corticosteroid-binding globulin, and physical activity in mice selectively bred for high voluntary wheel-running behavior'. *General and Comparative Endocrinology*, 156(2). pp. 210-7. doi: 10.1016/j.ygcen.2008.01.020.

Mangos, G. J., Walker, B. R., Kelly, J. J., Lawson, J. A., Webb, D. J., Whitworth, J. A., BR, W., JR, S., DJ, W. and GCM, W. (2000) 'Cortisol inhibits cholinergic vasodilatation in the human forearm', *American Journal of Hypertension*, 13(11), pp. 1155–1160. doi: 10.1016/S0895-7061(00)01201-2.

Mantovani, A., Sozzani, S., Locati, M., Allavena, P. And Sica, A. (2002) 'Macrophage polarization: tumor-associated macrophages as a paradigm for polarized M2 mononuclear phagocytes', *Trends in Immunology*, 23(11), pp. 549–555. doi: 10.1016/S1471-4906(02)02302-5.

Maragoudakis, M. E., Sarmonika, M. and Panoutsacopoulou, M. (1989) 'Antiangiogenic action of heparin plus cortisone is associated with decreased collagenous protein synthesis in the chick chorioallantoic membrane system', *Journal of Pharmacology and Experimental Therapeutics*, 251(2), pp. 679-82.

Martinez, F.O., Gordon, S., Locati, M. & Mantovani, A. (2006), 'Transcriptional profiling of the human monocyte-to-macrophage differentiation and polarization: new molecules and patterns of gene expression', *Journal of Immunology*, 177(10), pp. 7303-11.

Maser, E., Völker, B. & Friebertshäuser, J (2002), '11β-Hydroxysteroid Dehydrogenase Type 1 from Human Liver: Dimerization and Enzyme Cooperativity Support Its Postulated Role as Glucocorticoid Reductase', *Biochemistry*, 41(7), pp. 2459-2465. doi: 10.1021/bi015803t.

Masoud, G. N., & Li, W. (2015), 'HIF-1α pathway: role, regulation and intervention for cancer therapy', *Acta Pharmaceutica Sinica B,* 5(5) pp. 378-389. doi: 10.1016/j.apsb.2015.05.007.

Maxwell, S. R. J., Moots', R. J. and Kendall, M. J. (1994) 'Corticosteroids: do they damage the cardiovascular system?', *Postgraduate Medical Journal*, 70(830), pp. 863-70.

McCarty, M. F., Somcio, R. J., Stoeltzing, O., Wey, J., Fan, F., Liu, W., Bucana, C. and Ellis, L. M. (2007) 'Overexpression of PDGF-BB decreases colorectal and pancreatic cancer growth by increasing tumor pericyte content', *Journal of Clinical Investigation*, 117(8), pp. 2114–2122. doi: 10.1172/JCI31334.

McGregor, K., Mylonas, K. J., White, C., Walker, B. R. and Gray, G. (2014) '216 Immediate Pharmacological Inhibition of Local Glucocorticoid Generation increases Angiogenesis and Improves Cardiac Funcion after Myocardial Infarction', *Heart*, 100 Suppl, p. A118. doi: 10.1136/heartjnl-2014-306118.216.

McIntyre, A. and Harris, A. L. (2015) 'Metabolic and hypoxic adaptation to anti-angiogenic therapy: a target for induced essentiality', *EMBO Molecular Medicine*, 7(4), pp. 368–379. doi: 10.15252/emmm.201404271.

McKenna, N. J. and O'Malley, B. W. (2002) 'Combinatorial control of gene expression by nuclear receptors and coregulators', *Cell*, 108(4), pp. 465–74.

McLean, G. W., Komiyama, N. H., Serrels, B., Asano, H., Reynolds, L., Conti, F., Hodivala-Dilke, K., Metzger, D., Chambon, P., Grant, S. G. N. and Frame, M. C. (2004), 'Specific deletion of focal adhesion kinase suppresses tumor formation and blocks malignant progression', *Genes and Development,* 18, pp. 2998-3003. doi: 10.1101/gad.316304.

McSweeney, S. J., Hadoke, P. W. F., Kozak, A. M., Small, G. R., Khaled, H., Walker, B. R. and Gray, G. A. (2010) 'Improved heart function follows enhanced inflammatory cell recruitment and angiogenesis in 11β-HSD1-deficient mice post-MI', *Cardiovascular Research*, 88(1), pp. 159–167. doi: 10.1093/cvr/cvq149.

Menakuru, S. R., Brown, N. J., Staton, C. A. and Reed, M. W. R. (2008) 'Angiogenesis in pre-malignant conditions', *British Journal of Cancer*, 99(12), pp. 1961–1966. doi: 10.1038/sj.bjc.6604733.

Menetrier-Caux, C., Montmain, G., Dieu, M. C., Bain, C., Favrot, M.C., Caux, C., Blay, J.Y. (1998), 'Inhibition of the differentiation of dendritic cells from CD34(+) progenitors by tumor cells: role of interleukin-6 and macrophage colony-stimulating factor', *Blood*, 92(12), pp. 4778-91.

Meyer, W. J. and Nichols, N. R. (1981) 'Mineralocorticoid binding in cultured smooth muscle cells and fibroblasts from rat aorta', *Journal of Steroid Biochemistry*, 14(11), pp. 1157–68.

Michailidou, Z., Turban, S., Miller, E., Zou, X. T., Schrader, J., Ratcliffe, P. J., Hadoke, P. W. F., Walker, B. R., Iredale, J. P., Morton, N. M. and Seckl, J. R. (2012) 'Increased Angiogenesis Protects against Adipose Hypoxia and Fibrosis in Metabolic Disease-resistant 11 beta-Hydroxysteroid Dehydrogenase Type 1 (HSD1)-deficient Mice', *Journal of Biological Chemistry*, 287(6), pp. 4188–4197. doi: 10.1074/jbc.M111.259325.

Mikosz, C. A., Brickley, D. R., Sharkey, M. S., Moran, T. W. and Conzen, S. D. (2001) 'Glucocorticoid Receptor-mediated Protection from Apoptosis Is Associated with Induction of the Serine/Threonine Survival Kinase Gene, sgk-1', *Journal of Biological Chemistry*, 276(20), pp. 16649–16654. doi: 10.1074/jbc.M010842200.

Mikucki, M. E., Fisher, D. T., Matsuzaki, J., Skitzki, J. J., Gaulin, N. B., Muhitch, J. B., Ku, A. W., Frelinger, J. G., Odunsi, K., Gajewski, T. F., Luster, A. D. and Evans, S. S. (2015) 'Non-redundant requirement for CXCR3 signalling during tumoricidal T-cell trafficking across tumour vascular checkpoints', *Nature Communications*, 6, p. 7458. doi: 10.1038/ncomms8458.

Mishra, P., Banerjee, D. and Ben-Baruch, A. (2011) 'Chemokines at the crossroads of tumor-fibroblast interactions that promote malignancy', *Journal of Leukocyte Biology*, 89(1), pp. 31–39. doi: 10.1189/jlb.0310182.

Mishra, P. J., Mishra, P. J., Humeniuk, R., Medina, D. J., Alexe, G., Mesirov, J. P., Ganesan, S., Glod, J. W. and Banerjee, D. (2008) 'Carcinoma-Associated Fibroblast-Like Differentiation of Human Mesenchymal Stem Cells', *Cancer Research*, 68(11), pp. 4331–4339. doi: 10.1158/0008-5472.CAN-08-0943.

Möhle, R., Green, D., Moore, M. A., Nachman, R. L. and Rafii, S. (1997) 'Constitutive production and thrombin-induced release of vascular endothelial growth factor by human megakaryocytes and platelets.', *Proceedings of the National Academy of Sciences of the United States of America*, 94(2), pp. 663–8.

Moloney, F. J., Comber, H., Conlon, P. J. and Murphy, G. M. (2006) 'The role of immunosuppression in the pathogenesis of basal cell carcinoma', *British Journal of Dermatology*, 154(4), pp. 790–791. doi: 10.1111/j.1365-2133.2006.07156.x.

Monder, C. and Lakshmi, V. (1989) 'Evidence for kinetically distinct forms of corticosteroid 11 beta-dehydrogenase in rat liver microsomes', *Journal of Steroid Biochemistry*, 32(1A), pp. 77–83.

Morikawa, S., Baluk, P., Kaidoh, T., Haskell, A., Jain, R. K. and McDonald, D. M. (2002) 'Abnormalities in Pericytes on Blood Vessels and Endothelial Sprouts in Tumors', *The American Journal of Pathology*, 160(3), pp. 985–1000. doi: 10.1016/S0002-9440(10)64920-6.

Morgan, S. A., McCabe, E. L., Gathercole, L. L., Hassan-Smith, Z. K., Larner, D. P., Bujalska, I. J., Stewart, P. M., Tomlinson, J. W. & Lavery, G. G. (2014), '11β-HSD1 is the major regulator of the tissue-specific effects of circulating glucocorticoid excess', *Proceedings of the National Academy of Sciences of the United States of America*, 111(24), pp. 2482-91. doi: 10.1073/pnas.1323681111.

Morris, D. J., Brem, A. S., Ge, R. S., Jellinck, P. H., Sakai, R. R. and Hardy, M. P. (2003) 'The functional roles of 11 beta-HSD1: vascular tissue, testis and brain', *Molecular and Cellular Endocrinology*, 203(1–2), pp. 1–12. doi: 10.1016/s0303-7207(03)00094-7.

Morton, N. M., Holmes, M. C., Fievet, C., Staels, B., Tailleux, A., Mullins, J. J. and Seckl, J. R. (2001) 'Improved Lipid and Lipoprotein Profile, Hepatic Insulin Sensitivity, and Glucose Tolerance in 11β-Hydroxysteroid Dehydrogenase Type 1 Null Mice', *Journal of Biological Chemistry*, 276(44), pp. 41293–41300. doi: 10.1074/jbc.M103676200.

Morton, N. M. & Seckl, J. R., '11β-hydroxysteroid dehydrogenase type 1 and obesity', *Frontiers of Hormone Research*, 36, pp. 146-64. doi: 10.1159/0000115363.

Motoo, Y. and Sawabu, N. (1994) 'Antitumor effects of saikosaponins, baicalin and baicalein on human hepatoma cell lines', *Cancer Letters*, 86(1), pp. 91–95. doi: 10.1016/0304-3835(94)90184-8.

Mulatero, P., Panarelli, M., Schiavone, D., Rossi, A., Mengozzi, G., Kenyon, C. J., Chiandussi, L. and Veglio, F. (1997) 'Impaired cortisol binding to glucocorticoid receptors in hypertensive patients', *Hypertension*, 30(5), pp. 1274–8.

Murakami, M., Nguyen, L. T., Zhuang, Z. W., Zhang, Z. W., Moodie, K. L., Carmeliet, P., Stan, R. V and Simons, M. (2008) 'The FGF system has a key role in regulating vascular integrity.', *The Journal of Clinical Investigation*, 118(10), pp. 3355–66. doi: 10.1172/JCI35298.

Murdoch, C., Muthana, M., Coffelt, S. B. and Lewis, C. E. (2008) 'The role of myeloid cells in the promotion of tumour angiogenesis', *Nature Reviews Cancer*, 8(8), p. 618. doi: 10.1038/nrc2444.

Mylonas, K. J., Turner, N. A., Bageghni, S. A., Kenyon, C. J., White, C. I., McGregor, K., Kimmitt, R. A., Sulston, R., Kelly, V., Walker, B. R., Porter, K. E., Chapman, K. E. and Gray, G. A. (2017) '11β-HSD1 suppresses cardiac fibroblast CXCL2, CXCL5 and neutrophil recruitment to the heart post MI.', *The Journal of Endocrinology*, 233(3), pp. 315–327. doi: 10.1530/JOE-16-0501.

Nagy, J. A., Chang, S.-H., Shih, S.-C., Dvorak, A. M. and Dvorak, H. F. (2010) 'Heterogeneity of the tumor vasculature', *Seminars in Thrombosis and Hemostasis*, 36(3), pp. 321–31. doi: 10.1055/s-0030-1253454.

Nauck, M., Karakiulakis, G., Perruchoud, A. P., Papakonstantinou, E. and Roth, M. (1998) 'Corticosteroids inhibit the expression of the vascular endothelial growth factor gene in human vascular smooth muscle cells', *European Journal of Pharmacology*, 341(2–3), pp. 309–315. doi: 10.1016/s0014-2999(97)01464-7.

Newman, A. C. and Hughes, C. C. W. (2012) 'Macrophages and angiogenesis: a role for Wnt signaling', *Vascular Cell*, 4(1), p. 13. doi: 10.1186/2045-824X-4-13.

Nicosia, R. F. and Ottinetti, A. (1990), 'Growth of microvessels in serum-free matrix culture of rat aorta. A quantitative assay of angiogenesis in vitro', *Laboratory investigation*, 63(1), pp. 115-122.

Nixon, M., Upreti, R. and Andrew, R. (2012) '5 -Reduced glucocorticoids: a story of natural selection', *Journal of Endocrinology*, 212(2), pp. 111–127. doi: 10.1530/JOE-11-0318.

Nishimura, K., Nonomura, N., Satoh, E., Harada, .Y, Nakayama, M., Tokizane, T., Fukui, T., Ono, Y., Inoue, H., Shin, M., Tsujimoto, Y., Takayama, H., Aozasa, K. & Okuyama A. (2001), 'Potential mechanism for the effects of dexamethasone on growth of androgen-independent prostate cancer', *Journal of the National Cancer Institute*, 93(22), pp. 1739-46.

Nomura, S., Fujitaka, M., Sakura, N. and Ueda, K. (1997) 'Circadian rhythms in plasma cortisone and cortisol and the cortisone/cortisol ratio', *Clinica Chimica Acta*, 266(2), pp. 83–91. doi: 10.1016/S0009-8981(97)00142-3.

Nowell, P. C. (1976) 'The clonal evolution of tumor cell populations', *Science*, 194(4260), pp. 23–8.

Nuotio-Antar, A. M., Hachey, D. L. and Hasty, A. H. (2007) 'Carbenoxolone treatment attenuates symptoms of metabolic syndrome and atherogenesis in obese, hyperlipidemic mice', *American Journal of Physiology-Endocrinology and Metabolism*, 293(6), pp. E1517–E1528. doi: 10.1152/ajpendo.00522.2007.

Oakley, R. H. and Cidlowski, J. A. (2013) 'The biology of the glucocorticoid receptor: New signaling mechanisms in health and disease', *Journal of Allergy and Clinical Immunology*, 132(5), pp. 1033–1044. doi: 10.1016/j.jaci.2013.09.007.

Oberleithner, H., Schneider, S. W., Albermann, L., Hillebrand, U., Ludwig, T., Riethmüller, C., Shahin, V., Schäfer, C. and Schillers, H. (2003) 'Endothelial Cell Swelling by Aldosterone', *Journal of Membrane Biology*, 196(3), pp. 163–172. doi: 10.1007/s00239-003-0635-6.

Odermatt, A. and Klusonova, P. (2015) '11β-Hydroxysteroid dehydrogenase 1: Regeneration of active glucocorticoids is only part of the story', *The Journal of Steroid Biochemistry and Molecular Biology*, 151, pp. 85–92. doi: 10.1016/j.jsbmb.2014.08.011.

Öhlund, D., Handly-Santana, A., Biffi, G., Elyada, E., Almeida, A. S., Ponz-Sarvise, M., Corbo, V., Oni, T. E., Hearn, S. A., Lee, E. J., Chio, I. I. C., Hwang, C.-I., Tiriac, H., Baker, L. A., Engle, D. D., Feig, C., Kultti, A., Egeblad, M., Fearon, D. T., Crawford, J. M., Clevers, H., Park, Y. and Tuveson, D. A. (2017) 'Distinct populations of inflammatory fibroblasts and myofibroblasts in pancreatic cancer', *The Journal of Experimental Medicine*, 214(3), p. jem.20162024. doi: 10.1084/jem.20162024.

Oishi, Y., Fu, Z. W., Ohnuki, Y., Kato, H. and Noguchi, T. (2002) 'Molecular basis of the alteration in skin collagen metabolism in response to in vivo dexamethasone treatment: effects on the synthesis of collagen type I and III, collagenase, and tissue inhibitors of metalloproteinases', *The British Journal of Dermatology*, 147(5), pp. 859–68.

Olive, K. P., Jacobetz, M. A., Davidson, C. J., Gopinathan, A., McIntyre, D., Honess, D., Madhu, B., Goldgraben, M. A., Caldwell, M. E., Allard, D., Frese, K. K., DeNicola, G., Feig, C., Combs, C., Winter, S. P., Ireland-Zecchini, H., Reichelt, S., Howat, W. J., Chang, A., Dhara, M., Wang, L. F., Ruckert, F., Grutzmann, R., Pilarsky, C., Izeradjene, K., Hingorani, S. R., Huang, P., Davies, S. E., Plunkett, W., Egorin, M., Hruban, R. H., Whitebread, N., McGovern, K., Adams, J., Iacobuzio-Donahue, C., Griffiths, J. and Tuveson, D. A. (2009) 'Inhibition of Hedgehog Signaling Enhances Delivery of Chemotherapy in a Mouse Model of Pancreatic Cancer', *Science*, 324(5933), pp. 1457–1461. doi: 10.1126/science.1171362.

Orimo, A., Gupta, P. B., Sgroi, D. C., Arenzana-Seisdedos, F., Delaunay, T., Naeem, R., Carey, V. J., Richardson, A. L. and Weinberg, R. A. (2005) 'Stromal Fibroblasts Present in Invasive Human Breast Carcinomas Promote Tumor Growth and Angiogenesis through Elevated SDF-1/CXCL12 Secretion', *Cell*, 121(3), pp. 335–348. doi: 10.1016/j.cell.2005.02.034.

Oster, H., Damerow, S., Kiessling, S., Jakubcakova, V., Abraham, D., Tian, J., Hoffmann, M. W. and Eichele, G. (2006) 'The circadian rhythm of glucocorticoids is regulated by a gating mechanism residing in the adrenal cortical clock', *Cell Metabolism*, 4(2), pp. 163–173. doi: 10.1016/j.cmet.2006.07.002.

Ozawa, M. G., Yao, V. J., Chanthery, Y. H., Troncoso, P., Uemura, A., Varner, A. S., Kasman, I. M., Pasqualini, R., Arap, W. and McDonald, D. M. (2005) 'Angiogenesis with pericyte abnormalities in a transgenic model of prostate carcinoma', *Cancer*, 104(10), pp. 2104–2115. doi: 10.1002/cncr.21436.

Özdemir, B. C., Pentcheva-Hoang, T., Carstens, J. L., Zheng, X., Wu, C.-C., Simpson, T. R., Laklai, H., Sugimoto, H., Kahlert, C., Novitskiy, S. V., De Jesus-Acosta, A., Sharma, P., Heidari, P., Mahmood, U., Chin, L., Moses, H. L., Weaver, V. M., Maitra, A., Allison, J. P., LeBleu, V. S. and Kalluri, R. (2014) 'Depletion of Carcinoma-Associated Fibroblasts and Fibrosis Induces Immunosuppression and Accelerates Pancreas Cancer with Reduced Survival', *Cancer Cell*, 25(6), pp. 719–734. doi: 10.1016/j.ccr.2014.04.005.

Pácha, J., Lisá, V. and Mikšík, I. (2002) 'Effect of cellular differentiation on 11β-hydroxysteroid dehydrogenase activity in the intestine', *Steroids*, 67(2), pp. 119–126. doi: 10.1016/S0039-128X(01)00143-X.

Pàez-Ribes, M., Allen, E., Hudock, J., Takeda, T., Okuyama, H., Viñals, F., Inoue, M., Bergers, G., Hanahan, D. and Casanovas, O. (2009) 'Antiangiogenic Therapy Elicits Malignant Progression of Tumors to Increased Local Invasion and Distant Metastasis', *Cancer Cell*, 15(3), pp. 220–231. doi: 10.1016/j.ccr.2009.01.027.

Paleolog, E. M. (2002) ‘Angiogenesis in rheumatoid arthritis’, *Arthritis Research*, 4(Suppl 3), p. S81. doi: 10.1186/ar575.

Pardali, E., Goumans, M.-J. and ten Dijke, P. (2010) ‘Signaling by members of the TGF-β family in vascular morphogenesis and disease’, *Trends in Cell Biology*, 20(9), pp. 556–567. doi: 10.1016/j.tcb.2010.06.006.

Parente, L. (2001) ‘The development of synthetic glucocorticoids’, in *Glucocorticoids*. Basel: Birkhäuser Basel, pp. 35–51. doi: 10.1007/978-3-0348-8348-1_3.

Parker, M. G. (1993) ‘Steroid and related receptors’, *Current Opinion in Cell Biology*, 5(3), pp. 499–504. doi: 10.1016/0955-0674(93)90016-j.

Patenaude, A., Parker, J. and Karsan, A. (2010) ‘Involvement of endothelial progenitor cells in tumor vascularization’, *Microvascular Research*, 79(3), pp. 217–223. doi: 10.1016/j.mvr.2010.01.007.

Pearson, O. H. And Eliel, L. P. (1950) ‘Use of pituitary adrenocorticotropic hormone (ACTH) and cortisone in lymphomas and leukemias’, *JAMA* , 144(16), pp. 1349–53.

Peckett, A. J., Wright, D. C. and Riddell, M. C. (2011) ‘The effects of glucocorticoids on adipose tissue lipid metabolism’, *Metabolism*, 60(11), pp. 1500–1510. doi: 10.1016/j.metabol.2011.06.012.

Peng, K., Pan, Y., Li, J., Khan, Z., Fan, M., Yin, H., Tong, C., Zhao, Y., Liang, G. & Zheng, C. (2016). ‘11β-Hydroxysteroid Dehydrogenase Type 1(11β-HSD1) mediates insulin resistance through JNK activation in adipocytes’. *Scientific Reports*, 6(1), 37160. doi.org/10.1038/srep37160.

Phillips, D. M., Lakshmi, V. And Monder, C. (1989) ‘Corticosteroid 11β-Dehydrogenase in Rat Testis’, *Endocrinology*, 125(1), pp. 209–216. doi: 10.1210/endo-125-1-209.

Phng, L.-K. and Gerhardt, H. (2009) ‘Angiogenesis: A Team Effort Coordinated by Notch’, *Developmental Cell*, 16(2), pp. 196–208. doi: 10.1016/j.devcel.2009.01.015.

Pitt, B., Zannad, F., Remme, W. J., Cody, R., Castaigne, A., Perez, A., Palensky, J. and Wittes, J. (1999) ‘The Effect of Spironolactone on Morbidity and Mortality in Patients with Severe Heart Failure’, *New England Journal of Medicine*, 341(10), pp. 709–717. doi: 10.1056/NEJM199909023411001.

Pitulescu, M. E. and Adams, R. H. (2010) ‘Eph/ephrin molecules--a hub for signaling and endocytosis’, *Genes & Development*, 24(22), pp. 2480–2492. doi: 10.1101/gad.1973910.

Polverini, P. J. and Leibovich, S. J. (1984) ‘Induction Of Neovascularization Invivo And Endothelial Proliferation Invitro By Tumor-Associated Macrophages’, *Laboratory Investigation*, 51(6), pp. 635–642.

Potente, M., Gerhardt, H. and Carmeliet, P. (2011) ‘Basic and Therapeutic Aspects of Angiogenesis’, *Cell*, 146(6), pp. 873–887. doi: 10.1016/j.cell.2011.08.039.

Provencher, P. H., Saltis, J. and Funder, J. W. (1995) ‘Glucocorticoids but not mineralocorticoids modulate endothelin-1 and angiotensin II binding in SHR vascular smooth muscle cells.’, *The Journal of Steroid Biochemistry and Molecular Biology*, 52(3), pp. 219–25.

Provezano, P. P., Cuevas, C., Chang, A. E., Goel, V. K., Von Hoff, D. D., Hingorani, S. R. (2012), ‘Enzymatic Targeting of the Stroma Ablates Physical Barriers to Treatment of Pancreatic Ductal Adenocarcinoma’, *Cancer Cell*, 21(3), pp. 418-429. doi: 10.1016/j.ccr.2012.01.007.

Pufall, M. A. (2015) ‘Glucocorticoids and Cancer’, in *Advances in Experimental Medicine and Biology*, Spinger, pp. 315–333. doi: 10.1007/978-1-4939-2895-8_14.

Pufe, T., Scholz-Ahrens, K. E., Franke, A. T. M., Petersen, W., Mentlein, R., Varoga, D., Tillman, B., Schrezenmeir, J. & Glüer, C. C., (2003), ‘The role of vascular endothelial growth factor in glucocorticoid-induced bone loss: evaluation in a minipig model’. *Bone*,.33(6), pp. 869–876.

Qian, B.-Z. and Pollard, J. W. (2010) ‘Macrophage diversity enhances tumor progression and metastasis.’, *Cell*, 141(1), pp. 39–51. doi: 10.1016/j.cell.2010.03.014.

Quante, M., Tu, S. P., Tomita, H., Gonda, T., Wang, S. S. W., Takashi, S., Baik, G. H., Shibata, W., DiPrete, B., Betz, K. S., Friedman, R., Varro, A., Tycko, B. and Wang, T. C. (2011) ‘Bone Marrow-Derived Myofibroblasts Contribute to the Mesenchymal Stem Cell Niche and Promote Tumor Growth’, *Cancer Cell*, 19(2), pp. 257–272. doi: 10.1016/j.ccr.2011.01.020.

Quax, R. A., Manenschijn, L., Koper, J. W., Hazes, J. M., Lamberts, S. W., van Rossum, E. F. & Feelders, R. A. (2013), ‘Glucocorticoid sensitivity in health and disease’, *Nature Reviews: Endocrinology*, 9(11), pp. 670-86. doi: 10.1038/nrendo.2013.183.

Rabbitt, E. H., Ayuk, J., Boelaert, K., Sheppard, M. C., Hewison, M., Stewart, P. M. and Gittoes, N. J. L. (2003a) ‘Abnormal expression of 11β-hydroxysteroid dehydrogenase type 2 in human pituitary adenomas: a prereceptor determinant of pituitary cell proliferation’, *Oncogene*, 22(11), pp. 1663–1667. doi: 10.1038/sj.onc.1206293.

Rabbitt, E. H., Gittoes, N. J. L., Stewart, P. M. and Hewison, M. (2003b) ‘11β-Hydroxysteroid dehydrogenases, cell proliferation and malignancy’, *The Journal of Steroid Biochemistry and Molecular Biology*, 85(2), pp. 415–421. doi: 10.1016/S0960-0760(03)00224-3.

Rabbitt, E. H., Lavery, G. G., Walker, E. A., Cooper, M. S., Stewart, P. M. and Hewison, M. (2002) ‘Prereceptor regulation of glucocorticoid action by 11beta-hydroxysteroid dehydrogenase: a novel determinant of cell proliferation’, *The FASEB Journal*, 16(1), pp. 36–44. doi: 10.1096/fj.01-0582com.

Rae, M., Mohamad, A., Price, D., Hadoke, P. W. F., Walker, B. R., Mason, J. I., Hillier, S. G. and Critchley, H. O. D. (2009) ‘Cortisol Inactivation by 11 beta-Hydroxysteroid dehydrogenase-2 May Enhance Endometrial Angiogenesis via Reduced Thrombospondin-1 in Heavy Menstruation’, *Journal of Clinical Endocrinology & Metabolism*, 94(4), pp. 1443–1450. doi: 10.1210/jc.2008-1879.

Rajan, V., Chapman, K. E., Lyons, V., Jamieson, P., Mullins, J. J., Edwards, C. R. W. and Seckl, J. R. (1995) ‘Cloning, sequencing and tissue-distribution of mouse 11β-hydroxysteroid dehydrogenase-1 cDNA’, *The Journal of Steroid Biochemistry and Molecular Biology*, 52(2), pp. 141–147. doi: 10.1016/0960-0760(94)00159-J.

Rajan, V., Edwards, C. and Seckl, J. (1996) ‘11 beta-Hydroxysteroid dehydrogenase in cultured hippocampal cells reactivates inert 11-dehydrocorticosterone, potentiating neurotoxicity’, *Journal of Neuroscience*, 16(1), pp. 65-70

Raza, A., Franklin, M. J. and Dudek, A. Z. (2010) ‘Pericytes and vessel maturation during tumor angiogenesis and metastasis’, *American Journal of Hematology*, 85(8), pp. 593–598. doi: 10.1002/ajh.21745.

Reddy, T. E., Pauli, F., Sprouse, R. O., Neff, N. F., Newberry, K. M., Garabedian, M. J. and Myers, R. M. (2009) ‘Genomic determination of the glucocorticoid response reveals unexpected mechanisms of gene regulation’, *Genome Research*, 19(12), pp. 2163–2171. doi: 10.1101/gr.097022.109.

Rehman, J., Li, J., Orschell, C. M. and March, K. L. (2003) 'Peripheral blood endothelial progenitor cells are derived from monocyte/macrophages and secrete angiogenic growth factors', *Circulation*, 107(8), pp. 1164–9.

Reinmuth, N., Liu, W., Jung, Y. D., Ahmad, S. A., Shaheen, R. M., Fan, F., Bucana, C. D., McMahon, G., Gallick, G. E. and Ellis, L. M. (2001) 'Induction of VEGF in perivascular cells defines a potential paracrine mechanism for endothelial cell survival.', *The FASEB Journal*, 15(7), pp. 1239–41.

Rettura, G., Seitter, J., Zisblatt, M., Levenson, S. M., Levine, N. and Seifter, E. (1973) 'Metyrapone-Inhibited Oncogenesis in Mice Inoculated With a Murine Sarcoma Virus2', *JNCI: Journal of the National Cancer Institute*, 51(6), pp. 1983–1985. doi: 10.1093/jnci/51.6.1983.

Rhim, A. D., Oberstein, P. E., Thomas, D. H., Mirek, E. T., Palermo, C. F., Sastra, S. A., Dekleva, E. N., Saunders, T., Becerra, C. P., Tattersall, I. W., Westphalen, C. B., Kitajewski, J., Fernandez-Barrena, M. G., Fernandez-Zapico, M. E., Iacobuzio-Donahue, C., Olive, K. P. and Stanger, B. Z. (2014) 'Stromal Elements Act to Restrain, Rather Than Support, Pancreatic Ductal Adenocarcinoma', *Cancer Cell*, 25(6), pp. 735–747. doi: 10.1016/j.ccr.2014.04.021.

Risau, W. (1997) 'Mechanisms of angiogenesis', *Nature*, 386(6626), pp. 671–674. doi: 10.1038/386671a0.

Rog-Zielinska, E. A., Craig, M.-A., Manning, J. R., Richardson, R. V, Gowans, G. J., Dunbar, D. R., Gharbi, K., Kenyon, C. J., Holmes, M. C., Hardie, D. G., Smith, G. L. and Chapman, K. E. (2015) 'Glucocorticoids promote structural and functional maturation of foetal cardiomyocytes: a role for PGC-1α', *Cell Death and Differentiation*, 22(7), pp. 1106–1116. doi: 10.1038/cdd.2014.181.

Rog-Zielinska, E. A., Thomson, A., Kenyon, C. J., Brownstein, D. G., Moran, C. M., Szumska, D., Michailidou, Z., Richardson, J., Owen, E., Watt, A., Morrison, H., Forrester, L. M., Bhattacharya, S., Holmes, M. C. and Chapman, K. E. (2013) 'Glucocorticoid receptor is required for foetal heart maturation', *Human Molecular Genetics*, 22(16), pp. 3269–3282. doi: 10.1093/hmg/ddt182.

Rohan, R. M., Fernandez, A., Udagawa, T., Yuan, J. and D'Amato, R. J. (2000) 'Genetic heterogeneity of angiogenesis in mice', *FASEB Journal*, 14(7), pp. 871–6.

Rosenbaum, R. M., Cheli, C. D. and Gerritsen, M. E. (1986) 'Dexamethasone inhibits prostaglandin release from rabbit coronary microvessel endothelium', *The American Journal of Physiology*, 250(6 Pt 1), pp. C970-7.

Rosewicz S., McDonald A. R., Maddux, B. A., Goldfine, I. D., Miesfeld, R. L. & Logsdon, C.D., (1988), 'Mechanism of glucocorticoid receptor down-regulation by glucocorticoids', *Journal of Biological Chemistry*, 263(6), pp. 2581-4.

Rousselle, A., Qadri, F., Leukel, L., Yilmaz, R., Fontaine, J. F., Sihn, G., Bader, M., Ahluwalia, A. & Duchene, J. (2013), 'CXCL5 limits macrophage foam cell formation in atherosclerosis', *Journal of Clinical Investigation*, 123(3), pp. 1343-7. doi: 10.1172/JCI66580.

Ruoslahti, E. (2002) 'specialization of tumour vasculature', *Nature Reviews Cancer*, 2(2), pp. 83–90. doi: 10.1038/nrc724.

Rutz, H. P., Mariotta, M., von Knebel Doeberitz, M. and Mirimanoff, R. O. (1998) 'Dexamethasone-induced radioresistance occurring independent of human papilloma virus gene expression in cervical carcinoma cells', *Strahlentherapie und Onkologie* , 174(2), pp. 71–4.

Saharinen, P., Eklund, L., Miettinen, J., Wirkkala, R., Anisimov, A., Winderlich, M., Nottebaum, A., Vestweber, D., Deutsch, U., Koh, G. Y., Olsen, B. R. and Alitalo, K. (2008) 'Angiopoietins assemble distinct Tie2 signalling complexes in endothelial cell–cell and cell–matrix contacts', *Nature Cell Biology*, 10(5), pp. 527–537. doi: 10.1038/ncb1715.

Sahu, B., Laakso, M., Pihlajamaa, P., Ovaska, K., Sinielnikov, I., Hautaniemi, S. & Janne, O. A. (2013) 'FoxA1 Specifies Unique Androgen and Glucocorticoid Receptor Binding Events in Prostate Cancer Cells', *Cancer Research*, 73(5), pp. 1570–1580. doi: 10.1158/0008-5472.CAN-12-2350.

Sakamoto, H., Kitano, M., Suetomi, Y., Maekawa, K., Takeyama, Y. & Kudo, M. (2008), 'Utility of contrast-enhanced endoscopic ultrasonography for diagnosis of small pancreatic carcinomas', *Ultrasound in Medicine and Biology*, 34(4), pp. 525-32. doi: 10.1016/j.ultrasmedbio.2007.09.018.

Salvesen, H. B. and Akslen, L. A. (1999) 'Significance of tumour-associated macrophages, vascular endothelial growth factor and thrombospondin-1 expression for tumour angiogenesis and prognosis in endometrial carcinomas', *International Journal of Cancer*, 84(5), pp. 539–543.

Sanchis, A., Alba, L., Latorre, V., Sevilla, L. M., Pérez, P., Demonacos, C. and Krstic-Demonacos, M. (2012) 'Keratinocyte-Targeted Overexpression of the Glucocorticoid Receptor Delays Cutaneous Wound Healing', *PLoS ONE*, 7(1), p. e29701. doi: 10.1371/journal.pone.0029701.

Sapolsky, R. M., Romero, L. M. and Munck, A. U. (2000) 'How do glucocorticoids influence stress responses? Integrating permissive, suppressive, stimulatory, and preparative actions', *Endocrine reviews*, 21(1), pp. 55–89. doi: 10.1210/edrv.21.1.0389.

Sarabdjitsingh, R. A., Zhou, M., Yau, J. L. W, Webster, S. P., Walker, B. R., Seckl, J. R., Joëls, M., Krugers, H. J. (2014), 'Inhibiting 11b-hydroxysteroid dehydrogenase type 1 prevents stress effects on hippocampal synaptic plasticity and impairs contextual fear conditioning', *Neuropharmacology*, 81, pp. 231-236. doi: 10.1016/j.neuropharm.2014.01.042.

Sato, A., Suzuki, H., Nakazato, Y., Shibata, H., Inagami, T. and Saruta, T. (1994) 'Increased expression of vascular angiotensin II type 1A receptor gene in glucocorticoid-induced hypertension', *Journal of Hypertension*, 12(5), pp. 511–6.

Sato, T. N., Tozawa, Y., Deutsch, U., Wolburg-Buchholz, K., Fujiwara, Y., Gendron-Maguire, M., Gridley, T., Wolburg, H., Risau, W. and Qin, Y. (1995) 'Distinct roles of the receptor tyrosine kinases Tie-1 and Tie-2 in blood vessel formation', *Nature*, 376(6535), pp. 70–74. doi: 10.1038/376070a0.

Schäfer, M. and Werner, S. (2008) 'Cancer as an overhealing wound: an old hypothesis revisited', *Nature Reviews Molecular Cell Biology*, 9(8), pp. 628–638. doi: 10.1038/nrm2455.

Schaper, W. (2009) 'Collateral circulation', *Basic Research in Cardiology*, 104(1), pp. 5–21. doi: 10.1007/s00395-008-0760-x.

Schlossmacher, G., Stevens, A., & White, A. (2011). 'Glucocorticoid receptor-mediated apoptosis: mechanisms of resistance in cancer cells'. *The Journal of Endocrinology*, 211(1), pp. 17–25. doi.org/10.1530/JOE-11-0135.

Schiffelers, R. M., Metselaar, J. M., Fens, M. H. A. M., Janssen, A. P. C. A., Molema, G. and Storm, G. (2005) 'Liposome-encapsulated prednisolone phosphate inhibits growth of established tumors in mice.', *Neoplasia*, 7(2), pp. 118–27. doi: 10.1593/neo.04340.

Schoors, S., Bruning, U., Missiaen, R., Queiroz, K. C. S., Borgers, G., Elia, I., Zecchin, A., Cantelmo, A. R., Christen, S., Goveia, J., Heggermont, W., Goddé, L., Vinckier, S., Van Veldhoven, P.

P., Eelen, G., Schoonjans, L., Gerhardt, H., Dewerchin, M., Baes, M., De Bock, K., Ghesquière, B., Lunt, S. Y., Fendt, S.-M. and Carmeliet, P. (2015) 'Fatty acid carbon is essential for dNTP synthesis in endothelial cells', *Nature*, 520(7546), pp. 192–197. doi: 10.1038/nature14362.

Schoors, S., De Bock, K., Cantelmo, A. R., Georgiadou, M., Ghesquière, B., Cauwenberghs, S., Kuchnio, A., Wong, B. W., Quaegebeur, A., Goveia, J., Bifari, F., Wang, X., Blanco, R., Tembuyser, B., Cornelissen, I., Bouché, A., Vinckier, S., Diaz-Moralli, S., Gerhardt, H., Telang, S., Cascante, M., Chesney, J., Dewerchin, M. and Carmeliet, P. (2014) 'Partial and Transient Reduction of Glycolysis by PFKFB3 Blockade Reduces Pathological Angiogenesis', *Cell Metabolism*, 19(1), pp. 37–48. doi: 10.1016/j.cmet.2013.11.008.

Schrama, D., thor Straten, P., Fischer, W. H., McLellan, A.D., Bröcker, E. B., Reisfeld, R. A., Becker, J. C. (2001) 'Targeting of lymphotoxin-alpha to the tumor elicits an efficient immune response associated with induction of peripheral lymphoid-like tissue', *Immunity*, 14, pp. 111–121.

Scott, B. A., Lawrence, B., Nguyen, H. H. and Meyer, W. J. (1987) 'Aldosterone and dexamethasone binding in human arterial smooth muscle cells', *Journal of Hypertension*, 5(6), pp. 739–44.

Seckl, J. R. and Walker, B. R. (2001) 'Minireview: 11β-Hydroxysteroid Dehydrogenase Type 1— A Tissue-Specific Amplifier of Glucocorticoid Action 1', *Endocrinology*, 142(4), pp. 1371–1376. doi: 10.1210/endo.142.4.8114.

Serrels, A., McLeod, K., Canel, M., Kinnaird, A., Graham, K., Frame, M. C., & Brunton, V. G. (2012). 'The role of focal adhesion kinase catalytic activity on the proliferation and migration of squamous cell carcinoma cells'. *International Journal of Cancer*, 131(2), 287–297. doi.org/10.1002/ijc.26351.

Serrels, A., Lund, T., Serrels, B., Byron, A., McPherson, R. C., von Kriegsheim A., Gómez-Cuadrado, L., Canel, M., Muir, M., Ring, J. E., Maniati, E., Sims, A. H., Pachter, J. A., Brunton, V. G., Gilbert, N., Anderton, S. M., Nibbs, R. J. and Frame, M. C. (2015), 'Nuclear FAK controls chemokine transcription, Tregs, and evasion of anti-tumor immunity', *Cell*, 163(1), pp. 160-73. doi: 10.1016/j.cell.2015.09.001.

Seyfried, T. N., Shelton, L. M. and Mukherjee, P. (2010) 'Does the existing standard of care increase glioblastoma energy metabolism?', *The Lancet Oncology*, 11(9), pp. 811–813. doi: 10.1016/S1470-2045(10)70166-2.

Shaheen, R. M., Tseng, W. W., Davis, D. W., Liu, W., Reinmuth, N., Vellagas, R., Wieczorek, A. A., Ogura, Y., McConkey, D. J., Drazan, K. E., Bucana, C. D., McMahon, G. and Ellis, L. M. (2001) 'Tyrosine kinase inhibition of multiple angiogenic growth factor receptors improves survival in mice bearing colon cancer liver metastases by inhibition of endothelial cell survival mechanisms.', *Cancer Research*, 61(4), pp. 1464–8.

Shalaby, F., Ho, J., Stanford, W. L., Fischer, K. D., Schuh, A. C., Schwartz, L., Bernstein, A. and Rossant, J. (1997) 'A requirement for Flk1 in primitive and definitive hematopoiesis and vasculogenesis.', *Cell*, 89(6), pp. 981–90.

Shankaran, V., Ikeda, H., Bruce, A. T., White, J. M., Swanson, P. E., Old, L. J. and Schreiber, R. D. (2001) 'IFNgamma and lymphocytes prevent primary tumour development and shape tumour immunogenicity.', *Nature*, 410(6832), pp. 1107–1111. doi: 10.1038/35074122.

Shiga, K., Hara, M., Nagasaki, T., Takafumi, S., Takahashi, H. & Takeyama, H. (2015), 'Cancer-Associated Fibroblasts: Their Characteristics and Their Roles in Tumor Growth', *Cancers (Basel)*, 7(4), pp. 2443-2458. doi: 10.3390/cancers7040902.

Shpilberg, Y., Connor, M. K. & Riddell, M. C. (2015), 'The direct and indirect effects of corticosterone and primary adipose tissue on MCF7 breast cancer cell cycle progression', *Hormone Molecular Biology and Clinical Investigation*, 22(2), pp. 91-100. doi: 10.1515/hmbci-2015-0003.

Sica, A. and Bronte, V. (2007) 'Altered macrophage differentiation and immune dysfunction in tumor development', *Journal of Clinical Investigation*, 117(5), pp. 1155–1166. doi: 10.1172/jci31422.

Sica, A., Saccani, A. and Mantovani, A. (2002) 'Tumor-associated macrophages: A molecular perspective', *International Immunopharmacology*, 2(8), pp. 1045–1054. doi: 10.1016/S1567-5769(02)00064-4.

Sidler, D., Renzulli, P., Schnoz, C., Berger, B., Schneider-Jakob, S., Flück, C., Inderbitzin, D., Corazza, N., Candinas, D. and Brunner, T. (2011) 'Colon cancer cells produce immunoregulatory glucocorticoids', *Oncogene*, 30(21), pp. 2411–2419. doi: 10.1038/onc.2010.629.

Sinha P., Chornoguz, O., Clements, V.K., Artemenko, K. A., Zubarev, R. A., Ostrand-Rosenberg, S. (2011), 'Myeloid-derived suppressor cells express the death receptor Fas and apoptose in response to T cell-expressed FasL', *Blood*, 117(20), pp. 5381-90. doi: 10.1182/blood-2010-11-321752.

Slominski, A. T., Manna, P. R. and Tuckey, R. C. (2014) 'Cutaneous glucocorticosteroidogenesis: securing local homeostasis and the skin integrity', *Experimental Dermatology*, 23(6), pp. 369–374. doi: 10.1111/exd.12376.

Small, G. R., Hadoke, P. W. F., Sharif, I., Dover, A. R., Armour, D., Kenyon, C. J., Gray, G. a and Walker, B. R. (2005) 'Preventing local regeneration of glucocorticoids by 11beta-hydroxysteroid dehydrogenase type 1 enhances angiogenesis.', *Proceedings of the National Academy of Sciences of the United States of America*, 102(34), pp. 12165–12170. doi: 10.1073/pnas.0500641102.

Smith, B. T., Tanswell, A. K., Minshall, D., Bogues, W. N. and Vreeken, E. (1982) 'Influence of corticosteroids on glycogen content and steroid 11-reductase activity in lung and liver of the fetal and newborn rat.', *Biology of the Neonate*, 42(5–6), pp. 201–7.

Smith, R. E., Little, P. J., Maguire, J. A., Stein-Oakley, A. N. and Krozowski, Z. S. (1996) 'Vascular localization of the 11 beta-hydroxysteroid dehydrogenase type II enzyme.', *Clinical and experimental pharmacology & physiology*, 23(6–7), pp. 549–51.

Soberman, J. E. and Weber, K. T. (2000) 'Spironolactone in congestive heart failure', *Current Hypertension Reports*, 2(5), pp. 451–6.

Sofuni, A., Iijima, H., Moriyasu, F., Nakayama, D., Shimizu, M., Nakamura, K., Itokawa, F., Itoi, T., (2005) 'Differential diagnosis of pancreatic tumors using ultrasound contrast imaging', *Journal of Gastroenterology*, 40(5), pp. 518-25. doi: 10.1007/s00535-005-1578-z.

Sooy, K., Noble, J., McBride, A., Binnie, M., Yau, J. L. W., Seckl, J. R., Walker, B. R. and Webster, S. P. (2015) 'Cognitive and Disease-Modifying Effects of 11β-Hydroxysteroid Dehydrogenase Type 1 Inhibition in Male Tg2576 Mice, a Model of Alzheimer's Disease', *Endocrinology*, 156(12), pp. 4592–4603. doi: 10.1210/en.2015-1395.

Sooy, K., Webster, S. P., Noble, J., Binnie, M., Walker, B. R., Seckl, J. R. and Yau, J. L. W. (2010) 'Partial Deficiency or Short-Term Inhibition of 11β-Hydroxysteroid Dehydrogenase Type 1 Improves Cognitive Function in Aging Mice', *Journal of Neuroscience*, 30(41), pp. 13867–13872. doi: 10.1523/JNEUROSCI.2783-10.2010.

Souverein, P. C., Berard, A., Van Staa, T. P., Cooper, C., Egberts, A. C. G., Leufkens, H. G. M. and Walker, B. R. (2004) 'Use of oral glucocorticoids and risk of cardiovascular and cerebrovascular disease in a population based case-control study', *Heart*, 90(8), pp. 859–865. doi: 10.1136/hrt.2003.020180.

Spiegelman, V. S., Budunova, I. V, Carbajal, S. and Slaga, T. J. (1997) 'Resistance of transformed mouse keratinocytes to growth inhibition by glucocorticoids', *Molecular carcinogenesis*, 20(1), pp. 99–107.

Stewart, P. M., Corrie, J. E., Shackleton, C. H. and Edwards, C. R. (1988) 'Syndrome of apparent mineralocorticoid excess. A defect in the cortisol-cortisone shuttle', *The Journal of Clinical Investigation*, 82(1), pp. 340–9. doi: 10.1172/JCI113592.

Stewart, P. M. and Krozowski, Z. S. (1999) '11 beta-hydroxysteroid dehydrogenase', *Vitamins and Hormones - Advances in Research and Applications*, 57, pp. 249–324.

Stewart, P. M., Whorwood, C. B., Barber, P., Gregory, J., Monder, C., Franklyn, J. A. And Sheppard, M. C. (1991) 'Localization of Renal 1 β-Dehydrogenase by in Situ Hybridization: Autocrine not Paracrine Protector of the Mineralocorticoid Receptor', *Endocrinology*, 128(4), pp. 2129–2135. doi: 10.1210/endo-128-4-2129.

Stewart, P. M, Valentino, R., Wallace, A. M., Burt, D., Shackleton, C. L. and Edwards, C. W. (1987) 'Mineralocorticoid activity of liquorice: 11-beta-hydroxysteroid dehydrogenase deficiency comes of age', *The Lancet*, 330(8563), pp. 821–824. doi: 10.1016/S0140-6736(87)91014-2.

Stimson, R. & Walker, B. R. (2007), 'Glucocorticoids and 11beta-hydroxysteroid dehydrogenase type 1 in obesity and the metabolic syndrome', *Minerva endocrinologica*, 32(3), pp. 141-159.

Stockmann, C., Doedens, A., Weidemann, A., Zhang, N., Takeda, N., Greenberg, J. I., Cheresh, D. A. and Johnson, R. S. (2008) 'Deletion of vascular endothelial growth factor in myeloid cells accelerates tumorigenesis', *Nature*, 456(7223), pp. 814–818. doi: 10.1038/nature07445.

Stojadinovic, O., Lee, B., Vouthounis, C., Vukelic, S., Pastar, I., Blumenberg, M., Brem, H. and Tomic-Canic, M. (2006) 'Novel Genomic Effects of Glucocorticoids in Epidermal Keratinocytes: inhibition of apoptosis, interferon-pathway, and wound healing along with promotion of terminal differentiation', *Journal of Biological Chemistry*, 282(6), pp. 4021–4034. doi: 10.1074/jbc.M606262200.

Strauss, D. C. and Thomas, J. M. (2010) 'Transmission of donor melanoma by organ transplantation', *The Lancet Oncology*, 11(8), pp. 790–796. doi: 10.1016/S1470-2045(10)70024-3.

Sudhir, K., Jennings, G. L., Esler, M. D., Korner, P. I., Blombery, P. A., Lambert, G. W., Scoggins, B. and Whitworth, J. A. (1989) 'Hydrocortisone-induced hypertension in humans: pressor responsiveness and sympathetic function.', *Hypertension*, 13(5). 416-21.

Sui, M., Chen, F., Chen, Z. and Fan, W. (2006) 'Glucocorticoids interfere with therapeutic efficacy of paclitaxel against human breast and ovarian xenograft tumors', *International Journal of Cancer*, 119(3), pp. 712–717. doi: 10.1002/ijc.21743.

Sun, K. and Myatt, L. (2003) 'Enhancement of Glucocorticoid-Induced 11β-Hydroxysteroid Dehydrogenase Type 1 Expression by Proinflammatory Cytokines in Cultured Human Amnion Fibroblasts', *Endocrinology*, 144(12), pp. 5568–5577. doi: 10.1210/en.2003-0780.

Suri, C., Jones, P. F., Patan, S., Bartunkova, S., Maisonpierre, P. C., Davis, S., Sato, T. N. and Yancopoulos, G. D. (1996) 'Requisite Role of Angiopoietin-1, a Ligand for the TIE2 Receptor, during Embryonic Angiogenesis', *Cell*, 87(7), pp. 1171–1180. doi: 10.1016/S0092-8674(00)81813-9.

Suzuki, S., Suzuki, T., Tsubochi, H., Koike, K., Tateno, H., Krozowski, Z. S. and Sasano, H. (2000) 'Expression of 11 beta-hydroxysteroid dehydrogenase type 2 and mineralocorticoid receptor in primary lung carcinomas', *Anticancer Research*, 20(1A), pp. 323–8.

Swift, M. R. and Weinstein, B. M. (2009) 'Arterial–Venous Specification During Development', *Circulation Research*, 104(5).

Swerdlow, S. H., Angermeier, P. A. & Hartman, A. L. (1988), 'Intrathymic ontogeny of the T cell receptor associated CD3 (T3) antigen', *Laboratory Investigation,* 58(4), pp.421-7.

Takahashi, K., Sasano, H., Fukushima, K., Hirasawa, G., Miura, H., Sasaki, I., Matsuno, S., Krozowski, Z. S. and Nagura, H. (1998) '11 beta-hydroxysteroid dehydrogenase type II in human colon: a new marker of fetal development and differentiation in neoplasms', *Anticancer Research*, 18(5A), pp. 3381–8.

Tammela, T., Zarkada, G., Wallgard, E., Murtomäki, A., Suchting, S., Wirzenius, M., Waltari, M., Hellström, M., Schomber, T., Peltonen, R., Freitas, C., Duarte, A., Isoniemi, H., Laakkonen, P., Christofori, G., Ylä-Herttuala, S., Shibuya, M., Pytowski, B., Eichmann, A., Betsholtz, C. and Alitalo, K. (2008) 'Blocking VEGFR-3 suppresses angiogenic sprouting and vascular network formation', *Nature*, 454(7204), pp. 656–660. doi: 10.1038/nature07083.

Tannin, G. M., Agarwal, A. K., Monder, C., New, M. I. and White, P. C. (1991) 'The human gene for 11 beta-hydroxysteroid dehydrogenase. Structure, tissue distribution, and chromosomal localization', *The Journal of Biological Chemistry*, 266(25), pp. 16653–8.

Tasker, J. G., Di, S. and Malcher-Lopes, R. (2006) 'Minireview: rapid glucocorticoid signaling via membrane-associated receptors', *Endocrinology*. NIH Public Access, 147(12), pp. 5549–56. doi: 10.1210/en.2006-0981.

Teelucksingh, S., Mackie, A. D., Burt, D., McIntyre, M. A., Brett, L. and Edwards, C. R. (1990) 'Potentiation of hydrocortisone activity in skin by glycyrrhetinic acid', *The Lancet*, 335(8697), pp. 1060–3.

Temkin, S., Nacharaju, V. L., Hellman, M., Lee, Y. C. & Abulafia, O. (2006), Type 2 11beta-hydroxysteroid dehydrogenase activity in human ovarian cancer, *Steroids,* 71(11-12), pp. 1019-23. doi: 10.1016/j.steroids.2006.09.001.

Terao, M., Itoi, S., Murota, H. and Katayama, I. (2013) 'Expression profiles of cortisol-inactivating enzyme, 11β-hydroxysteroid dehydrogenase-2, in human epidermal tumors and its role in keratinocyte proliferation', *Experimental Dermatology*, 22(2), pp. 98–101. doi: 10.1111/exd.12075.

Terao, M. and Katayama, I. (2016) 'Local cortisol/corticosterone activation in skin physiology and pathology', *Journal of Dermatological Science*, 84(1), pp. 11–16. doi: 10.1016/j.jdermsci.2016.06.014.

Terao, M., Murota, H., Kimura, A., Kato, A., Ishikawa, A., Igawa, K., Miyoshi, E. and Katayama, I. (2011) '11β-Hydroxysteroid Dehydrogenase-1 Is a Novel Regulator of Skin Homeostasis and a Candidate Target for Promoting Tissue Repair', *PLoS ONE*, 6(9), p. e25039. doi: 10.1371/journal.pone.0025039.

Terao, M., Tani, M., Itoi, S., Yoshimura, T., Hamasaki, T., Murota, H. and Katayama, I. (2014) '11β-hydroxysteroid dehydrogenase 1 specific inhibitor increased dermal collagen content and promotes fibroblast proliferation', *PloS ONE*, 9(3), p. e93051. doi: 10.1371/journal.pone.0093051.

Thiele, S., Baschant, U., Rauch, A. & Rauner, M. (2014), 'Instructions for producing a mouse model of glucocorticoid-induced osteoporosis', *BoneKEy Reports,* 3, pp. 552. doi: 10.1038/bonekey.2014.47.

Thieringer, R., Le Grand, C. B., Carbin, L., Cai, T. Q., Wong, B. M., Wright, S. D. and Hermanowski-Vosatka, A. (2001) '11 beta-hydroxysteroid dehydrogenase type 1 is induced in human monocytes upon differentiation to macrophages', *Journal of Immunology*, 167(1), pp. 30–35.

Thurston, G., Noguera-Troise, I. and Yancopoulos, G. D. (2007) 'The Delta paradox: DLL4 blockade leads to more tumour vessels but less tumour growth', *Nature Reviews Cancer*, 7(5), pp. 327–331. doi: 10.1038/nrc2130.

Tiganescu, A., Tahrani, A. A., Morgan, S. A., Otranto, M., Desmoulière, A., Abrahams, L., Hassan-Smith, Z., Walker, E. A., Rabbitt, E. H., Cooper, M. S., Amrein, K., Lavery, G. G. and Stewart, P. M. (2013) '11β-Hydroxysteroid dehydrogenase blockade prevents age-induced skin structure and function defects', *Journal of Clinical Investigation,* 123(7), pp. 3051–3060. doi: 10.1172/JCI64162.

Tiganescu, A., Walker, E. A., Hardy, R. S., Mayes, A. E. and Stewart, P. M. (2011) 'Localization, Age- and Site-Dependent Expression, and Regulation of 11β-Hydroxysteroid Dehydrogenase Type 1 in Skin', *Journal of Investigative Dermatology*, 131(1), pp. 30–36. doi: 10.1038/jid.2010.257.

Trapnell, C., Pachter, L and Salzberg, S. L., (2009), 'TopHat: discovering splice junctions with RNA-Seq', *Bioinformatics,* 25(9), pp. 1105-1111. doi: 10.1093/bioinformatics/btp120.

Trapnell, C., Roberts, A., Goff, L., Pertea, G., Kim, D., Kelley, D. R., Pimentel, H., Salzberg, S. L., Rinn, J. L., Pachter, L. (2012), 'Differential gene and transcript expression analysis of RNA-seq experiments with TopHat and Cufflinks', *Nature Protocols,* 7(3), pp. 562-578. doi: 10.1038/nprot.2012.016.

Tvorogov, D., Anisimov, A., Zheng, W., Leppänen, V.-M., Tammela, T., Laurinavicius, S., Holnthoner, W., Heloterä, H., Holopainen, T., Jeltsch, M., Kalkkinen, N., Lankinen, H., Ojala, P. M. and Alitalo, K. (2010) 'Effective Suppression of Vascular Network Formation by Combination of Antibodies Blocking VEGFR Ligand Binding and Receptor Dimerization', *Cancer Cell,* 18(6), pp. 630–640. doi: 10.1016/j.ccr.2010.11.001.

Uhrenholt, T. R., Schjerning, J., Hansen, P. B., Nørregaard, R., Jensen, B. L., Sorensen, G. L. and Skøtt, O. (2003) 'Rapid Inhibition of Vasoconstriction in Renal Afferent Arterioles by Aldosterone', *Circulation Research*, 93(12), pp. 1258-66.

Usami, Y., Satake, S., Nakayama, F., Matumoto, M., Ohnuma, K., Komori, T., Semba, S., Ito, A. & Yokozaki, H. (2008), 'Snail-associated epithelial-mesenchymal transition promotes oesophageal squamous cell carcinoma motility and progression', *Journal of Pathology,* 215(3), pp. 330-9. doi: 10.1002/path.2365.

Usher, M.G., Duan, S.Z., Ivaschenko, C.Y., Frieler, R.A., Berger, S., Schütz, G., Lumeng, C.N. & Mortensen, R. M. (2010), 'Myeloid mineralocorticoid receptor controls macrophage polarization and cardiovascular hypertrophy and remodeling in mice', *Journal of Clinical Investigation,* 120(9), pp. 3350-64. doi: 10.1172/JCI41080.

Vajdic, C. M. and van Leeuwen, M. T. (2009) 'Cancer incidence and risk factors after solid organ transplantation', *International Journal of Cancer*, 125(8), pp. 1747–1754. doi: 10.1002/ijc.24439.

Van Amerongen, M. J., Harmsen, M. C., van Rooijen, N., Petersen, A. H. and van Luyn, M. J. A. (2007) 'Macrophage depletion impairs wound healing and increases left ventricular remodeling after

myocardial injury in mice', *American Journal of Pathology*, 170(3), pp. 818–829. doi: 10.2353/ajpath.2007.060547.

Van Cutsem, E., Vervenne, W. L., Bennouna, J., Humblet, Y., Gill, S., Van Laethem, J. L., Verslype, C., Scheithauer, W., Shang, A., Cosaert, J. & Moore, M. J. (2009), 'Phase III trial of bevacizumab in combination with gemcitabine and erlotinib in patients with metastatic pancreatic cancer', *Journal of Clinical Oncology,* 27(13), pp. 2231-7. doi: 10.1200/JCO.2008.20.0238.

Vandekeere, S., Dewerchin, M. and Carmeliet, P. (2015) 'Angiogenesis Revisited: An Overlooked Role of Endothelial Cell Metabolism in Vessel Sprouting', *Microcirculation,* 22(7), pp. 509–517. doi: 10.1111/micc.12229.

Vanderbilt, J N., Miesfeld, R., Maler, B. A. &Yamamoto, K. R. (1987), 'Intracellular Receptor Concentration Limits Glucocorticoid-Dependent Enhancer Activity', *Molecular Endocrinology,* 1(1), pp. 68-74. doi: 10.1210/mend-1-1-68.

Varga, G., Ehrchen, J., Tsianakas, A., Tenbrock, K., Rattenholl, A., Seeliger, S., Mack, M., Roth, J. and Sunderkoetter, C. (2008) 'Glucocorticoids induce an activated, anti-inflammatory monocyte subset in mice that resembles myeloid-derived suppressor cells', *Journal of Leukocyte Biology*, 84(3), pp. 644–650. doi: 10.1189/jlb.1107768.

Vedeckis, W. V., Ali, M & Allen, H. R. (1989), 'Regulation of glucocorticoid receptor protein and mRNA levels', *Cancer Research,* 49 (8 Suppl), pp. 2295s-2302s.

Veilleux, A., Laberge, P. Y., Morency, J., Noël, S., Luu-The, V. and Tchernof, A. (2010) 'Expression of genes related to glucocorticoid action in human subcutaneous and omental adipose tissue', *The Journal of Steroid Biochemistry and Molecular Biology*, 122(1–3), pp. 28–34. doi: 10.1016/j.jsbmb.2010.02.024.

Verdegem, D., Moens, S., Stapor, P. and Carmeliet, P. (2014) 'Endothelial cell metabolism: parallels and divergences with cancer cell metabolism', *Cancer & Metabolism*, 2, p. 19. doi: 10.1186/2049-3002-2-19.

Vernieri, F., Pasqualetti, P., Matteis, M., Passarelli, F., Troisi, E., Rossini, P. M., Caltagirone, C. and Silvestrini, M. (2001) 'Effect of collateral blood flew and cerebral vasomotor reactivity on the outcome of carotid artery occlusion', *Stroke*, 32(7), pp. 1552–1558.

Viaje, A., Slaga, T. J., Wigler, M. & Weinstein, B. I. (1977), 'Effects of Anti-inflammatory Agents on Mouse Skin Tumor Promotion, Epidermal DNA Synthesis, Phorbol Ester-induced Cellular Proliferation, and Production of Plasminogen Activator', *Cancer Research,* 37, pp. 1530-1536.

Viña, J., & Lloret, A. (2010), 'Why women have more Alzheimer's disease than men: gender and mitochondrial toxicity of amyloid-beta peptide', *Journal of Alzheimer's Disease,* 20 Suppl 2, pp. S527-33. doi: 10.3233/JAD-2010-100501.

Volden, P. A. & Conzen, S. D. (2013), 'The influence of glucocorticoid signalling on tumor progression', *Brain, Behaviour and Immunity,* 30(0), pp. S26-S31. doi: 10.1016/j.bbi.2012.10.022.

Waddell, B. J., Benediktsson, R., Brown, R. W. and Seckl, J. R. (1998) 'Tissue-Specific Messenger Ribonucleic Acid Expression of 11β-Hydroxysteroid Dehydrogenase Types 1 and 2 and the Glucocorticoid Receptor within Rat Placenta Suggests Exquisite Local Control of Glucocorticoid Action 1', *Endocrinology*, 139(4), pp. 1517–1523. doi: 10.1210/endo.139.4.5900.

Walker, B. R. (2007) 'Glucocorticoids and cardiovascular disease', *European Journal of Endocrinology*, 157(5), pp. 545–59. doi: 10.1530/EJE-07-0455.

Walker, B. R., Campbell, J. C., Fraser, R., Stewart, P. M. and Edwards, C. R. W. (1992) 'Mineralocorticoid excess and inhibition of 11 β-hydroxysteroid dehydrogenase in patients with ectopic ACTH syndrome', *Clinical Endocrinology*, 37(6), pp. 483–492. doi: 10.1111/j.1365-2265.1992.tb01478.x.

Walker, B. R., Connacher, A. A., Lindsay, R. M., Webb, D. J. and Edwards, C. R. (1995) 'Carbenoxolone increases hepatic insulin sensitivity in man: a novel role for 11-oxosteroid reductase in enhancing glucocorticoid receptor activation', *The Journal of Clinical Endocrinology & Metabolism*, 80(11), pp. 3155–3159. doi: 10.1210/jcem.80.11.7593419.

Walker, B. R., Yau, J. L., Brett, L. P., Seckl, J. R., Monder, C., Williams, B. C. And Edwards, C. R. W. (1991) '11 β -Hydroxysteroid Dehydrogenase in Vascular Smooth Muscle and Heart: Implications for Cardiovascular Responses to Glucocorticoids', *Endocrinology*, 129(6), pp. 3305–3312. doi: 10.1210/endo-129-6-3305.

Walker, E. A., Ahmed, A., Lavery, G. G., Tomlinson, J. W., Kim, S. Y., Cooper, M. S., Ride, J. P., Hughes, B. A., Shackleton, C. H. L., McKiernan, P., Elias, E., Chou, J. Y. and Stewart, P. M. (2007) '11beta-Hydroxysteroid Dehydrogenase Type 1 Regulation by Intracellular Glucose 6-Phosphate Provides Evidence for a Novel Link between Glucose Metabolism and Hypothalamo-Pituitary-Adrenal Axis Function', *Journal of Biological Chemistry*, 282(37), pp. 27030–27036. doi: 10.1074/jbc.M704144200.

Wamil, M., Battle, J. H., Turban, S., Kipari, T., Seguret, D., de Sousa Peixoto, R., Nelson, Y. B., Nowakowska, D., Ferenbach, D., Ramage, L., Chapman, K. E., Hughes, J., Dunbar, D. R., Seckl, J. R. and Morton, N. M. (2011) 'Novel Fat Depot-Specific Mechanisms Underlie Resistance to Visceral Obesity and Inflammation in 11 -Hydroxysteroid Dehydrogenase Type 1-Deficient Mice', *Diabetes*, 60(4), pp. 1158–1167. doi: 10.2337/db10-0830.

Wang, L., Liu, J., Zhang, A., Cheng, P., Zhang, X., Lv, S., Wu, L., Di, W., Zha, J., Kong, X., Qi, H., Zhong, Y., Ding, G. (2012) 'BVT.2733, a selective 11β-hydroxysteroid dehydrogenase type 1 inhibitor, attenuates obesity and inflammation in diet-induced obese mice'. *PloS One*, 7(7), e40056. doi.org/10.1371/journal.pone.0040056.

Wang, R., Jiao, H., Zhao, J., Wang, X. and Lin, H. (2016) 'Glucocorticoids Enhance Muscle Proteolysis through a Myostatin-Dependent Pathway at the Early Stage.', *PloS ONE*, 11(5), p. e0156225. doi: 10.1371/journal.pone.0156225.

Wang, Z., Malone, M. H., He, H., McColl, K. S. and Distelhorst, C. W. (2003) 'Microarray Analysis Uncovers the Induction of the Proapoptotic BH3-only Protein Bim in Multiple Models of Glucocorticoid-induced Apoptosis', *Journal of Biological Chemistry*, 278(26), pp. 23861–23867. doi: 10.1074/jbc.M301843200.

Warburg, O. (1956) 'On the Origin of Cancer Cells', *Science*, 123(3191), pp. 309-14.

Warren, C. M. and Iruela-Arispe, M. L. (2010) 'Signaling circuitry in vascular morphogenesis', *Current Opinion in Hematology*, 17(3), p. 1. doi: 10.1097/MOH.0b013e32833865d1.

Webster, S. P., Seckl, J. R., Walker, B. R., Ward, P., Pallin, T. D., Dyke, H. J. and Perrior, T. R., (2011), '(4-Phenyl-piperidin-1-yl)-[5-(1H-pyrazol-4-yl)-thiophen-3-yl]-methanone compounds and their use', *Int PCT Application*, WO2011033255.

Webster, S. P., McBride, A., Binnie, M., Sooy, K., Seckl, J. R., Andrew, R., Pallin, T. D., Hunt, H. J., Perrior, T. R., Ruffles, V. S., Ketelbey, J. W., Boyd, A. and Walker, B. R. (2017) 'Selection and early clinical evaluation of the brain-penetrant 11β-hydroxysteroid dehydrogenase type 1

(11β-HSD1) inhibitor UE2343 (XanamemTM)', *British Journal of Pharmacology*, 174(5), pp. 396–408. doi: 10.1111/bph.13699.

Weidner, N. (2008), 'Measuring intratumoral microvessel density', *Methods in Enzymology,* 444, pp. 305-323. doi: 10.1016/S0076-6879(08)02814-0.

Weinberg, R. A., Hahn, W. C., Counter, C. M., Lundberg, A. S., Beijersbergen, R. L. and Brooks, M. W. (1999) 'Creation of human tumour cells with defined genetic elements.', *Nature*, 400(6743), pp. 464–468. doi: 10.1038/22780.

Weitzman, E. D., Fukushima, D., Nogeire, C., Roffwarg, H., Gallagher, T. F. And Hellman, L. (1971) 'Twenty-four Hour Pattern of the Episodic Secretion of Cortisol in Normal Subjects', *The Journal of Clinical Endocrinology & Metabolism*, 33(1), pp. 14–22. doi: 10.1210/jcem-33-1-14.

Wen, F. Q., Liu, X., Manda, W., Terasaki, Y., Kobayashi, T., Abe, S., Fang, Q., Ertl, R., Manouilova, L. & Rennard S. I. (2003), 'TH2 Cytokine-enhanced and TGF-beta-enhanced vascular endothelial growth factor production by cultured human airway smooth muscle cells is attenuated by IFN-γ and corticosteroids'. *Journal of Allergy and Clinical Immunology*, 111(6), pp. 1307–1318.

Whatcott, C. J., Han, H., Posner, R. G. & Von Hoff, D. (2013), 'Tumor-Stromal Interactions in Pacnreatic Cancer', *Critical Reviews in Oncogenesis,* 18(0), pp. 135-151.

Wheelan, N., Webster, S. P., Kenyon, C. J., Caughey, S., Walker, B. R., Holmes, M. C., Seckl, J. R. & Yau, J. L. W. (2015), 'Short-term inhibition of 11β-hydroxysteroid dehydrogenase type 1 reversibly improves spatial memory but persistently impairs contextual fear memory in aged mice', *Neuropharmacology,* 91, pp. 71-76. doi: 10.1016/j.neuropharm.2014.12.005.

White, C. I., Jansen, M. A., McGregor, K., Mylonas, K. J., Richardson, R. V, Thomson, A., Moran, C. M., Seckl, J. R., Walker, B. R., Chapman, K. E. and Gray, G. A. (2015) 'Cardiomyocyte and vascular smooth muscle independent 11β-hydroxysteroid dehydrogenase 1 amplifies infarct expansion, hypertrophy and the development of heart failure following myocardial infarction in male mice.', *Endocrinology*, p. en20151630. doi: 10.1210/en.2015-1630.

Whitworth, J. A., Mangos, G. J. and Kelly, J. J. (2000) 'Cushing, cortisol, and cardiovascular disease', *Hypertension*, 36(5), pp. 912–6.

Whorwood, C. B., Donovan, S. J., Flanagan, D., Phillips, D. I. W. and Byrne, C. D. (2002) 'Increased Glucocorticoid Receptor Expression in Human Skeletal Muscle Cells May Contribute to the Pathogenesis of the Metabolic Syndrome', *Diabetes*, 51(4).

Whorwood CB, Franhlyn JA, Sheppard MC, S. P. and Stewart P. M., (1992) 'Tissue localization of 11 beta-hydroxysteroid dehydrogenase and its relationship to the glucocorticoid receptor', *Journal of Steroid Biochemistry and Molecular Biology*, 41(1), pp. 21-8.

Wiegers, G. J., Croiset, G., Reul, J. M., Holsboer, F. and de Kloet, E. R. (1993) 'Differential effects of corticosteroids on rat peripheral blood T-lymphocyte mitogenesis in vivo and in vitro.', *The American Journal of Physiology*, 265(6 Pt 1), pp. E825-30.

Wiegers, G. J., Labeur, M. S., Stec, I. E., Klinkert, W. E., Holsboer, F. and Reul, J. M. (1995) 'Glucocorticoids accelerate anti-T cell receptor-induced T cell growth.', *The Journal of Immunology*, 155(4).

Wiegers, G. J., Reul, J. M., Holsboer, F. and de Kloet, E. R. (1994) 'Enhancement of rat splenic lymphocyte mitogenesis after short term preexposure to corticosteroids in vitro', *Endocrinology*, 135(6), pp. 2351–2357. doi: 10.1210/endo.135.6.7988417.

Willhauck, M. J., Mirancea, N., Vosseler, S., Pavesio, A., Boukamp, P., Mueller, M. M., Fusenig, N. E. and Stark, H.-J. (2006) 'Reversion of tumor phenotype in surface transplants of skin SCC cells by scaffold-induced stroma modulation', *Carcinogenesis*, 28(3), pp. 595–610. doi: 10.1093/carcin/bgl188.

Woitge, H. W., Harrison, J. R., Ivkosic, A., Krozowski, Z. and Kream, B. E. (2001) 'Cloning and in Vitro Characterization ofα 1(I)-Collagen 11β-Hydroxysteroid Dehydrogenase Type 2 Transgenes as Models for Osteoblast-Selective Inactivation of Natural Glucocorticoids 1', *Endocrinology*, 142(3), pp. 1341–1348. doi: 10.1210/endo.142.3.8044.

Wong, C. E., Yu, J. S., Quigley, D. A., To, M. D., Jen, K-Y., Huang, P. Y., Rosario, R. D. & Balmain, A. (2013), 'Inflammation and Hras signaling control epithelial–mesenchymal transition during skin tumor progression', *Genes and Development*, 27, pp. 670-682. doi: 10.1101/gad.210427.112.

World Health Organization (2017), Department of Information, Evidence and Research, mortality database (accessed on 04/09/2017).

Wu, W., Chaudhuri, S., Brickley, D. R., Pang, D., Karrison, T. and Conzen, S. D. (2004) 'Microarray analysis reveals glucocorticoid-regulated survival genes that are associated with inhibition of apoptosis in breast epithelial cells', *Cancer Research*, 64(5), pp. 1757–64.

Yancopoulos, G. D., Davis, S., Gale, N. W., Rudge, J. S., Wiegand, S. J. and Holash, J. (2000) 'Vascular-specific growth factors and blood vessel formation', *Nature*, 407(6801), pp. 242–248. doi: 10.1038/35025215.

Yano, A., Fujii, Y., Iwai, A., Kawakami, S., Kageyama, Y. and Kihara, K. (2006) 'Glucocorticoids suppress tumor lymphangiogenesis of prostate cancer cells', *Clinical Cancer Research*, 12(20 Pt 1), pp. 6012–7. doi: 10.1158/1078-0432.CCR-06-0749.

Yau, J. L. W., Noble, J., Thomas, S., Kerwin, R., Morgan, P. E., Lightman, S., Seckl, J. R. and Pariante, C. M. (2007) 'The Antidepressant Desipramine Requires the ABCB1 (Mdr1)-Type p-Glycoprotein to Upregulate the Glucocorticoid Receptor in Mice', *Neuropsychopharmacology*, 32(12), pp. 2520–2529. doi: 10.1038/sj.npp.1301389.

Yau, J. L. W., Wheelan, N., Noble, J., Walker, B. R., Webster, S. P., Kenyon, C. J., Ludwig, M. and Seckl, J. R. (2015) 'Intrahippocampal glucocorticoids generated by 11β-HSD1 affect memory in aged mice', *Neurobiology of Aging*, 36(1), pp. 334–343. doi: 10.1016/j.neurobiolaging.2014.07.007.

Zachary, I. and Morgan, R. D. (2011) 'Therapeutic angiogenesis for cardiovascular disease: biological context, challenges, prospects', *Heart*, 97(3), pp. 181–9. doi: 10.1136/hrt.2009.180414.

Zeeb, M., Strilic, B. and Lammert, E. (2010) 'Resolving cell–cell junctions: lumen formation in blood vessels', *Current Opinion in Cell Biology*, 22(5), pp. 626–632. doi: 10.1016/j.ceb.2010.07.003.

Zhang, C., Kolb, A., Büchler, P., Cato, A. C., Mattern, J., Rittgen, W., Edler, L., Debatin, K.-M., Büchler, M. W., Friess, H. and Herr, I. (2006a) 'Corticosteroid co-treatment induces resistance to chemotherapy in surgical resections, xenografts and established cell lines of pancreatic cancer', *BMC Cancer*, 6(1), p. 61. doi: 10.1186/1471-2407-6-61.

Zhang, C., Mattern, J., Haferkamp, A., Pfitzenmaier, J., Hohenfellner, M., Rittgen, W., Edler, L., Debatin, K.-M., Groene, E. and Herr, I. (2006b) 'Corticosteroid-induced chemotherapy resistance in urological cancers', *Cancer Biology & Therapy*, 5(1), pp. 59–64.

Zhang, C., Wenger, T., Mattern, J., Ilea, S., Frey, C., Gutwein, P., Altevogt, P., Bodenmüller, W., Gassler, N., Schnabel, P.A., Dienemann, H., Marmé, A., Hohenfellner, M., Haferkamp, A.,

Pfitzenmaier, J., Gröne, H.J., Kolb, A., Büchler, P., Büchler, M., Friess, H., Rittgen, W., Edler, L., Debatin, K. M., Krammer, P.H., Rutz, H.P. & Herr I. (2007), 'Clinical and mechanistic aspects of glucocorticoid-induced chemotherapy resistance in the majority of solid tumors', *Cancer Biology and Therapy*, 6(2), pp. 278-87.

Zhang, L., Dong, Y., Zou, F., Wu, M., Fan, C. & Ding Y (2013), '11β-Hydroxysteroid dehydrogenase 1 inhibition attenuates collagen-induced arthritis', *International Immunopharmacology'*, 17(3), pp. 489-94. doi: 10.1016/j.intimp.2013.07.015.

Zhang, T. Y., Ding, X. and Daynes, R. A. (2005) 'The expression of 11 beta-hydroxysteroid dehydrogenase type I by lymphocytes provides a novel means for intracrine regulation of glucocorticoid activities', *Journal of Immunology*, 174(2), pp. 879–89.

Zhang, Y., Zhong, X., Gjoka, Z., Li, Y., Stochaj, W., Stahl, M., Kriz, R., Tobin, J. F., Erbe, D. and Suri, V. (2009) 'H6PDH interacts directly with 11β-HSD1: Implications for determining the directionality of glucocorticoid catalysis', *Archives of Biochemistry and Biophysics*, 483(1), pp. 45–54. doi: 10.1016/j.abb.2008.12.004.

Zhang, Z., Coutinho, A. E., Man, J. T. Y., Kipari, T. M. J., Hadoke, P., Salter, D. M., Seckl, J. R. and Chapman, K. (2017) 'Macrophage 11β-HSD1 deficiency promotes inflammatory angiogenesis.', *The Journal of Endocrinology*, p. JOE-17-0223. doi: 10.1530/JOE-17-0223.

Zheng, Y., Izumi, K., Li, Y., Ishiguro, H. and Miyamoto, H. (2012) 'Contrary Regulation of Bladder Cancer Cell Proliferation and Invasion by Dexamethasone-Mediated Glucocorticoid Receptor Signals', *Molecular Cancer Therapeutics*, 11(12), pp. 2621–2632. doi: 10.1158/1535-7163.MCT-12-0621.

Zhou, H.-Y., Hu, G.-X., Lian, Q.-Q., Morris, D. and Ge, R.-S. (2012) 'The metabolism of steroids, toxins and drugs by 11β-hydroxysteroid dehydrogenase 1', *Toxicology*, 292(1), pp. 1–12. doi: 10.1016/j.tox.2011.11.012.

Zhu, W. H., Iurlaro, M., MacIntyre, A., Fogel, E. and Nicosia, R. F. (2003) 'The mouse aorta model: influence of genetic background and aging on bFGF- and VEGF-induced angiogenic sprouting', *Angiogenesis*, 6(3), pp. 193–9. doi: 10.1023/B:AGEN.0000021397.18713.9c.